TARGETING AUTOPHAGY IN COLORECTAL CANCER

AIKATERINI LAMPADA

This dissertation is submitted to University College London for the examination of Doctor of Philosophy

University College London, 2016

DECLARATION

I, Aikaterini Lampada, confirm that the work presented in this thesis is my own. Where information has been derived from other sources, I have indicated this in the thesis.

ACKNOWLEDGEMENTS

Firstly, I would like to express my sincere gratitude to my supervisors Prof. Daniel Hochhauser and Prof. Paolo Salomoni for giving me the opportunity to work in this PhD project. Their continuous support, advice, patience, motivation and stimulating scientific discussions helped me to mature as a scientist. Paolo and Daniel thank you for believing in me, for your guidance throughout my PhD research and thesis writing and for mentoring me.

I would like to thank UCL Grand Challenges PhD funding body for investing in me and giving me the opportunity to pursue research at the UCL Cancer Institute for the past four years.

A great thank you goes to Dr Gyorgy Szabadkai for his guidance and advice in confocal microscopy. Additionally, I would like to thank all research groups that helped this project by kindly providing reagents.

I would also like to thank Christopher Barrington and Andreas Giannopoulos for reading parts of my PhD thesis manuscript and providing constructive comments.

I thank all members, past and present, of the “Nuclear function and metabolism in cancer pathogenesis” research group that accommodated me for the past four years. My PhD life would not have been the same without their constant support, great company and friendly environment. In particular, I would like to thank Sara Galavotti and David Michod for their warm welcome when I firstly joined the lab. Life in the lab would not have been the same without my “PhD-mate”, Deli A (Justin). Justin thanks for being a great lab-mate and friend. Thanks for your support and for making endless days in the lab easy. A special thanks goes to Julia Hofmann for taking the brave decision to share the lab-bench and house with me. Julia thanks for your friendship and support (especially during my thesis writing), for our funny moments at work and at house and most importantly for teaching me German. I would like to thank Valeria Amodeo for being a great friend and company during sleepless nights in the lab. Valeria thanks for your support in the lab and during my thesis writing and for dancing with me sirtaki when I needed it! Special thanks goes to Ketty Kessler and Sara Bianco, my desk-mates, for being patient with the pile of papers covering my desk and listening my complaint when the computer stopped working during thesis writing. Ketty and Sara thanks for your support and funny moments in the lab. I thank Manav Pathania for his great company, for listening patiently my immunofluorescence analysis queries and for his help. Great thanks goes to Ana Paula Leite for her support and her meaningful help with bioinformatics queries. I thank Nicola Maestro for his kind help and for the funny moments in the lab. I thank Qingyi Liang for all the funny

western blotting moments and for her great company. I would like to thank Natalia Izotova, Teresa Sposito and Aditya Shroff that recently joined the lab. Finally, I would like to thank Susanne Scheipl and Lucia Cottone for their support and funny moments in the lab.

I thank all lab members of the “Drug-DNA Interactions” research group, past and present for their kind help. Especially, I would like to thank Valeria Santoro, a great colleague and friend. Valeria thank you for your support and for our endless conversations.

I am also thankful to my great friends Nikolas, Panagiota, Efi and Manolis along with all my colleagues at the UCL Cancer Institute for supporting me throughout this PhD. Special thanks goes in particular to Demetra, Sabine, Eva and Nancy for sharing this experience with me and for making work in UCL Cancer Institute unforgettable.

I am really thankful for having the love and support of my family; my parents, Sakis and Stella and my sister Giota. Thank you all for believing in me, actively supporting my studies and my dreams. Thank you for being on my side in both successes and failures. Last but not least, I would like to express my gratitude to Andreas. Andrea thank you for your understanding, patience and constant support throughout these years. Thanks for believing in me, making me happy and helping me evolve! Thanks for sharing this long journey with me!

To my wonderful parents and sister

ABSTRACT

Alterations of metabolism have been implicated in cancer pathogenesis and response to therapy. Autophagy is a metabolic pathway providing the cell with intermediates of metabolism and limiting cellular damage via degradation of intracellular components in vesicular structures called autophagosomes/ autolysosomes. Basal autophagy plays a dual role in cancer: in normal tissues suppresses neoplastic transformation, whereas in established cancers sustains tumour growth. Therefore, it is important to evaluate the role of basal autophagy in CRC. Additionally, oncogenic tyrosine kinases (TKs) inhibit autophagy either directly, or indirectly via activation of the PI3K/mTOR pathway. Work from our group and others have shown that i) autophagy is induced upon TK-targeted therapeutics and ii) autophagy pharmacological inhibition increases sensitivity to TK targeted therapy. In colorectal cancer (CRC), which is the 3rd most common cancer type often characterised by *PI3K* and *KRAS* mutations, targeted inhibition of the Epithelial Growth Factor Receptor (EGFR) is used for the treatment of metastatic patients albeit with limited therapeutic benefit. It is presently unclear whether autophagy inhibition could potentiate EGFR targeted therapy in CRC. More generally, our knowledge on whether or how autophagy *vice versa* could control RTK activation is limited.

The main aims of this research are: i) investigating the effect of EGFR inhibition on autophagy and the potential benefit of autophagy suppression in CRC; ii) exploring the role of basal autophagy in CRC and its relationship to signalling.

I have shown that activating mutations in *KRAS* and *PI3K* genes make CRC cells resistant to EGFR inhibition as well as to autophagy induction, mainly through differential regulation of MAPK/ERK and PI3K/AKT pathways activation; thus suggesting that autophagy targeting would have limited impact in CRC. Conversely, PI3K mutant CRC cells display basal levels of autophagy despite the presence of constitutive PI3K/mTOR signalling and basal autophagy controls RTK activation and cell signalling. Finally, basal autophagy is suggested to play a tumour suppressive role under anchorage-independent cell growth conditions.

Overall, these findings suggest a complex relationship between RTKs and autophagy: on one hand, autophagy activation upon RTK targeted therapy is dependent on *PI3K* mutational status; on the other hand, inhibition of basal autophagy affects RTK activation and downstream AKT and/or MAPK signalling independently of *KRAS/PI3K* mutations.

TABLE OF CONTENTS

LIST OF FIGURES

LIST OF TABLES

LIST OF ABBREVIATIONS

3-MA	3-Methyladenine
4E-BP1	eIF4E-Binding Protein 1
A	Adenine
ACD	Autophagic Cell Death
ADCC	Antibody-Dependent Cellular cytotoxicity
AMBRA1	Activating Molecule in Beclin1 Regulated Autophagy Protein 1
AMPK	5'-AMP-Activated Protein Kinase
APC	Adenomatous Polyposis Coli
ARG	AmphiReGulin
ATGs	Autophagy Genes
BCL-2	B-cell lymphoma-2
bFGF	basic Fibroblast Growth Factor
BIF-1	Bax-Interacting Factor 1
BSA	Bovine Serum Albumin
BTC	BeTaCellulin
Cbl	Casitas B-lineage lymphoma protein
CDK2	Cyclin Dependent Kinase 2
Chk1	Checkpoint kinase 1
CIMP	CpG Island Methylator Phenotype
CIN	Chromosomal Instability
C-lobe	Carboxy-lobe
CMA	Chaperone-Mediated Autophagy
CML	Chronic Myeloid Leukaemia
CQ	Chloroquine
CRC	ColoRectal Cancer
DMEM	Dulbecco's Modified Eagle's Medium

DMSO	DiMethyl SulfOxide
DOX	Doxycycline hyclate
ECL	Enhanced ChemiLuminescence
EGF	Epithelial Growth Factor
EGFR	Epithelial Growth Factor Receptor
EGN	EpiGeN
eIF4E	eukaryotic translation initiation Factor 4E
EMT	Epithelial to Mesenchymal Transition
Eph	Ephrin
EphB2	EPH Receptor B2
EPR	EPiRegulin
ER	Endoplasmatic Reticulum
ERGIC	ER-Golgi Intermediate Compartment
ESCRT	Endosomal Sorting Complexes Required for Transport
F	Phenylalanine
FAP	Familial Adenomatous Polyposis
FBS	Fetal Bovine Serum
FDA	Food and Drug Administration
FGFR	Fibroblast Growth Factor Receptor
FIP200	Focal adhesion kinase family-Interacting Protein 200kDa
FOXO	Forkhead boX O
GABARAP	γ-Amino Butyric Acid Receptor-Associated Protein
GAP	GTPase-Activating Protein
GDP	Guanosine DiPhosphates
GEF	GTP Exchange Factor
GFP	Green Fluorescence Protein
GIAP	G alpha-interacting protein
Grb2	Growth Factor Receptor Bound Protein 2

GSK-3	Glycogen Synthase Kinase 3
GTPase	Guanosine Triphosphatase
HB-EGF	Heparin-Binding EGF
HBV	Hepatitis B Virus
HCQ	Hydroxychloroquine
HGF	Hepatocyte Growth Factor
HGFR	Hepatocyte Growth Factor Receptor
HNPCC	Hereditary Non-Polyposis Colorectal Cancer
HNSCC	Head And Neck Squamous Cell Carcinoma
hrHGF	human recombinant Hepatocyte Growth Factor
HRP	HorseRadish Peroxidase
hsc70	heat shock-cognate protein of 70kDa
I	Isoleucine
IF	ImmunoFluoresence
IGF	Insulin-like Growth Factor
IGFR	Insulin-like Growth Factor Receptor
IL-8	InterLeukin-8
IMDM	Iscove's Modified Dulbecco's Medium
IP	ImmunoPercipitation
IP3	Inositol 1,4,5-triPhosphate
IR	Insulin Receptor
JNK	Jun N-terminal Kinase
L	Leucine
LAMP-2A	Lysosome-Associated Membrane Protein type 2A
LAPTM4B	Lysosomal Protein TransMembrane 4 Beta
LB	Luria Broth
LC3	microtubule-associated protein Light Chain 3
LIR	LC3-Interacting Region

M	Molar
MAPK	Mitogen-Activated Protein Kinase
MAPK/ERK	Mitogen-Activated Protein Kinase / Extracellular-signal-Regulated Kinase
mCRC	metastatic ColoRectal Cancer
MEFs	Mouse Embryonic Fibroblasts
MEK	MAPK/ERK Kinase
MEM	Minimum Essential Medium
mM	miliMolar
MGMT	O^6-methylguanine DNA methyltransferase
MMP-9	Matrix Metalloproteinase 9
MMR	DNA MisMatch Repair
MOI	Multiplicity of Infection
MSI	Microsatellite Instability
mTOR	mechanistic Target Of Rapamycin
mTORC1	mTOR Complex 1
mTORC2	mTOR Complex 2
NBR1	Neighbor of BRCA1 Gene 1
ng	nanogram
NGF	Nerve Growth Factor
NGFR	Nerve Growth Factor Receptor
N-lobe	amino-lobe
NRF2	Nuclear factor erythroid 2-Related Factor 2
NRGs	NeuReGulins
NSCLC	Non-Small Cell Lung Cancer
OD	Optical Density
p27KIP	p27 Kinase Inhibitory Protein
PanIN	Pancreatic Intraepithelial Neoplasia

PBS	Phosphate Buffered Saline
PCR	Polymerase Chain Reaction
PDAC	Pancreatic Ductal AdenoCarcinomas
PDGFR	Platelet-Derived Growth Factor Receptors
PDK1	3-Phosphoinositide-Dependent Kinase 1
PDK1	Pyruvate Dehydrogenase lipoamide Kinase isozyme 1
PE	PhosphatidylEthanolamine
PEG	PolyEthylene Glycol
PES	PolyEtherSulfone
PET	PolyEthylene Terephtalate
PHLPP1	Pleckstrin Homology Domain and Leucine-Rich Repeat Protein Phosphatase1
PI3K	PhosphatidylInositol 3-Kinase
PI3P	PhosphatidylInositol 3-Phosphate
PIP2	PhosphatidylInositol 4,5 bi-Phosphate
PIP3	PhosphatidylInositol 3,4,5 tri-Phosphate
PP2A	Protein Phosphatase 2A
PSSM	Position-Specific Scoring Matrix
PtdIns	PhosphatidylInositols
PTEN	Phosphatase and TENsin
PVDF	PolyVinyliDene Fluoride
RAS	Rat Sarcoma Protein
Rb	RetinoBlastoma
RET	Rearranged During Transfection
Rheb	Ras homolog enriched in brain
RLU	Relative Light Units
RNAi	RNA Interference
ROI	Region Of Interest

ROR	Receptor Tyrosine kinase-like orphan Receptor
ROS	Reactive Oxygen Species
RTK	Receptor Tyrosine Kinase
Rubicon	RUN domain protein as Beclin 1 interacting and cysteine-rich containing
S6K1	S6 kinase 1
SAPK	Stress-Activated Protein Kinase
SD	Standard deviation
SDS	Sodium Dodecyl Sulfate
SEM	Standard Error of Mean
SH2	Src Homology 2 domains
shRNA	short hairpin RNA
SNAREs	SNAP (Soluble NSF Attachment Protein) Receptor
SOS	Son Of Sevenless
SQSTM1/p62	Sequestosome 1
SRB	Sulforhodamine B
TBS	Tris Buffer Saline
TetR	Tet Repressor
TGF-a	Transforming Growth Factor-alpha
TIE	Tyrosine kinase with Immunoglobulin-like and EGF-like domains
TKIs	Tyrosine Kinase Inhibitors
TRE	Tet-Responsive Elements
TSC1/2	Tuberous SClerosis 1 and 2
ULK1/2	Unc-51-Like Kinase
UPS	Ubiquitin Proteasome System
UVRAG	UltraViolet irradiation Resistance-Associated Gene
V	Valine
VEGF	Vascular Endothelial Growth Factor

Vps34	Vacuolar protein sorting 34
W	Tryptophan
WIPI-1/2	WD repeat domain phosphoinositide interacting 1 or 2
WT	Wild Type
Y	Tyrosine
µM/uM	microMolar

Chapter 1

Introduction

1. Introduction

1.1. Autophagy

The term autophagy that derives from the Greek words “auto” (self) and “phagein” (to eat) and literally means self-eating was originally described by Christian de Duve in 1963 primed by his earlier discovery of the lysosome as a degradation organelle, in 1955. The term autophagy is used to describe observations linked to the transmission of cytoplasmic components into lysosomes for degradation. For many years, autophagy was considered as a non-selective “bulk” degradation process until 1978 when the first evidence regarding different types of autophagy was discovered (Ohsumi, 2014). Hitherto, autophagy is considered as a tightly regulated catabolic self-renewal pathway that helps cells to maintain their homeostasis and overcome stressing stimuli. Autophagy is conserved through evolution and is categorized into three types that differ in their mechanisms of function namely: 1) chaperone-mediated autophagy (CMA), 2) microautophagy and 3) macroautophagy (usually referred to as autophagy) (Feng *et al.*, 2014). Macroautophagy is the most extensively studied type of autophagy and is the main focus of this study.

In CMA, cytoplasmic proteins are selectively recognized and interact with the abundantly expressed chaperone, heat shock-cognate protein of 70kDa (hsc70), which is responsible for their translocation to lysosomes. Once at lysosomes, cytoplasmic proteins are interacting with the lysosome-associated membrane protein type 2A (LAMP-2A). This interaction promotes LAMP-2A multimerisation and in association with other proteins the formation of the translocation complex. Ensuing translocation and unfolding of the cytoplasmic protein, is its internalisation to the lysosomal lumen and degradation (Cuervo and Wong, 2014).

Microautophagy refers to the degradation of small portions of cytoplasm along with its contents into lysosomes following their engulfment into single-membrane vacuoles that originate by invagination of the lysosomal membrane. Even though the term microautophagy described shortly after the discovery of autophagy, its regulation, molecular mechanism and role in disease in mammalian cells is still unclear (Mijaljica *et al.*, 2011).

Macroautophagy (referred to hereafter as autophagy) mediates the degradation of cytoplasmic long-lived proteins and organelles into lysosomes via their previous engulfment into cytoplasmic double membrane vacuoles, called autophagosomes (Mizushima *et al.*, 2008, Ravikumar *et al.*, 2010, Mizushima and Komatsu, 2011). Autophagosome formation is a dynamic process where an open-ended, cup-shaped double-membrane structure, called phagophore, appears in the cytoplasm and

gradually increases in size until it gets closed. Autophagosome formation takes around 5-10mins to complete and autophagosome diameter varies between 0.5-1.5μm in mammals (Shibutani and Yoshimori, 2014). Fusion of an autophagosome with a lysosome follows forming an autolysosome. Autolysosome formation could be either direct or have an intermediate step where autophagosome initially fuses with late endosomes to form an amphisome and then the latter fuses with lysosomes. Inside the lysosome the cytoplasmic content along with the inner-autophagosome membrane are degraded by lysosomal hydrolases (Birgisdottir *et al.*, 2013). Autophagy could be either selective or non-selective depending on the way that the cargo is delivered inside the autophagosome. Non-selective autophagy refers to the “bulk” sequestration of cytoplasmic compartments into the autophagosome while selective autophagy describes the selective sequestration of proteins and organelles like mitochondria (a procedure called mitophagy) into the autophagosome through selective autophagy receptors such as Sequestosome 1 (SQSTM1/p62) and Neighbor of BRCA1 Gene 1 (NBR1) (Singh and Cuervo, 2011, Birgisdottir *et al.*, 2013).

Autophagy can be further subclassified into “basal autophagy” and “induced autophagy” based on the absence or presence of an autophagy-inducing stressful stimuli, respectively (Mizushima, 2007). As a physiological and homeostatic process for the cell, basal autophagy is present in most cells and tissues in a non-stressing environment to provide quality control of proteins and organelles. However, under a stressing stimulus induced autophagy is massively upregulated in the cell providing nutrient and energy precursors that enable survival. Such stressing stimuli include nutrient/growth factor deprivation, metabolic stress, endoplasmatic reticulum (ER) stress, hypoxia, oxidative stress, pathogen infection and cancer therapy (He and Klionsky, 2009, Kroemer *et al.*, 2010, Birgisdottir *et al.*, 2013). Even though the majority of *in vitro* studies are focused on induced autophagy, *in vivo* studies revealed an important role of basal autophagy in the maintenance of organismal physiology. Dysfunction of basal autophagy has been linked with various pathophysiological conditions from heart-related diseases and neurodegeneration to cancer. Mice with cardiac-specific deletion of *ATG5* gene develop cardiomyopathy, suggesting that basal autophagy represents a homeostatic mechanism in the heart maintaining correct size and function of cardiomyocytes and cardiac structure (Nakai *et al.*, 2007). Similarly, basal autophagy was identified as an important regulator of neurodegenerative diseases since mice with neural-specific deletion of *ATG5* gene are presenting accumulation of abnormal intracellular proteins forming aggregates and inclusions, which ultimately leads to neurodegeneration (Hara *et al.*, 2006). Finally, basal autophagy has been found to play an important albeit controversial role in cancer initiation and progression that will be discussed in more detail in Chapter 1.2. Briefly,

basal autophagy is suggested to play a tumour suppressive role in cancer initiation while basal autophagy in cancer progression and cancer treatment has a tumour-promoting role. Increased levels of basal autophagy have been found in a variety of cancer tissues including CRC where basal autophagy supports tumour growth and confers tumour aggressiveness.

1.1.1. Autophagosome biogenesis machinery

The revolution in autophagy research came in 1990s when autophagy in yeast was established and the isolation and characterization of autophagy genes (refereed as ATGs) starts providing important knowledge for the autophagic machinery. Currently, 38 ATG genes have been identified in yeast, many of which are sharing orthologs with mammals (Birgisdottir *et al.*, 2013). The autophagic process and machinery are complex and can be divided into four distinct steps based on the molecular effectors taking part and the morphological changes of the autophagosome that occur. These are the: initiation, elongation, maturation and degradation of the autophagosome (Ravikumar *et al.*, 2010, Kimmelman, 2011). 15 ATG genes conserved from yeast to human are implicated in these four steps. They are common between non-selective and selective autophagy and therefore are composing the autophagic core machinery (Shibutani and Yoshimori, 2014). Next I will briefly discuss the most important ATGs in the autophagic core machinery in relation to their function in each step of autophagosome biogenesis.

1.1.1.1. Initiation of autophagosome biogenesis

The first step for the initiation of autophagosome biogenesis is the formation and nucleation of the membrane that will lead to phagophore formation. The origin of the autophagosome membrane is not yet fully elucidated and recent studies indicate various membrane sources for autophagosome biogenesis. Even though good candidates for membrane sources suggested being the Endoplasmic Reticulum (ER), the Golgi apparatus, the ER-Golgi Intermediate Compartment (ERGIC), the outer membrane of the mitochondria, the plasma membrane and recycling endosomes, the precise mechanism of membrane assembly is not yet clear (Tooze and Yoshimori, 2010, Shibutani and Yoshimori, 2014).

The most important molecular components of the autophagic core machinery in this step are the Unc-51-Like Kinase (**ULK1/2**) **complex** and **Class-III** phosphatidylinositol 3-kinase (**PI3K**) **complex**. ULK1/2 complex regulates autophagy induction and is the

most upstream complex to be formed upon an autophagy-induction stimulus. ULK1/2 complex is composed of **ULK1/2**, **Atg13**, Focal adhesion kinase family-Interacting Protein 200kDa (**FIP200)** and **ATG101**. ULK1/2 directly interacts with ATG13 and this interaction primes the binding of ATG13 to FIP200 to form the ULK1/2 complex (Feng *et al.*, 2014, Shibutani and Yoshimori, 2014). **Class-III PI3K complex** is formed downstream of ULK1/2 and is important for nucleation of the phagophore membrane and production of PhosphatidylInositol 3-Phosphate (PI3P) lipid; an important component of the autophagosome membrane. Class-III PI3K complex is mainly composed of PI3K Vacuolar protein sorting 34 (**Vps34**), **p150,** and **Beclin1.** Vps34 kinase is responsible for production of PI3P and its activity is dependent on the formation of either an activation or inhibitory complex of p150:Beclin1 with either Beclin1-activating or -inhibitory effector proteins, respectively. There are two Beclin1-activating complexes structured either by Activating molecule in Beclin1 Regulated Autophagy protein 1 (**AMBRA1**) and **ATG14** or UltraViolet irradiation Resistance-Associated Gene (**UVRAG**) and Bax-Interacting Factor 1 (**BIF-1**) proteins. For the formation of Beclin1-inhibitory complexes AMBRA1 and BIF-1 proteins are replaced by B-cell lymphoma-2 (**BCL-2**) and RUN domain protein as Beclin 1 interacting and cysteine-rich containing (**Rubicon**), respectively. BCL-2 directly inhibits Beclin1 whereas Rubicon deactivates UVRAG to de-activate the Beclin1 complex (He and Klionsky, 2009, Ravikumar *et al.*, 2010, Kimmelman, 2011, Rubinsztein *et al.*, 2012, Feng *et al.*, 2014, Shibutani and Yoshimori, 2014). The accumulation of synthesized PI3P triggers more ATGs proteins to the phagophore membrane and primes its elongation.

1.1.1.2. Phagophore elongation

The **elongation** of the phagophore membrane needs the constant supply of lipids; **ATG9** protein has been implicated in membrane delivery from membrane sources to the phagophore. Elongation of the phagophore is still not well defined but there are evidence supporting that **ATG2** - WD repeat domain phosphoinositide interacting 1 or 2, (**WIPI-1/2**) - **ATG9** complex to play a role in this process (Shibutani and Yoshimori, 2014).

Key molecular events of the phagophore elongation step are the formation of two ubiquitin-like conjugation systems: 1) **ATG8** and 2) **ATG12**. In mammals there are two ATG8 subfamilies composed of microtubule-associated protein light chain 3 (**LC3**) and γ-amino butyric acid receptor-associated protein (**GABARAP**) proteins. LC3 subfamily has 3 isoforms: LC3A, LC3B and LC3C whereas GABARAP subfamily has two:

GABARAPL1 and GABARAPL2. In mammals **LC3B** isoform is the best-studied marker used for autophagy research (Birgisdottir *et al.*, 2013). Two post-translational modifications conform LC3B able to associate to phagophore membrane. Firstly, a proteolytic cleavage in its C-terminal tail catalysed by ATG4 enzyme, creates a free cytoplasmic form of LC3B called LC3-I. Secondly, LC3-I protein is conjugated to phosphatidylethanolamine (PE) at its cleaved-C-terminal tail to create a phagophore-associated form of LC3 protein, called **LC3-II**. Lipidation of LC3-I is a reaction involving the E1-and E2-like ubiquitin enzymes, ATG7 and ATG3, respectively. ATG7 protein binds, activates and then facilitates LC3-I transfer to ATG3. Even though the mechanism of PE conjugation is not clear yet, it is believed that ATG12 ubiquitin-like conjugation complex acts as an E3-like ubiquitin enzyme for LC3-I lipidation. ATG12 ubiquitin-like system is composed of **ATG12, ATG5** and **ATG16L1** proteins. Initially ATG12 protein is activated by ATG7 through which is transferred to the E2-like ubiquitin enzyme, ATG10. An intermediate complex composed of ATG12 and ATG10 is formed until ATG12 is covalently conjugated with ATG5. Finally, ATG16L1 is conjugated to the ATG12-ATG5 complex by directly interacting with ATG5. (He and Klionsky, 2009, Ravikumar *et al.*, 2010, Kimmelman, 2011, Rubinsztein *et al.*, 2012, Feng *et al.*, 2014). LC3-II in addition to its function in phagophore elongation is an important component for selective autophagy since is directly binding to selective-autophagy receptors such as p62 and NBR1 (Birgisdottir *et al.*, 2013). LC3-II protein is associated with both outer- and inner-membranes of the phagophore/autophagosome. After the autophagosome is formed, the responsible ATG proteins for phagophore elongation are detached and recycled back to the cytoplasm for mediating another round of autophagosome biogenesis. The only known exception is LC3-II protein that remains associated with autophagosomes until the very last step of the process, characteristic that makes it the main marker for autophagy research. While ATG12, ATG5 and ATG16L1 are usually used as markers of the early steps of autophagosome biogenesis since they are dissociating from the phagophore membrane as long as the autophagosome is formed (Shibutani and Yoshimori, 2014).

1.1.1.3. Maturation and degradation of the autophagosome

After the phagophore closes, follows maturation and degradation of the autophagosome. **UVRAG** is an important component of the **maturation** step through fusion of autophagosomes with late endosomes and lysosomes promotion. Additionally, the fusion step involves proteins like ESCRT, SNAREs, Rab7 and the class-III Vps proteins. **Degradation** of the autolysosome consists the last step of the autophagic machinery; a process dependent on the proper function of lysosomic

hydrolases, proteinases and lipases. At this step the inner-autophagosome membrane along with autophagic cargo are degraded and the new precursor molecules are released to the cytoplasm in order to maintain cellular homeostasis and physiological function (He and Klionsky, 2009, Ravikumar *et al.*, 2010, Kimmelman, 2011, Rubinsztein *et al.*, 2012).

1.1.2. Molecular pathways regulating autophagy

Different molecular pathways controlling signalling cascades of growth factor/nutrient availability, energy levels, ER stress, hypoxia, oxidative stress and pathogen infection responses in the cell, have been found to control autophagy. The majority of them are upstream regulators of ULK1 and/or class III PI3K complexes of the core autophagic machinery and thus regulating autophagosome biogenesis. The best characterised mechanism that an autophagic stimulatory/inhibitory signal is transmitted to the core autophagic machinery for autophagy regulation is through the mechanistic Target Of Rapamycin (mTOR) kinase. This type of autophagy is called mTOR-dependent or canonical autophagy. However, there are exceptions in this rule and accumulating evidence highlight the presence of mTOR-independent mechanisms of autophagy regulation, wherein an autophagic stimulus is transmitted to the core autophagic machinery without the involvement of mTOR kinase (Sarkar, 2013). Below, I am going to discuss how nutrient, growth factor, energy and stress-mediated signalling pathways, which are commonly deregulated in cancer, control autophagy in mTORC1-dependent and -independent manners.

1.1.2.1. Nutrient-dependent signalling pathway: mTOR pathway

mTOR is a serine/threonine protein kinase that exists in two distinct complexes, named mTOR Complex 1 (mTORC1) and 2 (mTORC2). mTORC1 is activated in response to nutrients, growth factors, stress, energy status and oxygen. Full activation of mTORC1 requires both nutrients and growth factors (Laplante and Sabatini, 2012, Efeyan *et al.*, 2015). In the presence of nutrients, mTORC1 translocates to the outer surface of the lysosome where it interacts with Rag Guanosine Triphosphatase (GTPase) complexes responsible for its activation. Rag GTPases are localised to the lysosome by a complex named Ragulator, which is also necessary for mTORC1 lysosomal recruitment. Rag GTPases interact with mTORC1 and facilitate its translocation to a compartment that mTORC1-kinase activator, Ras homolog enriched

in brain (Rheb) GTPase resides (Sancak *et al.*, 2008, Sancak *et al.*, 2010). When mTORC1 complex is fully active, it controls protein and lipid synthesis as well as energy production in the cell. Two best-known downstream substrates of mTORC1 are eukaryotic translation initiation factor 4E (eIF4E)-binding protein 1 (4E-BP1) and S6 kinase 1 (S6K1).

In addition to its anabolic functions, active mTORC1 is a master negative regulator of autophagy induction (Yang and Klionsky, 2010, Laplante and Sabatini, 2012, Efeyan *et al.*, 2015). Under nutrient replete conditions, mTORC1 is activated and directly interacts with components of the ULK1 complex. In particular, mTORC1 directly phosphorylates ATG13 and ULK1 to restrain ULK1 kinase activity and consequently autophagy induction. In turn, upon nutrient-deplete conditions where mTORC1 is inactivated, ULK1 and ATG13 are de-phosphorylated and ULK1 complex can be activated, leading in that way to autophagy induction (Hosokawa *et al.*, 2009, Jung *et al.*, 2009, Kim *et al.*, 2011a, Russell *et al.*, 2014). Apart from regulating autophagosome initiation, mTORC1 has been recently suggested to control later stages of the autophagic process. Specifically, in nutrient-replete conditions, mTORC1 phosphorylates UVRAG and this phosphorylation event enhances the interaction of UVRAG with Rubicon. This interaction inhibits UVRAG-mediated autophagosome maturation (Kim *et al.*, 2015).

1.1.2.2. Growth factor-dependent signalling pathways

Growth factors bind and activate Receptor Tyrosine Kinases (RTKs) in the plasma membrane stimulating in that way downstream signalling cascades such as PI3K/AKT and mitogen-activated protein kinase / extracellular - signal-regulated kinase (MAPK/ERK) pathways (RTKs are discussed in session 1.5.1.) (Lemmon and Schlessinger, 2010). In growth factor deprived conditions, RTKs and their downstream effectors are deactivated, thus resulting to autophagy induction in the majority of the cases (Galluzzi *et al.*, 2015). Well-characterized growth factor-dependent signalling pathways that regulate autophagy are: a) **PI3K/AKT** and b) **MAPK/ERK** pathways. Additionally, **RTKs** have been recently found to be direct modulators of autophagy induction.

PI3K/AKT pathway

PI3K is a family of lipid kinases, which catalyse the phosphorylation of the 3-hydroxyl group of the inositol ring in phosphatidylinositols (PtdIns). Based on structure

and substrate specificity differences, PI3K isoforms have been classified into three classes: class I, class II and class III. While class III PI3Ks are directly participating in autophagy induction (discussed in 1.1.1.), class I PI3Ks could modulate autophagy mainly indirectly.

Class I PI3Ks are downstream effectors of RTKs. They form heterodimers composed of a catalytic subunit, p110 (has four isoforms named α, β, γ and δ), and a regulator subunit, p85. In basal unstimulated conditions, p85 regulatory subunits function to stabilize p110 and inactivate its kinase activity. Whereas in stimulated conditions, p85 subunits through their Src homology 2 domains (SH2) domains, recruit p110 to the phosphorylated tyrosine residues of RTKs, where they release their p85-mediated inhibition of p110 enabling p110 kinase activation (Vanhaesebroeck *et al.*, 2010). They generate phosphatidylinositol 3,4,5 tri-phosphate (PIP3) from phosphatidylinositol 4,5 bi-phosphate (PIP2), which recruits AKT protein kinase and 3-phosphoinositide-dependent kinase 1 (PDK1) to the plasma membrane. AKT is fully activated in two-steps reaction. Firstly, PDK1 phosphorylates AKT Tyrosine residue 308 and secondly mTORC2 phosphorylates its serine residue 473 (Engelman *et al.*, 2006, Mendoza *et al.*, 2011). Class I PI3K and AKT are upstream regulators of mTORC1 and in such an indirect way can regulate autophagy induction. In particular when AKT is active, it inhibits autophagy by activating mTORC1. AKT-mediated mTORC1 activation is catalysed through inhibition of its upstream negative regulator, Tuberous sclerosis 1 and 2 (TSC1/2) complex, responsible for disseminating growth factor signals to mTORC1. TSC1/2 is a GTPase-activating protein (GAP) for the Rheb GTPase. The GTP-bound form of Rheb directly interacts with mTORC1 and activates its kinase function. On the contrary, TSC1/2 as a Rheb GAP, converts Rheb in its inactive, GDP-bound form that negatively regulates mTORC1 activity (Laplante and Sabatini, 2012). Additionally, RAS signalling has been implicated in autophagy regulation through its ability to directly activate Class I PI3K and inhibit autophagy induction in an mTORC1-dependent manner (Furuta *et al.*, 2004, He and Klionsky, 2009, Ravikumar *et al.*, 2010).

Apart from the indirect, AKT/mTORC1-mediated regulation of autophagy previously discussed, an isoform of PI3K, named p110β, was recently found to regulate autophagy in an mTORC1-independent manner. Specifically, p110β interacts with Rab5 intracellularly and this interaction promotes Rab5 activity over Vps34-Vps15 complex to induce autophagy both in basal and growth factor deprived conditions (Dou *et al.*, 2013). Moreover, AKT can directly regulate autophagy in an mTORC1-independent manner since it phosphorylates Beclin1 at S295 (and possibly S234) and inhibit autophagosome biogenesis (Wang *et al.*, 2012). Finally, AKT can transcriptionally regulate and inhibit autophagy induction through phosphorylation-

dependent inactivation of the transcription factor Forkhead box O3 (FoxO3). Activation of FoxO3 has been found to elevate the expression of autophagy related genes such as LC3B, GABARAPL1, Vps34, ULK2 and ATG12L and consequently promote autophagy induction in an mTORC1-independent manner in skeletal muscle (Mammucari *et al.*, 2007, Zhao *et al.*, 2007).

MAPK/ERK pathway

MAPK/ERK pathway is a downstream RTK effector that is composed of the Raf, MAPK/ERK kinase (MEK) and ERK1/2 kinases. When a RTK is active, it can activate ERK1/2 through a multistep cascade of phosphorylation events. A key event for MAPK/ERK activation in the plasma membrane is the sequestration and binding of the adaptor protein Growth Factor Receptor Bound Protein 2 (Grb2) to the phosphorylated tyrosine residues of a RTK, through its specific SH2 domain. Concurrently with Grb2, Son Of Sevenless (SOS), a GTP Exchange Factor (GEF), translocates to the plasma membrane (McKay and Morrison, 2007). SOS physically interacts with rat sarcoma protein (RAS) GTPase and catalyses its activation through the exchange of Guanosine DiPhosphates (GDP) with GTP. RAS as a GTPase can hydrolyze bound GTP to GDP and in that way switches constantly from an inactive GDP-bound state to an active GTP-bound state. The activated GTP-bound RAS catalyses the activation of RAF protein, which in turn phosphorylates MEK and finally leads to the phosphorylation of ERK1/2 proteins (Roberts and Der, 2007). Activated ERK1/2 translocate to the nucleus controlling various transcription factors and in that way expression of various genes involved in cell proliferation and survival (McKay and Morrison, 2007).

MAPK/ERK pathway has been suggested to play a role in autophagy induction with dichotomous observations though regarding its role. Like AKT, ERK1/2 when is active can inhibit autophagy by activating mTORC1 through direct inactivation of its upstream inhibitory complex TSC1/2 (Yang and Klionsky, 2010, Laplante and Sabatini, 2012). On the other hand, a non-canonical AMPK-MEK/ERK-TSC-mTOR pathway that regulates autophagy through controlling Beclin 1 levels has been described. In fact, upon various autophagic stimuli MEK/ERK residing downstream of AMPK was activated and mediated the disassembly and inactivation of mTORC1 and/or mTORC2 complexes, resulting in the up-regulation of Beclin 1 levels and autophagy induction (Wang *et al.*, 2009). Additionally, it is found that ERK1/2 activates autophagy through phosphorylation of the G alpha-interacting protein (GIAP); a regulator of G protein signalling (Ogier-Denis *et al.*, 2000, Pattingre *et al.*, 2003, Helgason *et al.*, 2013). In particular, autophagy inhibition in the presence of amino acids is correlated with

reduced ERK1/2 activation, which mediated GAIP phosphorylation inhibition in intestinal derived cancer cells (Ogier-Denis *et al.*, 2000).

RTKs (discussed in 1.5.1 page 49)

RTKs are traditionally believed to modulate autophagy indirectly in an mTORC1-dependent manner through their downstream effectors, PI3K and MAPK/ERK that described above.

It was only recently that the first evidence came to light for direct regulation of the autophagic machinery by RTKs in an mTORC1/AKT-independent manner and has been mainly illustrated for Epithelial Growth Factor Receptor (EGFR). Research from Wei *et al*., (2013) has shown that active EGFR (either ligand-activated WT EGFR or constantly active mutant EGFR) binds and phosphorylates Beclin 1 protein. These phosphorylation events enhance interaction of Beclin 1 protein with autophagy-negative regulators Bcl-2 and Rubicon and in turn eliminate interaction with the autophagy-positive regulator Vps34 kinase further leading to autophagy inhibition in human Non-Small Cell Lung Cancer (NSCLC) cells (Wei *et al.*, 2013). Additionally, a recent study has shown a kinase-independent role of EGFR in autophagy regulation. They show that EGFR downregulation results in autophagy suppression both in normal and starved conditions. The mechanism suggested is that inactive-EGFR translocates to lysosomal protein transmembrane 4 beta (LAPTM4B) positive endosomal compartments and creates a complex with Sec5 exocyst subunit. Inactive-EGFR/LAPTM4B/Sec5 complex is responsible for dissociation of Rubicon from Beclin 1 and in that way initiate autophagy (Tan *et al.*, 2015).

Additionally, EphB2 receptor ectopic expression was found to increase autophagy in 293T cells. EphB2-regulated autophagy induction was proposed to be controlled by increased ERK and class III PI3K pathway activity and in turn downregulated AKT activity (Kandouz *et al.*, 2010). Recent findings of the same group are showing that EphB2 expression upregulates autophagy and the increase in autophagy induction downstream EphB2 was associated with increased expression of ATG5 and ATG12 proteins (Chukkapalli *et al.*, 2014).

1.1.2.3. Energy-dependent signalling pathway: AMPK pathway

5'-AMP-activated protein kinase (AMPK) is a fundamental regulator for cellular metabolism and is a great energy sensor in the cell. AMPK is stimulated upon decreased energy levels in the cell that is translated to low ATP/AMP ratio (Efeyan *et*

al., 2015). Since autophagy is induced as a homeostatic mechanism to energetic stress, AMPK has been shown to be a positive regulator of autophagy. AMPK has been described both as indirect (mTORC1-dependent) and direct modulator of autophagy induction (mTORC1-independent) (Russell *et al.*, 2014). Regarding its indirect nature of function, when AMPK is activated, phosphorylates TSC2 and inactivates Rheb, which leads to mTORC1 inhibition and autophagy induction (Laplante and Sabatini, 2012, Russell *et al.*, 2014). Alternatively, AMPK directly phosphorylates Raptor subunit of the mTORC1 complex and inhibits mTORC1 activity (Gwinn *et al.*, 2008).

Finally, AMPK can directly phosphorylate and activate ULK1 kinase from the core autophagic machinery and in that way induce autophagy in an mTORC1-independent manner (Kim *et al.*, 2011a).

1.1.2.4. Other mTORC1-independent pathways regulating autophagy

Pathways susceptible to chemical perturbations in the cell have been described to control autophagy in an mTORC1-independent manner. More specific inositol, cAMP/Epac/Inositol 1,4,5-triphosphate (IP3) and Ca2+/calpain pathways have been found to inhibit autophagy when activated (Sarkar *et al.*, 2005, Williams *et al.*, 2008, Ravikumar *et al.*, 2010, Sarkar, 2013). Components of the class III PI3K pathway, such as Beclin 1, have been found to control autophagy induction in an mTORC1-independent manner in starvation conditions. In particular, activation of the JNK1 signalling pathway has been identified as a positive regulator of autophagy induction during starvation through phosphorylating Bcl-2 protein and resulting in disruption of the autophagy-inhibitory complex Bcl-2/Beclin 1 (Wei *et al.*, 2008). Additionally, a recent genome-wide siRNA screen has identified a variety of growth factors and cytokines that are negatively regulating autophagy under normal nutrient-replete conditions through Class III PI3K inhibition (Lipinski *et al.*, 2010). Induction of basal autophagy in an mTORC1-independent manner has been previously reported in RAS-expressing cancer cells with the precise mechanism remaining unknown (Guo *et al.*, 2011). However, a recent publication by Perera *et al*., 2015, describes that increased levels of basal autophagy in pancreatic ductal adenocarcinoma (PDA) is transcriptionally controlled by accelerated nuclear translocation and consequent activation of the MiT/TFE proteins that concomitantly regulate lysosome biogenesis (Perera *et al.*, 2015).

1.2. Role of autophagy in Cancer

Progress in the scientific field of autophagy over the last two decades revealed autophagy to be linked with various pathophysiological conditions such as neurodegenerative, cardiovascular and immunological disorders, infectious diseases and most importantly cancer (Ravikumar *et al.*, 2010). In this report, I will mainly focus on the controversial role of autophagy in cancer initiation and progression.

1.2.1. Tumour suppressive role of autophagy

Autophagy has been suggested to play a tumour suppressive role in early tumourigenesis events due to its ability to mitigate cellular stress, via maintenance of cellular homeostasis and prevention of stress-induced transformation in normal tissues (Kimmelman, 2011, Rosenfeldt and Ryan, 2011, Yang *et al.*, 2011b, White, 2012).

Indirect evidence of a tumour suppressive role of autophagy in early tumourigenesis comes from the identification of mutations and/or amplifications in a number of cancer-related genes, in a variety of cancer types that cause malignant transformation and result in autophagy suppression. Such examples include inactivation or loss of tumour suppressor genes such as *PTEN* whereas oncogenes like *PI3K* and *AKT1* are activated (Galluzzi *et al.*, 2015).

There is also increasing direct evidence supporting a tumour suppressive role of autophagy in cancer initiation, arising mainly from autophagy-deficient mouse models studies. The first evidence came from studies on the essential autophagy gene *Beclin1*. It was observed that Beclin1 expression is frequently low in breast carcinoma cell lines and tissues compared to normal breast epithelium. Additionally, Beclin1 overexpression could suppress tumourigenesis of breast cancer cell lines *in vitro* and in a mouse xenograft model (Liang *et al.*, 1999, Kimmelman, 2011). On support of these observations, ensuing work from the same group showed that *Beclin1* monoallelic loss in mice results in increased incidence of spontaneous neoplasm development and accelerated Hepatitis B virus (HBV)-induced hepatocellular carcinoma development (Qu *et al.*, 2003, White, 2012). Moreover a recent study on Ambra1 gene, an activator protein of Beclin1, supports the tumour suppressive role of autophagy in cancer initiation (Cianfanelli *et al.*, 2015).

1.2.1.1.Tumour suppressive mechanisms of autophagy

A variety of different mechanisms regulating the tumour suppressive function of autophagy in cancer initiation have been suggested. Autophagy could suppress cancer initiation by maintaining genomic integrity of a cell. Karantza-Wadsworth *et al*., (2007) have shown that autophagy-deficient cells with monoallelic loss in *Beclin1* resulted in increased DNA damage under metabolic stress conditions in breast cancer *(Karantza-Wadsworth et al., 2007)*. Another study has shown that ATG7 and ATG5-mediated autophagy suppression in mouse embryonic fibroblasts impaired homologous recombination DNA repair mechanism by downregulating the phosphorylation of checkpoint kinase 1 (Chk1) that potentially could lead to accumulation of DNA damage (Liu *et al.*, 2015).

An additional mechanism that autophagy could suppress tumourigenesis is through maintenance of mitochondria quality control through mitophagy (a selective lysosomal degradation of dysfunctional mitochondria) and by controlling cellular antioxidant defense. The latter function of autophagy is supported by a study showing that autophagy impairment, results in accumulation of the autophagic substrate protein p62 known to control indirectly nuclear factor erythroid 2-related factor 2 (NRF2) activation leading in that way to the production of reactive oxygen species (ROS)-detoxification genes and promotion of cell survival (Inami *et al.*, 2011, Kimmelman, 2011, White, 2012).

Inflammation has been suggested as a hallmark of cancer since prolonged inflammation could lead to the development of cancer (Colotta *et al.*, 2009). It is believed that defects in the autophagic machinery could result in inflammation-induced cancer and the best examples describing that phenomenon are inflammatory bowel disease (Crohn's disease) and pancreatitis (Rosenfeldt and Ryan, 2011). In the study of Cadwell *et al*., (2009) was observed that mice with defects in autophagy related genes such as *Atg16L1*, *Atg5* or *Atg7* present abnormalities in small intestinal Paneth cells that resembles the abnormalities occurring in Crohn's disease patients (Cadwell *et al.*, 2009).

Additionally, autophagy could suppress tumourigenesis by inducing cell death or senescence in RAS-induced transformation events. Work from Elgendy *et al*., (2011) suggested that HRAS-induced autophagy upregulation limits clonogenic survival of human ovarian surface epithelial cells by accelerating autophagy-mediated cell death. Autophagy inhibition (shBeclin1, siRNA ATG5 and ATG7) rescues this phenotype (Elgendy *et al.*, 2011). On the other hand, work from Young *et al*., (2009) showed that RAS-induced autophagy upregulation promotes senescence of human diploid

fibroblasts and autophagy inhibition (shATG5 and shATG7) reversed this phenotype (Young *et al.*, 2009).

Finally, autophagy may suppress cancer initiation by promoting defense against viral and bacterial infections with high tumourigenic potential, such as HBV (which promotes hepatocellular carcinoma) and *Streptococcus bovis* (which causes colorectal carcinoma), respectively (Galluzzi *et al.*, 2015).

1.2.2. Tumour-promoting role of autophagy

Opposing to the tumour suppressive role of autophagy in cancer initiation, autophagy has been suggested to promote cancer progression. Generally, autophagy helps cancer cells to overcome and survive stressing stimuli of the cancer microenvironment like nutrient/growth factors deprivation, defects in metabolism, hypoxia and cancer treatment (Galluzzi *et al.*, 2015). Additionally, growing evidence indicates a positive correlation between high autophagic status and tumour invasive/metastatic phenotype as well as poor clinical outcome (Galavotti *et al.*, 2013, Galluzzi *et al.*, 2015).

Recently, direct insight into the tumour-promoting role of autophagy in cancer progression came from studies using mouse models for tissue-specific, oncogenic-driven cancers with or without autophagy. *In vivo* work on the autophagy-related genes, ATG7 and ATG5, are revealing a more complex oncogene-regulated role of autophagy in cancer initiation and progression. Even though systemic deletion of ATG5 and conditional liver-specific deletion of ATG7 showed autophagy to play a tumour suppressive role in hepatocellular carcinoma development (Takamura *et al.*, 2011), recent studies on pancreatic cancer development failed to prove this (Rosenfeldt *et al.*, 2013, Yang *et al.*, 2014). These two studies reported that conditional deletion of either ATG5 or ATG7 genes in pancreatic tissue does not lead to malignant transformation whereas autophagy-deficient mice present increased tissue destruction and die earlier.

Interestingly though they showed that autophagy plays a tumour suppressive role in pancreatic cancer initiation in an activated-*KRAS*-dependent context (Rosenfeldt *et al.*, 2013, Yang *et al.*, 2014). Accelerated neoplasmatic initiation upon ATG5 and ATG7-mediated autophagy suppression was observed in *KRAS* G12D and *BRAF* V600E driven lung cancer models, respectively. However, benign neoplasms were dependent on autophagy to progress into a malignant state (Strohecker *et al.*, 2013, Rao *et al.*, 2014). In line with the aforementioned observations the study of Rosenfeldt *et al*., (2013) showed that concurrent *KRAS* G12D activation and ATG7 or ATG5 deletion

leads to increased pre-cancerous pancreatic intraepithelial neoplasia (PanIN) formation while eliminated the progression of PanINs into pancreatic ductal adenocarcinomas (PDAC) (Rosenfeldt *et al.*, 2013). Intriguingly, the role of autophagy in *KRAS*-driven cancer progression was switched from tumour-promoting to tumour suppressive when *p53* was concurrently deleted, in both pancreatic and lung tissues (Rosenfeldt *et al.*, 2013, Rao *et al.*, 2014). The tumour suppressive role of autophagy in the *p53*-deletion context was attributed to increased glucose uptake of autophagy-deficient cells. On the contrary, in *KRAS* G12D-driven pancreatic carcinoma mouse model where *p53* was abolished through loss of heterozygosity, autophagy inhibition restricts cancer progression (Yang *et al.*, 2014). Finally, a tumour-promoting role of autophagy in intestinal cancer initiation and progression was observed in an *APC* conditional knockout model. Reduced intestinal neoplasms were formed in ATG7-deficient mice and this inadequacy of ATG7-deficient mice to form intestinal neoplasms was due to increased microbiome-induced immune response. However, the decreased intestinal tumour growth of ATG7-deficient mice was attributed to metabolic defects such as p53-growth arrest and AMPK activation rather that increased immune responses (Levy *et al.*, 2015).

1.2.2.1. Tumour-promoting mechanisms of autophagy

Different mechanisms have been suggested to be responsible for the tumour-promoting role of autophagy in cancer progression. Cancer cells could depend on autophagy for growth, survival and fulfillment of their elevated metabolic requirements. A variety of studies have shown that established tumours display autophagy addiction (Guo *et al.*, 2011, Kim *et al.*, 2011b, Lock *et al.*, 2011). These tumours are characterized by activated *RAS* oncogene expression resulting in elevated levels of autophagy not only in stressed conditions but in basal levels as well. High levels of basal autophagy in *RAS* activated cancers maintain tumour growth, survival and mitochondrial function (Guo *et al.*, 2011, Yang *et al.*, 2011a).

Another interesting aspect of tumourigenesis is the requirement of tumours for functional mitochondrial respiration, induced by *RAS* oncogene. It has been demonstrated that autophagy is required for maintaining mitochondrial function and in that way promoting tumourigenesis (Guo *et al.*, 2011, White, 2012, Guo *et al.*, 2013, Rosenfeldt *et al.*, 2013, Strohecker *et al.*, 2013, Rao *et al.*, 2014, Yang *et al.*, 2014).

Sustained angiogenesis represents another important hallmark for cancer development and progression (Hanahan and Weinberg, 2011). There are some studies proposing a role of autophagy in controlling angiogenesis, which could

possibly support the tumour-promoting role of autophagy. In the study by Du *et al*., (2012) it was observed that pharmacological and genetic (by Atg5 siRNA) inhibition of autophagy reduces angiogenesis possibly through elimination of autophagy-mediated ROS production and AKT activation (Du *et al.*, 2012). Additionally, the role of autophagy in inducing angiogenesis is supported by cancer-related studies showing that pharmacological and genetic (*ATG5* and *Beclin-1*) inhibition of autophagy potentiates anti-angiogenic cancer treatment in colon cancer cells (Selvakumaran *et al.*, 2013).

Recently, autophagy has also been proposed to regulate migration/invasion in cancer. Work from Salomoni's group and others showed that inhibition of autophagy inhibits migration/invasion in glioma-initiating cells and established cell lines (Macintosh *et al.*, 2012, Galavotti *et al.*, 2013). Another study showed that autophagy is induced in cells undergoing Epithelial to Mesenchymal Transition (EMT) and regulates migration in this context (Li *et al.*, 2013a) (unpublished work from our laboratory shows the same). Taken together, these findings suggest that autophagy could be involved in regulating tumour metastasis, a key factor underlying cancer progression.

Collectively, in healthy tissues autophagy maintains cellular equilibrium and eliminates cancer initiation. However, if the autophagic barrier in tumour development fails and a malignancy is established then autophagic function needs to be restored in order cancer cells to survive (Galluzzi *et al.*, 2015). However, recent contradictory observations are indicating the urgency of extensive research in the field in order to deconvolute the complex role of autophagy in cancer initiation and progression.

1.3. Autophagy modulation in cancer treatment

Taking into account the predominant tumour-promoting role of autophagy in cancer progression, it was expected that the role and function of autophagy upon cancer treatment would favor cancer cell survival. However, some studies in the literature suggest an opposing pro-death role of autophagy upon cancer treatment. The pro-death and pro-survival roles of autophagy upon cancer treatment will be discussed below.

1.3.1. Pro-death role of autophagy in cancer treatment

The role of autophagy as a pro-death mechanism is under a long lasting debate. The definition of autophagic cell death (ACD) has been introduced to describe the type of cell death caused by autophagy, characterized by increased autophagic flux but not increased apoptosis or necroptosis and in which inhibition of autophagy suppresses cell death (Marino *et al.*, 2014). Even though there is evidence in the literature supporting that autophagy induction could lead to cell death, it is still under question whether autophagy could execute cell death by itself or is just present when cell death occurs (Fuchs and Steller, 2015). Under physiological conditions, ACD has been implicated to the removal of salivary gland and midgut in the fruitfly *Drosophila melanogaster* during development. ACD rather than caspace-dependent apoptosis has been found to be responsible for *Drosophila melanogaster* midgut cell death and removal, while both autophagy and caspase-dependent cell death are important for salivary gland removal (Berry and Baehrecke, 2007, Denton *et al.*, 2009). In mammals, the role of ACD remains elusive under physiological conditions while ACD has been described to eliminate cell survival under drug-induced conditions including cancer therapy (Marino *et al.*, 2014). Indeed ACD is induced in imipramine-treated glioma cell lines and mice bearing glioma tumours. Ticlopidine, which inhibits the purinergic receptor $P2Y_{12}$ and enhances autophagy induction, accelerated imipramine-induced autophagy and potentiated imipramine treatment response. Genetic inhibition of autophagy (shRNA for Beclin1 and ATG7) blocked imipramine and ticlopidine-induced cell death while pharmacological inhibition of apoptosis and necroptosis did not affect levels of cell death (Shchors *et al.*, 2015). The best example of a pro-death role of autophagy came from studies with apoptosis-deficient cells, lacking both Bak and Bax pro-apoptotic proteins. In particular, apoptosis-deficient mouse embryonic fibroblasts (MEFs) underwent autophagy-dependent cell death under etoposide treatment. Inhibition of autophagy either pharmacologically (3-methyladenine) or genetically (siRNA for ATG5 or Beclin1) rescued etoposide-induced cell death in these cells (Shimizu *et al.*, 2004). Additionally, it has been shown that the pan-BCL-2 inhibitor (-)-Gossypol induces autophagic cell death in apoptosis-resistant glioma cells; genetic manipulation (Beclin-1 and ATG5 knockdown) reduces the cell death induced by (-)-Gossypol (Voss *et al.*, 2010). In the study by Goussetis *et al*., (2010) it is shown that autophagy is induced upon arsenic trioxide in leukemia cells and that pharmacological (CQ) and genetic modulation (ATG7 and Beclin1 siRNA) of autophagy increased the clonogenic potential of these cells upon arsenic trioxide treatment (Goussetis *et al.*, 2010). Similarly, EGFR targeted therapy by Erlotinib was found to induce autophagy in NSCLC cells and mouse xenografts harbouring an Erlotinib-sensitive EGFR mutation.

Autophagy induction upon EGFR targeted therapy was due to increased Beclin1 interaction with Vps34 and genetic inhibition of autophagy (via shATG7 and an inhibitory phosphomimetic mutant of Beclin1 were used) resulted in increased clonogenic survival *in vitro* and partial resistance to Erlotinib in mouse xenografts (Wei *et al.*, 2013). Although autophagy could function as a compensatory cell death mechanism in an apoptotic-deficient context, there are a lot of studies that show a concomitant activation of autophagy and cell death mechanisms upon treatment (Rebecca and Amaravadi, 2015). For example, although glioma cells found to induce autophagic cell death upon arsenic trioxide, pharmacological inhibition of autophagy (bafilomycin A1) in combination with arsenic trioxide found to enhance the anti-tumour effect of arsenic trioxide through the induction of apoptosis (Kanzawa *et al.*, 2003). Additionally, autophagy has been found to increase sensitivity to chemotherapeutic agents (mitoxantrone or oxaliplatin) *in vivo* by increasing immunogenic cell death. In particular, autophagy increases the secretion of ATP in dying cells that leads to recruitment of dendritic cells and T lymphocytes into the tumour bed and increases chemosensitivity (siRNAs and shRNAs against ATG5 or ATG7 were used) (Michaud *et al.*, 2011).

Overall, even though the existence of autophagic cell death is under question, it is a matter of fact that in some experimental models autophagy induction reduced cell survival. Whether autophagy is directly responsible for cell death execution or other cell death mechanisms, like apoptosis or necrosis are it remains to be elucidated.

1.3.2. Pro-survival role of autophagy in cancer treatment

Following the realization that autophagy could be a survival pathway for tumour cells, the hypothesis that it could have a pro-survival role in cancer treatment was inevitable. Additionally, the fact that the mode of action of anti-cancer drugs resembles some natural stimuli inducing autophagy strengthened this hypothesis. Since then, an increasing number of studies investigating the pro-survival role of autophagy upon cancer treatment started. In that setting, pharmacological and genetic autophagy manipulation approaches are used.

A variety of pharmacological agents that target different steps in the autophagic process have been described in the literature and summarized in Table 1.1. The majority of these agents are lysosomotropic compounds targeting later steps in the autophagic process; in particular they are inhibiting the autophagosome turnover by inhibiting lysosomal function. Agents such as, Chloroquine (CQ), Hydroxychloroquine (HCQ) and Mefloquine are Food and Drug Administration (FDA)-approved and have been in clinical use for many years for the treatment of diseases such as malaria,

autoimmune and psychiatric disorders. It was only recently however that their connection with the autophagic pathway has been proven (Amaravadi *et al.*, 2011, Yang *et al.*, 2013). Recently, SAR405 and PIK-III Vps34-specific inhibitors, targeting Vps34-kinase domain, have been developed and shown to inhibit autophagosome formation (Dowdle *et al.*, 2014, Ronan *et al.*, 2014). However, caution should be taken when used since Vps34 inhibition may additionally interfere with vesicle trafficking, as was already shown for SAR405 inhibitor (Ronan *et al.*, 2014, Galluzzi *et al.*, 2015, Rebecca and Amaravadi, 2015). Moreover, an ULK1 kinase inhibitor has been developed and shown to block autophagy induction (Egan *et al.*, 2015). Amongst all the currently known autophagic inhibitors, CQ and its more potent analog HCQ are the most commonly used for *in vitro* as well as *in vivo* studies.

It is possible that cancer therapy induces autophagy by increasing DNA damage, metabolic stress and malfunctioned organelles. Indeed, it has been found that autophagy is a pro-survival mechanism after radiation and arsenic trioxide in glioma cells (Ravikumar *et al.*, 2010). In addition, a variety of chemotherapeutic agents have been found to induce autophagy and inhibition of autophagy found to improve their therapeutic potential (Amaravadi *et al.*, 2011). Targeted therapy has been also found to induce autophagy possibly by resembling nutrient/growth factor deprivation.

Table 1. 1: Agents used for autophagy inhibition

Agent Name	Mechanism of action	Autophagic Step	Clinical usage	References
Chloroquine	Lysosome deacidification	Autophagolysosome degradation	Malaria Autoimmune disorders	Amaravadi *et al.*, 2011; Y. P. Yang *et al.*, 2013
Hydroxycloroquine	Lysosome deacidification	Autophagolysosome degradation	Malaria Autoimmune disorders	Amaravadi *et al.*, 2011; Y. P. Yang *et al.*, 2013
Mefloquine	Lysosome deacidification	Autophagolysosome degradation	Malaria	Sharma *et al.*, 2012
Lys05	Lysosome deacidification	Autophagolysosome degradation	No	McAfee *et al.*, 2012
Desmethylclomipramine	Lysosomal deacidification	Autophagolysosomal Degradation	Psychiatric disorders	Rossi *et al.*, 2009
SAR405	Vps34 kinase inhibitor	Autophagosome biogenesis	No	Ronan *et al.*, 2014 Rebecca&Amaravadi 2015
PIK-III	Vps34 kinase inhibitor	Autophagosome biogenesis	No	Dowdle *et al.*, 2014 Rebecca&Amaravadi 2015
VATG-027	Lysosome deacidification	Autophagolysosomal Degradation	No	Goodall *et al.*, 2014 Rebecca&Amaravadi 2015
SBI-0206965	ULK1 kinase inhibitor	Autophagosome biogenesis	No	Egan *et al.*, 2015

1.3.2.1. Pro-survival role of autophagy in tyrosine kinase targeted therapy

A number of studies in the last few years have proposed a role of autophagy downstream inhibition of oncogenic tyrosine kinases via targeted therapy agents. Work from our group (Bellodi *et al.*, 2009) has shown that autophagy inhibition potentiates BCR-ABL tyrosine kinase targeted therapy (Imatinib) in Chronic Myeloid Leukaemia (CML) cells, by using pharmacological and genetic modulation of autophagy (shRNA for Atg5 and Atg7). It was observed that Imatinib-induced autophagy was associated with ER stress (Bellodi *et al.*, 2009). This work led to a clinical trial for the use of the autophagy inhibitor HCQ (See Table 1. 1 and Appendix I, page 231) in combination with the BCR/ABL-targeting drug Imatinib (Calabretta and Salomoni, 2011). Additionally, Li *et al*., (2010) showed that autophagy has a pro-survival role upon EGFR targeting antibody Cetuximab (See Table 1.2) treatment and that pharmacological and genetic modulation of autophagy (Beclin-1 ot Atg7 shRNA) sensitise Cetuximab-treated cells to apoptosis. They showed that Cetuximab-induced autophagy is controlled by PI3K/mTOR pathway inhibition and it was accompanied by activation of the Beclin1/Vps34 complex, by Cetuximab (Li and Fan, 2010). The same group published another paper showing that the pro-survival role of autophagy was a characteristic only of cancer cells undergoing apoptosis upon Cetuximab treatment (Li *et al.*, 2010). These contradictory observations warrant further examination since the precise mechanism causing this cell-type specific effect of autophagy upon cetuximab treatment was not found. Additionally, work in glioblastoma showed that autophagy inhibition can potentiate treatment by the EGFR kinase inhibitor Erlotinib (See Table 1.2), proposing a pro-survival role of autophagy (Eimer *et al.*, 2011). A similar pro-survival role of autophagy upon EGFR inhibition (Erlotinib or Gefitinib; See Table 1.2) was observed in lung cancer as well. This study also demonstrated that pharmacological or genetic inhibition of important autophagy regulators (Atg5 and Atg7 siRNA) potentiates targeted therapy (Han *et al.*, 2011). In line with *in vivo* studies underlining the importance of autophagy as a tumour-promoting mechanism in an oncogene-activation context (*KRAS* and *BRAF*) is a recent study in melanoma. It is reported that autophagy plays a cytoprotective role in *BRAF* V600E melanoma cell lines and mouse xenografts upon *BRAF* inhibiting targeted therapy. Additionally, increased autophagy was observed in *BRAF* V600E patients' samples that were resistant to *BRAF* inhibition treatment. Both pharmacological (Lys05) and genetic (shATG5) inhibition of autophagy *in vitro* and only pharmacological in mouse xenografts potentiated *BRAF* inhibition-mediated cell death in melanoma (Ma *et al.*, 2014).

The continuous need for potentiation of cancer therapy efficacy along with the growing evidence supporting a pro-survival role of autophagy in cancer progression and cancer treatment led to the development of several clinical trials where conventional cancer treatment therapeutics are combined with autophagy modulation compounds. Below I will discuss the current status of clinical trials involving autophagy inhibitors focusing mainly on targeted therapy compounds.

1.3.3. Modulation of autophagy in clinical trials

Currently, an increasing number of clinical trials combining different targeted therapy agents with autophagy inhibitors is ongoing or are being developed for cancer types such as lung, colorectal, prostate and renal carcinomas; melanoma and sarcoma (Appendix I, page 231). In a variety of clinical trials in lung and colorectal cancer, the antiangiogenic monoclonal antibody Bevacizumab is used in combination with different chemotherapeutic agents along with HCQ as an autophagy inhibitor. Additionally, EGFR tyrosine kinase inhibitors such as, Erlotinib and Gefitinib are used in combination with HCQ in lung cancer clinical trials. AKT or mTOR inhibitors in combination with HCQ are in use in prostate and renal carcinomas.

Recently, results from Phase I and II clinical trial have been published regarding the combinational treatment of HCQ autophagy inhibitor with various cancer treatment agents (temozolomide and radiation in glioblastoma multiforme; temozolomide in melanoma and solid tumours; temsirolimus in solid tumours and melanoma; vorinostat in advanced solid tumours; erlotinib in NSCLC) (Goldberg *et al.*, 2012, Mahalingam *et al.*, 2014, Rangwala *et al.*, 2014a, Rangwala *et al.*, 2014b, Rosenfeld *et al.*, 2014). These trials provided important information for the applicability of autophagy inhibition in a clinical setting and for dose-limiting toxicity in cancer patients. The majority of the trials found HCQ to be well-tolerated in patients and no dose-limiting toxicity of HCQ was observed; with the higher HCQ concentrations tested going up to 1200 mg/day (Goldberg *et al.*, 2012, Mahalingam *et al.*, 2014, Rangwala *et al.*, 2014a, Rangwala *et al.*, 2014b). The only study that reported dose-limiting toxicity at 800 mg/day HCQ was in glioblastoma multiforme patients that HCQ was combined with radiation therapy and temozolomide. HCQ treatment at this concentration resulted in myelosuppression development in three out of three patients (Rosenfeld *et al.*, 2014). Importantly, all these trials evaluated that HCQ can inhibit autophagy in a clinical setting and additionally established biomarkers for assessing autophagy modulation in clinical trials. Some of the biomarkers consist of: i) monitoring autophagosome accumulation by electron microscopy in peripheral blood mononuclear cells, ii) assessment of LC3B lipidation by western blotting and iii) investigation of LC3B-positive

immunohistochemical samples (Goldberg *et al.*, 2012, Mahalingam *et al.*, 2014, Rangwala *et al.*, 2014a, Rangwala *et al.*, 2014b, Rosenfeld *et al.*, 2014, Rebecca and Amaravadi, 2015).

Even though it is too early for generalisation of results, autophagy inhibition was shown to prolong stable-disease and partially improved treatment response in some patients with melanoma, colorectal cancer (CRC), renal cell carcinoma and NSCLC (Goldberg *et al.*, 2012, Mahalingam *et al.*, 2014, Rangwala *et al.*, 2014a, Rangwala *et al.*, 2014b). However, inconsistent autophagy inhibition between patients and no clinical benefit of HCQ- combinational treatment (temozolomide and radiation therapy) versus monotherapy was observed in glioblastoma and metastatic pancreatic patients, respectively (Rosenfeld *et al.*, 2014, Wolpin *et al.*, 2014).

Nevertheless the high number of clinical trials using autophagy inhibitors to potentiate efficacy of conventional cancer therapy, a tumour suppressive role of autophagy is demonstrated in various cancer types following cancer treatment. These observations suggest that autophagy-inhibiting therapeutic approaches should not be considered a panacea and in some cases autophagy-inducing agents may potentiate cancer treatment outcome. For example ticlopidine, a purinergic receptor $P2Y_{12}$ inhibitor, enhanced imipramine-induced autophagic cell death and increased survival in glioma-bearing mice (Shchors *et al.*, 2015). Additionally, our knowledge on the status of autophagy in different cancer types is limited. Human cancers are characterised by high heterogeneity (Vogelstein *et al.*, 2013) and heterogeneity is an outstanding issue in cancer biology and cancer therapy having a key role in therapeutic resistance. Research from our lab has shown that among the different molecular subgroups of glioma, only the mesenchymal subgroup could be associated with high autophagy gene expression. This work suggests that only the mesenchymal subtype of glioblastoma may respond to autophagy inhibition (Galavotti *et al.*, 2013). Apart from the variability characterising tumours of the same subtype, intra-tumour metabolic heterogeneity (Cantor and Sabatini, 2012) could also play an important role in how tumours respond to autophagy inhibition. Furthermore, the differential role of autophagy in oncogene-driven cancers, as discussed above, points out that autophagy inhibition approaches could have adverse effects than expected. Heterogeneity of autophagic status is expected to be a critical factor affecting response to autophagy inhibition therapeutic approaches.

1.4 Colorectal Cancer (CRC)

1.4.1. Epidemiology

CRC is the 3rd most common cancer type in males and the 2nd in females worldwide, accounted for approximately 1.4 million of new cancer cases and 693.900 deaths on 2012. The incidence rates of CRC are almost twice higher in developed countries compared to less developed countries. Australia/New Zealand, Europe and North America are the countries exhibiting the highest incidence rates of CRC (Torre *et al.*, 2015). CRC incidence markedly varies between countries and this could be due to different environmental risks and genetic predisposition between populations (Arvelo *et al.*, 2015). Even though there is a marked higher incidence rate of CRC in developed countries, the mortality rate is lower compared to less developed countries. The increased survival of CRC patients in developed countries could be attributed to the improved healthcare system as well as the higher socioeconomic status. CRC screening, reduced exposure to high risk factors and better treatment approaches are some of the factors that could enhance CRC patient survival (Torre *et al.*, 2015). In general, 64.9% of patients with CRC will reach an average of 5-year survival after diagnosis. Early diagnosis is an important factor determining CRC patients' survival; 90.3% of patients that were diagnosed with a localised tumour will achieve a 5-year survival compared to only 12.5% of patients that were diagnosed with a metastatic CRC (DeSantis *et al.*, 2014).

The risks for developing CRC are both environmental and genetic. Consequently, CRC is divided into three main categories based on the risk factors affecting its development: i) hereditary, ii) sporadic and iii) familial. Hereditary CRC accounts for approximately 5% of total CRC cancer cases and develops due to the presence of hereditary genetic mutations of known genes. Hereditary CRC can be further subdivided into Familial Adenomatous Polyposis (FAP) and hereditary non-polyposis colorectal cancer (HNPCC) based on the presence of adenomatous polyps or not, respectively. Sporadic CRC is the most common type of CRC cancers and is responsible for approximately 75% of total CRC cases. Sporadic CRC cancer development has been linked to risk factors such as ageing, western dietary, chronic inflammation and various environmental factors. Finally, approximately 20% of total CRC cases are classified into the familial group. Familial CRC patients have a family history of CRC but hitherto there is no known association with a specific gene, as in hereditary CRC (Al-Sohaily *et al.*, 2012, Arvelo *et al.*, 2015). Below the molecular alterations that lead to CRC development will be discussed.

1.4.2. Molecular pathology of CRC

CRC develops through the accumulation of genetic and epigenetic alterations leading to the transformation of a normal colon mucosa to adenoma, then to a carcinoma and finally to a metastatic cancer (Vogelstein *et al.*, 2013). This process is heterogeneous regarding the order and grade of genetic alterations taking place as well as the location of the colorectum and each patient (Manne *et al.*, 2010).

Genomic instability is a common characteristic of CRC and three different molecular pathways have been linked to this phenomenon. These are the: i) Chromosomal Instability (CIN) pathway, ii) Microsatellite Instability (MSI) pathway, and iii) CpG Island Methylator Phenotype (CIMP) pathway; these could either act cooperatively or independently one from each other to cause genomic instability. Additionally, a variety of oncogenes and tumour suppressor genes were found altered in CRC (Lengauer *et al.*, 1998, Markowitz and Bertagnolli, 2009, Manne *et al.*, 2010)

Chromosomal instability is the most common type of genomic instability in CRC and involves the loss/gain of a chromosome or a part of it. This type of instability could lead to loss/gain of important tumour suppressor genes/oncogenes resulting in CRC malignant transformation (Markowitz and Bertagnolli, 2009). Amplifications in a big part of the chromosome usually appear at chromosomes 8q, 13, and 20q and losses at chromosomes 8p, 17p, and 18q in CRC (Fearon, 2011).

Microsatellite instability is a consequence of loss of function of important proteins implicated in the DNA mismatch repair (MMR) pathway. Microsatellites are short nucleotide sequences present all over the genome that they are prone to errors during replication. MMR proteins are responsible for correcting such base-pair errors. A variety of different MMR genes were found mutated in HNPCC patients with the most common being the *MSH2* and *MLH1* genes. Even though only 2%-4% of sporadic CRC patients found to harbour mutations in MMR genes, a higher percentage (~15%) of patients occurred with MSI characteristics. In sporadic CRC patients with high MSI occurrence, *MLH1* gene was silenced due to hypermethylation of its promoter (Fearon, 2011, Al-Sohaily *et al.*, 2012).

The existence of a hypermethylated *MLH1* promoter along with observations of methylation in other genes termed the CIMP pathway in CRC. CIMP refers to epigenetic alterations in gene expression due to DNA methylation. Usually methylation of a gene promoter results to silencing of the gene (Issa, 2004). Even though CRC cells are characterized by low methylation rates compared to normal surrounding tissue, a variety of gene promoters are found to be hypermethylated, resulting to gene silencing. Genes found to be silenced by hypermethylation of their promoter in CRC

are *Adenomatous Polyposis Coli* (*APC)* and O^6- *Methylguanine DNA Methyltransferase* (*MGMT)* (Fearon, 2011, Al-Sohaily *et al.*, 2012).

Finally, a broad range of oncogenes and tumour suppressor genes have been found mutated in CRC. The first gene identified to be in association with hereditary CRC was the *APC*, which is responsible for FAP development. In the majority of FAP cases, *APC* gene found to harbour frameshift mutations leading to truncation of APC protein. Additionally, *APC* mutations have been found to be present in sporadic CRC as well. Approximately 70-80% of CRC patients appear to harbour *APC* inactivating mutations. *APC* gene is characterised as a "gatekeeper" gene since it is believed to be one of the first mutation events leading to malignant transformation in CRC (Fearon, 2011, Vogelstein *et al.*, 2013). The small malignant clone that appears and grows after *APC* inactivation, named adenoma, needs a second mutation event in order to enhance its clonal growth and form a carcinoma. Usually, *KRAS* activating mutations are responsible for carcinoma development. This process continues with mutations in other genes such as *PI3K*, *TGF-β* and *p53* to develop a metastatic cancer that can expand to lymph nodes and distant organs (Vogelstein *et al.*, 2013). The most common mutated pathways in CRC are WNT, RAS/MAPK, PI3K, TGF-β and p53 (Fearon, 2011, Cancer Genome Atlas, 2012).

1.4.3. CRC treatment

Treatment of CRC depends on the stage of the cancer at the time of diagnosis. At early-diagnosed CRC, patients are referred to surgeons for tumour resection. At later stages of CRC, patients are treated by surgery that is followed by approximately 6 months of chemotherapy. Chemotherapy is usually the main treatment of patients with advanced metastatic CRC (DeSantis *et al.*, 2014). The main chemotherapeutic agents used for CRC treatment are 5-fluorouracil, irinotecan and oxaliplatin. Additionally, targeted therapy agents against two different RTKs have been recently used either as combinational treatment with chemotherapy or as a monotherapy to total refractory metastatic CRC patients. These are two monoclonal antibodies against EGFR, Cetuximab and Panitumumab and a monoclonal antibody against VEGF receptor, bevacizumab. Part of this thesis will be focused on the role of autophagy upon EGFR targeted therapy (Cetuximab) in CRC. EGFR targeted therapy will be therefore discussed below.

1.5. Epidermal Growth Factor Receptor (EGFR) and EGFR targeted therapy

1.5.1. EGFR

RTKs are a family of cell surface receptors with an intrinsic, growth factor-regulated tyrosine kinase activity (Gschwind *et al.*, 2004). As tyrosine kinases, they catalyse the transfer of the γ phosphate of ATP to hydroxyl groups of tyrosines on other target proteins (Schlessinger, 2000). 58 different RTKs have been discovered in humans and are categorized into 20 families. All RTKs share similar structural characteristics: i) a ligand-binding domain in their extracellular region, ii) a single transmembrane helix and iii) a cytoplasmic region containing a conserved protein tyrosine kinase domain and additional carboxy-terminal and juxtamembrane regulatory domains. Even though, different growth factors act as RTKs' ligands, the mechanism of activation as well as the downstream intracellular signalling pathways stimulated by RTKs are common between them. The majority of RTKs, with the exception of insulin receptor (IR) and IGF1 receptor, are monomers in the plasma membrane and they dimerise only upon ligand binding in their extracellular domain. Dimerisation stimulates activation of their tyrosine kinase domains and transphosphorylation of tyrosines in adjacent RTKs. The phosphorylated RTKs will then recruit proteins of intracellular downstream pathways and prime signalling cascades (Lemmon and Schlessinger, 2010).

RTKs are controlling various cellular processes such as proliferation, differentiation, metabolism, survival and migration. Interestingly, more than half of the RTKs have been found deregulated in cancer. Such examples are members of the ErbB, PDGFR, HGFR and FGFR families (Gschwind *et al.*, 2004, Lemmon and Schlessinger, 2010).

1.5.1.1. EGFR architecture and function

EGFR RTK was identified by G. Carpenter on 1978, (Carpenter *et al.*, 1978) an important discovery in the RTK signalling field along with the earlier discoveries of nerve growth factor (NGF) and epithelial growth factor (EGF) by R. Levi-Montalcini and S. Cohen, respectively (Levi-Montalcini, 1952, Cohen, 1962, 1965). Since then our knowledge on RTKs has massively increased and EGFR consists one of the best studied amongst RTKs (Gschwind *et al.*, 2004, Schlessinger, 2014).

The Epidermal Growth Factor Receptor (EGFR/ErbB1/HER1) is a 170kDa transmembrane glycoprotein belonging to the ErbB family, one of the 20 RTKs' families. Along with EGFR another three RTKs consist ErbB family: i) ErbB2/HER2, ii) ErbB3/HER3 and iii) ErbB4/HER4 proteins. All four members share common structure and an activation mechanism that is dimerisation dependent (either homodimers or heterodimers could be formed between ErbB RTKs). Like all RTKs, they are

composed of an extracellular ligand-binding region, a transmembrane region and a cytoplasmic tyrosine kinase region. Their extracellular region can be further subdivided into four domains, named I, II, III and IV. The single transmembrane helix is connected with both extracellular and intracellular regions via a small extracellular and intracellular juxtamembrane domain, respectively. The tyrosine kinase domain in their cytoplasmic region is linked with a carboxy-terminus tail that contains tyrosine residues, responsible for autophosphorylation events of the RTK (Hynes and Lane, 2005, Zandi *et al.*, 2007, Lemmon and Schlessinger, 2010, Lemmon *et al.*, 2014). With the exception of ErbB2, all other ErbB family members are competent for growth factor-ligand stimulation. Epidermal Growth Factor (EGF), Transforming Growth Factor-alpha (TGF-a), amphiregulin (ARG) and epigen (EGN) ligands can only activate EGFR. Another class of ligands that bind and activates ErbB4, such as betacellulin (BTC), Heparin-Binding EGF (HB-EGF) and epiregulin (EPR), can also activate EGFR. ErbB3 and ErbB4 RTKs are stimulated by another class of ligands, which is called neuregulins (NRGs). While NRG-1 and 2 bind both ErbB3 and ErbB4, NRG-3 and 4 are ErbB4 specific (Hynes and Lane, 2005, Lemmon *et al.*, 2014). EGFR ligands are usually type I transmembrane proteins with their amino-terminus domain exposed extracellularly. In their amino-terminus a conserved motif is located, named EGF domain that is responsible for EGFR binding (with exception EGF ligand that has eight EGF domains). They also have a transmembrane domain that links the extracellular amino-terminus domain with a cytoplasmic carboxy-terminus tail. Ligands cannot bind to RTKs in their transmembrane form; therefore they need to be processed by proteases in order to become activated secreted ligands. Known proteases responsible for EGFR-ligand proteolytic cleavage are ADAMs (Adrain and Freeman, 2014).

Upon ligand binding (to a pocket structure formed by I and III extracellular EGFR subdomains), the extracellular domain of EGFR totally changes conformation enabling its dimerisation with another receptor. It needs to be mentioned that in contrast to all other RTKs where usually ligand plays an active role in receptor-receptor dimerisation, dimerisation of EGFR is solely mediated by receptor-receptor contacts; mainly between the extracellular domains II (dimerisation arm). This dimerisation event results in activation of the cytoplasmic tyrosine kinase domain of the dimer in an allosteric mediated way. Activation of EGFR cytoplasmic tyrosine kinase domains is accompanied by the formation of an asymmetric dimer, whereby one kinase acts as an activator while the other one as the receiver. Both the activator and the receiver have an amino-lobe (N-lobe) and a carboxy-lobe (C-lobe). The model suggested for allosteric EGFR tyrosine kinase activation describes that the C-lobe of the activator tyrosine kinase, contacts the N-lobe of the receiver tyrosine kinase and in a

conformation change-dependent manner switch the inactive state of the receiver to active. Finally, the active-receiver transphosphorylates tyrosine residues in the carboxy-terminus tail of the activator (Lemmon and Schlessinger, 2010, Lemmon *et al.*, 2014). Activated tyrosines in EGFR recruit adaptor proteins such as Grb2 and PI3K to activate the two major downstream signalling pathways MAPK/ERK and PI3K/AKT, respectively (previously discussed in session 1.1.2.2.) (Zandi *et al.*, 2007).

EGFR signalling is controlling various physiological cellular processes, thus it was no surprise when deregulations in its activation were linked with cancer development and progression. In 1980s, studies reported the presence of EGFR overexpression in epithelial tumours and linked EGFR with cancer. Since then more mechanisms contributing to disruption of EGFR tight regulation have been described such as: i) increased ligand production, ii) EGFR mutations and iii) defective EGFR downregulation (Gschwind *et al.*, 2004, Zandi *et al.*, 2007).

The linkage between EGFR and other members of the ErbB family with the biology of various cancer types such as colorectal, lung, breast, glioblastoma as well as head and neck cancer led to the development of drugs specifically targeting EGFR activation (Lemmon *et al.*, 2014).

1.5.2. EGFR Targeted Therapy

Targeted therapy is a major advance in cancer therapeutics and it refers to the generation of drugs that specifically target and regulate molecular alterations exclusively for tumour cells. Two different categories of EGFR-targeting agents are currently available in the cancer-pharmaceutical market including: monoclonal antibodies that specifically bind to EGFR extracellular domain and tyrosine kinase inhibitors (TKIs), which target the intracellular tyrosine kinase domain of EGFR (Gschwind *et al.*, 2004, Lemmon and Schlessinger, 2010). In Table 1. 2, EGFR-targeting agents used clinically are summarised. Although these agents represent a major step forward for personalized cancer therapy their clinical outcome is still limited. In this report I will focus on the monoclonal antibody category and more specifically to the chimeric antibody called Cetuximab (distributed under the trade name Erbitux).

Table 1. 2: Summary of FDA approved EGFR targeting agents

EGFR inhibitor	Mode of action	FDA approved
Cetuximab	EGFR Monoclonal Ab	1) KRAS WT colorectal cancer
		2) Metastatic head and neck cancer
Panitumumab	EGFR Monoclonal Ab	EGFR expressing colorectal cancer
Gefitinib (Iressa)	EGFR Tyrosine kinase inhibitor	Non-small cell lung cancer
Erlotinib (Tarceva)	EGFR Tyrosine kinase inhibitor	1) First-line treatment of metastatic non-small cell lung cancer with EGFR exon 19 deletions or exon 21 L858R substitution
		2) Maintenance treatment of Non-small cell lung cancer
		3) Along with gemcitabine for pancreatic cancer
Afatinib	EGFR and HER2 Tyrosine kinase inhibitor	First-line treatment of metastatic non-small cell lung cancer with EGFR exon 19 deletions or exon 21 L858R substitution
Lapatinib	EGFR and HER2 Tyrosine kinase inhibitor	1) Hormone receptor positive metastatic breast cancer that overexpresses the HER2 receptor
		2) Along with capecitabine for HER2 overexpressing breast cancer

1.5.2.1. Cetuximab

Cetuximab is a 152 kDa chimeric human-murine immunoglobulin G1 developed from the full murine M-225 antibody by replacement of its murine backbone with a human one in order to reduce hypersensitivity reactions to patients. The variable antigen binding domain of the murine M-225 antibody, responsible for EGFR recognition, was kept intact through Cetuximab development (Vincenzi *et al.*, 2008). Cetuximab structural studies have shown that Cetuximab binds to domain III of the EGFR extracellular domain antagonizing in that way ligand binding. Cetuximab prevents EGFR from obtaining its post ligand-binding specific structural conformation that blocks EGFR dimerisation and in that way ensures that ligand will not displace bound-Cetuximab even in ligand-high abundance conditions. In such way Cetuximab directly inhibits EGFR activation and the subsequent activation of its downstream pathways (Li *et al.*, 2005). Although direct inhibition of EGFR activation is believed to be the main anti-tumour mechanism of Cetuximab action, there are other mechanisms suggested to play important role in Cetuximab-mediated anti-tumour activity. Firstly,

antibody-dependent cellular cytotoxicity (ADCC) has been implicated to play a role in Cetuximab anti-tumour action by recruiting cytotoxic host cells like monocytes and natural killer cells to the tumour microenvironment; a positive correlation between EGFR expression levels and ADCC was observed (Ashraf *et al.*, 2012). EGFR internalisation was also suggested to play key role in Cetuximab-mediated anti-tumour activity since the intracellular fate of EGFR-Cetuximab complex seems to differ from the EGFR-ligand complex. It is found that EGFR-Cetuximab complex is more stable to endosomal acidic pH, avoiding in that way EGFR endosomal sorting and promoting EGFR lysosomal degradation; EGFR degradation leads to downregulation of its levels (Li *et al.*, 2005, Vincenzi *et al.*, 2008). Inhibition of cell cycle progression through increased levels of p27 Kinase Inhibitory Protein (p27KIP) is suggested by studies as another anti-tumour effect of Cetuximab. p27KIP is bound to cyclin dependent kinase 2 (CDK2) resulting in its decreased activation and G1-phase cell cycle arrest in DiFi colorectal cell line (Vincenzi *et al.*, 2008). Increased apoptotic capacity has also been suggested as an anti-tumour effect of Cetuximab and the main pathways involved in this process were p27KIP/CDK2, NF-kB and Insulin Growth Factor Receptor (IGFR) (Vincenzi *et al.*, 2008). Inhibition of angiogenesis through the decreased production of angiogenesis growth factors such as, Vascular Endothelial Growth Factor (VEGF), Interleukin-8 (IL-8) and basic Fibroblast Growth Factor (bFGF) and inhibition of invasion and metastasis through decreased expression and activity of the Matrix Metalloproteinase 9 (MMP-9) are two other mechanisms of the anti-tumour activity of Cetuximab (Vincenzi *et al.*, 2008).

Food and Drugs Administration (FDA) has approved Cetuximab use for the treatment of *KRAS* WT, EGFR-expressing metastatic colorectal cancer (mCRC) as single agent or in combination with irinotecan-based chemotherapy. Cetuximab is also used for recurrent locoregional and/or metastatic head and neck squamous cell carcinoma (HNSCC) in combination with platinum-based chemotherapy as a first-line treatment.

Unfortunately, treatment response to Cetuximab is limited and with poor outcome in a subset of patients mainly due to the presence of primary or the development of acquired resistance (Bertotti and Sassi, 2015).

1.5.3. Molecular mechanisms controlling Cetuximab resistance

1.5.3.1. Primary resistance

Molecular heterogeneity of CRC is a factor with pivotal role in Cetuximab treatment response and a variety of studies have focused their research identifying the molecular

components that are responsible for primary resistance to Cetuximab treatment. The main mechanisms underlying primary Cetuximab resistance are i) *EGFR* genetic alterations (including mutations and gene copy number), ii) genetic alterations of EGFR downstream effectors and iii) genetic alterations of other RTKs such as ErbB2 and c-MET.

EGFR mutations are not found in CRC while increased *EGFR* copy number has been positively correlated with Cetuximab response. Additionally, increased expression of the EGFR ligands amphiregulin and epiregulin has been positively correlated with response to Cetuximab treatment. However, these biomarkers are not in use for the selection of CRC patients in clinic (Bardelli and Siena, 2010).

Until now the most important biomarker that is clinically used for patient selection in Cetuximab treatment is *KRAS* gene mutational status (Misale *et al.*, 2014). Specifically, the mutational status of *KRAS* gene has been suggested to be the most important mechanism regulating primary Cetuximab resistance since *KRAS* activating mutations in the codon 12 and 13 of exon 2 have been shown to be negative predictors of Cetuximab response (Lièvre *et al.*, 2006, Benvenuti *et al.*, 2007). Additionally, activating mutations in *NRAS* oncogene are found in CRC (De Roock *et al.*, 2010, Vaughn *et al.*, 2011) and have been implicated to primary EGFR-targeted therapy resistance (Misale *et al.*, 2014). However, not all *KRAS* WT patients benefit from Cetuximab treatment and research focused on identifying other molecular biomarkers to explain heterogeneity in Cetuximab treatment response. Genetic alterations and specifically gene amplification of the RTKs ErbB2 (Bertotti *et al.*, 2011, Yonesaka *et al.*, 2011) and c-MET (Inno *et al.*, 2011, Bardelli *et al.*, 2013) have been found to deteriorate Cetuximab response mainly by maintaining MAPK/ERK pathway active.

Beyond *KRAS*, other EGFR downstream signal transducers, which have been implicated to Cetuximab primary resistance, compose of activating mutations in *BRAF* (V600E) and *PIK3CA* (encoding for the PI3K catalytic subunit, p110) genes as well as loss of function mutations in *Phosphatase and Tensin* (*PTEN*) gene. However, no robust statistical correlation with Cetuximab response was observed for these genes yet (Bardelli and Siena, 2010, Sartore-Bianchi *et al.*, 2010, De Roock *et al.*, 2011) (Misale *et al.*, 2014).

1.5.3.2. Acquired Cetuximab resistance

Another important issue implicated in Cetuximab response is the development of acquired Cetuximab resistance after a period of 3-12 months in patients that were initially responsive to treatment (Bardelli *et al.*, 2013). The main mechanisms

implicated in acquired Cetuximab resistance are: i) ErbB2 up-regulation, ii) *Met* amplification, iii) *EGFR* ectodomain mutation acquisition, iv) selection of mutations in the *KRAS* gene or *KRAS* amplification, v) Nuclear EGFR up-regulation and vi) deregulation of EGFR internalisation and degradation.

A recent study described increased signalling through ErbB2 as responsible for development of acquired resistance and in some cases primary resistance of CRC patients. They found that either amplification of *ErbB2* or overexpression of the ERBB3/ERBB4 ligand heregulin are responsible through sustained activation of ERK1/2 (Vlacich and Coffey, 2011).

In a work of Bardelli *et al*., (2013) it was demonstrated that *MET* gene amplification observed in circulating tumour DNA was responsible for acquired and primary Cetuximab resistance in *KRAS* WT metastatic CRC patients (Bardelli *et al.*, 2013). The same group has also recently shown that secondary mutations in *KRAS* gene were a frequent phenomenon in metastatic CRC patients that acquired Cetuximab resistance (Misale *et al.*, 2012). In contrast, another group suggested that Cetuximab acquired resistance caused by *KRAS* activating mutations is due to the existence of expanded *KRAS* mutant subclones within the tumour before treatment initiation (Diaz *et al.*, 2012). It was also found that amplification of the *KRAS* gene even though a rare event could account for Cetuximab resistance in small resistant patient subgroups (Misale *et al.*, 2012, Valtorta *et al.*, 2013).

The acquired *EGFR* ectodomain mutation S492R has been suggested to play an important role in Cetuximab resistance by blocking Cetuximab antibody binding to EGFR receptor (Montagut *et al.*, 2012). In a study using as a NSCLC model of Cetuximab resistance, it was observed that increased levels of nuclear EGFR may represent an additional mechanism underlying Cetuximab resistance (Li *et al.*, 2009). Finally, there is evidence showing that alterations of EGFR internalisation and degradation represent another mechanism of acquired resistance. In particular, it was shown that Cetuximab resistant cell lines presenting higher levels of EGFR compared to their parental cell lines due to reduced association of EGFR with Casitas B-lineage lymphoma protein (Cbl) ubiquitin ligase E3 leading to decreased EGFR degradation (Brand *et al.*, 2011).

1.6. Outstanding questions

Extensive research is still needed to improve survival and life quality of the CRC patient aiming the development of new effective therapeutic strategies.

Targeting metabolism in cancer is a promising therapeutic approach (Tennant *et al.*, 2010). Cancer cells have evolved survival mechanisms like autophagy to overcome metabolic challenges of stressing stimuli of the tumour microenvironment and/or cancer therapeutics (Rabinowitz and White, 2010). Additionally, autophagy has been linked with the regulation of many acquired capabilities of a cancerous cell. This knowledge led to the development of new therapeutic strategies where conventional cancer treatment is combined with autophagy enhancing/inhibiting compounds. Although research in the autophagy field the last decades answered fundamental questions, the role of autophagy in cancer and cancer treatment remains controversial and needs further research in order to revolutionize cancer therapy and improve clinical outcomes. In particular, contrary to the high number of ongoing clinical trials our knowledge in CRC heterogeneity regarding autophagy regulation and function under basal and cancer treatment-induced conditions is still limited. Intensive research in these fields is still needed to ensure beneficial outcome of clinical trials testing the effect of autophagy inhibition in combination with conventional cancer therapy in CRC.

Previous published work from our lab has shown that autophagy inhibition potentiates BCR-ABL tyrosine kinase targeted therapy efficacy in CML cells (Bellodi *et al.*, 2009). This work prompted us to investigate in more detail the role of autophagy in the context of RTK inhibition in epithelial cancers, such as CRC. Specifically in CRC, our knowledge about the role of autophagy upon targeted therapy remains limited. It is known that RTKs could regulate autophagy either directly or indirectly through downstream effectors. PI3K/mTOR pathway residing downstream of RTKs is an established master negative regulator of autophagy induction and *PI3K* activating mutations are frequently present in a variety of cancers including CRC (Samuels *et al.*, 2004). Therefore, an open question remains whether tumours with constantly active PI3K pathway would induce autophagy downstream of RTKs inhibition and whether autophagy inhibition approaches would potentiate RTK inhibition therapy. Although increasing evidence in the autophagy field supports a direct regulation of autophagy via RTKs, our knowledge on whether or how autophagy *vice versa* could control RTK activation is limited.

Most cell biology studies use starvation or inhibition of PI3K/mTOR models for autophagy induction. However, the majority of *in vivo* studies are investigating autophagy inhibition in the absence of specific stimuli (apart from intratumoural/intratissutal stress) and are revealing a differential impact of basal autophagy in cancer progression depending on tumour-type and -mutational status. Therefore, it is important to evaluate the role of basal autophagy in CRC. Recent studies have identified a novel, non-catabolic role of autophagy in regulation of cell signalling albeit the relationship between autophagy and cell signalling in cancer and

specifically in CRC remains elusive and requires further investigation. Characterisation of basal autophagy even in the absence of stressful stimuli like cancer treatment would provide insight on the response to autophagy inhibitors in clinical settings.

1.7. Aims of the project

The main aims of this research are:

1. To investigate the effect of RTK inhibition on autophagy induction and the potential benefit of autophagy suppression in CRC
2. To explore the role of basal autophagy in CRC and its relationship to signalling

Potential impact

By achieving these objectives we will be able to better understand the role of autophagy as part of the metabolic rewiring used by CRC cells to expand and resist stress. This knowledge would not be limited to CRC only, as novel insights into the fundamental mechanism underlying the role and regulation of autophagy in cancer would be uncovered. Finally, this work will potentially inform clinicians on how to rationally design clinical trials based on autophagy inhibitors and RTK targeted therapy.

Chapter 2

Materials and Methods

2. Materials and Methods

2.1. Materials

2.1.1. Cell lines

HCT-116 and DLD-1 *KRAS* WT and G13D isogenic cell lines were kindly provided by Prof. Bert Vogelstein (Johns Hopkins University, USA). SW48 *KRAS* isogenic cell lines were purchased from the Horizon Discovery Company. DiFi cells were kindly provided by Prof. Alberto Bardelli (University of Torino, Italy). CaCo2 cells were in stock in Prof. Daniel Hochhauser's laboratory. HEK 293T and Phoenix A cell lines, which were used for virus production procedures, were available in Prof. Paolo Salomoni's laboratory.

2.1.2. Chemical compounds and drugs

All chemical compounds and drugs were dissolved to the indicated stock concentration and then in cell culture media to reach the final working concentration. Sterile conditions were followed throughout the preparation of all reagents and sterile filtering through a 0.22 μm pore hydrophilic polyethersulfone (PES) membrane was applied when required. Fresh aliquots were used for each independent experiment.

Chloroquine diphosphate salt (CQ) (C6628, Sigma) was dissolved in sterile Phosphate Buffered Saline (PBS) at a stock concentration of 10 mM and was used at a working concentration of 10 μM. Doxycycline hyclate (DOX) powder (D9891, Sigma) was resuspended into sterile H_2O at a stock concentration of 50 mg/ml and was stored protected from light. DOX, which was used for stimulation of shRNA expression in the pLKO-Tet-On inducible CRC cell lines, was used at the optimal working concentration of each CRC cell line (10 ng/ml for HCT-116 and 100 ng/ml for DLD-1, SW48 and CaCo2 cells). Clinical-grade Cetuximab, Gefitinib and Lapatinib were used. Cetuximab (Merck Serono, Germany) was already diluted in a colorless solution for infusion at a stock concentration of 5 mg/ml. All following drugs were dissolved in dimethyl sulfoxide (DMSO) (D2650, Sigma). Clinical-grade Gefitinib (Iressa; AstraZeneca) was used at a concentration of 1 μM and Lapatinib at 2 or 5 μM (Tykerb; GSK). The dual PI3K and mTOR inhibitor, PI103 hydrochloride (2930, R&D systems), was dissolved at a stock concentration of 10 mM and 1 μM was used to assess competence of CRC cells to autophagy induction. The selective AKT inhibitor vIII (124018, Calbiochem) was prepared in a stock concentration of 9 mM. 2 and 5 μM of AKT vIII inhibitor were used to investigate the role of AKT activation in Cetuximab-mediated autophagy induction in

CRC cells. The proteasome activity inhibitor MG132 (C2211, Sigma) was resuspended at a stock concentration of 10 mM and 2.5 µM was used to inhibit proteasome activity in HCT-116 cells. The specific c-MET kinase inhibitor, SGX 523 was kindly provided by Prof. Tony Ng (University College London, UK). SGX 523 was prepared at a stock concentration of 5 mM and 0.5 µM was used to treat HCT-116 cells. In all experiments wherein cells were treated with compounds diluted in DMSO, the corresponding untreated conditions were treated with equal concentrations of DMSO.

EGF (Sigma-Aldrich) and HGF (R&D) ligands were dissolved in accordance to supplier instructions and were used at concentrations of 100 ng/ml and 50 ng/ml, respectively.

For endocytosis studies, Transferrin-555 and the clathrin inhibitor Pitstop2 were kindly provided by Prof. Clare Futter (University College London, UK). Dynamin inhibitor, Dynasore, was a kind gift by Prof. Kerry Chester (University College London, UK).

Iodonitrotetrazolium Chloride (A6248.0001, VWR), which was used at anchorage independent cell growth assay, was kindly provided by Dr Pablo Rodriguez-Viciana (University College London, UK). Iodonitrotetrazolium Chloride was dissolved in sterile PBS at a stock concentration of 8 mg/ml and was used at a final working concentration of 145 µg/ml.

The phosphatase inhibitors Sodium Fluoride (NaF) (201154, Sigma-Aldrich) and Sodium Orthovanadate (Na_3VO_4; S6508, Sigma) were prepared at a stock concentration of 1 M and 100 mM, respectively. The protease inhibitors Pepstatin A (P5318, Sigma), Aprotinin (A6279, Sigma) and Leupeptin (L8511, Sigma) or the protease inhibitor cocktail (11697498001, Roche) were used at corresponding concentrations (See 2.1.6.) to supplement cell lysis buffers.

2.1.3. Plasmids

pGIPZ vectors were purchased from the UCL Cancer Institute, pGIPZ lentiviral shRNA human library. pLKO-Tet-On backbone was purchased from Addgene. pLXSN and pLXSN_myrAKT plasmids were kindly provided by Dr Pablo Rodriguez-Viciana (University College London, UK).

2.1.4. Antibodies

Tables 2.1-2.4 are summarizing all primary and secondary antibodies used in this work. Important information such as supplier name, catalogue number as well as

working concentrations are provided. Anti-Ubiquitin, anti-PP2A, anti-pRb, anti-total IGF-IR beta and anti-HGF antibodies were kindly provided by Prof. Henning Walczak, Dr Pablo Rodriguez-Viciana, Dr Alexander Hergovich, Prof. Bart Vanhaesebroeck and Prof. Adrienne Flanagan (University College London, UK), respectively.

Table 2. 1: Primary antibodies used for western blotting. Antibodies noted as ♯ were diluted into 5% BSA in TBS-T. All other antibodies were diluted into 5% milk in PBS-T.
Note: Anti-LC3B antibody * was discontinued and replaced with the Anti-LC3B antibody from Cell Signalling.

a/a	Primary Antibody	Species	Dilution	Catalogue No	Supplier
1	Anti-LC3B *	Rabbit	1:1000	L7543	Sigma-Aldrich
2	Anti-LC3B	Rabbit	1:1000	2775	Cell Signaling
3	Anti-ATG7	Rabbit	1:500	2631	Cell Signaling
4	Anti-p62	Rabbit	1:1000	BML-PW9860	Enzo Life Sciences
5	Anti-pAKT S473 ♯	Rabbit	1:1000	4060	Cell Signaling
6	Anti-pAKT T308 ♯	Rabbit	1:500	4056	Cell Signaling
7	Anti-Total AKT ♯	Rabbit	1:1000	9272	Cell Signaling
8	Anti-pERK 1/2 T202/ Y204 ♯	Rabbit	1:1000	4370	Cell Signaling
9	Anti-Total ERK 1/2 ♯	Mouse	1:1000	9107	Cell Signaling
10	Anti-Beta actin clone AC-15	Mouse	1:5000-1:10000	A5441	Sigma-Aldrich
11	Anti-pEGFR Y1068 ♯	Rabbit	1:500	2234	Cell Signaling
12	Anti-Total EGFR ♯	Rabbit	1:500-1:1000	2232	Cell Signaling
13	Anti-Calnexin ♯	Rabbit	1:1000	2433	Cell Signaling
14	Anti pSTAT3 Y705 ♯	Rabbit	1:1000	9145	Cell Signaling
15	Anti-Total STAT3 ♯	Rabbit	1:1000	9132	Cell Signaling
16	Anti-Ubiquitin	Rabbit	1:1000	07-375	Millipore
17	Anti-PP2A Catalytic A ♯	Mouse	1:10000	610555	BD Transduction Laboratories
18	Anti-pS6 Ribosomal protein S240/244 ♯	Rabbit	1:1000	2215	Cell Signaling
19	Anti-Total S6 Ribosomal protein ♯	Mouse	1:500	2317	Cell Signaling
20	Anti-pMEK1/2 S217/221 ♯	Rabbit	1:1000	9121	Cell Signaling
21	Anti-Total MEK1/2 ♯	Mouse	1:500	4694	Cell Signaling
22	Anti-p-p38 MAPK T180/ Y182 ♯	Rabbit	1:1000	4511	Cell Signaling
23	Anti-p-AMPK alpha T172 ♯	Rabbit	1:1000	2535	Cell Signaling
24	Anti-Total AMPK alpha ♯	Rabbit	1:1000	5831	Cell Signaling
25	Anti-p-SAPK/JNK T183/ Y185 ♯	Rabbit	1:1000	9251	Cell Signaling
26	Anti-Total-SAPK/JNK ♯	Rabbit	1:1000	9258	Cell Signaling
27	Anti-p-Rb S807/811 ♯	Rabbit	1:500	9308	Cell Signaling
28	Anti-PTEN ♯	Rabbit	1:1000	9552	Cell Signaling
29	Anti-Total IGF-IR beta ♯	Rabbit	1:1000	3027	Cell Signaling
30	Anti-p-c-MET Y1234/1235 ♯	Rabbit	1:1000	3077	Cell Signaling
31	Anti-Total c-MET ♯	Rabbit	1:1000	8198	Cell Signaling
32	Anti-phosphotyrosine clone 4G10 ♯	Mouse	1:500-1:1000	05-321	Millipore
33	Anti-HGF	Rabbit	1:1000	ab83760	Abcam

Table 2. 2: Secondary antibodies used for western blotting.

a/a	Secondary Antibody	Dilution	Catalogue No	Supplier
1	Goat Anti-Rabbit IgG, DyLight 800	1:5000	35571	Thermo Scientific
2	Goat Anti-Mouse IgG, DyLight 680	1:5000	35518	Thermo Scientific
3	ECL Anti-Rabbit IgG, Horseradish Peroxidase linked whole antibody (from donkey)	1:5000	NA934V	GE Healthcare UK Limited
4	ECL Anti-Mouse IgG, Horseradish Peroxidase linked whole antibody (from sheep)	1:5000	NA931V	GE Healthcare UK Limited

Table 2. 3: Antibodies used for immunoprecipitation studies.

a/a	Antibody	Species	Catalogue No	Supplier
1	Anti-pERK 1/2 T202/Y204	Rabbit	4370	Cell Signaling
2	Anti-Total IGF-IR beta	Rabbit	3027	Cell Signaling
3	Anti-p-c-MET Y1234/1235	Rabbit	3077	Cell Signaling
4	Anti-Total c-MET	Rabbit	8198	Cell Signaling
5	Anti-Total EGFR	Rabbit	4267	Cell Signaling
6	Anti-Normal IgG	Rabbit	2729	Cell Signaling

Table 2. 4: Primary and Secondary antibodies used for immunofluorescence studies.

a/a	Primary Antibody	Species	Dilution	Catalogue No	Supplier
1	Anti-LC3B, clone 5F10	Mouse	1:50	0231-100/ LC3-5F10	nanotools
2	Anti-Total c-MET	Rabbit	1:150	8198	Cell Signaling
3	Anti-Total EGFR	Rabbit	1:50	4267	Cell Signaling
a/a	Secondary Antibody	Species	Dilution	Catalogue No	Supplier
1	Anti-Rabbit IgG Alexa Fluor 488	Goat	1:1000	A11008	Life Technologies
2	Anti-Mouse IgG Alexa Fluor 568	Goat	1:1000	A11019	Life Technologies

2.1.5. Oligonucleotides

Polymerase chain Reaction (PCR) primers and pLKO-Tet-On cloning oligos were generated and purchased from Invitrogen. Lyophilized oligos were resuspended in appropriate volume of sterile nuclease free H_2O to yield a stock of 100 µM and were thoroughly mixed by vortexing. PCR primers were further diluted using sterile nuclease free H_2O in a working concentration of 5µM.

Table 2. 5: Primers used for determination of *PIK3CA* and *KRAS* mutational status by sequencing.

a/a	Primer name	Primer Sequence (5' to 3')	PCR amplicon	Tm (°C)	Supplier
1	Forward_PIK3CA_ Exon15-16	ATGATTTACGGCAAGATATGC	794bp	60	Life Technologies
2	Reverse_PIK3CA_ Exon20	TCAGTTCAATGCATGCTGTTT		60	Life Technologies
3	Forward_PIK3CA_ Exon4-5	AAGATCTATGTTCGAACAGGT	694bp	60	Life Technologies
4	Reverse_PIK3CA_ Exon11-10	ACATCTGGGCTACTTCATCTC		60	Life Technologies
5	Forward_KRAS_ Exon1-2	AGGCCTGCTGAAAATGACTGAA	220bp	62.1	Life Technologies
6	Reverse_KRAS_ Exon3	GGTCCCTCATTGCACTGTACTCC		62.1	Life Technologies

Table 2. 6: Single-stranded oligos used to develop the desired shRNA duplex sequence, which was cloned into the pLKO-Tet-On vector

a/a	Oligos name	Oligos Sequence (5' to 3')
1	Forward shEGFP	CCGGTCCGCAAGCTGACCCTGAAGTTCTTCAAGAGAGAACTTCAGGGTCAGCTTGCTTTTTG
2	Reverse shEGFP	AATTCAAAAAGCAAGCTGACCCTGAAGTTCTCTCTTGAAGAACTTCAGGGTCAGCTTGCGGA
3	Forward shATG7 E8	CCGGTCCCCCAGTTCAGAGCTAAATAATATTCAAGAGATATTATTTAGCTCTGAACTGGGTTTTTG
4	Reverse shATG7 E8	AATTCAAAAACCCAGTTCAGAGCTAAATAATATCTCTTGAATATTATTTAGCTCTGAACTGGGGGA
5	Forward shATG7 G7	CCGGTCCACCTCTCTATGAGTTTGAAGATTTCAAGAGAATCTTCAAACTCATAGAGAGGTTTTTTG
6	Reverse shATG7 G7	AATTCAAAAAACCTCTCTATGAGTTTGAAGATTCTCTTGAAATCTTCAAACTCATAGAGAGGTGGA
7	Forward shATG7 F12	CCGGTCCCGCCCACAGCATCATCTTCGAATTCAAGAGATTCGAAGATGATGCTGTGGGCGTTTTTG
8	Reverse shATG7 F12	AATTCAAAAACGCCCACAGCATCATCTTCGAATCTCTTGAATTCGAAGATGATGCTGTGGGCGGGA

2.1.6. Buffer Recipes

2X HEPES Buffer, pH 7.05: 280 mM NaCl; 10 mM KCl; 1.5 mM Na_2HPO_4; 12 mM D(+)-Glucose Monohydrate and 50 mM HEPES.

5X Polyethylene glycol (PEG), pH 7.2: 50 mM PEG; 0.41 M NaCl and 0.2% Tris 1 M, pH 7.5.

10X annealing Buffer: 1 M NaCl and 100 mM Tris-HCl pH 7.4.

RIPA Lysis Buffer: 20 mM Tris pH 7.4; 150 mM NaCl; 1 mM EDTA pH 8; 1 mM EGTA pH 8; 0.5% (w/v) Sodium Deoxycholate; 0.1% (v/v) sodium dodecyl sulfate (SDS); 1%

(v/v) Nonidet P-40. Prior cell lysis 1X protease inhibitors cocktail and 1 mM Na_3VO_4 and 50 mM NaF of the phosphatase inhibitors were added.

Non-denaturing Lysis Buffer: 20 mM Tris pH 7.4; 137 mM NaCl; 2 mM EDTA pH 8; 1% (v/v) Nonidet P-40. Prior cell lysis 10 µg/ml of each protease inhibitor: i) Aprotinin, ii) Pepstatin A and iii) Leupeptin as well as 1 mM Na_3VO_4 and 50 mM NaF of the phosphatase inhibitors were added.

Protein Loading Buffer (5X Laemmli sample buffer): 10% (w/v) SDS; 50% (w/v) glycerol; 0.125% (w/v) bromophenol blue; 250 mM Tris pH 6.8; 2 mM 2-mercaptoethanol.

1X Running Buffer: 0.186M Glycine; 0.02 M Trisma Base and 0.15% (v/v) SDS.

1X Transfer Buffer: 0.186M Glycine; 0.02 M Trisma Base and 20% (v/v) Methanol.

PBS-T: 1X PBS pH 7.4 supplemented with 0.1% (v/v) Tween 20.

TBS-T: 1X TBS pH 7.4 (19.8 mM Trisma Base; 0.13 M NaCl; 0.05% (v/v) HCl) supplemented with 0.1% (v/v) Tween 20.

Tris-Acetate-EDTA Buffer (TAE 1X): 40 mM Trisma Base; 0.001% (v/v) Acetic acid; 1 mM EDTA pH 8.

5X DNA Loading Buffer: 100 mM Tris pH 8; 10 mM EDTA pH 8; 50% Glycerol and 0.5%w/v bromophenol blue.

2.2. Methods

2.2.1. Cell Culture

2.2.1.1.Cell line maintenance and cryopreservation

Eight different CRC cell lines were used and maintained in culture. Human colorectal carcinoma cell lines, HCT-116, DLD-1 and SW48 as well as their *KRAS* mutant isogenic versions were maintained in McCoy's 5A medium containing 2 mM L-Glutamine. The human colorectal carcinoma cell line, CaCo2, was maintained in Minimum Essential Medium (MEM) medium containing 2 mM L-Glutamine. The human rectal carcinoma cell line, DiFi, was maintained in Ham's F12 Nutrient mixture medium containing 1 mM L-Glutamine. The human embryonic kidney cell line HEK-293T (expresses the large T antigen from SV40 virus), which was used for lentiviral production, was maintained in Dulbecco's Modified Eagle's Medium (DMEM)

supplemented with 4.5 g/L D-Glucose and Sodium Pyruvate. The human embryonic kidney cell line, Phoenix A, which was used for retrovirus production, was maintained in Iscove's Modified Dulbecco's Medium (IMDM) containing 4.5 g/L D-Glucose and Sodium Pyruvate. All cell culture media were supplemented with 10% Fetal Bovine Serum (FBS, Life Technologies), and 1% Penicillin/Streptomycin (Gibco).

All inducible pLKO-Tet-On shRNA-expressing (shEGFP, shATG7-E8, -G7 and -F12) stable cell lines were maintained in corresponding medium supplemented with 10% Tet-Free Certified FBS (Life Technologies, 16000-044, Lot number 1221032) in the presence of puromycin selection (0.25 µg/ml for SW48, 0.5 µg/ml for HCT-116, 1.5 µg/ml for DiFi, 3 µg/ml for DLD-1 and 1.5 µg/ml for CaCo2 cells). DiFi LXSN and LXSN_myrAKT-expressing cells were cultured in the corresponding medium in the presence of neomycin selection (750 µg/ml). All experiments were conducted in the absence of either puromycin or neomycin selection.

Cells were cultured in tissue culture dishes at 37^{o}C in a humidified atmosphere of 5% CO_2. Cell culture procedures were carried out in sterile conditions in Class II biological safety cabinets. Cells were cultured until 80-90% confluence was reached and then were passaged to new culture dishes (every 2-3 days). Briefly, adhered cells were washed once with appropriate volume of sterile PBS, dependent on size of tissue culture dishes. PBS was removed and followed incubation with 1X Trypsin (Gibco) at 37^{o}C for 1-3 mins. Trypsin was used for efficient cell detachment of tissue culture dishes and neighboring cells. Adding cell culture medium deactivated trypsin and cells were pelleted down by centrifugation at 1200 rpm for 5 mins. Trypsin-containing cell culture medium was removed and replaced by fresh medium to resuspend cell pellet. Appropriate numbers of cells were replated to new tissue culture dishes for cell culture maintenance and/or experimental procedures. Cell number counting and cell viability examination was conducted using the Beckman coulter Vi-Cell XR machine and software. Optimization experiments were performed for each independent cell line in order to evaluate correct cell number plating for maximum cell viability. The maximum cell passage reached in culture was 20 wherein fresh cell cultures were set up.

Cryopreservation of cell lines was conducted by long-term storage in liquid nitrogen containers. Exponentially growing cells were trypsinised and pelleted down as previously described. Cell pellets were resuspended in freezing medium (45% corresponding medium for each cell line supplemented with 45% FBS and 10% DMSO) transferred in cryovials and were short-term stored in -80^{o}C to allow gradual decrease of temperature until their long-term storage in liquid nitrogen. For retrieval of frozen cell stocks from liquid nitrogen, cryovials were quickly thawed by incubation at 37^{o}C waterbath and cell suspensions were supplemented with 6 ml of fresh cell culture medium. Cells were pelleted down by centrifugation at 1200 rpm for 5 mins to remove

traces of DMSO. Cell pellets were resuspended in fresh cell culture medium and plated in appropriate tissue culture dishes.

2.2.1.2. Transient transfection for small interfering RNAs (siRNAs) delivery

RNA interference (RNAi) technology was used to knock down *EGFR* and *LC3B* gene expression. siRNAs sequences were received as lyophilized powders and dissolved in RNAse free H_2O at a stock concentration of 50 μM. Intermediate dilutions in RNAse free H_2O were applied to yield working concentrations.

Two different transfection reagents were used for the delivery of EGFR and LC3B siRNAs to CRC cell lines. SMARTpool: ON-TARGETplus EGFR siRNA (L-003114-00, Thermo Scientific) and siRNA negative control (Scramble, Thermo Scientific) were used in a concentration of 25 nM and/or 50 nM using DharmaFECT reagent 1 (T-2001-02, GE Dharmacon) in HCT-116 and DLD-1 cell lines. Silencer select LC3B siRNA (s37749 and s224886, Life Technologies) and negative control (Scramble, 4390843, Life Technologies) were used in a concentration of 10 nM using Lipofectamine RNAiMAX reagent (13778075, Thermo Scientific) in HCT-116 cells. Both DharmaFECT and Lipofectamine RNAiMAX transfection reagents are cationic liposome formulations that make complexes with siRNAs and allow efficient delivery of siRNAs into the cell through the cell membrane barrier.

Forward transfection protocol was followed with both transfection reagents. One day prior transfection, 1.0 - 1.5 x 10^5 cells were plated in 6-well tissue culture dishes and let to adhere overnight at 37^{o}C. The following day, cells were transfected according to the protocol of each manufacturer. Briefly, appropriate volume of each transfection reagent and siRNA was diluted in separate tubes containing Opti-MEM I reduced serum medium without serum. The diluted Opti-MEM siRNAs were combined with Opti-MEM containing the corresponding transfection reagent and let to incubate at room temperature for 20 mins. The transfection reagent-siRNA mixture was added dropwise to each corresponding well containing cells and let to incubate at 37^{o}C. Transfection medium was replaced with fresh complete medium after 24 hours. Cells were harvested 48 and/or 72 hours post-transfection by scraping. Protein knock down was assessed using western blotting (See 2.2.2.3.).

For examination of protein knock down by immunofluorescence (IF) (See 2.2.4.1.), the same experimental conditions were followed but cell number, volume of siRNAs and volume of transfection reagents were proportionally adjusted to the relative surface area of a 24-well tissue culture dish.

2.2.1.3. Calcium Phosphate transfection for virus particle production

The calcium phosphate transfection method was used to generate lenti- and retro-virus particles by transfecting HEK 293T and Phoenix A cells with the corresponding plasmids. Calcium phosphate transfection method is based on the generation of precipitates through the interaction of the negative charged phosphate groups contained in the HEPES buffer with the positive charged calcium groups in the calcium chloride solution. DNA is bound in the surface of these precipitates and in that way inserts the cell (Kingston *et al.*, 2001).

Lentivirus Particle Generation

Lentivirus particle production was employed for generation of stable CRC cell lines by viral transduction approaches (See 2.2.1.5.). 6 x 10^6 HEK 293T cells were plated in 15 cm dishes (two different dishes were combined for each different virus generation) containing 20 ml complete DMEM medium and were let to adhere overnight at 37^{o}C. The following day the calcium phosphate transfection approach was followed to perform a triple co-transfection of HEK 293T cells with lentivirus packaging vectors (pCMV-VSV-G and pCMV-HIV-1) and desired plasmid DNA. Briefly, 7.2 µg of pCMV-VSV-G (expressing VSV-G envelope gene), 15.6 µg pCMV-HIV-1 (expressing Gag, Pol, Rev and Tat genes) vectors along with 24 µg of shRNA encoding lentivirus vector (i.e. pLKO-Tet-On shATG7, pLKO-Tet-On shEGFP or pGIPZ) were diluted in sterile nuclease free H_2O containing 10% (v/v) 2.5 M calcium chloride to a final volume of 1 ml. The DNA-calcium chloride mixture was thoroughly mixed and allowed to equilibrate at room temperature for 30 mins. 37^{o}C pre-warmed 2X HEPES buffer (See 2.1.6.) was added to the DNA-calcium chloride solution in a ratio 1:1 and the mixture was thoroughly mixed for 1 min. DNA-calcium chloride-HEPES mixture was added dropwise to each 15 cm dish containing HEK 293T cells. Transfection medium was replaced with normal culture medium after 8 hours. Transfected HEK 293T cells were let to incubate for additional 48 hours when supernatants containing lentiviral particles collected. Viral particles concentration by PEG precipitation was followed.

Retrovirus Particle Generation

Retrovirus particle production was employed for generation of stable DiFi cell lines expressing myristoylated AKT by viral transduction approaches (See 2.2.1.5.). 2.5 x 10^6 Phoenix A cells were plated in 10 cm dishes (four different dishes were combined

for each different virus generation) containing 10 ml complete IMDM medium and were let to adhere overnight at 37^{o}C. The following day the calcium phosphate transfection approach was followed to co-transfect Phoenix A cells with 1.2 µg SARAIII retrovirus packaging vector and 20 µg desired plasmid DNA (i.e. pLXSN or pLXSN_myrAKT). DNA was diluted in sterile nuclease free H_2O containing 25% (v/v) 1 M calcium chloride to a final volume of 1 ml. The DNA-calcium chloride mixture was thoroughly mixed and allowed to equilibrate at room temperature for 30 mins. 37^{o}C pre-warmed 2X HEPES buffer was added to the DNA-calcium chloride solution in a ratio 1:1 and the mixture was thoroughly mixed for 1 min. DNA-calcium chloride-HEPES mixture was added dropwise to each 10 cm dish containing Phoenix A cells. Transfection medium was replaced with normal culture medium after 8 hours. Transfected Phoenix A cells were let to incubate for additional 36 hours when supernatants containing retrovirus particles collected and virus particle concentration by PEG precipitation was followed.

Virus Particle Concentration by PEG Precipitation

Supernatants containing lenti- or retro- virus particles were centrifuged at 3000 g for 15 mins to eliminate cells and cellular debris. Further cellular debris elimination was achieved by 0.45 µm PVDF filtration of the supernatant. 5X PEG solution (See 2.1.6.) was added to the supernatant containing the viral particles in a volume ratio 1:4 to concentrate the virus particles. Solution was refrigerated at 4^{o}C overnight. The next day the concentrated virus particles were pelleted down through centrifugation at 1500 g for 30 mins and PEG containing medium was discarded. Virus particle pellets were resuspended in sterile cold PBS in a volume ratio 50:1 and were aliquoted and stored at -80^{o}C. Fresh concentrated virus particles aliquots were used in each independent viral transduction experiment.

2.2.1.4. Virus tittering by antibiotic selection

For virus tittering, 1.0 x 10^5 HCT-116 cells were plated in 6-well plates and incubated overnight at 37^{o}C. Cell culture medium was replaced by medium supplemented with 5 µg/ml polybrene to enhance absorption and transduction of the virus particles. Cells were transduced by different serial dilutions of the virus particles. Two untransduced control wells were included. Transduced cells were let to incubate overnight at 37^{o}C and followed replacement of the virus-containing medium with fresh

medium. Cells were incubated for additional 24 hours at 37^{o}C to allow for sufficient expression of the antibiotic resistance gene in the transduced cells prior antibiotic selection. The following day, cell culture medium supplemented with appropriate volume of antibiotic was added in all viral transduced wells including one untransduced control well, named “mock-transduced”. Cell viability was assessed daily in the “mock-transduced” well by light microscopy. Antibiotic-containing medium was replaced every 48 hours and antibiotic selection was conducted as long as all cells in the “mock-transduced” well were eliminated. Followed quantitative assessment of virus titter by trypsinising and counting cells in each different viral transduced well. Percentage (%) of infectivity was expressed as number of cells in each of virally transduced wells divided by the number of cells in the positive control well (“no transduced/no antibiotic”) multiplied with 100. Multiplicity of infection (MOI) of 1 considered as equal to 50% of infectivity.

2.2.1.5. Viral Transduction of CRC cell lines

Viral transduction method was used to generate stable (pGIPZ) and inducible-expressing (pLKO-Tet-On) shRNA CRC cell lines as well as myristoylated AKT-expressing (pLXSN) DiFi cells. 1.0 x 10^5 of each cell line was plated in 6-well plates and let to incubate overnight at 37^{o}C. Cells were transduced with the appropriate volume of each virus based on virus tittering at an MOI of 10 in media containing 5 μg/ml polybrene. Selection of transduced cell populations was performed using TurboGFP expression sorting for pGIPZ shRNA-expressing cells; puromycine selection for pLKO-Tet-On-shRNA expressing cells and neomycin selection for LXSN_myrAKT and control cells. Subsection 2.2.1.1. annotates the specific concentration of puromycin and neomycin was used for each CRC cell line. Of note, for generation of pLKO-Tet-On CRC cell lines all transduction steps were performed by using medium containing 10% (v/v) Tetracycline-Free Certified FBS in order to avoid stimulation of shRNA expression by traces of tetracycline contained in the regular FBS.

2.2.2. Biochemistry

2.2.2.1. Total cell protein extraction

2.5 - 4 x 10^5 of CRC cells (depending on each CRC cell line) were plated in 6 cm tissue culture dishes and let to adhere for approximately 48 hours at 37^{o}C until

approximately 70% of confluence was reached. Drug treatment was applied under sterile conditions for the indicated incubation time and total cell protein extraction followed. Cell culture medium was removed and adhered cells were washed once with PBS. 100 - 150 µl of RIPA Lysis Buffer or Non-Denaturing Lysis Buffer supplemented with protease and phosphatase inhibitors was added to the cells on ice. Cell scraping was used to harvest cells from the culture dishes and cell lysates were transferred to microcentrifuge tubes. Cell lysates were incubated on ice for 30 mins and then centrifuged at 13200 rpm for 15 mins at 4^{o}C. Supernatants containing total cell protein extracts were transferred to new microcentrifuge tubes and kept on ice as long as the total cell protein concentration of extracts was quantified (See 2.2.2.2.). Following total cell protein concentration quantification, 5X protein loading buffer was added to cell lysates in a ratio 1:4 in order to yield a final concentration of 1X protein loading buffer to the cell extracts. Total cell extracts were boiled at 95^{o}C for 5 mins and then were stored at -20^{o}C until further use.

2.2.2.2. Determination of total cell protein concentration

For total cell protein concentration determination the BCA protein assay kit (23227, Pierce) or Bradford assay (500-0006, BioRad) were used dependent on the Lysis Buffer used. For RIPA Lysis Buffer only the BCA protein assay kit was performed being compatible with SDS content. Both assays were conducted according to instructions of the manufacturer. A standard linear curve, which was designed by using known concentrations (0.5 - 10 µg/µl) of BSA, was employed for quantification of undetermined protein concentration of total cell extracts. Optical Density (O.D.) was measured in a spectrophotometer at 562 nm and 595 nm for BCA protein assay kit and Bradford assay, respectively.

2.2.2.3. Western Blotting

Equal concentration of total cell extracts (30 - 50 µg) were separated in 8%, 10%, 15% SDS-polyacrylamide gel electrophoresis (SDS-PAGE) and Criterion™ TGX Stain-Free™ Precast Gels as required and transferred for $2^{1/2}$ hours onto nitrocellulose membrane in a wet blotter. 1X Running Buffer was used for protein electrophoresis and 1X Transfer Buffer was used for protein transfer (See 2.1.6.). Efficiency of protein transfer onto nitrocellulose membranes was examined by shortly incubating membranes in Ponceau S (Sigma) solution that reversibly removed by PBS-T or TBS-

T washes. Nitrocellulose membranes were blocked in 5% BSA (w/v) TBS-T for phosphorylated studies and in 5% milk (w/v) PBS-T for all other studies with 1 hour incubation time. Immunodetection performed by incubating the membranes with different primary antibodies (Table 2. 1) overnight at 4^{o}C. After 3 washes in TBS-T (phosphorylated proteins detection) or PBS-T, membranes were incubated with a secondary antibody conjugated with horseradish peroxidase (HRP) or fluorescent dye diluted in 5% milk (w/v) PBS-T (Table 2. 2) for 1 hour. Protein expression was detected on medical X-Ray films (Fujifilm) using the Enhanced Chemiluminescence System (ECL) when HRP-conjugated secondary antibodies used. The LI-COR Odyssey Imaging System scanner was used for detection of protein expression when fluorescent dye-conjugated secondary antibodies were used.

2.2.2.4. Densitometric Analysis

LI-COR Odyssey software or Fiji (Image-J) software was used for densitometric analysis of protein bands detected either via LI-COR Odyssey Imaging System scanner or ECL, respectively. For both densitometric methods, the protein bands of interest were selected in high quality (minimum 300 dpi) images and background intensity was subtracted.

2.2.2.5. Phospho-RTK array

The human phospho-RTK array (ARY001B, R&D) was used for the determination of changes in phosphorylation of RTKs between autophagy-proficient and -compromised samples. The Phospho-RTK array includes nitrocellulose membranes whereby mouse antibodies from 49 different RTKs and control antibodies are previously captured. The array was conducted with the specific reagents provided and based on the instructions of the manufacturer. Briefly, 1.5 - 2 x 10^{6} autophagy-proficient or -compromised cells (depending on the cell line used) were plated in 10 cm tissue culture dishes at day 3 of DOX treatment and let to adhere for another 48 hours at 37^{o}C in the presence of DOX. Then cells were lysed using Lysis Buffer 17 supplemented with protease and phosphatase inhibitors and protein quantification of total cell extracts was conducted using Bradford assay (See 2.2.2.2.). 1500 µg of total cell extracts was diluted into array buffer 1 to reach a volume of 1.5 ml and samples of each autophagy-proficient or -compromised condition were applied onto the nitrocellulose membrane with the RTK-captured antibodies. Followed overnight

incubation at 4^{o}C on a rocking platform shaker and the next day nitrocellulose membranes were washed and incubated with a pan anti-phospho-tyrosine antibody conjugated to HRP in a dilution 1:5000 for 2 hours at room temperature. The phosphorylated tyrosines on RTKs were detected by chemilluminescence using X-ray Films and multiple exposure times (20 secs - 10 mins) were used to detect the majority of RTKs. Nitrocellulose membranes incubated with autophagy-proficient or -compromised lysates were placed into the same autoradiography cassette and developed concomitantly to allow comparison between conditions. For densitometric analysis of phospho-RTK array results, X-ray films were scanned in high resolution (1200 dpi) and the GS-800 Calibrated Densitometer (BioRad) was used to quantify the intensity of each independent RTK spot. Numerical results were analysed by determining the average signal (pixel intensity) of the pair of duplicate spots presenting each RTK and followed by subtraction of an averaged background signal for each RTK independently. Differences in RTK phosphorylation were determined by comparing phosphorylation of RTKs between autophagy-proficient and -compromised cells.

2.2.2.6. Immunoprecipitation (IP)

Preparation of protein A Sepharose beads slurry

Protein A Sepharose beads (71-7090-00AF, GE Healthcare) were supplied lyophilized and 50 ml of distilled H_2O was used to hydrate them with overnight incubation at 4^{o}C by rolling. Beads were pelleted down by centrifugation at 450 g for 5 mins at 4^{o}C and the supernatant was removed by aspiration. Followed two washes in 50 ml of distilled H_2O and 3 washes in sterile 1X PBS with intermediate centrifugations as described above for pelleting down the beads. Hydrated protein A Sepharose beads were diluted in a ratio 1:2 into sterile 1X PBS solution containing 25% (v/v) Ethanol and Sodium Azide. The stock solution containing beads was stored at 4^{o}C until further use.

Coupling of Antibodies to Protein A Sepharose

Antibodies used in IP studies (Table 2. 3) were firstly coupled to protein A Sepharose beads. Briefly, the Sepharose protein A slurry was gently mixed by vortexing and 10 µl of beads were washed twice with non-denaturing lysis buffer by intermediate centrifugations of 20 secs at 13200 rpm to remove the excess of the slurry solution containing ethanol. Followed coupling of beads with the required

volume of antibody in 300 µl of non-denaturing lysis buffer via rotation at 4°C for 4 hours. Preceding IP, antibody-Sepharose A coupled beads were washed 4 times in non-denaturing lysis buffer containing protease and phosphatase inhibitors with intermediate centrifugation steps as abovementioned.

IP

IP was performed via incubating 500 - 1000 µg of total cell protein extracts (into non-denaturing lysis buffer containing phosphatase and protease inhibitors; 0.5% (v/v) Nonidet P-40 instead of 1% (v/v) was used in non-denaturing lysis buffer for c-MET/p-c-MET and LC3B co-immunoprecipitation experiments) with 10 µl antibody-Sepharose A coupled beads in a total volume of 1000 µl with rotating for 3 hours at 4°C. Then beads were washed 4 times with 1000 µl non-denaturing lysis buffer containing phosphatase and protease inhibitors followed by centrifugation for 20 sec at 13200 rpm. The pellet was resuspended in 50 µl of 1X protein loading buffer, incubated at 95°C for 5 mins and centrifuged at 13200 rpm for 1 min. The supernatant containing the immunoprecipitated proteins was then analysed using western blotting (See 2.2.2.3.).

2.2.3. Functional Assays

2.2.3.1. Sulforhodamine B (SRB) Cell Proliferation / Survival assay

Using the Sulforhodamine B (SRB) colorimetric assay, cell proliferation/survival was assessed upon normal conditions and drug treatments. SRB assay is used for cell density determination by measuring cellular protein content. SRB binds through its sulfonic groups to basic amino acids under acidic condition and it releases from them under basic conditions. The amount of dye released from the cells is proportional to the cell number (Vichai and Kirtikara, 2006).

3000 cells / 200 µl of medium were seeded in each well of flat 96-well plates. 48 hours post-seeding cells were treated with Cetuximab (0, 0.01, 0.1, 1, 5, 10, 50, 100 µg/ml) or Cetuximab (0, 10, 50 and 100 µg/ml) -/+ 10 µM CQ, depending on the experiment. A separate control plate that has been seeded with the same number of cells was fixed before treatment and considered as the “day 0” control. The control plate was stored at room temperature and processed along with the experimental plates. Cetuximab/Cetuximab along with CQ-treated cells were incubated for 87 hours at 37°C. Cell proliferation in autophagy-proficient and -compromised HCT-116 *KRAS*

WT and G13D cells was assessed by plating 2000 - 3000 cells / 200µl of medium in each well of 96-well plates and cell density measured every day for 10 days. Briefly, media was aspirated from the wells and cells fixed in 10% (w/v) of Trichloroacetic acid for 20 mins at 4^{o}C. Cells stained in 0.4% (w/v) SRB solution for 20 mins at room temperature. Traces of the unbound dye were removed by washing cells 5 times with 1% (w/v) Trichloroacetic acid and the plates air-dried overnight. The dye was solubilized with 10 mM Tris base (pH 10.5) for 30 mins at room temperature and absorbance was measured at 540 nm.

2.2.3.2. Anchorage-independent cell growth Assay

Anchorage independent cell growth assay was used to examine differences in cell growth of HCT-116 *KRAS* WT cells in autophagy-proficient and -compromised conditions. Briefly, 6% (w/v) low melting point agarose (16520, Invitrogen) was prepared in distilled H_2O and mixture was autoclaved. The following day, 6% agarose was solubilized via microwaving until uniformly in solution and was diluted in cell culture medium to reach a concentration of 2%. 2% agarose was thoroughly mixed by pipetting and was further diluted in cell culture medium to reach a concentration of 0.6%. The remaining 2% agarose was kept at 40^{o}C waterbath for use in later steps of the procedure. 2 ml of 0.6% agarose was plated in 6-well culture dishes and let to polymerase at room temperature to create the agarose bottom layer. In the meantime, cells were trypsinised, counted (See 2.2.1.1.) and 2000 cells were transferred to tubes containing the appropriate volume of medium to further dilute 2% agarose in a concentration of 0.35%. 2 ml of 0.35% agarose containing cells was placed onto the 0.6% agarose bottom layer. The top layer of agarose containing cells was shortly incubated at room temperature to enable polymerization and then placed at 37^{o}C in a humidified atmosphere of 5% CO_2 incubator. The next day, 2 ml of medium was added on top of the 0.35% agarose layer and followed regular medium changes every 3 days for a duration of 21 days. For visualisation of cell colonies 145 µg/ml of Iodonitrotetrazolium Chloride dye was added in each well and cells let to incubate for another 24 hours at 37^{o}C. Images were acquired using the Image Quant LAS 4000 machine and automatic quantification of cell colonies was conducted by using the ImageQuant software by following instructions of the manufacturer.

2.2.3.3. Cell Migration/Invasion Assay

Cell migration and invasion assays were performed using BD Falcon™ cell culture inserts and BD BioCoat™ Matrigel™ Invasion Chambers (BD Biosciences, 353097, 354480), respectively. 5 x 10^4 cells in cell culture medium not containing FBS were seeded at migration or invasion chambers of a 24-well plate and allowed to migrate or invade for 60 hours through 8-micron pore Polyethylene Terephthalate (PET) membrane or 8-micron pore PET membrane coated with matrigel, respectively. As a chemoattractant, cell culture medium containing 10% FBS was used at the bottom of each well. Untreated and 10 μM CQ-treated conditions were included. Non-migrated and non-invaded cells were removed from the top of the PET membranes by gently cleaning with cotton swabs. Migrated and invaded cells fixed in 100% methanol for 2 mins and stained with 1:5000 Hoescht/PBS for 30 mins at room temperature. Inserts kept in PBS at 4^{o}C. To quantitate migratory or invasive cells, the surface of each well was photographed under inverted fluorescence microscope at 10X magnification. The total number of cells per condition was counted by using the Cell profiler program. Invasion was calculated by dividing the number of cells that invaded through the matrigel insert membrane with the number of cells that migrated through the control insert membranes (For schematic representation of the procedure see Figure 4. 28). Histograms represent the average ±Standard Deviation (SD) of three independent experiments.

2.2.3.4. Determination of Proteasome activity

Proteasome-Glo assay (G8660, Promega) was used for determination of proteasome activity of CRC cells based on the instructions of the manufacturer. Briefly, 6 x1 0^3 HCT-116 *KRAS* WT and G13D cells were plated in white-walled 96-well plates, containing 100 μl of cell culture medium and let to adhere overnight at 37^{o}C. The next day cells were treated with appropriate compounds for the indicated timepoints based on each experiment. For proteasome activity dose response, HCT-116 *KRAS* WT cells were treated with serial dilutions of the proteasome inhibitor MG132 (0.01, 0.05, 0.1, 0.25, 0.5, 1 and 2.5 μM) for 6 hours. For determination of proteasome activity between autophagy-proficient and -compromised conditions, HCT-116 cells (5 days in the presence of DOX) were treated with 10 μM CQ or 2.5 μM MG132 for 6 hours to pharmacologically inhibit autophagy or proteasome activity, respectively. After drug treatment cells were equilibrated at room temperature for approximately 10 mins and the Proteasome-Glo Cell-Based Reagent was added to each corresponding well in a ratio 1:1. Plates were kept on dark and the content of the

wells were mixed by shaking at 700 rpm for 2 mins. Followed an additional incubation for 10 mins at room temperature and luminescence of each sample was measured in a Varioskan Flash plate-reader.

2.2.4. Microscopy

2.2.4.1. Immunofluorescence (IF)

6 x 10^4 HCT-116 *KRAS* WT cells were plated on sterile glass coverslips in 24-well plates and let to adhere for 48 hours at 37^{o}C. Cells were either untreated or treated with 10 µM CQ for 6 hours or stimulated with 50 ng/ml hrHGF for 3 hours (on ice) -/+ 10 µM CQ. Cells were fixed with 100% methanol for 15 mins in -20^{o}C and followed three washes in 1X PBS for 5 mins each. Fixed cells were blocked in blocking buffer (5% goat serum in PBS - 0.3%Triton-X100) for 1 hour at room temperature and were stained with primary antibody (Table 2. 4) overnight at 4^{o}C. After primary antibody incubation, cells were washed 3 times with PBS-T to remove traces for unspecifically bound antibody and followed incubation in dark with secondary fluorescent-conjugated antibodies (Table 2. 4) at room temperature for 1 hour. Traces of secondary antibody were removed by washing 3 times with PBS-T. Nuclear staining was performed via incubating cells with Hoechst dye in a dilution 1:5000 in PBS for 30 mins. Coverslips were mounted on microscope slides, let to dry and stored at 4^{o}C. Images were acquired using a Zeiss epifluorescence microscope or a Zeiss LSM 700 confocal microscope using x63 objective/1.4 numerical aperture. Z-stack images thickness was set to 0.4 µm and images in each experiment were acquired at same settings and exposure times. Post-acquisition brightness adjustments were identical between images of the same experiment and performed in Fiji software. Quantification of intracellular c-MET was performed by manually specifying the intracellular region of interest (ROI) of every cell in a single z-stack image using Fiji software. Plasma membrane staining was excluded from quantification analysis. Colocalisation analysis was performed via using Image J plugin JaCoP enabling manual adjustment of threshold of single channel z-stack images to eliminate background staining. Manders' coefficients were used for evaluation of colocalising fractions. Autophagosomes/cell were calculated automatically by using Imaris software. A manual adjustment of threshold of single channel z-stack images to eliminate background staining was performed identically to images from the same experiment.

2.2.4.2. Transferrin Internalisation Assay

Transferrin internalisation assay was employed to assess differences in endocytosis between autophagy-proficient and -compromised HCT-116 *KRAS* WT cells. 7 x 10^4 HCT-116 cells (3 days in the presence of DOX) were plated on sterile glass coverslips into 24-well plates containing 1 ml medium supplemented with DOX and let to adhere for 48 hours at 37^{o}C. Then medium was removed and replaced with 300 µl fresh medium not containing FBS (FBS high in transferrin) supplemented with 0.5% BSA and DOX. Cells were incubated at 37^{o}C in the absence of FBS for 4 hours and followed treatment with or without the endocytosis inhibitors Pitstop2 (10 or 20 µM) and Dynasore (80 µM) for 100 mins at 37^{o}C. Cells were placed on ice for 5 mins and Transferrin-555 was added to the corresponding conditions. Followed short incubation at 37^{o}C for 15 mins to let transferrin get endocytosed and cells were fixed using 4% Formaldehyde for 15 mins at room temperature. Formaldehyde traces were removed by washing 3 times with 1X PBS and cells were permeabilised in 0.1% (w/v) Saponin (S4521, Sigma) in 1X PBS for 15 mins. Nuclear staining was performed via incubating cells with Hoechst dye in a dilution 1:5000 in PBS for 30 mins. Coverslips were mounted on microscope slides, let to dry and stored at 4^{o}C. Images were acquired using a Zeiss LSM 700 confocal microscope as described above.

2.2.5. Molecular Biology

2.2.5.1. RNA Extraction

2 x 10^6 CRC cells were harvested by trypsinisation, pelleted down and subjected to RNA extraction by using the RNeasy Plus Mini Kit (74134, Qiagen). The procedure conducted based on the instructions of the manufacturer. Briefly, cells were lysed in the appropriate volume of RLT Plus buffer containing 1% (v/v) β-mercaptoethanol and cell lysates were homogenized by vortexing for 30 secs. Homogenized lysates were transferred to gDNA eliminator spin columns and followed centrifugation at 10000 rpm for 30 secs to eliminate genomic DNA from lysates. One volume of 70% (v/v) ethanol was added to the flow-through to enable binding conditions of RNA and samples were transferred to an RNeasy mini spin column. Total RNA (longer than 200 nucleotides) bound to the RNeasy spin column membrane was washed twice using RPE buffer and RNA was eluted in 30 µl RNase-free H_2O.

2.2.5.2. Reverse-Transcription PCR

The high capacity cDNA reverse transcription kit (4368814, Thermo Fisher Scientific) was used to retrotranscribe 1 µg of RNA isolated from CRC cells based on the instructions of the manufacturer. Briefly, reverse-transcription PCR reaction was performed in a total volume of 20 µl containing RNA and 2X RT mastermix (10X RT buffer; 25X dNTP Mix; 10X RT random primers; multiscribe reverse transcriptase; RNA inhibitors and nuclease-free H_2O) in a 1:1 ratio. The conditions of reverse-transcription PCR were 25^oC for 10 mins, 37^oC for 120 mins and 85^oC for 5 mins. cDNAs were stored in -20^oC until further use.

2.2.5.3. PCR

PCR reactions were performed in a total volume of 50 µl, containing 5 µM of each forward and reverse primers (Table 2. 5), 46 µl PCR Master Mix ($MgCl_2$ buffer; dNTPs; and nuclease-free H_2O) with 1 Unit of FastStart Taq DNA Polymerase (Roche). The conditions of PCR reactions were for *KRAS* fragments: 35 cycles of 95^oC for 1 min, 62.1^oC for 45 secs and 72^oC for 45 secs with an initial denaturation cycle of 95^oC for 5 mins and a final extension cycle of 70^oC for 7 mins; and *PIK3CA* fragments: 35 cycles of 95^oC for 1 min, 60^oC for 45 secs and 72^oC for 1 min with an initial denaturation cycle of 95^oC for 5 mins and a final extension cycle of 72^oC for 10 mins.

2.2.5.4. Determination of oligonucleotide concentration

The concentration and the quality of DNA/RNA were determined by using the NanoDrop Spectrophotometer (Thermo Scientific).

2.2.5.5. Analysis of DNA fragments by Agarose Gel Electrophoresis

Fractionation of nucleic acids was performed by electrophoresis in 1 - 1.5% Agarose (A9539, Sigma) / TAE gel containing ethidium bromide. DNA was mixed with 5X DNA Loading Buffer (See 2.1.6.) and electrophoresed at 100 V for approximately 30 mins. DNA bands were visualised under ultraviolet light.

2.2.5.6. Purification of DNA fragments from Agarose / TAE gel

Purification of DNA fragments from Agarose / TAE gel was performed by GeneJet Gel Extraction kit (K0691, Thermo Scientific) following the instructions of the manufacturer. DNA fragments were visualised in 1.5% Agarose / TAE gel using UV Transilluminator (365 nm). The desired DNA fragment was excised from the gel with a clean scalpel and an equal volume of Binding Buffer was added to the gel slice. Gel slices were solubilised by heating at 60^{o}C for 10 mins and samples were transferred to GeneJet purification columns. GeneJet column-bound DNA was washed twice with Wash Buffer and DNA fragments were eluted in 50 µl of nuclease-free H_20 with centrifugation at 13200 rpm for 1 min.

2.2.5.7. DNA Sequence Analysis

Sequencing of plasmid DNA (insert) or PCR amplified fragments was performed in the UCL CI sequencing facility by using the appropriate primers. Sequencing results were visualised using Finch TV software and were further analysed by using the EMBOSS Pairwise Alignment Algorithm from the EMBL-EBI Database (http://www.ebi.ac.uk/Tools/emboss/align/).

2.2.5.8. Cloning of shRNA oligos to pLKO-Tet-On plasmid

To generate shRNA-expressing plasmids, single-stranded oligos encoding the desired shRNA sequence (Table 2. 6) were firstly annealed and then cloned into the inducible lentiviral shRNA pLKO-Tet-On vector.

Annealing of single-stranded oligos

For the annealing of single-stranded oligos, 11.25 µl of each forward and reverse oligo (100 µM) were mixed with 2.5 µl of 10X annealing buffer (See 2.1.6.) and a PCR program was used to perform the reaction. The conditions of the PCR program used are: 10 mins at 98^{o}C, 5 mins at 95^{o}C, 5 mins at 90^{o}C, 5 mins at 88^{o}C, 5 mins at 85^{o}C, 5 mins at 80^{o}C, 5 mins at 78^{o}C, 5 mins at 75^{o}C, 5 mins at 70^{o}C, 5 mins at 68^{o}C, 5 mins at 65^{o}C, 5 mins at 60^{o}C, 5 mins at 58^{o}C, 5 mins at 55^{o}C, 5 mins at 50^{o}C, 5 mins at 45^{o}C, 5 mins at 40^{o}C, 10 mins at 37^{o}C and cooling down to 4^{o}C. The annealed oligo mixture was diluted in 0.5X of annealing buffer in a ratio 1:400 and ligated to the

cloning sites of pLKO-Tet-On vector created by *AgeI*/*EcoRI* digestion. Transformation into Stbl3 *E.coli* cells (See 2.2.5.9.) of the different ligation reactions followed and colonies were grown to purify plasmid DNA (See 2.2.5.10.). Verification of the inserted oligos was conducted by sequencing (See 2.2.5.7.).

DNA Restriction Digestion

pLKO-Tet-On vector was digested by using the restriction endonucleases *Age I* (Promega) and *EcoRI* (Roche) in Multicore buffer (Promega). The reaction was incubated at 37^{o}C for 1$^{1/2}$ hours and the restriction digestion products were visualised on 1% Agarose / TAE gel (See 2.2.5.6.). Followed purification of the digested pLKO-Tet-On vector from Agarose / TAE gel

Ligation of shRNA oligos to pLKO-Tet-On vector

Ligation reaction was performed in a total volume of 10 µl, containing double-stranded oligos, the digested pLKO-Tet-On vector, 2X Rapid Ligase buffer (C671B, Promega) and T4 DNA ligase (M180B, Promega). Ligation mixture was incubated at room temperature for 15 mins and transformation of ligated products in Stbl3 cells followed.

2.2.5.9. Transformation of plasmid DNA into High Efficiency Competent E.coli cells

50 µl of chemically competent *E.coli* cells - DH5α (Invitrogen) or Stbl3 (for pLKO-Tet-On vector transformation; Invitrogen) were thawed on ice and transformed with approximately 10 - 50 ng of plasmid DNA by incubating for 30 mins on ice. DH5α cells were heat shocked for 20 secs at 42^{o}C, were placed again on ice for 2 mins and 950 µl of SOC medium was added. Stbl3 cells were heat shocked for 45 secs at 42^{o}C, were placed again on ice for 2 mins and 250 µl of SOC medium was added. Bacteria incubated at 37^{o}C with shaking at 225 rpm for 1 hour and bacteria suspensions were spread to Luria Broth (LB)-Agar plates containing 100 µg/ml ampicillin (A9518, Sigma).

2.2.5.10. Purification of plasmid DNA

Plasmid DNA was purified using the JetStar 2.0 Plasmid Purification Kit (Genomed) according to the instructions of the manufacturer. For small- and large-scale purification of plasmid DNA, 1.5 ml and 200 ml of *E.coli* cells were cultured overnight in LB medium containing 100 μg/ml ampicillin, respectively. Overnight-cultured bacteria harvested by centrifugation at 12000 g for 3 mins and then lysed in Lysis buffer E2. The lysate was then transferred to the JetStar column in order the plasmid DNA to be captured. The column-bound DNA was then washed in wash buffer E5 and eluted in Elution buffer E6. Eluted plasmid DNA was precipitated using isopropanol and was washed in 70% ethanol at 4^{o}C. Precipitated DNA was air-dried for 10 mins and resuspended in appropriate volume of nuclease-free H_2O. Purified plasmid DNA was long-term sored in -20^{o}C.

2.2.6. Statistical analysis

Means of at least three independent experiments unless otherwise stated were statistically analysed using GraphPad Prism software. Determination of statistical significance in single-comparisons was performed using two-tailed unpaired Student's t-test and in multiple means comparisons using one-way or two-way ANOVA followed by the Bonferroni post-test.

Chapter 3

EGFR targeted therapy and autophagy in CRC

3. EGFR targeted therapy and autophagy in CRC

3.1. Background

EGFR targeted therapy is currently a promising approach for the treatment of many solid tumours including metastatic CRC. However, patients' response to EGFR targeted treatment is heterogeneous with limited potential mainly due to the presence of primary and acquired resistance mechanisms (Bertotti and Sassi, 2015). Autophagy has been previously suggested to play a pro-survival role upon targeted therapy and autophagy-inhibition combinational approaches have been found to potentiate cancer treatment (Bellodi *et al.*, 2009, Ravikumar *et al.*, 2010, Amaravadi *et al.*, 2011, Calabretta and Salomoni, 2011, Ma *et al.*, 2014). The activation of EGFR has been shown to inhibit either directly or indirectly autophagy induction and in turn EGFR inhibition has been shown to induce autophagy (discussed in 1.1.2.2., page 30). However, the specific role of autophagy upon EGFR targeted therapy remains controversial. On the one hand, EGFR inhibition-mediated autophagy plays a cytoprotective role for the survival of cancer cells and inhibition of autophagy potentiates cancer treatment (Han *et al.*, 2011, Dragowska *et al.*, 2013, Li *et al.*, 2013b, Zou *et al.*, 2013, Tang *et al.*, 2015). On the other hand, autophagy induction upon EGFR targeted therapy may potentiate treatment and inhibition of autophagy in this context may lead to refractory response to cancer treatment (Gorzalczany *et al.*, 2011, Wei *et al.*, 2013). Hitherto, our understanding on the role of autophagy upon EGFR targeted therapy in CRC is limited.

This chapter investigates the effect of EGFR targeted therapy on autophagy induction and aims to unravel the role of autophagy in EGFR targeted therapy response of CRC cells.

3.2. Results

3.2.1. *In vitro* model system to study autophagy in CRC

One of the main biomarkers used to predict EGFR targeted therapy response in CRC is *KRAS* status (Lièvre *et al.*, 2006, Benvenuti *et al.*, 2007, De Roock *et al.*, 2011, Misale *et al.*, 2014). CRC patients are screened for the presence of activating *KRAS* mutations and only *KRAS* WT patients are further refereed for EGFR targeted therapy with the monoclonal anti-EGFR antibody, Cetuximab. Previous studies have shown that activating mutations of the *RAS* oncogene results in upregulated basal autophagy, a phenomenon called "autophagy addiction". Autophagy addiction is considered to

potentiate tumour cell survival in starvation and tumourigenesis (Guo *et al.*, 2011). To examine the role of *KRAS* activation in response to Cetuximab treatment and investigate whether *KRAS*-mediated refractory response is driven by autophagy addiction, several isogenic *KRAS* WT and mutant CRC cell lines were included in our study. Table 3.1 summarizes the *KRAS* mutational status of CRC cell lines utilised in this work with information regarding their origin and technology used for their generation. To further confirm *KRAS* mutational status in all CRC cell lines, we designed sequencing primers specific for the identification of *KRAS* point mutations in codons 12 and 13 and all CRC cell lines were screened (Figure 3. 1). It was confirmed that HCT-116 and DLD-1 isogenic cell lines were homozygous for either *KRAS* WT or *KRAS* G13D mutation. SW48 isogenic cells were either homozygous for *KRAS* WT or heterozygous for *KRAS* G12D mutation. Finally, CaCo2 cells were found to be heterozygous for *KRAS* G12S point mutation and DiFi cells were homozygous for *KRAS* WT status.

Table 3. 1: *KRAS* mutational status of parental and *KRAS* isogenic CRC cell lines utilised in this study. Information regarding the technology used to generate *KRAS* isogenic cell lines as well as their provider is shown. G= Glycine, D= Aspartic acid and S= Serine.

Cell line	*KRAS* status of parental cell line	*KRAS* isogenic cell line	Generation of isogenic cell lines	KRAS isogenic cell lines provider
HCT-116	Heterozygous *KRAS* G13D	Homozygous *KRAS* WT	*KRAS* G13D knockout homologous recombination	Prof Bert Vogelstein
		Homozygous *KRAS* G13D	*KRAS* WT knockout homologous recombination	
DLD-1	Heterozygous *KRAS* G13D	Homozygous *KRAS* WT	*KRAS* G13D knockout homologous recombination	Prof Bert Vogelstein
		Homozygous *KRAS* G13D	*KRAS* WT knockout homologous recombination	
SW48	Homozygous *KRAS* WT	Homozygous *KRAS* WT	*KRAS* WT Parental cell line	Horizon Discovery
		Heterozygous *KRAS* G12D	*KRAS* G12D knockin homologous recombination	
CaCo2	Heterozygous *KRAS* G12S	Not available	-	-
DiFi	Homozygous *KRAS* WT	Not available	-	-

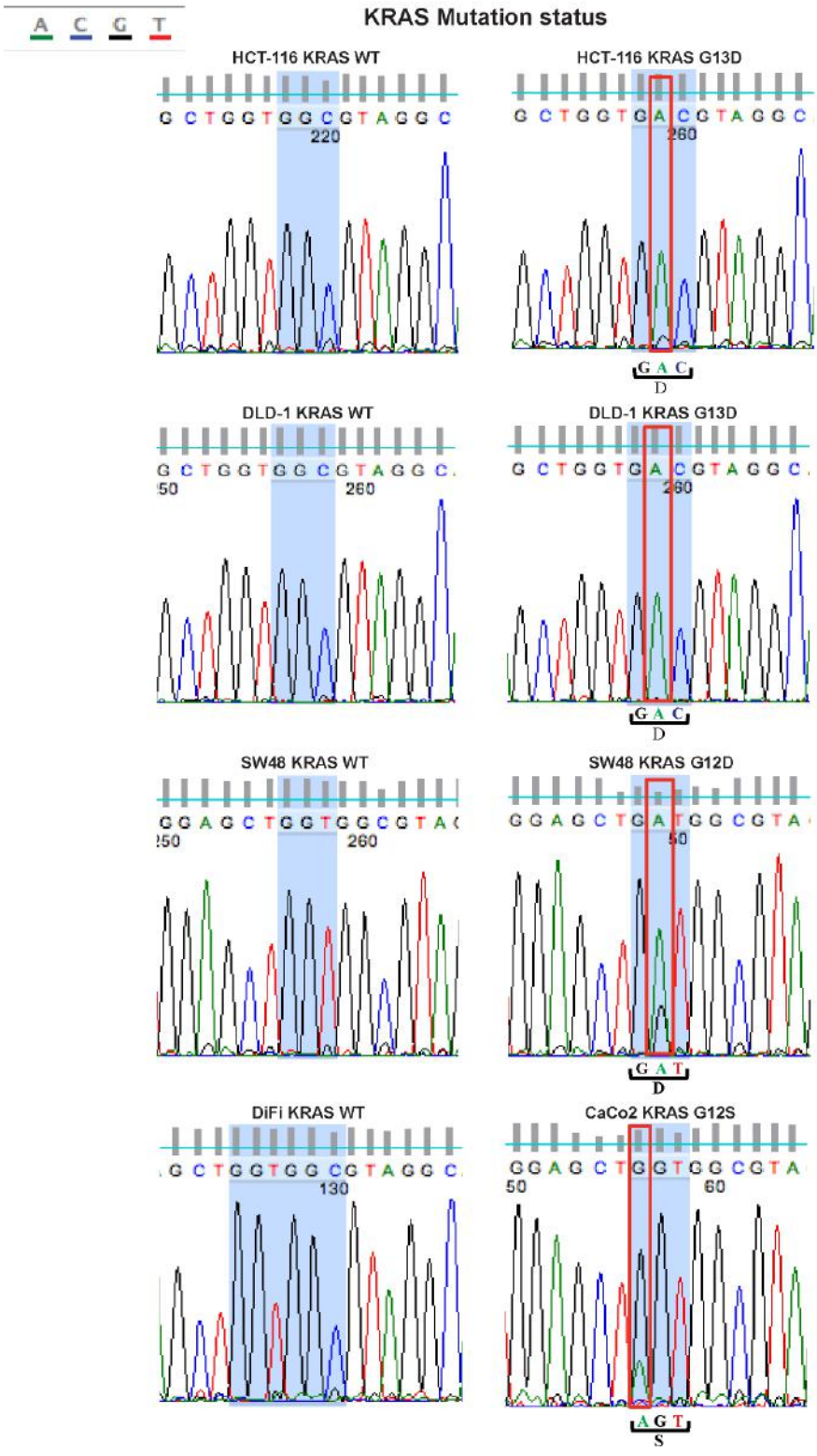

Figure 3. 1: Examination of *KRAS* codon 12 and 13 mutational status. The presence of *KRAS* activating mutations was confirmed in HCT-116, DLD-1 and SW48 *KRAS* mutant isogenic cell lines. DiFi cells were found not to harbour *KRAS* activating mutations and CaCo2 cells were found heterozygous for *KRAS* G12S activating mutation. D= Aspartic acid, S= Serine, Green/A= Adenine, Blue/C= Cytosine, Black/G= Guanine and Red/T=Thymine. *KRAS* codon 12 and 13 mutation screening experiment was conducted once in each cell line tested.

An *in vitro* pharmacological system for modulation of autophagy was required to examine the role of autophagy upon Cetuximab treatment. For pharmacological modulation of autophagy the anti-malaria and anti-rheumatoid drug Chloroquine (CQ) was used. CQ is known to inhibit vesicle acidification, including lysosomes, and is believed to block the last step of the autophagic process by inhibiting the clearance of autophagic vesicles into lysosomes (Solomon and Lee, 2009, Kimmelman, 2011). Due to its mode of action, the decreased number of side effects and its low price, an increasing number of clinical trials are using CQ in combination with conventional cancer therapy (Solomon and Lee, 2009, Kimura *et al.*, 2013).

Moreover, CQ is extensively used not only as an effective autophagy inhibitor but also to help monitoring autophagic flux upon normal and autophagy inducing or blocking conditions *in vitro* (Figure 3. 2.a) (Kimmelman, 2011, Klionsky *et al.*, 2012). CQ inhibits the fusion between autophagosomes and lysosomes, consequently resulting in accumulation of autophagosomes. The most important marker that is widely used for measuring autophagy is the LC3B protein. LC3 is synthesised as a proactive form and post-translational modifications give rise to two different forms: LC3-I (Carboxy-terminally cleaved) and LC3-II (lipidated LC3-I). LC3-II protein migrates faster that LC3-I in SDS-PAGE enabling the discrimination between the two forms by western blotting. As LC3-II is the only LC3 form that is present in both inner- and outer- autophagosome membranes, its expression level is used to measure autophagy. Measuring only LC3-II levels is an approach that does not take into account the dynamic nature of autophagy and could easily lead to misinterpretation of results. True determination of autophagic activity is obtained only by measuring the autophagic flux by using lysosomotropic compounds such as CQ. Since CQ blocks autophagosome degradation, an increase in LC3-II/LC3-I ratio in CQ-treated cells compared to untreated cells is considered a measure of autophagic flux (Kimmelman, 2011, Klionsky *et al.*, 2012). To determine differences in autophagic flux upon any kind of treatment in this study the CQ approach was used. Therefore, LC3-II/LC3-I ratio was compared between treated+CQ and untreated+CQ cells (Figure 3. 2.b).

10 μM CQ was used to monitor autophagic flux and assess the role of autophagy inhibition in CRC cells.

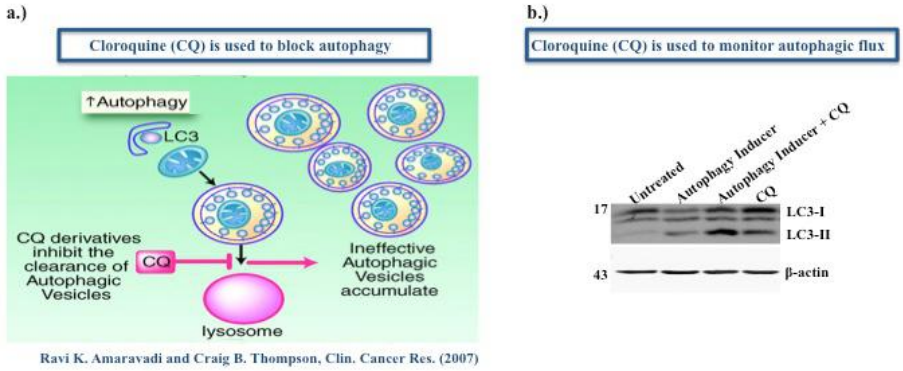

Figure 3. 2: Usage of Chloroquine in studying autophagy. a Chloroquine is used as an autophagic inhibitor since it blocks the degradation of autophagosomes by interfering with lysosomal acidification; **b** Chroroquine is used to monitor autophagic flux.

3.2.2. Activation of EGFR and its downstream signal effectors is cell-type specific

As a crucial first step preceding Cetuximab treatment experiments, the panel of CRC cell lines was screened for activation levels of EGFR and the EGFR downstream pathways PI3K and MAPK/ERK. Subsequently, *KRAS* isogenic cell lines were used in an attempt to unravel any differences in EGFR and its downstream effectors pathways regulated specifically by *KRAS* expression.

To address these, all CRC cell lines were cultured for 48 hours until they reached approximately 70% confluence. The levels of EGFR phosphorylation at tyrosine 1068 residue, as well as the levels of ERK 1/2 and AKT phosphorylation, were analysed in total cell lysates using western blotting. Measuring the phosphorylation levels of EGFR protein at specific tyrosine residues is a commonly used approach to detect EGFR activation/inactivation. Specifically, tyrosine 1068 residue of EGFR has been found to be responsible for Grb2 adaptor protein binding and is therefore highly implicated to MAPK/ERK downstream pathway activation (Rojas *et al.*, 1996). ERK 1/2 and AKT proteins constitute the last effectors of the MAPK/ERK and PI3K pathways, respectively (Engelman *et al.*, 2006, McKay and Morrison, 2007). Consequently, measurement of their phosphorylation levels is used to detect activation of the corresponding pathways, downstream of EGFR.

It was found that EGFR is highly activated in DiFi cells compared to all other CRC cell lines examined, followed by EGFR activation levels of SW48 and DLD-1 *KRAS* WT cells. In these two cell lines it was observed that EGFR was more active in *KRAS* WT cells compared to their mutant isogenic versions. HCT-116 cells showed the lowest EGFR activation compared to all other cell lines. Interestingly in these cells the presence of *KRAS* activating mutation accelerated EGFR activation compared to their

WT isogenic version (Figure 3. 3). Consequently, EGFR activation is cell-type specific and no correlation between EGFR activation and *KRAS* mutational status was found.

Discrepancies in MAPK/ERK pathway regulation were observed between the *KRAS* isogenic cell lines. As expected, higher ERK activation levels were observed in *KRAS* G13D HCT-116 cells compared to their *KRAS* WT isogenic version. No difference in ERK activation levels was found between *KRAS* WT and G12D SW48 cells and, surprisingly, lower ERK activation was found in *KRAS* G13D DLD-1 cells compared to their WT isogenic version (Figure 3. 3).

Regarding PI3K pathway regulation, it was found that AKT activation levels were higher at *KRAS* WT HCT-116 and SW48 cells compared to their *KRAS* mutated isogenic versions whereas the opposite effect was observed between the *KRAS* isogenic versions of DLD-1 cells (Figure 3. 3).

In conclusion, EGFR and its downstream effector pathways, PI3K and MAPK/ERK are regulated in a cell-type specific manner.

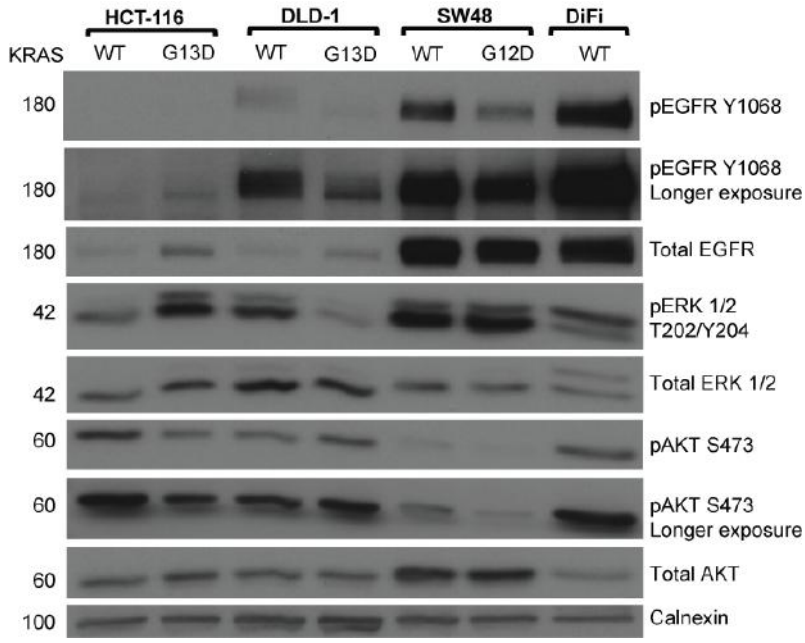

Figure 3. 3: Screening of CRC cell lines for EGFR, MAPK/ERK and PI3K activation levels. EGFR and its downstream effector pathways MAPK/ERK and PI3K are regulated in a cell-type specific manner. Phosphorylation levels of EGFR, ERK and AKT depict EGFR, MAPK/ERK and PI3K activation, respectively. Calnexin used as a loading control. p=phosphorylated. The experiment was performed once.

3.2.3. CRC cells respond to Cetuximab treatment in a cell-type specific manner – Activation of the *KRAS* oncogene is implicated in Cetuximab resistance

In order to identify the response of CRC cell lines to Cetuximab treatment, five different CRC cell lines, HCT-116, CaCo2, DLD-1, SW48 and DiFi were screened for

Cetuximab sensitivity using the SRB assay. Moreover, to investigate any possible implication of the *KRAS* mutational status in Cetuximab resistance three *KRAS* isogenic versions carrying activating mutations of the gene: HCT-116, DLD-1 *KRAS* G13D and SW48 *KRAS* G12D were also screened by SRB assay. Cetuximab response was examined after 87 hours of treatment and percentage (%) of cell growth for each condition was calculated by taking into account untreated controls and “day 0” of treatment controls for each cell line (discussed in 2.2.3.1).

The five cell lines examined were grouped into four different categories based on their sensitivity to Cetuximab treatment when compared to their untreated controls. It was found that HCT-116 *KRAS* WT and CaCo2 were the most resistant cell lines since no significant downregulation in their cell growth was observed compared to the untreated control (Figure 3. 4.a and b). SW48 *KRAS* WT cells showed intermediate resistance to Cetuximab treatment. A significant cell growth downregulation was observed in the majority of Cetuximab concentrations examined for this cell line but not beyond 50% (Figure 3. 4.c). DLD-1 *KRAS* WT cells were classified as Cetuximab sensitive due to a significant reduction in cell growth of 70% and beyond (Figure 3. 4.d). Finally, DiFi cells were classified to the Cetuximab high sensitivity group since not only a high percentage of downregulation in cell growth was observed but also a lower cell number compared to “day 0” control (Figure 3. 4.e). This observation could indicate that high concentrations of Cetuximab may induce cell death in this specific cell line.

As far as the implication of the *KRAS* mutational status in Cetuximab resistance is concerned, it was found that all isogenic *KRAS* mutated cell lines were not responsive to Cetuximab treatment when compared to their WT isogenic versions. Specifically, HCT-116 *KRAS* G13D cells did not show any difference in cell growth compared to their WT isogenic version since the aforementioned cell line did not respond to Cetuximab treatment (Figure 3. 4.a). SW48 *KRAS* G12D cells were more resistant compared to their isogenic WT version with approximately 28% higher cell growth, although this was not statistically significant (Figure 3. 4.c). Finally, DLD-1 *KRAS* G13D cells showed statistically significant difference in Cetuximab treatment response compared to their isogenic WT version since only 37% of cell growth inhibition observed in the higher Cetuximab concentration (Figure 3. 4.d). Of note, no *KRAS* WT and mutated isogenic cell lines were available for CaCo2 and DiFi cells, respectively.

In summary, response to Cetuximab treatment is cell-type specific and activating *KRAS* mutations may be implicated in Cetuximab resistance.

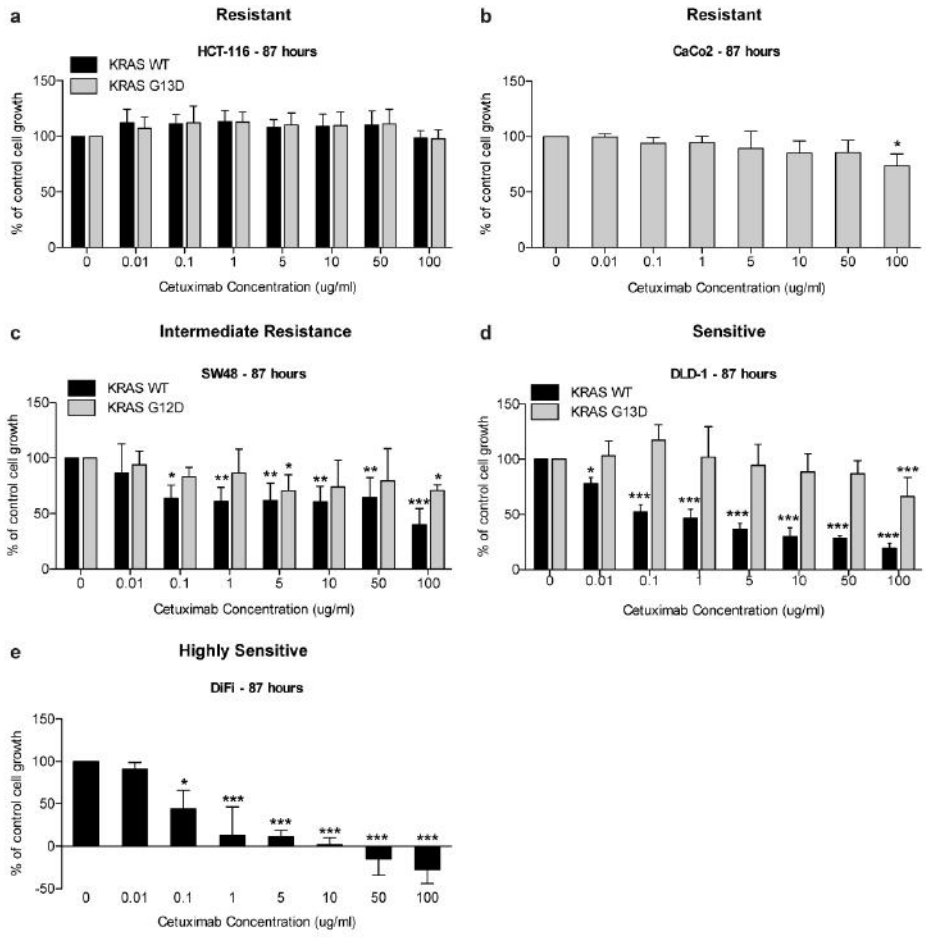

Figure 3. 4: Differential sensitivity of CRC cell lines to Cetuximab treatment – Implication of the *KRAS* mutation in Cetuximab resistance. **a** HCT-116 cells belong to the resistant group. No difference between *KRAS* WT and mutant cells to Cetuximab sensitivity; **b** CaCo2 cells are resistant to Cetuximab treatment; **c** SW48 cells belong to the intermediate resistance group. *KRAS* WT cells are more sensitive to Cetuximab treatment compared to mutant cells; **d** DLD-1 cells classified to the sensitive group. Statistically significant difference between *KRAS* WT and mutant cells in response to Cetuximab; **e** DiFi cells classified to the high sensitivity group. CRC cells were treated with 0, 0.01, 0.1, 1, 5, 10, 50 and 100 µg/ml Cetuximab for 87 hours. Bar plots represent % of control cell growth assessed by SRB assay. Error bars represent standard deviation of 4 independent SRB experiments. One-way ANOVA (CaCo2 and DiFi cells) or two-way ANOVA (HCT-116, DLD-1 and SW48 *KRAS* WT and mutant cells) statistical analysis followed by the Bonferroni post-test was used. *= $p<0.05$, **= $p<0.01$ and ***= $p<0.001$.

3.2.4. CRC cells are competent for autophagy induction

Prior to Cetuximab experiments, examination of autophagy-induction competence of CRC cells was important. To address this, the autophagy inducing stressor PI103, which inhibits both mTOR and PI3K, was used. Isogenic *KRAS* mutant cell lines were included in this examination in order to test whether activation of the *KRAS* oncogene affects autophagy induction levels under basal and autophagy-stimulated conditions.

All examined CRC cell lines were cultured either in the presence of 1 µM of PI103 combined or non-combined with CQ for 6 hours in order to monitor autophagic flux.

Based on the rate of LC3-I to LC3-II conversion, it was observed that all DLD-1, HCT-116, SW48 and CaCo2 CRC cell lines examined were capable of autophagy induction upon simultaneous inhibition of PI3K and mTOR, when untreated and PI103 treated or untreated+CQ and PI103+CQ conditions were compared (Figure 3. 5). When basal autophagy levels between *KRAS* WT and mutant cells were compared, it was observed that only DLD-1 and to a lower extent HCT-116 *KRAS* mutant cells had higher levels of basal autophagy compared to their WT isogenic versions (Figure 3. 5.a and b). Finally, *KRAS* activating mutation resulted in accelerated PI103-mediated autophagy induction only in SW48 cells compared to WT. In particular, SW48 *KRAS* G12D cells were found to induce higher levels of autophagy (approximately 1 fold difference) compared to their WT cells upon PI103 stimulation (Figure 3. 5.a, b and c)

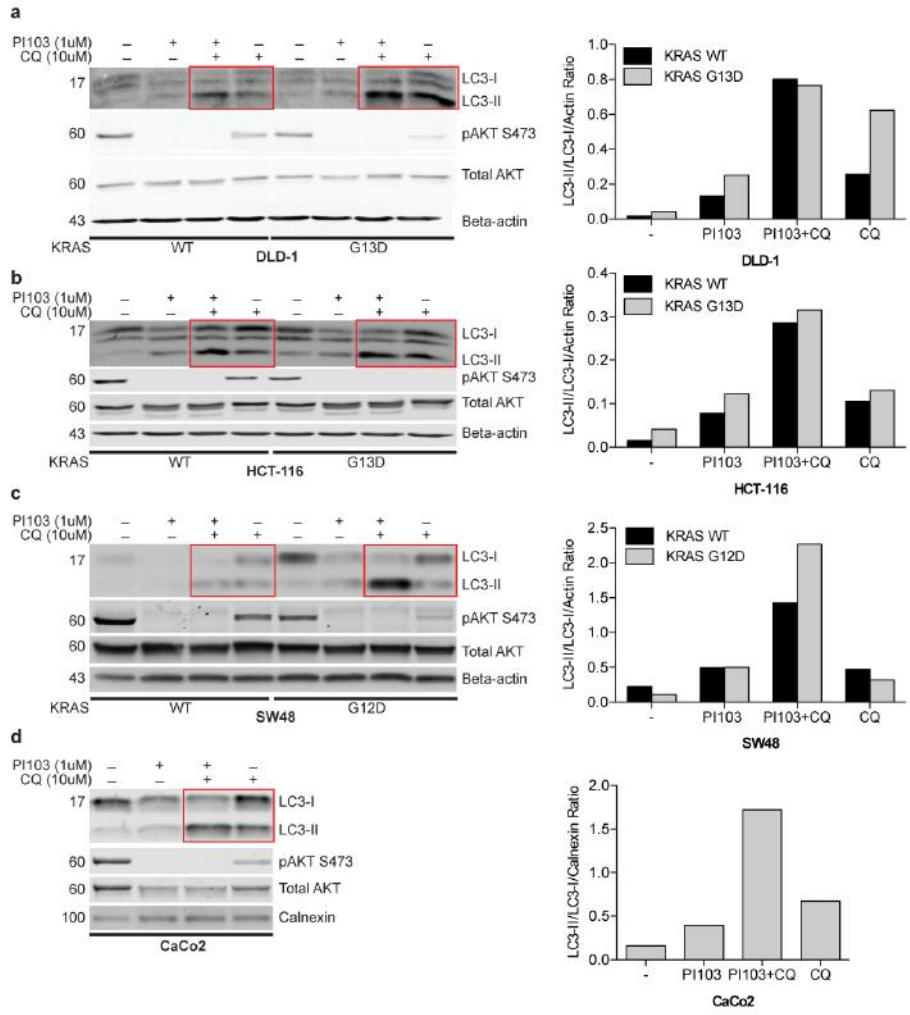

Figure 3. 5: Ability of CRC cell lines to induce autophagy upon PI103 treatment. Autophagy induction upon PI103 in **a** DLD-1; **b** HCT-116; **c** SW48 *KRAS* WT and mutant isogenic cell lines and; **d** CaCo2 cells. 1 μM PI103 used for induction of autophagy experiments. 10 μM CQ used to monitor autophagic flux. Protein expression levels were examined by western blotting. Beta-actin and calnexin used as loading controls. Bar plots represent densitometric analysis of LC3-II/LC3-I levels normalised to loading control. Western blotting images are representative of two independent experiments.

3.2.5. Cetuximab treatment only induces autophagy in DiFi cells

After confirming that CRC cells were capable of inducing autophagy upon PI3K and mTOR inhibition it was investigated whether Cetuximab targeted therapy induces autophagy and more specifically whether autophagy inhibition in this context sensitises CRC cells to therapy. Since Cetuximab blocks EGFR activation (Li *et al.*, 2005) it was hypothesised that it would induce autophagy by resembling growth factor deprivation autophagic stimulus. Another hypothesis examined was whether *KRAS* activation could affect levels of Cetuximab-induced autophagy and whether such an effect would affect Cetuximab resistance; *KRAS* activation plays an important role in Cetuximab primary and acquired resistance (Brand *et al.*, 2011, De Roock *et al.*, 2011, Misale *et al.*, 2012).

All cell lines examined were treated with two different Cetuximab concentrations (50 and 100 μg/ml) with and without CQ for 24 hours and LC3B levels were detected by western blotting. Only DiFi cells were found to induce moderate autophagy levels upon Cetuximab treatment at both concentrations examined (Figure 3. 6.e). DLD-1, HCT-116, SW48 both *KRAS* WT and mutant cells as well as CaCo2 cells failed to induce autophagy by Cetuximab treatment at any concentration examined (Figure 3. 6.a - d).

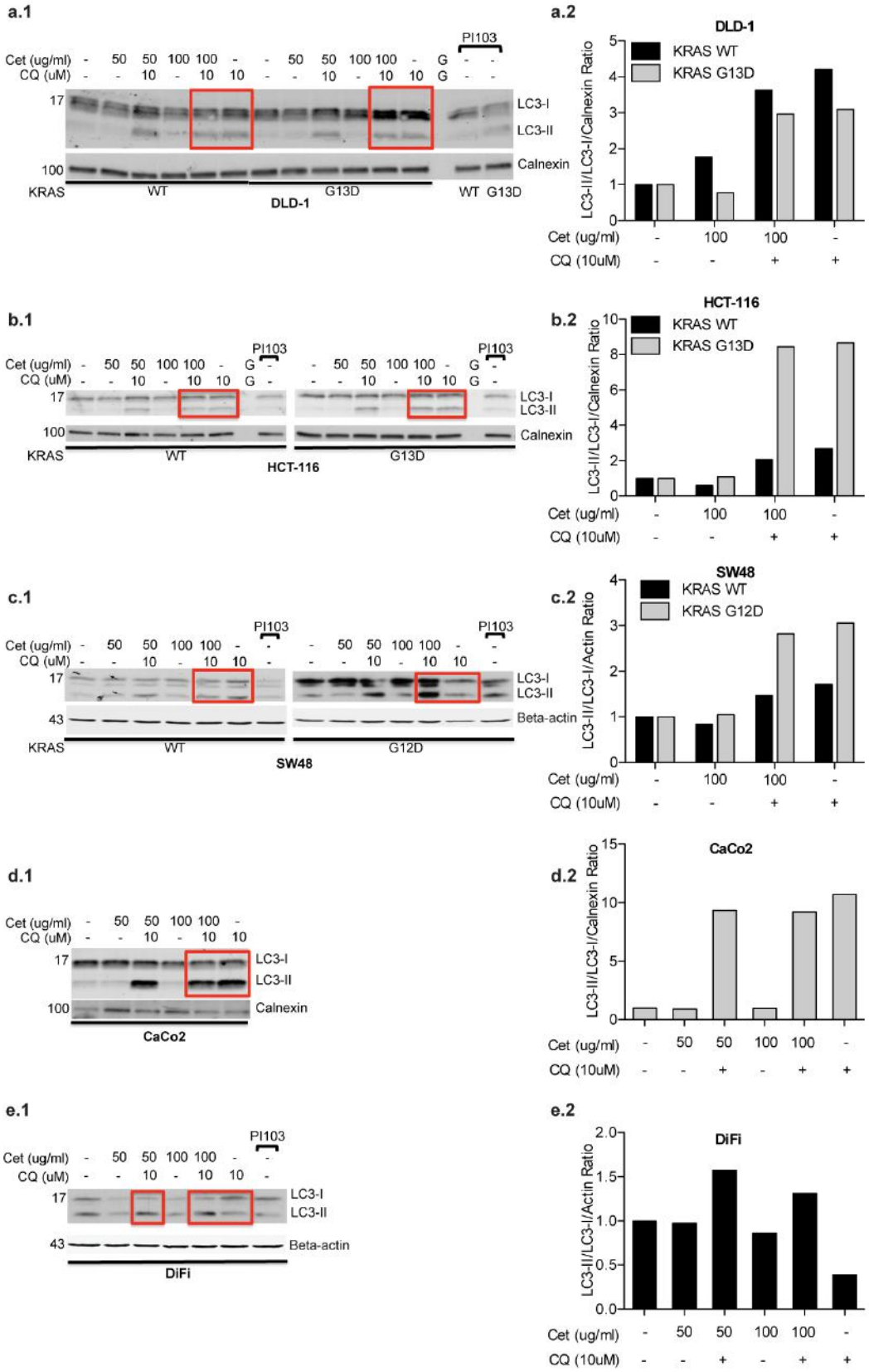

Figure 3. 6: Examination of autophagy induction upon Cetuximab treatment. Cetuximab did not induce autophagy in **a** DLD-1; **b** HCT-116; **c** SW48 *KRAS* WT and mutant isogenic cell lines and; **d** CaCo2 cells. Autophagy was induced in **e** DiFi cells. **1** depicts western blotting analysis of LC3 protein levels. Beta-actin or calnexin used as loading controls. **2** Bar plots represent densitometric analysis of LC3-II/LC3-I levels normalised to actin or calnexin. Cells treated with 50 and 100 µg/ml Cetuximab +/- 10 µM CQ for 24 hours. The experiment was performed once in each CRC cell line.

3.2.6. CQ fails to sensitise CRC cells to Cetuximab treatment

Based on the data shown in 3.2.5, most CRC cell lines do not induce autophagy upon Cetuximab treatment, suggesting that treatment with the lysosomotropic agent CQ would not sensitise CRC cells to Cetuximab with the potential exception of DiFi cells. To test this, all examined CRC cell lines were cultured in the presence of Cetuximab with or without 10 μM CQ for 87 hours and results were analysed using SRB assay.

Regarding HCT-116, SW48 and DLD-1 *KRAS* WT cell lines and their mutant isogenic versions, it was found that inhibition of autophagy via CQ does not potentiate Cetuximab treatment in any concentration examined (10, 50 and 100 μg/ml). In line with the aforementioned cell lines, CQ addition to CaCo2 cells did not have any effect in Cetuximab treatment response regardless of the concentrations examined (10, 50 and 100 μg/ml) (Figure 3. 7.a-d). Autophagy inhibition by CQ was found to marginally potentiate Cetuximab treatment in DiFi cells (Figure 3. 7.e). As previously described, DiFi cells were classified to the high sensitivity to Cetuximab response group and high concentrations of Cetuximab in these cells may induce cell death (Figure 3. 4.e). Herein SRB experiment in DiFi cells was performed using lower Cetuximab concentrations (0.01, 0.05 and 0.1 μg/ml) compared to all other CRC cells. Interestingly, CQ treatment alone provoked a statistically significant increase in the percentage of cell growth in SW48 *KRAS* G12D as opposed to the effect observed in DiFi cells (Figure 3. 7.c and e). CQ treatment alone did not have any effect on cell growth in all other CRC cell lines examined (Figure 3. 7.a, b and d).

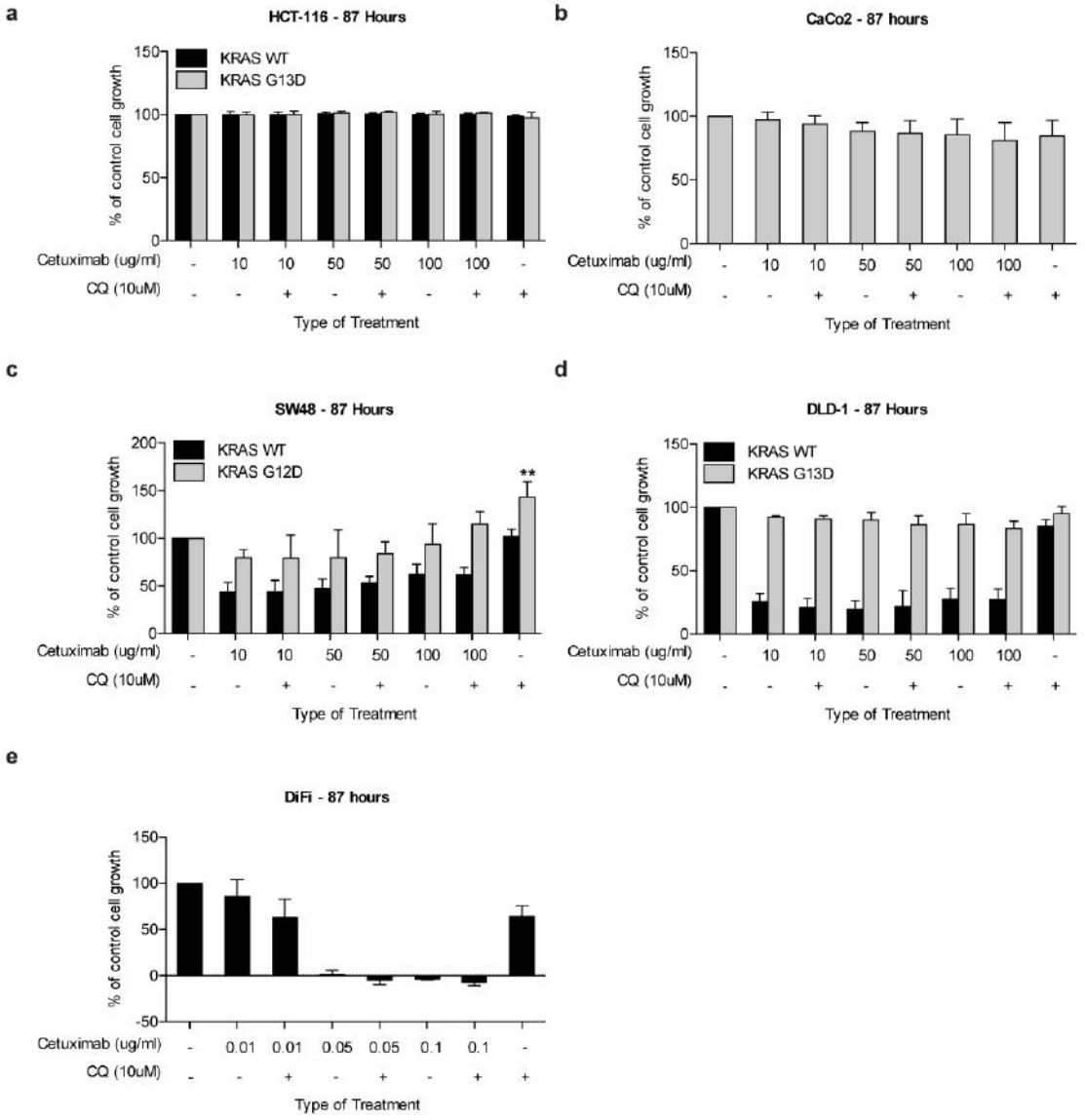

Figure 3. 7: Sensitivity of CRC cell lines to autophagy inhibition in combination with Cetuximab treatment. Autophagy inhibition by CQ does not potentiate Cetuximab treatment response in **a** HCT-116; **b** CaCo2; **c** SW48 and **d** DLD-1 cell lines. Autophagy inhibition by CQ potentiates Cetuximab treatment in **e** DiFi cells. 10, 50 and 100 µg/ml Cetuximal (a-d conditions) or 0.01, 0.05 and 0.1 µg/ml Cetuximab (e condition) +/- 10 µM CQ for 87 hours were used. Bar plots represent percentage (%) of control cell growth assessed by SRB assay. Error bars represent standard deviation of 4 independent SRB experiments. One-way ANOVA (CaCo2 and DiFi cells) or two-way ANOVA (HCT-116, DLD-1 and SW48 *KRAS* WT and mutant cells) statistical analysis followed by the Bonferroni post-test was used. **=p<0.01.

3.2.7. Cetuximab has variable effects on EGFR phosphorylation across different CRC cell lines

Amongst the five different CRC cell lines examined for autophagy induction upon Cetuximab treatment, it was observed that only DiFi cells were able to induce autophagy. Autophagy induction in DiFi cells was shown to have a marginal cyto-

protective role. The lack of consistent response to Cetuximab treatment, prompted us to investigate whether Cetuximab was equally potent at inhibiting EGFR phosphorylation across the different CRC cell lines. Cells were cultured in the presence of 50 and 100 µg/ml of Cetuximab for 24 hours with or without 10 µM CQ. It was found that both *KRAS* isogenic versions of DLD-1 cells, CaCo2 and DiFi cells had decreased phosphorylation levels of EGFR upon Cetuximab treatment (Figure 3. 8.a, d and e). For HCT-116 cells, no difference in EGFR phosphorylation level was observed upon Cetuximab treatment (Figure 3. 8.b) and SW48 cells showed an increase in EGFR phosphorylation levels upon Cetuximab treatment (Figure 3. 8.c). Interestingly, CQ treatment alone downregulated EGFR activation levels only in DiFi cells (Figure 3. 8.e).

Collectively, these data show that the response to Cetuximab treatment is variable across the CRC cell lines and that in DiFi cells decreased EGFR phosphorylation correlates with autophagy induction.

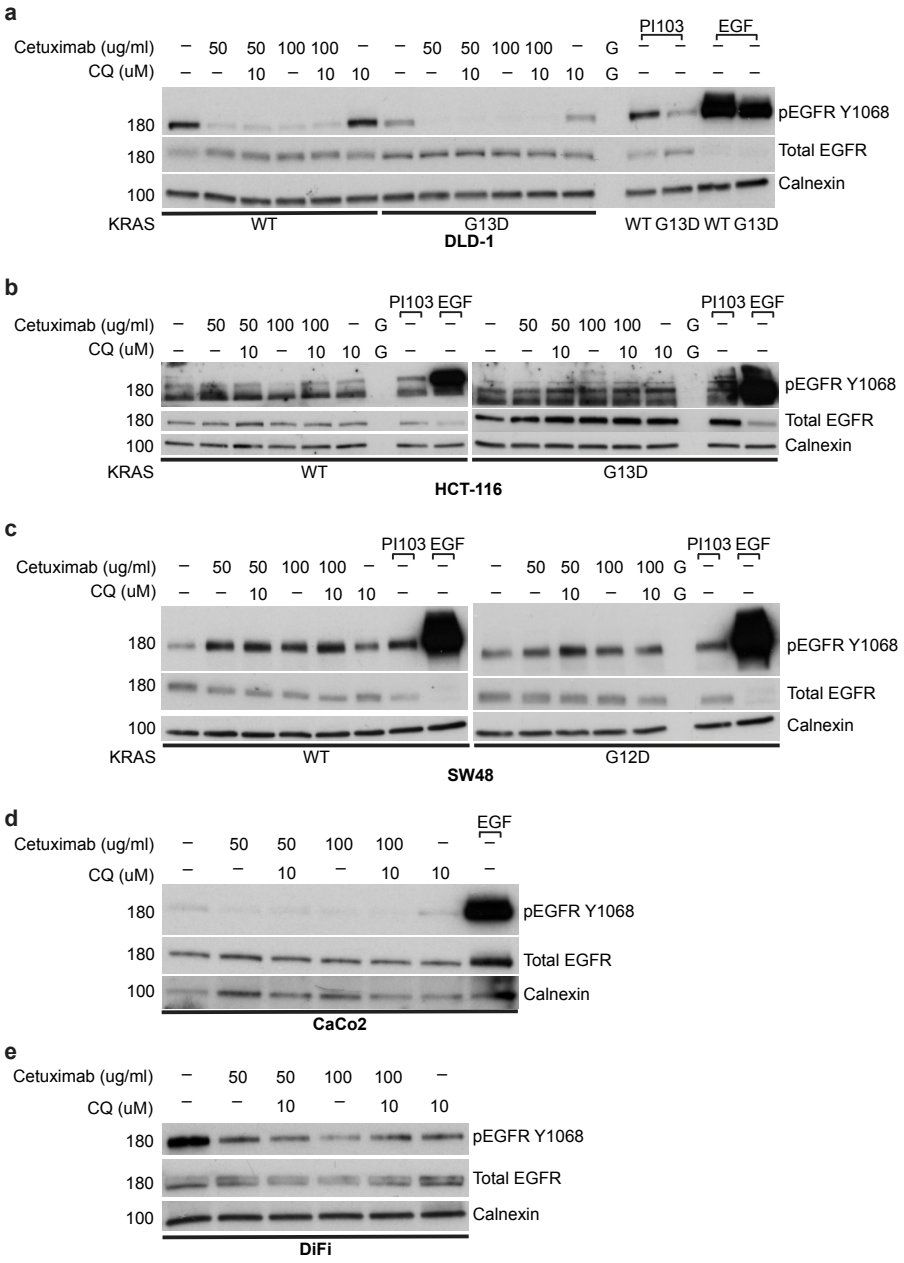

Figure 3. 8: EGFR activation levels upon Cetuximab treatment in **a** DLD-1; **b** HCT-116; **c** SW48 *KRAS* WT and mutant isogenic versions; **d** CaCo2 and **e** DiFi cells. Phosphorylation levels of EGFR depict EGFR activation. 50 and 100 µg/ml Cetuximab +/- 10 µM CQ for 24 hours were used. 1 µM PI103 used as autophagy induction positive control and EGF as EGFR activation positive control. Calnexin used as western blotting positive control. G= gap and p= phosphorylation. The experiment was performed once in each CRC cell line.

3.2.8. AKT phosphorylation upon Cetuximab treatment inversely correlates with autophagy induction and is affected by CQ treatment

The examination of EGFR activation levels alone cannot explain the differential response of CRC cell lines to Cetuximab treatment and their differential autophagy induction. To shed light on the mechanism controlling autophagy induction in response

to Cetuximab treatment, it was essential to examine the activation status of the PI3K/AKT pathway, which is a key downstream effector of EGFR and a known master regulator of autophagy induction (previously discussed in 1.1.2.2.).

To this end, CRC cell lines were cultured for 24 hours in the presence of 50 and 100 μg/ml Cetuximab with or without 10 μM CQ and the phosphorylation of AKT was analysed by western blotting. It was observed that the phosphorylation of S473 residue of AKT was not downregulated upon Cetuximab treatment in HCT-116, DLD-1 and SW48 *KRAS* WT and mutant cells as well as in CaCo2 cells (Figure 3. 9.a-d). Specifically, for DLD-1 and HCT-116 cells it was found that AKT phosphorylation levels were increased upon treatment. In contrast, AKT phosphorylation was reduced in DiFi cells upon Cetuximab treatment (Figure 3. 9.e). An interesting observation was that Cetuximab and CQ combinational treatment resulted in downregulation of AKT phosphorylation levels in all CRC cell lines examined (Figure 3. 9.a-e). In addition, HCT-116 and SW48 *KRAS* WT, CaCo2 and DiFi cells showed a downregulation of AKT phosphorylation levels following CQ treatment alone (Figure 3. 9.b-e). This observation will be further discussed in 4.2.2.

Collectively, AKT phosphorylation downregulation upon Cetuximab treatment correlates with autophagy induction following EGFR inhibition.

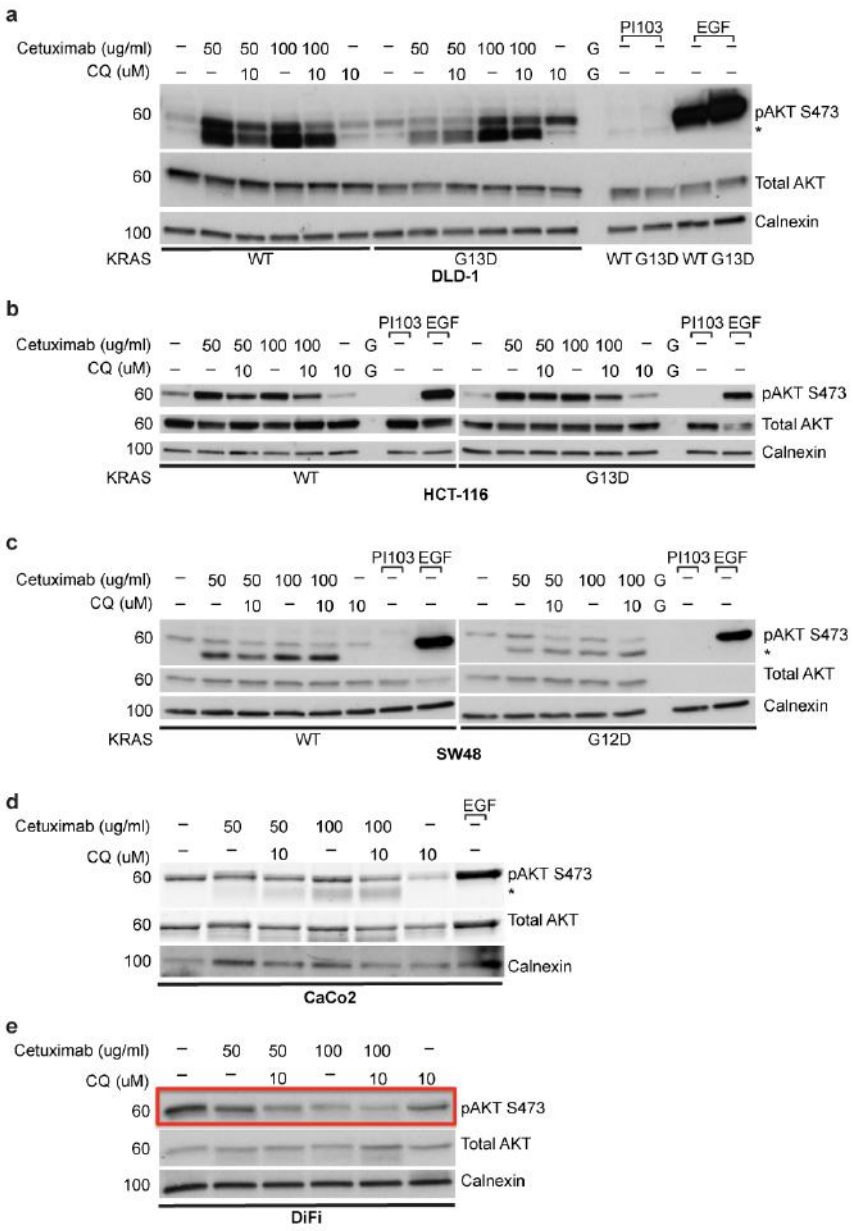

Figure 3. 9: PI3K activation levels upon Cetuximab treatment in **a** DLD-1; **b** HCT-116; **c** SW48 *KRAS* WT and mutant isogenic versions; **d** CaCo2 and **e** DiFi cells. Phosphorylation levels of AKT depict PI3K activation. 50 and 100 µg/ml Cetuximab +/- 10 µM CQ for 24 hours were used. 1 µM PI103 used as autophagy induction positive control and EGF as EGFR activation positive control. Calnexin used as western blotting positive control. G= gap, p= phosphorylation and * Cetuximab heavy chain. The experiment was performed once in each CRC cell line.

3.2.9. Downregulation of MAPK/ERK phosphorylation correlates with the growth suppressive response to Cetuximab treatment

Another downstream effector of EGFR pathway and known regulator of autophagy induction is MAPK/ERK pathway (previously discussed in 1.1.2.2.). In order to examine the importance of MAPK/ERK pathway in Cetuximab response and induction

of autophagy upon Cetuximab treatment, all CRC cells were cultured in 50 μg/ml or 100 μg/ml Cetuximab in the presence or absence of 10 μM CQ for 24 hours. ERK 1/2 protein activation levels, a downstream regulator of MAPK/ERK pathway, were analysed by western blotting. Downregulation of the activation levels of ERK protein, reflected by downregulation of its phosphorylation levels, was observed in all classified Cetuximab-responsive cell lines (Figure 3. 4.c-e) with the exception of the Cetuximab-resistant CaCo2 cell line (Figure 3. 4.b), which exhibited a marginal decrease in pERK levels (Figure 3. 10.d). Specifically, DiFi, DLD-1 and SW48 *KRAS* WT Cetuximab-responsive cells showed a decrease in ERK activation levels with DiFi cells having abolished pERK levels upon Cetuximab treatment (Figure 3. 10.a, c and e). As expected, *KRAS* mutated isogenic versions of DLD-1 and SW48 cells did not show any decrease in ERK activation levels due to the presence of the *KRAS* activating mutations G13D and G12D, respectively (Figure 3.10.a and c). HCT-116 was found to be the only cell line that MAPK/ERK pathway was not downregulated by Cetuximab, regardless of its *KRAS* mutational status. An increase in ERK activation levels was observed in both HCT-116 *KRAS* WT and G13D cells (Figure 3.10.b).

In contrast to the reduced pAKT levels observed upon Cetuximab and CQ combinational treatment in all CRC cell lines tested, no difference in pERK levels was found under the same conditions (Figure 3. 10). Interestingly, CQ treatment alone was found to upregulate pERK levels in both DLD-1 *KRAS* WT and G13D cells, as well as in SW48 *KRAS* WT and DiFi cells (Figure 3. 10.a, c and e). Finally, CQ treatment alone did not alter pERK levels in HCT-116 and CaCo2 cells (Figure 3. 10.b and d).

Collectively, MAPK/ERK pathway activation reduction is correlated with the growth suppressive response to Cetuximab treatment. No correlation could be made between MAPK/ERK activation levels and autophagy induction following EGFR inhibition.

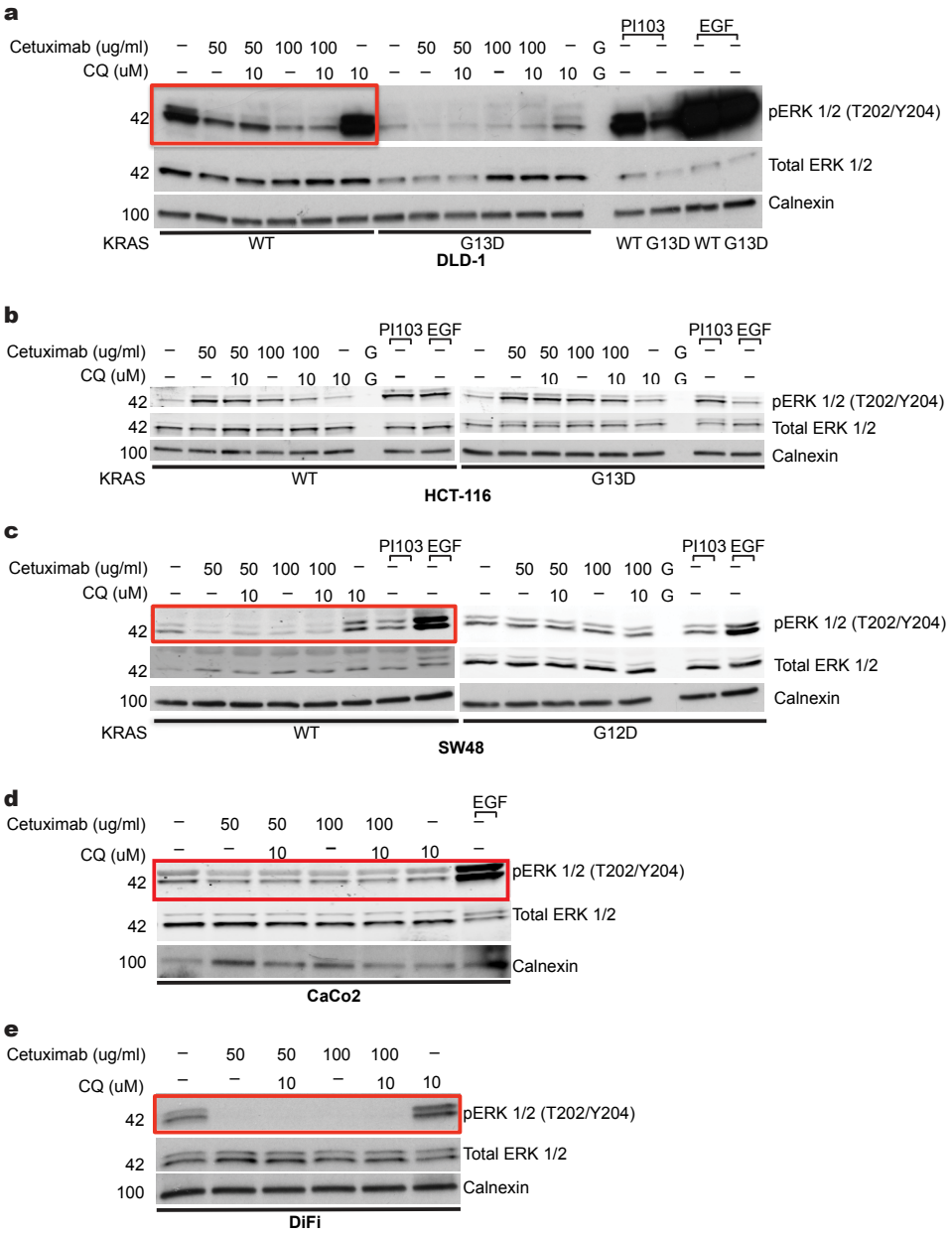

Figure 3. 10: MAPK/ERK activation levels upon Cetuximab treatment in **a** DLD-1; **b** HCT-116; **c** SW48 *KRAS* WT and mutant isogenic versions; **d** CaCo2 and **e** DiFi cells. Phosphorylation levels of ERK protein depict MAPK/ERK activation. 50 and 100 μg/ml Cetuximab +/- 10 μM CQ for 24 hours were used. 1 μM PI103 used as autophagy induction positive control and EGF as EGFR activation positive control. Calnexin used as western blotting positive control. G= gap and p= phosphorylation. The experiment was performed once in each CRC cell line.

3.2.10. EGFR downregulation and treatment with the EGFR tyrosine kinase inhibitor Gefitinib recapitulates the effect of Cetuximab on downstream signalling pathways

To further confirm the reliability of the already observed Cetuximab effects on EGFR pathway and downstream effectors, PI3K and MAPK/ERK, as well as

autophagy induction response upon EGFR inhibition, two different approaches were used. Firstly, EGFR protein expression was downregulated by siRNA and secondly EGFR activation was downregulated using an EGFR tyrosine kinase inhibitor, named Gefitinib. Western blotting was used to assess EGFR, AKT and ERK1/2 activation, based on the level of their phosphorylation.

For the EGFR siRNA approach, one of the most resistant in Cetuximab treatment cell line; HCT-116, and the sensitive cell line; DLD-1, as well as their isogenic *KRAS* G13D versions were examined after 48 and/or 72 hours of EGFR downregulation by using 25 nM and/or 50 nM of scramble and EGFR siRNAs. In both HCT-116 and DLD-1 cells EGFR levels were abolished by EGFR siRNA (Figure 3. 11.a.1 and 2). In line with Cetuximab results it was observed that both PI3K and MAPK/ERK pathways were not affected upon EGFR downregulation in both HCT-116 *KRAS* WT and G13D cells (Figure 3. 11.b.1 and c.1). Again in accordance with Cetuximab results, the MAPK/ERK pathway was found to be downregulated only in DLD-1 *KRAS* WT cells and remained stable in their isogenic cell line harbouring the activating *KRAS* G13D mutation (Figure 3. 11.b.2). The PI3K pathway remained stable upon EGFR downregulation in DLD-1 *KRAS* G13D cells and slightly decreased in DLD-1 *KRAS* WT cells (Figure 3. 11.c.2).

For the Gefitinib approach, HCT-116 KRAS WT and G13D isogenic cell lines were cultured in the presence of 1 μM Gefitinib for 6 hours with or without 10 μM CQ. In line with Cetuximab results, EGFR activation levels remained stable upon Gefitinib treatment in HCT-116 *KRAS* G13D cells. In contrast to Cetuximab and *KRAS* G13D Gefitinib results, a small decrease in EGFR activation levels was observed upon Gefitinib treatment in HCT-116 *KRAS* WT cells (Figure 3. 11.d). Similarly to Cetuximab and EGFR siRNA observations, Gefitinib experiment confirmed that MAPK/ERK and PI3K pathways were not affected upon EGFR activation inhibition in HCT-116 cells since both pERK and pAKT levels remained stable upon Gefitinib treatment (Figure 3. 11.e and f). Opposed to Cetuximab results (Figure 3. 10.b), combinational treatment of Gefitinib with CQ as well as CQ treatment alone showed a decrease in pERK levels compared to untreated controls in both HCT-116 *KRAS* WT and G13D cells (Figure 3. 11.e). In agreement with Cetuximab results (Figure 3. 9.b), Gefitinib and CQ combinational treatment along with CQ alone treatment resulted in PI3K pathway downregulated signalling, as depicted by reduced pAKT levels, in both *KRAS* isogenic versions of HCT-116 cells (Figure 3. 11.f).

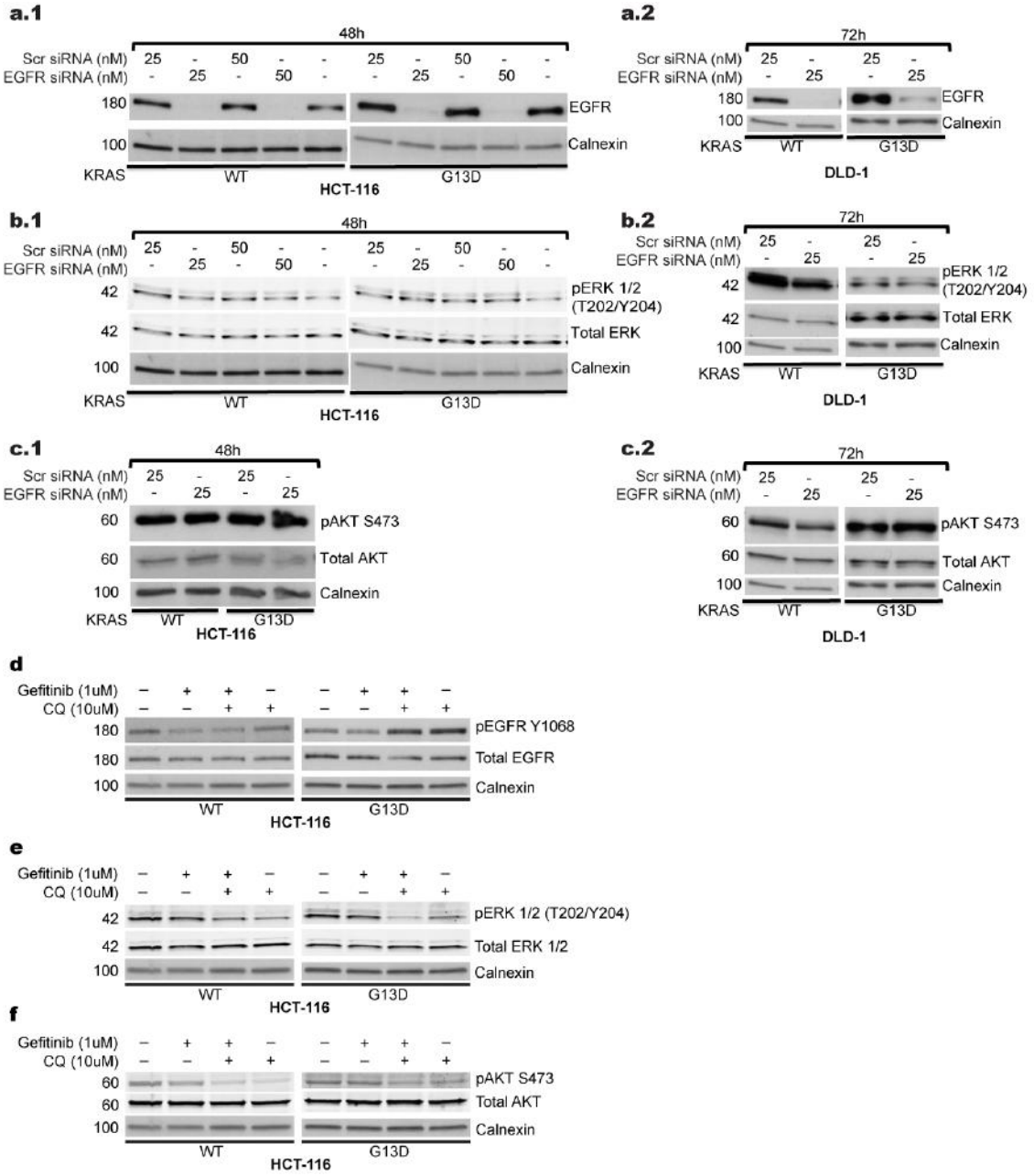

Figure 3. 11: EGFR downregulation and Gefitinib experiments. Total EGFR expression upon EGFR siRNA in **a.1** HCT-116 and **a.2** DLD-1 *KRAS* WT and G13D isogenic cell lines. MAPK/ERK pathway activation examination upon EGFR siRNA in **b.1** HCT-116 and **b.2** DLD-1 *KRAS* isogenic cell lines. PI3K pathway activation examination upon EGFR siRNA in **c.1** HCT-116 and **c.2** DLD-1 *KRAS* WT and G13D isogenic cell lines. Examination of **d** EGFR activation; **e** MAPK/ERK pathway and **f** PI3K pathway activation in HCT-116 *KRAS* WT and G13D isogenic cell lines upon Gefitinib +/- 10 μM CQ treatment. 25 and/or 50 nM of scramble and EGFR siRNAs were used and assessed using western blotting after 48 or 72 hours. Cells were treated with 1 μM of Gefitinib +/- 10 μM CQ for 6 hours. Phosphorylation levels of EGFR, ERK and AKT depict activation of EGFR, MAPK/ERK and PI3K pathways, respectively. Calnexin used as western blotting loading control. p= phosphorylated. The EGFR siRNA and Gefitinib experiment was performed once in each CRC cell line.

After confirming that the EGFR pathway and its downstream effectors MAPK/ERK and PI3K are regulated in a common way upon EGFR inhibition studies both by

Cetuximab and Gefitinib and that EGFR downregulation experiments are in line with these observations, it was of great importance to investigate whether autophagy induction upon EGFR siRNA and Gefitinib treatment follows the same pattern as with Cetuximab.

In order to monitor autophagic flux and to investigate if there is a kinase-independent role of EGFR in autophagy modulation, HCT-116 *KRAS* WT cells were treated with 25 nM of scramble or EGFR siRNAs for 48 hours; with or without 10 μM CQ treatment which started 6 hours prior the end of the experiment. Figure 3. 12.a shows that no autophagy induction was observed upon EGFR downregulation in HCT-116 *KRAS* WT cells. Similarly, it was observed that Gefitinib is unable to induce autophagy in both HCT-116 *KRAS* WT and G13D cells (Figure 3. 12.b).

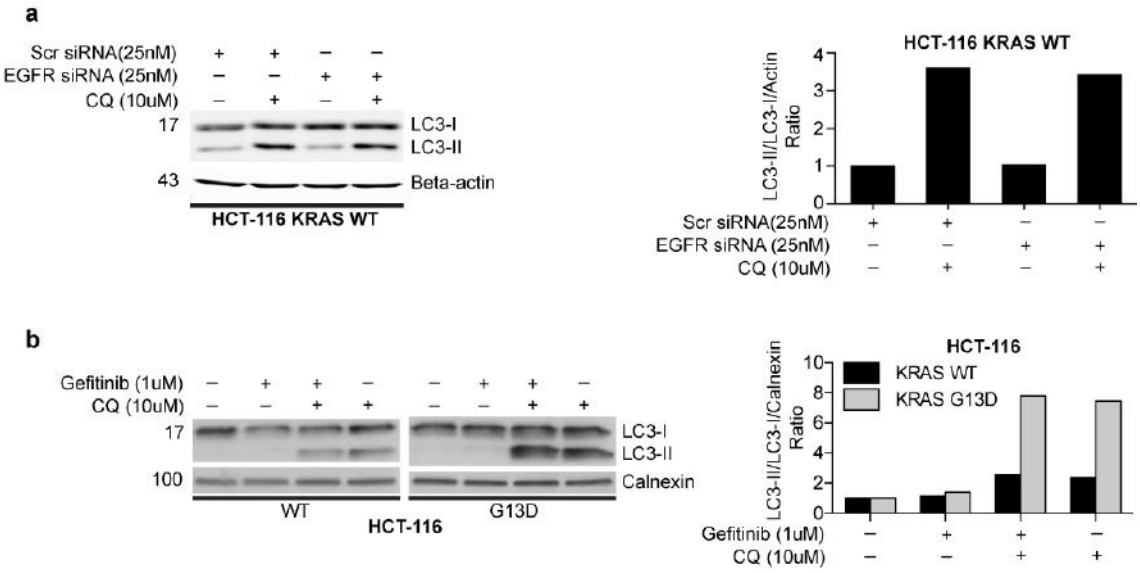

Figure 3. 12: Examination of autophagy induction upon EGFR siRNA and Gefitinib treatment in HCT-116 cells. Autophagy is not induced upon **a** EGFR siRNA and **b** Gefitinib treatment. Left: western blotting analysis of LC3B protein levels. Right: Bar plots represent densitometric analysis of LC3-II/LC3-I levels normalised to loading control observed by western blotting. Beta-actin or calnexin used as loading controls. Cells treated with 25 nM of scramble or EGFR siRNAs for 48 hours and +/- 10 μM CQ added to the culture medium 6 hours before cell lysis to enable monitoring of autophagic flux. For Gefitinib experiments, cells were treated with 1 μM Gefitinib +/- 10 μM CQ for 6 hours. Scr= scramble. Autophagy induction experiment following either EGFR siRNA or Gefitinib treatment in HCT-116 cells was performed once.

Overall, these findings show that inhibition of EGFR by multiple approaches fails to induce autophagy with the exception of DiFi cells. Autophagy induction following EGFR inhibition in DiFi cells correlates with the inhibitory effect of Cetuximab on AKT phosphorylation (Figure 3. 6.e).

3.2.11. Lack of autophagy induction upon EGFR inhibition correlates with *PI3K* mutational status or EGFR-independent mechanisms for AKT activation

The observation that there was a correlation between autophagy induction and AKT inhibition upon Cetuximab treatment prompted us to investigate in depth the mutational status of *PI3K* across the different CRC cell lines used. To address that, the Broad Institute Cancer Cell Line Encyclopedia and the Cosmic websites were used to investigate the mutational status of different components of the PI3K pathway in these cells.

It was found that HCT-116, DLD-1 and SW48 cell lines carry various mutations in different components of the PI3K pathway (Table 3. 2). For CaCo2 cells no mutations in PI3K pathway components were found implying that CaCo2 cells are WT for these genes. Finally, for DiFi cells there was no available information in either website.

Table 3. 2: Mutational status of HCT-116, DLD-1 and SW48 CRC cell lines.

Cell line	EGFR	KRAS	PIK3CA	PTEN	AKT	mTOR
HCT-116	-	p.G13D H	p.H1047R-low FI	3' UTR- del	-	-
DLD-1	-	p.G13D H p.P110H	p.E545K-medium FI p.D549N-medium FI	p.Q87P-low FI p.P96S-high FI p.D153Y-low FI	-	-
SW48	p.G719S H- high FI	-	p.G914R-medium FI	3' UTR-del	AKT3-p.R465Q-medium FI AKT2-p.R251W-high FI	p.V2389_splice

* H= Heterozygous **FI= Functional Impact

Data collected by the Broad Institute Cancer Cell Line Encyclopedia and Cosmic Websites

The mutations found in the *PIK3CA* gene warranted further investigation. *PI3KCA* encodes the catalytic subunit of PI3K, p110 and its mutations have been previously implicated in Cetuximab resistance (De Roock *et al.*, 2011). To confirm the mutations reported in the two search engines that were utilised, we designed sequencing primers specific for the identification of each point mutation and all CRC cell lines were screened for *PI3K* mutations (residues p.E545, p.D549, p.G914 and p.H1047). DLD-1 *KRAS* WT and G13D isogenic cell lines were found to harbour E545K and D549N activating mutations of the *PIK3CA* gene (Figure 3. 13 and 3. 14). SW48 *KRAS* isogenic cell lines instead harbour only the G914R *PIK3CA* mutation (Figure 3. 15). For the H1047R *PIK3CA* activating mutation, only HCT-116 *KRAS* isogenic cell lines were found to be positive (Figure 3. 16). Finally, CaCo2 and DiFi cells were shown to be WT for any of the four different point mutations screened (Figures 3. 13 - 3. 16).

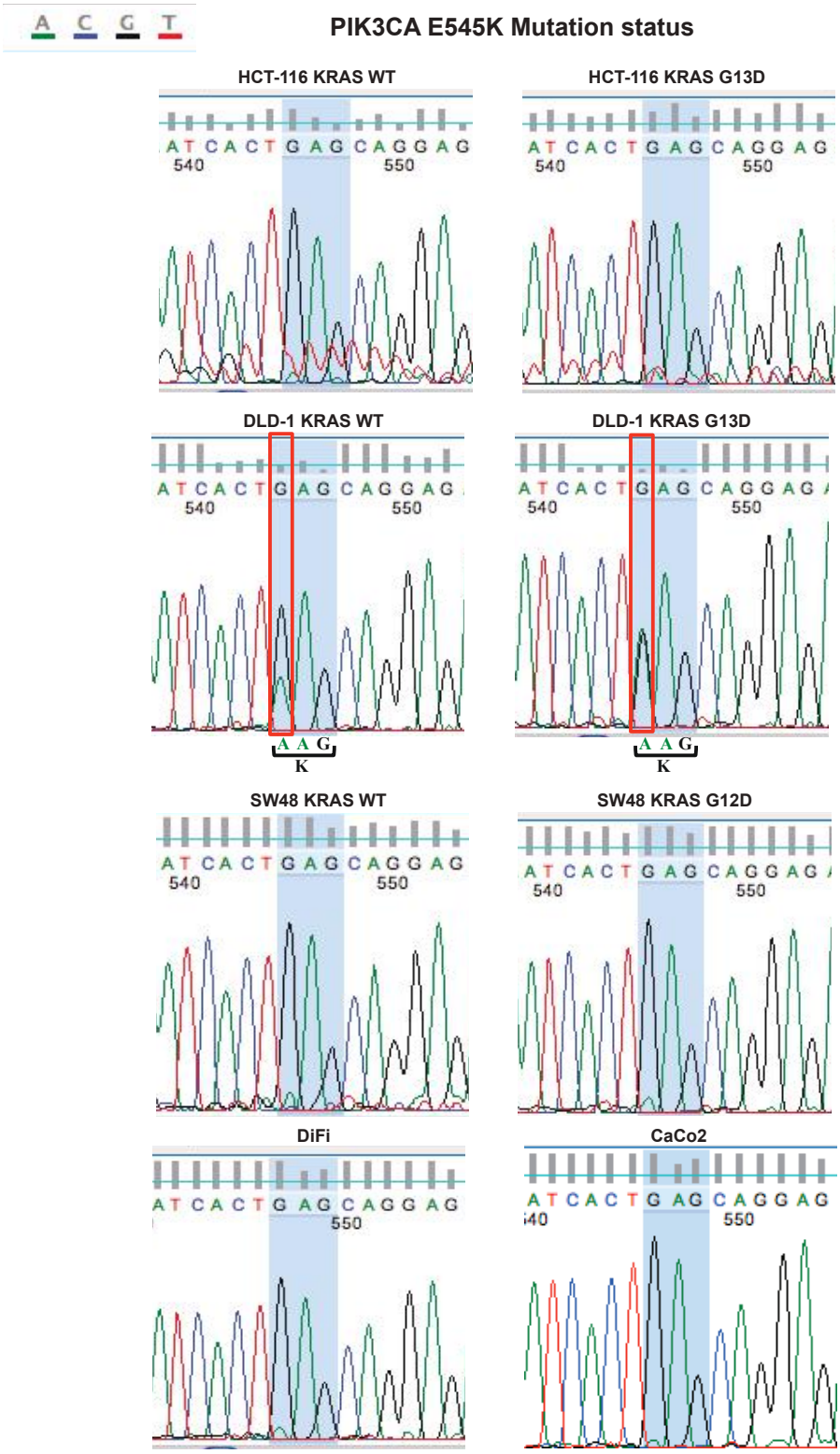

Figure 3. 13: Examination of *PIK3CA* mutational status at E545 residue. Only DLD-1 *KRAS* WT and G13D cells were found to harbour E545K *PIK3CA* activating mutation. E= Glutamic acid, K= Lysine, Green/A= Adenine, Blue/C= Cytosine, Black/G= Guanine and Red/T= Thymine. *PIK3CA* mutation screening experiment was conducted once in each cell line tested.

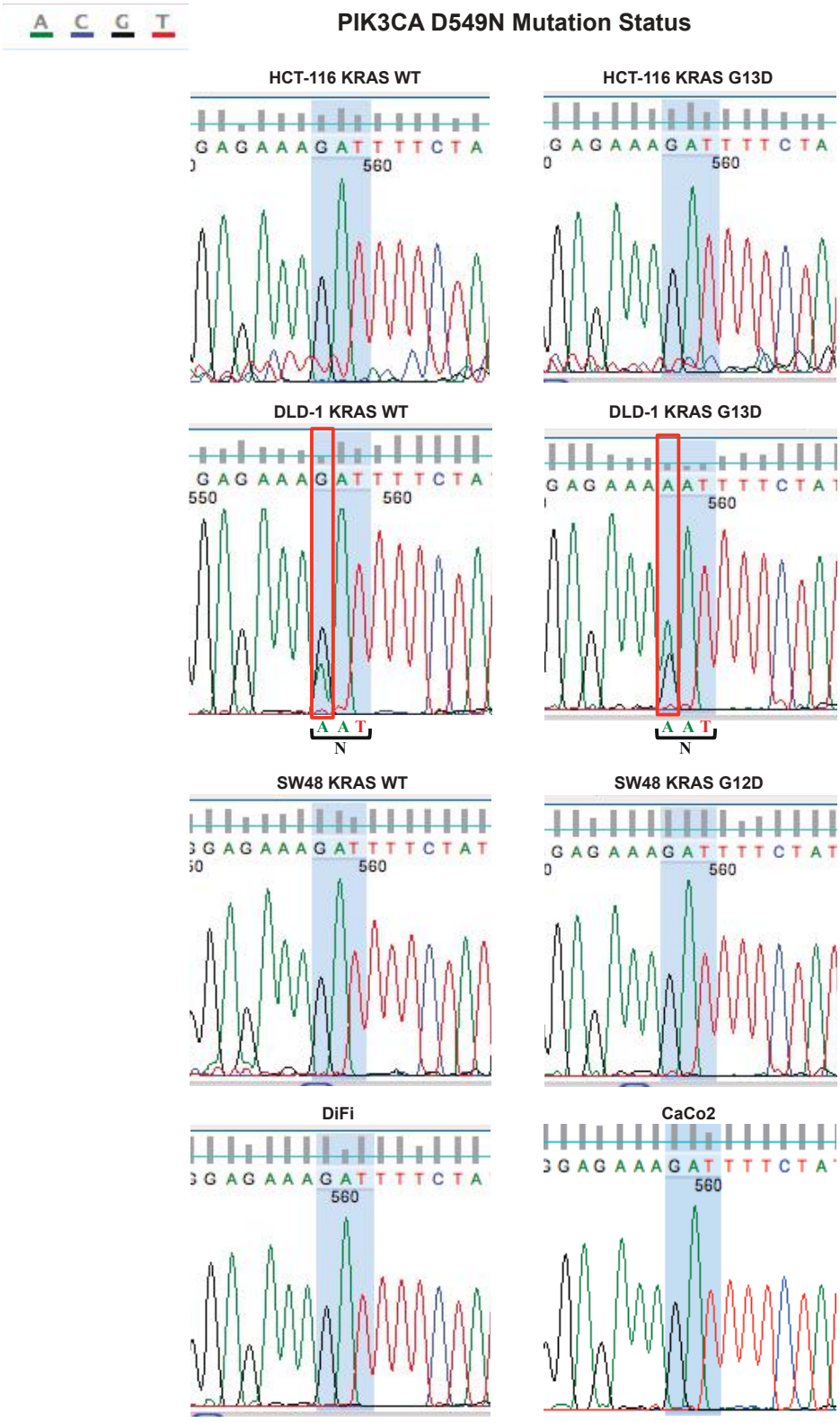

Figure 3. 14: Examination of *PIK3CA* mutational status at D549 residue. Only DLD-1 *KRAS* WT and G13D cells were found to harbour D549N *PIK3CA* activating mutation. D= Aspartic acid, N= Asparagine, Green/A= Adenine, Blue/C= Cytosine, Black/G= Guanine and Red/T= Thymine. *PIK3CA* mutation screening experiment was conducted once in each cell line tested.

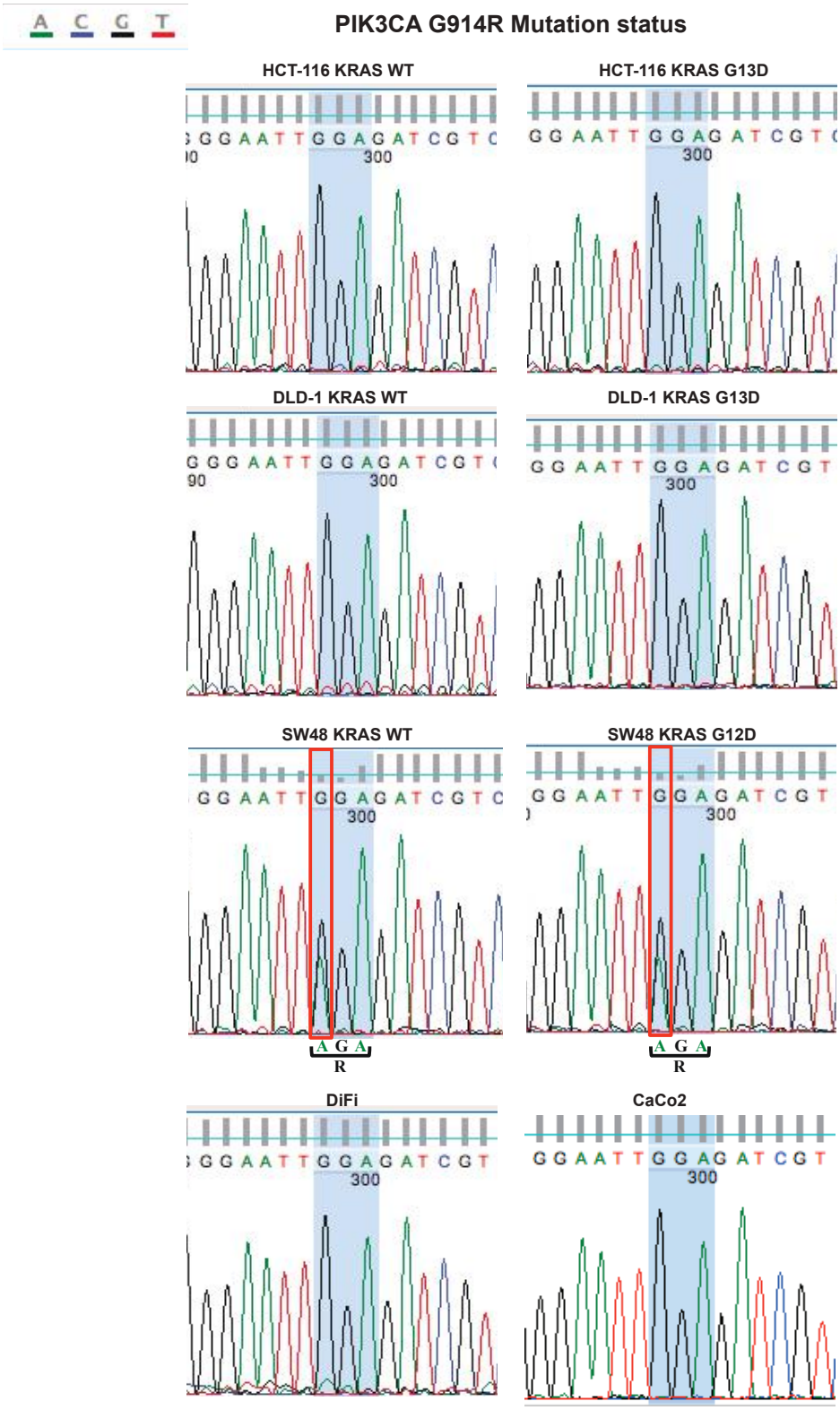

Figure 3. 15: Examination of *PIK3CA* mutational status at G914 residue. Only SW48 *KRAS* WT and G12D cells were found to harbour G914R *PIK3CA* activating mutation. G= Glycine, R= Arginine, Green/A= Adenine, Blue/C= Cytosine, Black/G= Guanine and Red/T= Thymine. *PIK3CA* mutation screening experiment was conducted once in each cell line tested.

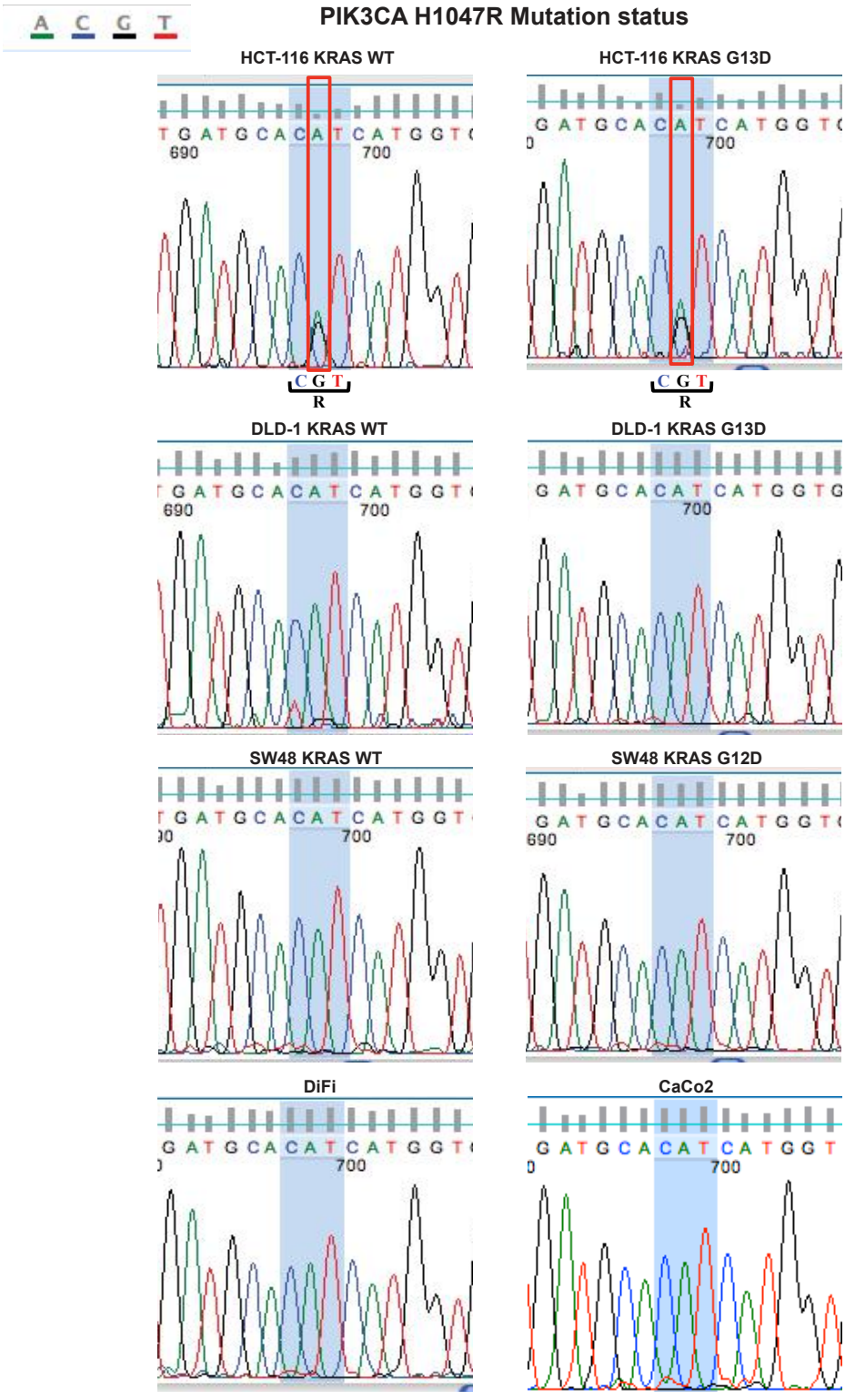

Figure 3. 16: Examination of *PIK3CA* mutational status at H1047 residue. Only HCT-116 *KRAS* WT and G13D cells were found to harbour H1047R *PIK3CA* activating mutation. H= Histidine, R= Arginine, Green/A= Adenine, Blue/C= Cytosine, Black/G= Guanine and Red/T= Thymine. *PIK3CA* mutation screening experiment was conducted once in each cell line tested.

In conclusion, *PIK3CA* activating mutations inversely correlated with inhibition of AKT phosphorylation and autophagy induction upon Cetuximab treatment, suggesting that the *PIK3CA* mutational status may be the main factor in dictating the autophagic response to EGFR inhibition. However, an exception to this rule is CaCo2 cells, which failed to downregulate the PI3K pathway and induce autophagy upon Cetuximab treatment despite their *PIK3CA* WT status. Which is the factor responsible for the lack of autophagy induction upon EGFR inhibition in CaCo2 cells? I hypothesised that a RTK other than EGFR alone controls PI3K activity in CaCo2 cells. I thought to investigate whether ErbB2 RTK is implicated. ErbB2 belongs to ErbB family of receptors, is incompetent for growth-factor stimulation and therefore creates heterodimers with EGFR, which are responsible for Cetuximab resistance in many cases (Vlacich and Coffey, 2011, Lemmon *et al.*, 2014). Thereby the potential implication of ErbB2 RTK was investigated.

To address this, a dual EGFR and ErbB2 tyrosine kinase inhibitor, Lapatinib, was used. CaCo2 cells were cultured in the presence of 1 μM or 2 μM of Lapatinib in combination with 50 μg/ml Cetuximab and/or 10 μM CQ for 24 hours. Activation levels of EGFR pathway and downstream effectors as well as autophagy induction were examined by western blotting. Lapatinib alone as well as Lapatinib and Cetuximab combinational treatment were more potently downregulating EGFR activation levels when compared to Cetuximab treatment alone (Figure 3. 17.b). The MAPK/ERK pathway was evenly downregulated in 1 μM Lapatinib and Cetuximab alone conditions and more potently upon 2 μM Lapatinib treatment alone or Lapatinib and Cetuximab combinational treatment (Figure 3. 17.c). PI3K pathway was downregulated evenly in 1 μM Lapatinib and Cetuximab alone treatments but more potently in the 2 μM Lapatinib treatment and Lapatinib and Cetuximab combinational treatments. Additionally, CQ treatment alone or in combination with Lapatinib; Cetuximab treatment alone or with Cetuximab and Lapatinib co-treatment downregulated AKT activation levels (Figure 3. 17.d). Finally, both 1 and 2 μM of Lapatinib were able to induce autophagy in CaCo2 cells with 2 μM of Lapatinib that more potently downregulated pAKT to induce autophagy in a higher level (Figure 3. 17.e). Even though Lapatinib and Cetuximab co-treatment resulted in a greater downregulation of pAKT levels, autophagy was not induced in a proportional way to pAKT downregulation (Figure 3. 17.e). This observation could imply that Cetuximab in combination with Lapatinib results in downregulation of autophagy. However, further investigation is needed since Lapatinib alone and Lapatinib and Cetuximab co-treatment samples were analysed in different western blotting gels and CQ alone control found to have a different pattern between the two examined gels.

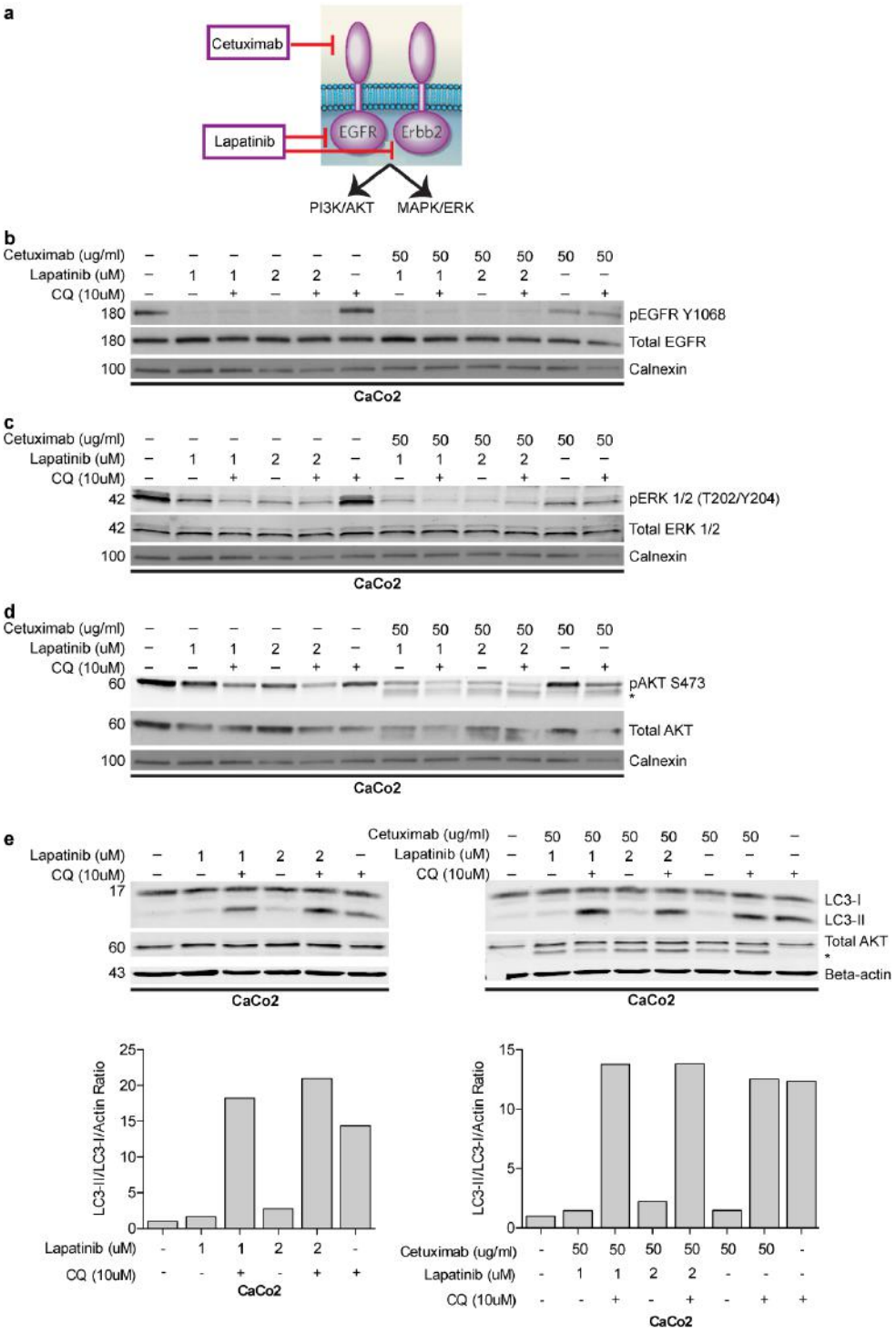

Figure 3. 17: EGFR and ErbB2 inhibition experiment by Lapatinib in Caco2 cells. a Schematic representation of Cetuximab and Lapatinib mode of action; **b** EGFR; **c** MAPK/ERK pathway; **d** PI3K pathway activation levels and **e** autophagy levels upon Lapatinib/Cetuximab treatment alone and Lapatinib/Cetuximab co-treatment. Bar plots represent densitometric analysis of LC3-II/LC3-I levels normalised to beta-actin observed by western blotting. 1 µM and 2 µM of Lapatinib, 50 µg/ml Cetuximab and 10 µM CQ were used for 24 hours. Phosphorylation levels of EGFR, ERK and AKT proteins reflect activation levels of EGFR, MAPK/ERK and PI3K pathways respectively. LC3-II/LC3-I levels normalised to beta-actin depicts levels of autophagy. Calnexin and beta-actin used as western blotting loading controls. ***** Represents heavy chain of Cetuximab antibody in Cetuximab treated cells that were detected at 55kDa below pAKT and total AKT bands. p= phosphorylated. **Note**: in **d** Total AKT antibody did not work well so total AKT results were re-blotted and are shown in **e**. Equal AKT levels were observed between all drug-treated conditions. The presented experiment was conducted once.

3.2.12 AKT pharmacological inhibition rescues autophagy induction in *PIK3CA*-mutated CRC cells, whereas constitutively active AKT inhibits autophagy in *PIK3CA*-WT cells

We next tested whether the use of the AKT vIII inhibitor could rescue induction of autophagy in *PIK3CA*-mutated cells. It is known that AKT can modulate autophagy either in an mTORC1 dependent manner or directly by phosphorylating Beclin1 (previously discussed in 1.1.2.2.). The E545K and D549N *PIK3CA* mutant DLD-1 *KRAS* WT and mutant cells were cultured in the presence of 2 μM and 5 μM of AKT vIII inhibitor alone or in combination with 50 μg/ml Cetuximab and/or 10 μM of CQ for 24 hours. AKT vIII treatment alone resulted in an upregulation of EGFR activation levels in DLD-1 *KRAS* mutant cells, whereas AKT vIII/Cetuximab co-treatment abolished EGFR activation in both *KRAS* isogenic versions of DLD-1 cells examined (Figure 3. 18.a). ERK activation levels were increased in DLD-1 *KRAS* WT cells but were unaffected in DLD-1 *KRAS* G13D cells upon AKT vIII treatment alone. Cetuximab treatment alone or in combination with AKT vIII inhibitor suppressed pERK levels in both DLD-1 *KRAS* WT and G13D cells (Figure 3. 18.b). Additionally, 6 hours of CQ treatment alone resulted in downregulation of pERK levels in both *KRAS* isogenic versions of DLD-1 cells examined (Figure 3. 18.b), in contrast to more extended CQ treatment (Figure 3. 10.a). Finally, the AKT vIII inhibitor alone or in combination with Cetuximab was able to downregulate pAKT levels compared to untreated or Cetuximab-only treated controls (Figure 3. 18.c). Critically, in the conditions where pAKT levels were abolished, apart from treatments with 5 μM of AKT vIII inhibitor or Cetuximab treatment alone, autophagy was induced upon AKT vIII inhibitor treatment alone or in combination with Cetuximab. As previously observed, Cetuximab treatment alone was unable to induce autophagy in both DLD-1 *KRAS* WT and G13D cells (Figure 3. 18.c).

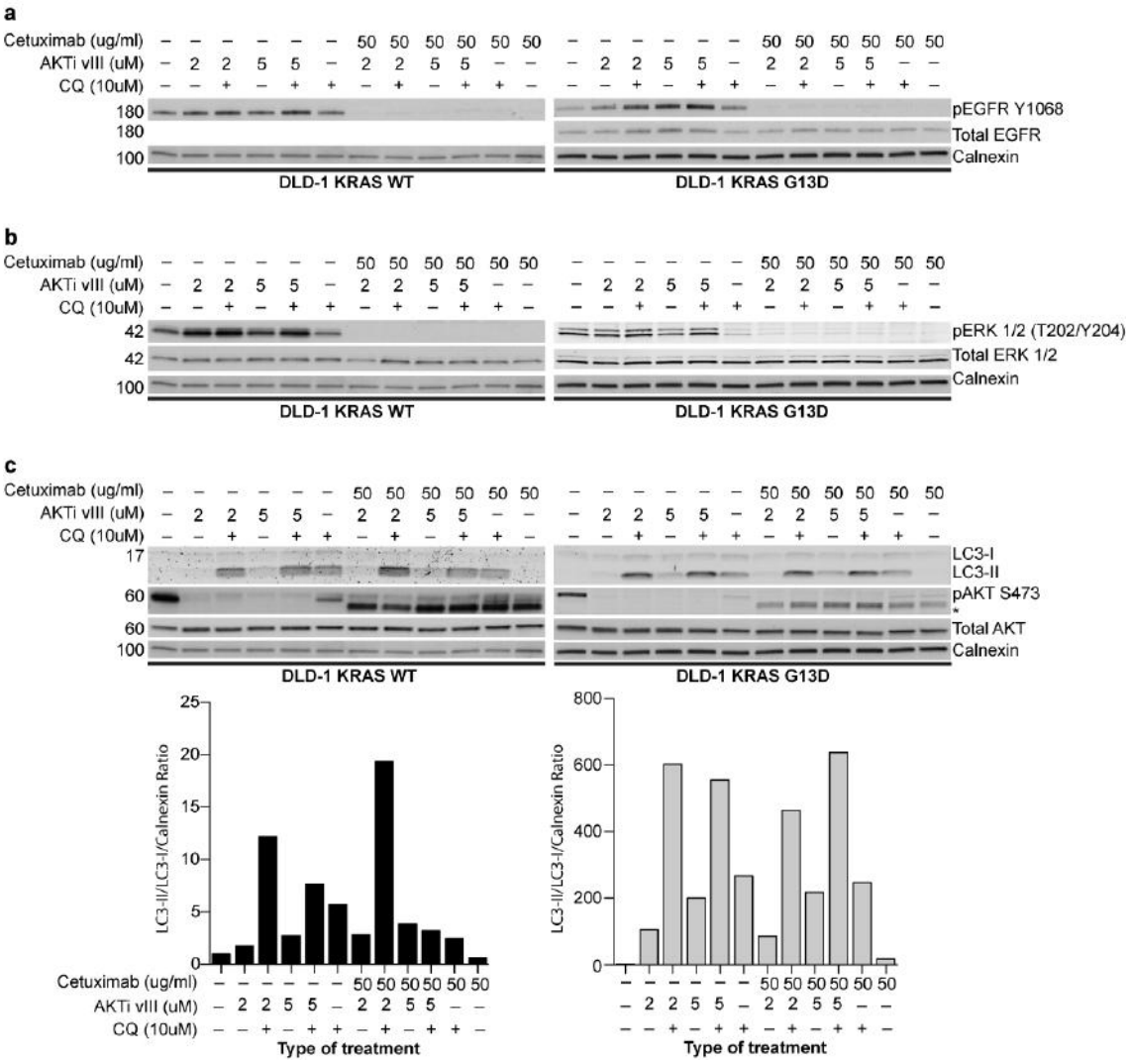

Figure 3. 18: AKT inhibition induces autophagy in *PIK3CA* mutant cells. a EGFR; **b** MAPK/ERK pathway and **c** PI3K pathway and autophagy levels upon AKT vIII inhibitor alone or in combination with Cetuximab in DLD-1 *KRAS* WT and G13D cells. Bar plots represent densitometric analysis of LC3-II/LC3-I levels normalised to calnexin observed by western blotting. 2 µM and 5 µM AKT vIII, 50 µg/ml Cetuximab and 10 µM CQ were used for 24 hours. Phosphorylation levels of EGFR, ERK and AKT proteins reflect activation levels of EGFR, MAPK/ERK and PI3K pathways respectively. LC3-II/LC3-I levels normalised to calnexin depicts levels of autophagy. Calnexin used as western blotting loading controls. ***** Represents heavy chain of Cetuximab antibody in Cetuximab treated cells that were detected at 55kDa below pAKT bands. **Note**: in **a** Total EGFR antibody did not work for DLD-1 *KRAS* WT cells and need to be repeated. p= phosphorylated. The experiment was conducted once.

Finally, in order to identify a direct link between AKT activation levels and autophagy induction upon Cetuximab treatment, I generated DiFi cells stably expressing myristoylated-AKT (LXSN_myrAKT). N-Myristoylation is a lipidation modification in which a 14-carbon fatty acid, myristate, is covalently attached to the N'-terminal glycine of a target protein by a N-myristoyltransferase either co- or post-translationally and results in its plasma membrane localisation (Martin *et al.*, 2011). It

has been shown that myristoylated-AKT protein is localised to the plasma membrane and remains constitutively active (Klippel *et al.*, 1996, Wang *et al.*, 2012).

We hypothesised that AKT constitutive activation would decrease Cetuximab-dependent autophagy induction in DiFi cells, which was the only cell line found to induce autophagy upon Cetuximab treatment (Figure 3. 6.e). For that reason, LXSN and LXSN_myrAKT DiFi cells were cultured in the presence of 50 µg/ml Cetuximab with or without 10 µM CQ for 24 hours. As expected, cells overexpressing myrAKT displayed higher pAKT levels at both steady state and upon Cetuximab treatment (Figure 3. 19.a). Interestingly, increased pERK levels were observed in LXSN_myrAKT DiFi cells at steady state. pERK and pEGFR levels were reduced upon Cetuximab treatment in both control and LXSN_myrAKT DiFi cells (Figure 3. 19.b). As initially hypothesised, the increased activation levels of AKT in LXSN_myrAKT DiFi cells resulted in lower autophagy induction levels upon Cetuximab treatment when compared with control DiFi cells (Figure 3. 19.a), implying a direct link between AKT activation status and autophagy induction in CRC cells upon Cetuximab treatment. In line with previous observations in Figure 3. 8.e and 3. 9.e, CQ treatment alone downregulated EGFR and AKT activation levels in control DiFi cells. However, CQ inhibited EGFR activation but not AKT activation in LXSN_myrAKT DiFi cells (Figure 3. 19.a and b).

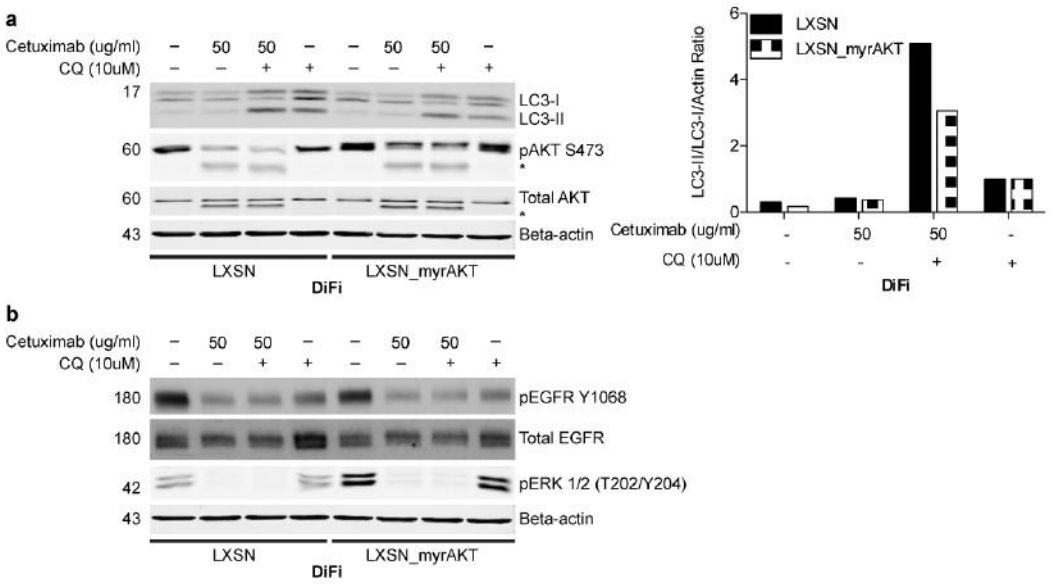

Figure 3. 19: Reduced autophagy induction upon Cetuximab treatment in myristoylated AKT overexpressing DiFi cell line. a autophagy and PI3K; **b** EGFR and MAPK/ERK pathway activation levels in control and myristoylated AKT overexpressing DiFi cell lines. Bar plot represents densitometric analysis of LC3-II/LC3-I levels normalised to beta-actin observed by western blotting. 50 µg/ml Cetuximab +/- 10 µM CQ for 24 hours were used. Phosphorylation levels of EGFR, ERK and AKT proteins reflect activation levels of EGFR, MAPK/ERK and PI3K pathways respectively. LC3-II/LC3-I levels normalised to beta-actin depicts levels of autophagy. Beta-actin used as western blotting loading controls. ***** Represents heavy chain of Cetuximab antibody in Cetuximab treated cells that were detected at 55kDa below pAKT and total AKT bands.

3.3. Discussion

3.3.1. Activation of MAPK/ERK and PI3K pathways may regulate the response of CRC cells to EGFR targeted therapy

EGFR is often deregulated in a variety of solid cancers and the development of EGFR targeted therapy revolutionised cancer therapeutics. However, primary or acquired resistance to targeted therapy limits the effectiveness of such approaches. *KRAS* oncogene represents the only molecular biomarker that is used for CRC patients' selection in EGFR targeted therapy approaches (information taken from FDA website). *KRAS* oncogene activation has been inversely correlated to Cetuximab response and patients with *KRAS* mutations were not found to benefit from Cetuximab treatment (Benvenuti *et al.*, 2007, Karapetis *et al.*, 2008). Although, Cetuximab treatment is only approved for *KRAS* WT metastatic CRC patients, their response to therapy is differential and only a small subgroup could benefit from it (De Roock *et al.*, 2011).

A panel of *KRAS* WT and mutant isogenic (when available) CRC cell lines was utilised in this work to investigate the response to Cetuximab treatment *in vitro*. In line with the literature, *KRAS* activating mutations were found to deteriorate responses to Cetuximab treatment in SW48 and DLD-1 *KRAS* isogenic cells (Figure 3. 4). Additionally, CaCo2 cells, which were heterozygous for *KRAS* G12S mutation, were resistant to Cetuximab treatment (Figure 3. 4.). However, activation of *KRAS* oncogene is not the only factor controlling response to Cetuximab treatment since *KRAS* WT CRC cells (HCT-116, SW48, DLD-1 and DiFi cells) present differential response to EGFR inhibition (Figure 3. 4). This work reinforces the theory that the existence of molecular factors other than *KRAS* activation, affect CRC patients' response to Cetuximab treatment.

Moroni *et al*., (2005) suggested EGFR amplification as a positive regulator of response to EGFR monoclonal antibody-targeted therapy in CRC (Moroni *et al.*, 2005). The correlation of high EGFR levels and sensitivity to Cetuximab that was observed in the high sensitivity group (DiFi; Figures 3. 3 - 3. 4) could be explained by the existence of *EGFR* gene amplification in these cells. DiFi cells were the first CRC cell line described to harbour *EGFR* amplification in the range of 60-80 copies per cell (Untawale *et al.*, 1993). However, *EGFR* amplification does not frequently occur in CRC (Shia *et al.*, 2005). If Cetuximab response was dictated by *EGFR* amplification, one might expect that refractory CRC cells would be characterised by low EGFR copy numbers. Although, HCT-116, DLD-1 and SW48 cells present low *EGFR* copy numbers (Moroni *et al.*, 2005), SW48 and DLD-1 cells have reduced cell growth following EGFR targeted therapy (Figure 3. 4). Additionally, EGFR expression in the

Cetuximab-sensitive group (DLD-1) is lower compared to the Cetuximab-intermediate resistance group (SW48) (Figures 3. 3 - 3. 4). Overall, these observations suggest that EGFR expression levels might not be implicated to Cetuximab treatment response. Similarly, previous studies have shown that there is no correlation between EGFR expression status and response to Cetuximab or Panitumumab treatment (Chung *et al.*, 2005, Hecht *et al.*, 2010). A possible scenario to explain the high sensitivity of DiFi cells to Cetuximab treatment could be that cells with *EGFR* amplification are highly dependent on EGFR activation for survival. Indeed, DiFi cells present the highest EGFR activation and respond to lower Cetuximab concentrations compared to the other responsive cells lines SW48 and DLD-1 (Figures 3. 3 - 3. 4). Based on these observations, we could hypothesise that EGFR activation may control response to Cetuximab treatment. However, SW48 cells, which exhibit higher EGFR activation compared to DLD-1 cells, are more resistant to Cetuximab treatment (Figures 3. 3 - 3. 4). The latter observation may rule out the likelihood EGFR activation to control CRC cells to Cetuximab treatment. A positive correlation between high gene expression of EGFR-ligands, like EREG and AREG and longer progression-free survival in Cetuximab-treated CRC patients has been described (Khambata-Ford *et al.*, 2007). Even though a correlation between EGFR-ligand production and Cetuximab response was not investigated in this work, a higher autocrine production of EGFR-ligands may be present in DLD-1 cells explaining their sensitivity to Cetuximab. Interestingly, EGFR expression levels were not positively correlated with activation levels of EGFR in DLD-1 cells. DLD-1 cells exhibit relatively high EGFR activation albeit low EGFR levels compared to SW48 and DiFi cells (Figure 3. 3), an observation that cannot be generalised for the other CRC cell lines. Collectively, factors such as: i) high *EGFR* amplification, ii) increased EGFR-ligand production and/or iii) increased dependency to EGFR in CRC cells could explain in certain cases the beneficial response to Cetuximab.

High genomic instability and genetic heterogeneity characterise the molecular pathology of CRC (discussed in 1.4.2., page 47). Aside from *KRAS* mutations, activation of *BRAF* and *PI3K* oncogenes have been described to occur in CRC (Misale *et al.*, 2014). A variety of studies have reported an implication of *BRAF* mutation V600E to Cetuximab resistance (Di Nicolantonio *et al.*, 2008, Laurent-Puig *et al.*, 2009, De Roock *et al.*, 2011, Ashraf *et al.*, 2012). However, this mechanism cannot explain the differential response to Cetuximab in this study, as all CRC cell lines examined were *BRAF* WT (Cosmic website).

PI3K oncogene activation has been suggested to confer resistance to EGFR targeted therapy in pre-clinical (Jhawer *et al.*, 2008, Ashraf *et al.*, 2012) and clinical studies (De Roock *et al.*, 2010). *PIK3CA* exon 9 and 20 activating mutations are

present in CRC patients, although only mutations in exon 20 positively correlate with resistance to Cetuximab (Ashraf *et al.*, 2012). Furthermore, *PIK3CA* exon 20 mutation was found to deteriorate Cetuximab response in HCT-116 *PIK3CA* isogenic cell lines (Jhawer *et al.*, 2008). On the other hand, *PIK3CA* exon 9 mutations were found unable to confer resistance to Cetuximab treatment in both pre-clinical and clinical models (Ashraf *et al.*, 2012, Pentheroudakis *et al.*, 2013, Karapetis *et al.*, 2014). Interestingly, three out of five CRC cell lines utilised in this work were harbouring activating mutations in *PIK3CA* gene (Figures 3. 13 - 3. 16). In particular, HCT-116 cells were heterozygous for H1047 *PIK3CA* mutation located at exon 20, whereas DLD-1 cells were heterozygous for both E545K and D549N *PIK3CA* mutations located at exon 9. The different exon localisation of *PIK3CA* mutations between HCT-116 and DLD-1 cells, may explain the total refractory response of HCT-116 cells to Cetuximab treatment and responsive phenotype of DLD-1 cells. G914R *PIK3CA* mutation present in SW48 cells has not been correlated to Cetuximab treatment response. A positive correlation between *PI3K* mutational status and sustained AKT activation levels following EGFR inhibition was identified in this work (Figure 3. 9). All cell lines with sustained AKT activation levels following EGFR inhibition were found to harbour *PI3K* activating mutations, with the exception of CaCo2 cells. CaCo2 cells despite their *PI3K* WT status, sustained AKT activation upon Cetuximab treatment. Nevertheless, when ErbB2 was concomitantly inhibited with EGFR in CaCo2 cells, AKT activation levels were downregulated (Figure 3. 17.d), suggesting that activation of ErbB2 restricts AKT inhibition. Work from Luca *et al*., (2014) shows that the response of CaCo2 cells to Cetuximab treatment was potentiated in EGFR and ErbB2 combinational therapy (Luca *et al.*, 2014). Of note, despite the fact that *PIK3CA* exon 20 mutations have been linked to Cetuximab refractory response, regulation of AKT downstream of *PI3K* mutations has not been evaluated in this setting (Jhawer *et al.*, 2008).

EGFR downstream signalling pathways are primarily MAPK/ERK and PI3K. It was therefore reasonable to investigate whether their activation is affecting Cetuximab resistance. This work suggests that differential activation/inhibition of MAPK/ERK and PI3K pathways downstream of EGFR may define Cetuximab response in *KRAS* WT CRC cells. Response to Cetuximab treatment was found to inversely correlate with the activation levels of PI3K/AKT and MAPK/ERK pathways downstream of EGFR. In particular, only the Cetuximab-high sensitivity group (DiFi) presenting a potential cytotoxic phenotype exhibited concomitantly PI3K/AKT and MAPK/ERK pathway inhibition (Figures 3. 9.e and 3. 10.e). On the contrary, the Cetuximab-resistant group (HCT-116) exhibiting neither a cytotoxic nor cytostatic phenotype, sustained high activation levels of both PI3K/AKT and MAPK/ERK pathways (Figures 3. 9.b and 3. 10.b). Cetuximab-intermediate resistance (SW48) and sensitive group (DLD-1)

presenting an intermediate and more profound cytostatic phenotype respectively, showed only MAPK/ERK pathway inhibition (Figures 3. 9 and 3. 10). In support of this, ERK activation levels were sustained in *KRAS* mutant SW48 and DLD-1 cells resulting in less potent Cetuximab response (Figures 3. 4 and 3. 10). A possible scenario could be that inhibition of ERK reduces cell growth and AKT regulates cell death response following EGFR inhibition. Previous studies in DiFi cells have shown that they induce apoptosis upon Cetuximab treatment (Karnes *et al.*, 1998, Liu *et al.*, 2000), confirming the suggested cytotoxic effect observed in our work. Nevertheless, the potential cytotoxic effect of Cetuximab in DiFi cells could be AKT activation-independent since DiFi cells are exceptionally sensitive to EGFR inhibition compared to other CRC cell lines. Whether ERK and AKT inhibition control cell growth and cell death, respectively following EGFR inhibition needs to be determined.

Genetic deregulation of *EGFR*, *KRAS*, *BRAF* and *PIK3CA* cannot systematically explain the differential response of CRC cells to Cetuximab treatment in our work. A more complex network of interactions having as end-point regulators, MAPK/ERK and PI3K pathways, may dictate differential response of CRC cells to EGFR inhibition.

3.3.2. The majority of CRC cell lines are refractory to autophagy induction following EGFR targeted therapy and do not benefit from EGFR-autophagy combinational therapy

Induction of autophagy following cancer treatment has been previously described as a resistance mechanism, enabling cancer cells to survive and fulfil their elevated metabolic needs (Amaravadi *et al.*, 2011, Rebecca and Amaravadi, 2015). Autophagy is induced in various cancer types such as NSCLC, breast cancer and glioblastoma following EGFR inhibition (Eimer *et al.*, 2011, Dragowska *et al.*, 2013, Wei *et al.*, 2013). Hitherto, the relationship between autophagy and EGFR inhibition in CRC is elusive and the role of autophagy in EGFR targeted therapy response of CRC has not been studied in depth. As was previously discussed, CRC cell lines present differential responses to EGFR targeted therapy and the molecular factors controlling their resistance are not fully characterised. This work aimed to identify whether autophagy is implicated in differential response and/or resistance of CRC cells to EGFR targeted therapy. It was shown that the majority of CRC cell lines tested were refractory to autophagy induction following EGFR inhibition by Cetuximab. Autophagy was solely induced in DiFi cells (Figure 3. 6). This phenomenon is not attributed to a general incompetence of CRC cells to induce autophagy since these cells efficiently respond to autophagy-inducing compounds (Figure 3. 5). Additionally, the refractory autophagic

response to Cetuximab treatment could not be caused by a specific inefficiency of Cetuximab to induce autophagy. Gefitinib and EGFR downregulation approaches that we used showed consistently with Cetuximab that EGFR modulation does not induce autophagy in HCT-116 cells (Figure 3. 12). Hitherto, there is no published work evaluating autophagy induction upon Cetuximab treatment in CRC. The only available information is limited to two studies, which included DiFi cells and confirm our findings for autophagy induction upon Cetuximab treatment (Li and Fan, 2010, Li *et al.*, 2010). Earlier studies reported that autophagy induction upon EGFR inhibition is a characteristic of sensitive to therapy-only NSCLC cells and that resistant cells do not induce autophagy (Li *et al.*, 2013b, Wei *et al.*, 2013). Other studies described that autophagy induction following EGFR inhibition is more pronounced in resistant NSCLC cell lines (Han *et al.*, 2011, Zou *et al.*, 2013). However, our results do not indicate such a correlation since both resistant (HCT-116 and CaCo2) and sensitive (DLD-1) CRC cells are refractory to autophagy induction following EGFR inhibition (Figures 3. 4 and 3. 6). Additionally, neither EGFR activation nor EGFR expression levels could be correlated with variability in autophagy induction following EGFR inhibition in my research. High EGFR expressing cells such as SW48 and DiFi cells were either refractory or competent to autophagy induction following EGFR inhibition, suggesting that EGFR expression levels may not determine autophagic behaviour of CRC cells following Cetuximab treatment (Figures 3. 3 and 3. 6.c and e). Similarly, EGFR activation levels could not determine autophagy induction upon Cetuximab treatment, since DLD-1 and SW48 cells exhibiting high pEGFR are refractory to autophagy induction (Figure 3. 3 and 3. 6.a and c).

The study by Li *et al.*, (2010) reported an apoptosis-dependent concept for autophagy induction following Cetuximab treatment in a panel of cancer cells. In particular, this study suggested a model where autophagy is induced only in cells presenting extensive or moderate levels of apoptosis upon Cetuximab treatment, whereas cells having only a cytostatic phenotype following Cetuximab treatment are refractory to autophagy induction. DiFi cells were included in this study and it was shown that Cetuximab treatment induced both apoptosis and autophagy. In turn, inhibition of Cetuximab-induced apoptosis (either by using a broad-spectrum caspase inhibitor or Cetuximab-resistant DiFi cells) abolished autophagy induction (Li *et al.*, 2010). Detailed investigation of apoptosis or cell growth arrest induction following EGFR inhibition has not been investigated in our work, however the latter model may apply to our findings. As was previously discussed, Cetuximab treatment was suggested to play a cytotoxic role in DiFi cells, which were competent for autophagy induction following EGFR inhibition. In turn, Cetuximab was suggested to play a cytostatic role in DLD-1 and SW48 cells that were refractory to autophagy induction

following EGFR inhibition. Further investigation defining any correlation between apoptosis and autophagy induction in CRC cells is warranted. However, findings by Li *et al*., (2010) should be considered with caution since results could be attributed to a cell-line specific biological behaviour to Cetuximab treatment rather than a generalisable biological phenomenon, as only one or two different cell lines in each category that originated from different cancer types were examined.

Earlier studies have reported that autophagy is induced following EGFR inhibition in a variety of cancer cell lines. However our work suggests that caution should be taken when generalising these findings. Not all cell lines induce autophagy following EGFR inhibition. Experimental differences may cause variability and misinterpretation of findings between studies. In our work, autophagic flux determination via western blotting was used to assess autophagy induction following EGFR inhibition, an approach not followed by a number of studies. Autophagy induction was monitored by either evaluating only the levels of LC3-II accumulation without using lysosomotropic compounds or where lysosomotropic compounds were used basal and EGFR-induced autophagic flux was not compared (Han *et al.*, 2011, Li *et al.*, 2013b, Zou *et al.*, 2013). Additionally in our work, autophagy induction following EGFR inhibition was mainly studied by using Cetuximab, which is a monoclonal antibody specifically targeting EGFR and limiting in such way non-specific inhibition/activation of molecular factors regulating autophagy. Reliability of findings was confirmed by investigating autophagy induction with alternative pharmacological EGFR inhibitors other than Cetuximab (i.e. Gefitinib) and EGFR downregulation approaches. Other studies evaluated autophagy induction by using solely a single EGFR inhibitor approach, which in some cases include TKI, such as Erlotinib and Gefitinib, in non-clinical relevant concentrations. For example, the study by Han *et al*., (2011) reported that autophagy was induced following EGFR inhibition in NSCLC in very high concentrations of Gefitinib and Erlotinib (up to 25 μM). Additionally these EGFR tyrosine kinase inhibitors failed to induce autophagy in an EGFR-dependent manner (Han *et al.*, 2011).

Even though EGFR targeted therapy has been characterised as a potent autophagy-inducing stimulus in cancer cells, the role of autophagy following EGFR inhibition remains biphasic. On one hand, autophagy induction following EGFR inhibition functions as a resistance mechanism and autophagy inhibition approaches potentiate response to EGFR targeted therapy (Han *et al.*, 2011, Dragowska *et al.*, 2013, Li *et al.*, 2013b, Zou *et al.*, 2013, Tang *et al.*, 2015). On the other hand, autophagy induction can potentiate EGFR targeted therapy and autophagy inhibition functions as a resistance mechanism (Gorzalczany *et al.*, 2011, Wei *et al.*, 2013). Our work aimed to characterise the role of autophagy following EGFR inhibition in CRC cells. In accordance with the autophagy-incompetent phenotype characterising the

majority of CRC cell lines following EGFR inhibition, concomitant EGFR and autophagy inhibition (CQ) did not affect CRC cell growth. However, autophagy was found to marginally potentiate Cetuximab treatment response in DiFi cells that were proficient for autophagy induction upon Cetuximab treatment, suggesting a pro-survival role of autophagy (Figures 3. 6 and 3. 7). Our findings suggest that a positive correlation between autophagy induction following EGFR inhibition and response to EGFR-autophagy combinational treatment occurs. In line with my findings, DiFi cells were previously reported to induce cyto-protective autophagy upon Cetuximab treatment (Li and Fan, 2010, Li *et al.*, 2010). Earlier studies have shown that autophagy inhibition (either genetic or pharmacological) potentiates EGFR targeted therapy response of cancer cells by accelerating levels of apoptosis (Li *et al.*, 2010, Li *et al.*, 2013b, Zou *et al.*, 2013, Tang *et al.*, 2015). We expect that EGFR targeted therapy in combination with autophagy suppression would exert a cytotoxic effect in DiFi cells by increasing levels of apoptosis, however further investigation is still needed.

CQ treatment alone did not affect CRC cell growth in the majority of the cell lines examined, weakening the possibility that CQ affects CRC cell growth in an autophagy-independent manner. However, CQ treatment alone diminished and potentiated cell growth in DiFi and SW48 *KRAS* G12D cells, respectively (Figure 3. 7.c and e). In particular for DiFi cells, the decrease in cell growth upon CQ treatment alone could be positively correlated with the reduced EGFR activation observed (Figure 3. 8.e and 3. 19.b). CQ treatment did not affect EGFR activation levels in any other CRC cell line examined. This may be linked to the high EGFR amplification in DiFi cells (discussed in 3.3.1) and a potential dependency of these cells on autophagy for cell growth/survival. A recent study reported that EGFR overexpressing cell lines and tumours are dependent on autophagy for survival. A positive correlation between EGFR and LC3 expression was reported in HNSSC xenografts, which was found to be sensitive to CQ treatment alone or in combination with irradiation. Additionally, this work revealed that pharmacological inhibition of autophagy (CQ) decreases proliferation more potently to high-EGFR expressing cells in comparison to low EGFR expressing cells (Jutten *et al.*, 2013). Nevertheless, this cannot explain the cell growth stimulatory effect of CQ in SW48 *KRAS* G12D cells presenting similar EGFR expression levels to DiFi cells. It could be that *KRAS*-driven basal autophagy regulates cell number of SW48 *KRAS* G12D cells by inducing cell death or senescence (discussed in 1.2.1.1., page 36) (Young *et al.*, 2009, Elgendy *et al.*, 2011). The role of autophagy in EGFR targeted therapy in a *KRAS*-dependent context could not be further evaluated in this work since all *KRAS* isogenic cell lines utilised, were refractory to autophagy induction (Figure 3. 7).

Overall, the majority of CRC cell lines were found refractory to autophagy induction following EGFR inhibition. The lack of autophagy induction upon EGFR inhibition could not be correlated to EGFR activation/expression levels and/or response to Cetuximab treatment. Importantly, this work highlights that heterogeneity of autophagy induction following EGFR inhibition is an important factor conferring differential response of CRC cells to EGFR-inhibition and autophagy combinational therapeutic approaches.

3.3.3. PI3K/AKT activation may render CRC cells refractory to autophagy induction following EGFR inhibition

It is generally accepted that RTKs' activation modulates autophagy induction. Activated EGFR can inhibit autophagy either indirectly through its downstream effectors or directly via interaction with Beclin1 protein (discussed in 1.1.2.2, page 30). Our work suggests that PI3K/AKT pathway downstream of EGFR may be responsible for autophagy induction following Cetuximab treatment in CRC cells. The majority of CRC cell lines were found to harbour *PI3K* activating mutations, which were positively correlated with sustained AKT activation levels upon EGFR inhibition (Figures 3. 9 and 3. 13 - 3. 16). Cells with *PI3K* activating mutations were refractory to autophagy induction following EGFR inhibition and AKT inhibition reversed their impotency to autophagy induction upon Cetuximab treatment (Figures 3. 6 and 3. 18). On the contrary, *PI3K* WT-DiFi cells potently downregulated AKT activation levels upon Cetuximab treatment and was the only cell line capable of inducing autophagy following EGFR inhibition (Figures 3. 6 and 3. 9). In turn, hyper-activation of AKT phosphorylation in DiFi cells reduced levels of Cetuximab-induced autophagy (Figure 3. 19). Even though CaCo2 cells are *PI3K* WT, they were not able to induce autophagy upon Cetuximab treatment (Figure 3. 6). This could be attributed to EGFR-independent sustained levels of pAKT following Cetuximab treatment, since ErbB2 and EGFR concomitant inhibition induced autophagy (Figure 3. 17.d and e). A positive correlation between autophagy induction and MAPK/ERK pathway upon Cetuximab treatment was not observed in our study. CRC cell lines with downregulated ERK activation were incompetent for autophagy induction following EGFR inhibition (Figures 3. 6 and 3. 10). The aforementioned observations highlight *PI3K* mutational status as a possible negative regulator of autophagy induction following EGFR inhibition by sustaining AKT activation levels. A positive correlation between PI3K pathway activation and EGFR-induced autophagy has been previously reported in the literature (Li and Fan, 2010, Han *et al.*, 2011, Dragowska *et al.*, 2013). The study by Li *et al*., (2010) has shown that PI3K pathway is important for autophagy induction upon

Cetuximab treatment in A431 cells since myristoylated -AKT and -PI3K transient expression rescued Cetuximab-induced autophagy (Li and Fan, 2010). In our work, myristoylated-AKT expression did not abolish but rather reduced Cetuximab-induced autophagy in DiFi cells. The remaining levels of Cetuximab-induced autophagy in the myristoylated-AKT condition can be attributed to the small albeit reduced AKT activation following Cetuximab treatment. PI3K/AKT pathway is known to regulate autophagy induction via controlling mTORC1 or Beclin1 activation (He and Klionsky, 2009, Ravikumar *et al.*, 2010, Laplante and Sabatini, 2012, Wang *et al.*, 2012). We can hypothesise that AKT downstream of PI3K may regulate either mTORC1 or Beclin1 activation and in that way Cetuximab-induced autophagy in CRC cells. mTORC1 or Beclin1 implication in regulating autophagy induction downstream of AKT has not been examined in this work and future studies are warranted to identify downstream regulators of PI3K/AKT pathway in autophagy regulation upon EGFR inhibition in CRC cells.

Recently, evidence for a direct role of EGFR (either tyrosine kinase -dependent or -independent) in autophagy regulation was introduced (discussed in 1.1.2.2., page 30) showing that EGFR targeted therapy may induce autophagy independently of mTORC1/AKT (Wei *et al.*, 2013, Tan *et al.*, 2015). Research from Wei *et al*., (2013) has shown that EGFR inhibition by Erlotinib blocked Beclin1/EGFR interaction at endosomes, rescued EGFR-mediated Beclin1 phosphorylation and increased autophagy only in Erlotinib-sensitive NSCLC cell lines and in tumour xenografts. Constitutively active mTOR could not rescue Erlotinib-induced autophagy (Wei *et al.*, 2013). Direct interaction of EGFR with Beclin1 in regulating autophagy induction was not tested in our work. In this manner we cannot exclude the possibility that Cetuximab-induced autophagy in DiFi cells is regulated by an EGFR/Beclin1 mechanism and future experiments in this direction are needed. Observations from our work, however might not support such a hypothesis and more specifically: i) AKT hyper-activation reduced Cetuximab-induced autophagy in DiFi cells suggesting an AKT-dependent mechanism for Cetuximab-induced autophagy and ii) DLD-1 cells that characterised by high EGFR activation levels and are sensitive to Cetuximab treatment they do not induce autophagy upon EGFR inhibition as was suggested for NSLCC cells in the latter study. Another approach, introduced by Tan *et al*., (2015) described a kinase-independent role of EGFR in autophagy regulation. In that context, Erlotinib- or Gefitinib-mediated inactive EGFR translocates to endosomes where a complex with Sec5 is created. Inactive EGFR/Sec5 complex dissociates Rubicon from Beclin1 and in that way autophagy is induced. This mechanism is suggested to be AKT-independent since Erlotinib and Gefitinib treatment potently downregulated EGFR activation levels without affecting pAKT. Additionally, EGFR expression was shown to

regulate basal autophagy induction in a variety of cells since EGFR downregulation abolished basal autophagy (Tan *et al.*, 2015). However, our work clearly shows that basal autophagic flux is not affected by EGFR downregulation in HCT-116 cells (Figure 3. 12.a) and that DLD-1 cells with sustained AKT activation levels and downregulated EGFR activation do not induce autophagy, as it would have been expected in the presence of an EGFR-kinase independent mechanism.

Variability in observations between studies may suggest the existence of various mechanisms responsible for autophagy induction following EGFR inhibition in different cell lines and tumour types. Collectively, our work suggests that autophagy induction downstream of EGFR may be regulated in a PI3K/AKT dependent manner and *PI3K* activating mutations may restrict CRC cells for autophagy induction following EGFR inhibition.

3.3.4. CRC cells display basal levels of autophagy independently of *PI3K* mutational status and AKT activation

PI3K/AKT pathway is a well-described negative regulator of autophagy induction through mTORC1-dependent and -independent mechanisms (discussed in 1.1.2.2., page 30). Given the fact that the majority of CRC cell lines utilised in this study are *PI3K* mutant and refractory to autophagy induction following a stressing stimulus like EGFR inhibition (due to high levels of AKT activation), it would have been expected that these cells would be incompetent for autophagy induction also in growth factor/nutrient replete basal-autophagy conditions. Interestingly, our work via monitoring autophagic flux using CQ clearly shows that all CRC cell lines utilised exhibit basal autophagy levels even in the presence of *PI3K* activating mutations and high AKT levels (HCT-116, DLD-1 and SW48 cells) (Figures 3. 5 and 3. 6). This observation suggests that basal autophagy levels are regulated in a PI3K/AKT independent manner in CRC cells, in contrast to the EGFR-induced autophagy. Additionally, basal autophagy in CRC cells occurred despite displaying active mTORC1 signalling, as levels of pS6 were found to be high in HCT-116, DLD-1 and CaCo2 cells examined (results are presented in 4.2.2., page 137; Figure 4. 6.c). These observations suggest the presence of an mTORC1-independent mechanism regulating basal autophagy in CRC. Earlier studies have described the presence of basal autophagy in cancer cells concomitantly with active mTORC1 signalling (Guo *et al.*, 2011, Perera *et al.*, 2015). Further investigation on the mechanism regulating basal levels of autophagy in CRC cells is warranted.

KRAS activating mutations have been shown to increase basal levels of autophagy a phenomenon named “autophagy addiction” (Guo *et al.*, 2011) and autophagy suppression in a variety of KRAS-driven cancer types has been found to attenuate cancer progression (Guo *et al.*, 2013, Rosenfeldt *et al.*, 2013, Yang *et al.*, 2014). In our study, the implication of *KRAS* activation in regulation of basal levels of autophagy was investigated via comparing *KRAS* WT and mutant CRC cells. It was found that *KRAS* activation increases basal levels of autophagy in a cell-type specific manner More specifically, *KRAS* activation increased basal levels of autophagy in DLD-1 and HCT-116 (to a lower extent) cells with the exception of SW48 cells, which exhibited marginally lower levels of basal autophagy compared to WT cells (Figure 3. 5). The variability in basal autophagy induction in the presence of *KRAS* could be attributed to a potential difference in the extent of *KRAS* activation between cell lines; HCT-116 and DLD-1 cells are homozygous for *KRAS* G13D mutation whereas SW48 cells are heterozygous for the G12D mutation. Furthermore, we cannot exclude the possibility that in SW48 cells *PI3K* activation restricts *KRAS* mutation to increase basal autophagy, since pharmacological inhibition of PI3K resulted in higher levels of PI103-induced autophagy in *KRAS* mutant cells.

3.3.5. Does inhibition of basal autophagy affect cell signalling?

CQ treatment was utilised in this work mainly to monitor autophagic flux and inhibit autophagy by a pharmacological manner. However, an interesting observation reported in this chapter was that inhibition of autophagic flux using CQ could alter the activation of AKT, ERK and EGFR. CQ treatment downregulated AKT activation in all CRC cell lines tested even in the presence of *PI3K* activating mutations. CQ treatment, as monotherapy, mainly resulted in attenuation of AKT activation, whereas when combined with Cetuximab decrease in AKT activation was not evident in most cell lines (Figures 3. 5, 3. 9, 3. 17 and 3. 18). CQ treatment was found to have variable outcomes on ERK activation levels in CRC cells and in some cases duration of CQ treatment differentially altered ERK activation. In particular, 24 hours of CQ treatment resulted in sustained ERK activation in HCT-116 and CaCo2 cells whereas in DLD-1, SW48 and DiFi cells pERK was upregulated (Figure 3. 10). CQ treatment for 6 hours resulted in reduction of ERK activation in HCT-116 cells, independently of *KRAS* mutational status (Figure 3. 11). As discussed in 3.3.2., DiFi cells were the only CRC cell line utilised that exhibited lower EGFR activation upon CQ treatment (Figures 3. 8 and 3. 19). In line with our findings, an earlier study investigating Erlotinib-induced autophagy in NSCLC has reported CQ to downregulate AKT and ERK activation in a

cell-type specific manner (Zou *et al.*, 2013). These observations suggest that inhibition of autophagic flux by CQ in CRC results in downregulation of AKT phosphorylation in a systematic manner, while ERK and EGFR activation are altered in a cell-type specific manner. However, pharmacological inhibition of autophagy via CQ cannot prove a direct role of autophagy in regulating cell signalling. As a lysosomotropic compound is only blocking the fusion of autophagosomes with lysosomes and we cannot exclude the possibility the effects on signalling we observed are caused by a non-autophagic-specific mechanism.

These observations along with evidence in the literature supporting a role of autophagy in regulation of ERK activation (Martinez-Lopez *et al.*, 2013), prompted us to investigate in depth whether autophagy plays a role in cell signalling of CRC cells. The role of autophagy in cell signalling is presented in Chapter 4.

3.3.6. Summary

The work presented in this chapter aimed to unravel the regulation and role of autophagy following EGFR targeted therapy in CRC cells. Our main findings suggest that CRC cells present differential response to EGFR targeted therapy possibly through differential regulation of MAPK/ERK and PI3K pathways activation downstream of EGFR. *PI3K* activating mutations and high AKT activation levels may render CRC cells refractory to autophagy induction following pharmacological inhibition or downregulation of EGFR. Additionally, concomitant EGFR and autophagy inhibition does not potentiate EGFR-targeted therapy response in CRC cells refractory to Cetuximab-induced autophagy. Only PI3K WT cells with deactivated AKT signalling following EGFR inhibition were found to induce cyto-protective autophagy. Even though *PI3K* mutated CRC cells are refractory to EGFR-mediated autophagy induction, they display basal levels of autophagy despite the presence of constitutive PI3K/mTOR signalling. Finally, inhibition of basal autophagic flux by CQ may affect cell signalling in CRC.

The main conclusions and future directions of this work are presented in Chapter 5.

Chapter 4

Basal autophagy and cell signalling in CRC

4. Basal autophagy and cell signalling in CRC

4.1. Background

An interesting observation described in Chapter 4 was that pharmacological modulation of autophagy by CQ treatment altered AKT and/or ERK phosphorylation in CRC cell lines. The role of the autophagosome in degradation of proteins either in a bulk or selective way is well defined. However, our knowledge on the role of autophagosomes and/or ATG proteins in regulation of cell signalling is still limited. Recently, publications in the field described a role for autophagy in the control of cell signalling and protein phosphorylation (Martinez-Lopez *et al.*, 2013, Cianfanelli *et al.*, 2015). Martinez-Lopez *et al*., (2013) described an atypical function of ATG proteins, in which ATG proteins and autophagosomes act as subcellular scaffolding compartments for MEK and ERK. Specifically, MEK and ERK were found to localise at the cytosolic side of the outer autophagosomal-membrane. Interestingly, ATG7 depletion in liver explants and brown adipose tissue as well as inhibition of LC3 lipidation in NIH/3T3 cells resulted in attenuation of ERK 1/2-phosphorylation levels, whereas phosphorylation levels of MEK protein remained stable (Martinez-Lopez *et al.*, 2013). Furthermore, Ambra1, a protein implicated in the early steps of autophagy (discussed in 1.1.1.1., page 26) has been found to control c-Myc phosphorylation by directly interacting with and enhancing PP2A phosphatase activity in an mTOR-dependent manner. Ambra1 depletion leads to increased c-Myc phosphorylation and stability, thus in turn promoting proliferation (Cianfanelli *et al.*, 2015).

This chapter investigates whether autophagy plays a direct role in regulation of cell signalling in CRC cells and aims to provide insights into the underlying molecular mechanism.

4.2. Results

4.2.1. Genetic modulation of autophagy in CRC cancer

In addition to the pharmacological modulation of autophagy by CQ, it was really important to generate an *in vitro* model system for genetic inhibition of autophagy. Genetic modulation of autophagy is the only way to confirm the direct role of autophagy in any observed phenotype since CQ can affect other cellular functions apart from autophagy (Kimura *et al.*, 2013). For genetic modulation of autophagy, the stable pGIPZ and the inducible pLKO-Tet-On (Wee *et al.*, 2008, Wiederschain *et al.*, 2009) lentiviral systems were used to downregulate the expression of ATG7 protein

and consequently autophagy. ATG7 protein downregulation blocks phagophore elongation through interruption of LC3-II formation resulting in autophagy inhibition (Mehrpour *et al.*, 2010). The mechanism that ATG7 facilitates LC3 lipidation has been previously discussed in 1.1.1. and is schematically represented in Figure 4. 1.

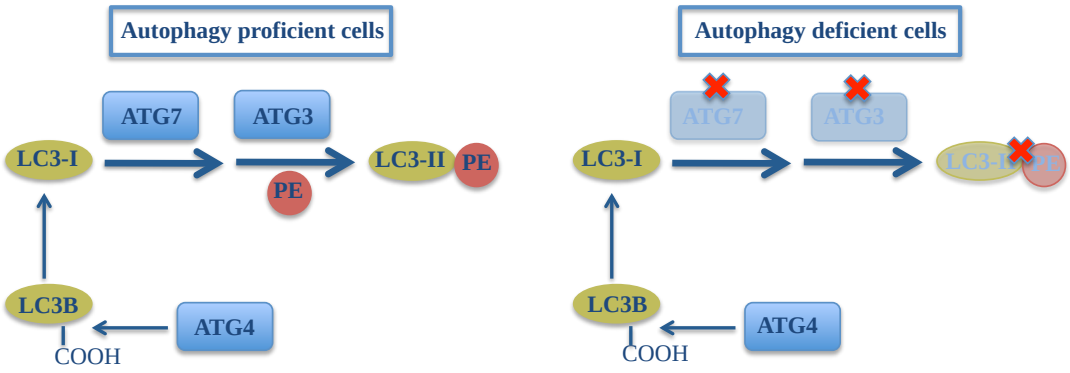

Figure 4. 1: **Autophagy inhibition through ATG7 protein downregulation.** ATG4 protein cleaves the carboxyl terminus of LC3B protein forming in that way the cytosolic form of LC3, called LC3-I. ATG7 protein is important for the lipidation process of LC3-I giving rise to the autophagosomal-associated form of LC3, called LC3-II. Autophagy-proficient cells would have a lipidated form of LC3 protein enabling their canonical autophagic function. Autophagy-compromised cells are incapable of inducing autophagy since ATG7 protein is downregulated resulting in blockade of LC3-I protein lipidation.

The UCL Cancer Institute has a whole genome shRNA library based on the pGIPZ lentiviral system, which enables the simultaneous expression of turbo Green Fluorescence Protein (turboGFP) along with shRNA expression through an IRES sequence located immediately after shRNA. We tested a number of shRNA vectors that were previously used in our lab (Galavotti *et al.*, 2013) for scramble and ATG7 shRNA (shATG7-E8, -G7 and -F12) expression via lentivirally transducing HCT-116 *KRAS* WT cells using an MOI of 10. It was found that both E8 and G7 shATG7 sequences potently downregulated ATG7 protein expression, while F12 sequence did not (Figure 4. 2.a). Then stable HCT-116 isogenic cells carrying WT or mutant *KRAS* were generated using scramble and shATG7 E8 lentivirus at an MOI of 10. Infected HCT-116 cells were GFP-sorted and expanded in culture. Western blotting was used to assess the efficiency of ATG7 protein downregulation. Approximately 75% of ATG7 downregulation was observed in both HCT-116 *KRAS* WT and G13D-shATG7 E8 expressing cells compared to scramble conditions (Figure 4. 2.b). To investigate the ability of autophagy-compromised cells (shATG7 E8) to induce autophagy upon autophagy-inducing stressors, we used the PI3K and mTOR dual inhibitor PI103 (Park *et al.*, 2008). Infected cells were treated with 1 μM of PI103 for 6 hours with and without 10 μM of CQ in order to enable autophagic flux monitoring, and LC3B protein

levels were assessed by western blotting. As is illustrated in Figure 4. 2.c, autophagy-compromised HCT-116 *KRAS* WT and G13D cells showed lower levels of autophagy induction compared to scramble cells. The problem that we encountered with the pGIPZ system was that pGIPZ-transduced cells tend to have decreased their ability to suppress autophagy through passages (approximately five passages), especially in basal conditions (Figure 4. 2.d).

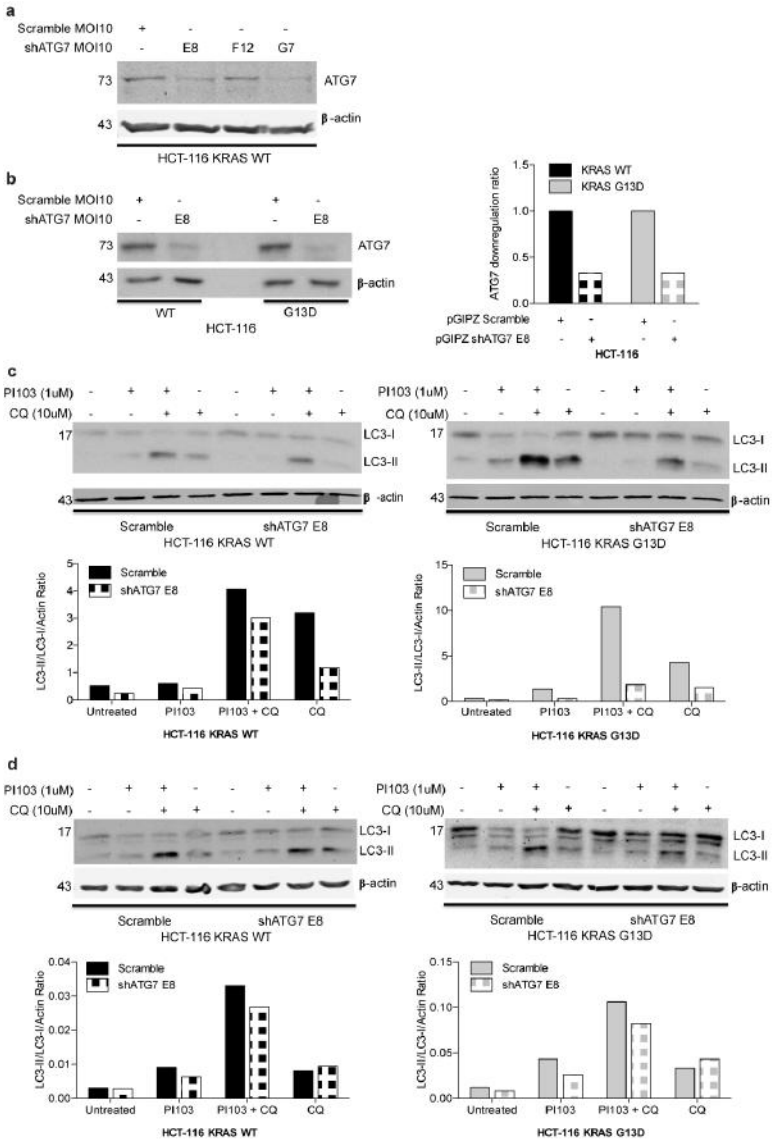

Figure 4. 2: **Genetic modulation of autophagy in HCT-116 *KRAS* WT and G13D cells using the stable pGIPZ lentiviral system. a** ATG7 protein expression in scramble and shATG7 E8, F12 and G7 expressing HCT-116 *KRAS* WT cells; **b** Left: Downregulation of ATG7 protein, Right: Bar plot represents ratio of ATG7 protein downregulation based on densitometric analysis of ATG7 protein expression levels normalised to actin; **c** ATG7 downregulation impairs autophagy induction in control and PI103-treated cells; **d** pGIPZ system for ATG7 downregulation lost its ability to impair autophagy through passages especially in basal autophagy conditions. 1 μM of PI103 used for induction of autophagy experiments. 10 μM of CQ used to monitor autophagic flux. Protein expression levels examined by western blotting and actin used as a loading control. Bar plots represent densitometric analysis of LC3-II/LC3-I levels normalised to actin.

To solve that problem and gain a better control of autophagy suppression between experiments, we decided to switch to the inducible pLKO-Tet-On system for genetic modulation of autophagy, which is described below.

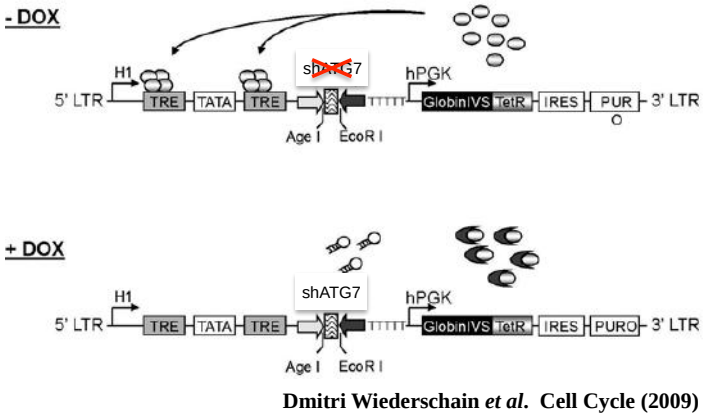

Dmitri Wiederschain *et al.* Cell Cycle (2009)

Figure 4. 3: **pLKO-Tet-On system mechanism of action.** pLKO–Tet-On system contains all important elements for lentiviral production and puromycin selection. shRNA and Tet repressor (TetR) expression are regulated by two different promoters, H1 and hPGK respectively. This allows the inducible expression of a desirable shRNA. In the absence of Doxycycline (DOX) TetR is expressed and blocks the expression of shRNA by binding to the Tet-responsive elements (TRE) downstream of H1 promoter. Upon DOX introduction TetR binds to DOX allowing the expression of the shRNA, thereby inhibiting the binding of TetR to TRE of the H1 promoter.

Three different shATG7 sequences, called E8, G7 and F12, as well as the control shRNA sequence, shEGFP, were cloned into the pLKO-Tet-On vector and lentiviral production ensued in HEK 293T cells. Four different CRC cell lines and their isogenic *KRAS* mutated versions where available, were lentivirally transduced at a MOI of 10. To assess the knockdown efficiency of ATG7 protein expression, cells were cultured in the presence of 10 ng/ml and/or 100 ng/ml doxycycline (DOX) for 72 and 120 hours and results analysed by western blotting. The E8 sequence displayed the highest downregulation of ATG7 protein expression in both HCT-116 *KRAS* WT and G13D cells after incubation with 10 ng/ml DOX for 120 hours (approximately 68% of ATG7 protein; Figure 4. 4.a.1 and 2). In DLD-1 *KRAS* WT and G13D cells, it was again found that the shATG7 E8 sequence was the most effective to downregulate ATG7 protein expression (approximately 49%) upon 100 ng/ml DOX treatment for 120 hours (Figure 4. 4.b.1 and 2). Similar results were observed in CaCo2 cells after 120 hours with 100 ng/ml DOX (approximately 48%; Figure 4. 4.c.1 and 2). In contrast, in SW48 *KRAS* WT and G12D cells all sequences were efficiently downregulated ATG7 protein expression (upon 100 ng/ml DOX after 120 and 72 hours, respectively; Figure 4. 4.d.1 and 2).

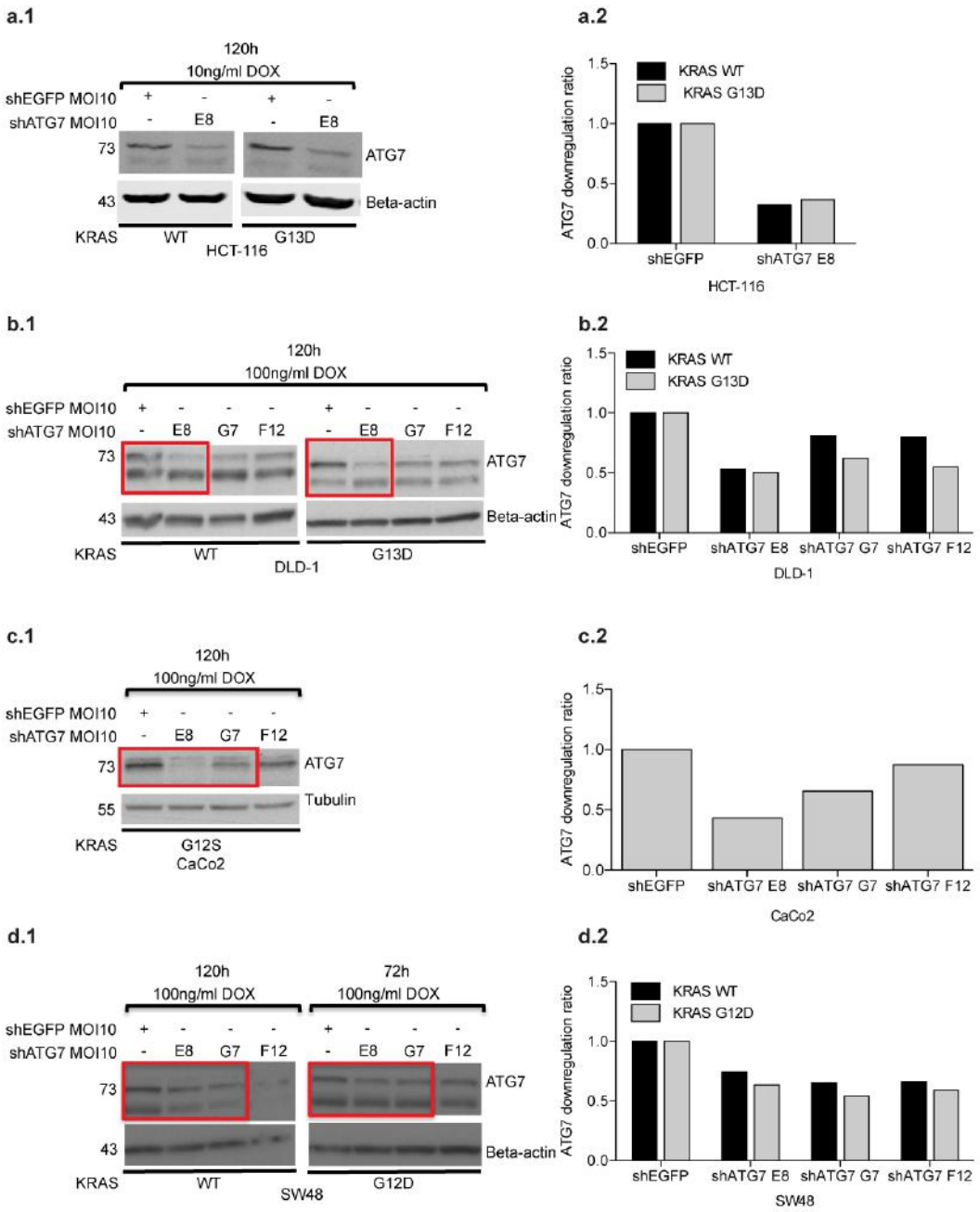

Figure 4. 4: ATG7 protein downregulation using the inducible pLKO-Tet-On lentiviral system. a. 1-2 HCT-116 *KRAS* WT and G13D; **b. 1-2** DLD-1 *KRAS* WT and G13D; **c. 1-2** CaCo2 and **d. 1-2** SW48 *KRAS* WT and G12D cell lines. Protein expression levels examined by western blotting with Beta-actin used as a loading control. Bar plots represent ATG7 protein downregulation ratio based on densitometric analysis of ATG7 protein expression levels normalised to Beta-actin. E8, G7, F12: refer to different sequences used for ATG7 protein downregulation. DOX= Doxycycline. ATG7 protein expression in autophagy-proficient and -compromised conditions was examined in all western blotting experiments conducted in this work.

Next, the reversibility of ATG7 downregulation was assessed by DOX withdrawal from the culture media. HCT-116 *KRAS* WT shEGFP and shATG7 E8 cells were cultured in the presence of 10 ng/ml of DOX for 11 days. Then, cells were further

cultured with DOX or DOX-free fresh media for a further 120 hours. ATG7 protein levels decreased in the presence of DOX but then fully recovered upon DOX withdrawal confirming that ATG7 downregulation is reversible (Figure 4. 5.a).

Finally, the ability of shATG7 E8 cells to induce autophagy upon autophagy-inducing stressors was assessed. HCT-116 shEGFP and shATG7 E8 cells (WT and mutant *KRAS*) were cultured in the presence of DOX for 168 hours and were then treated with the autophagy inducer PI103. Autophagy-compromised *KRAS* WT and G13D HCT-116 cells displayed reduced autophagy induction upon PI103 treatment at all three time points analysed (Figure 4. 5.b).

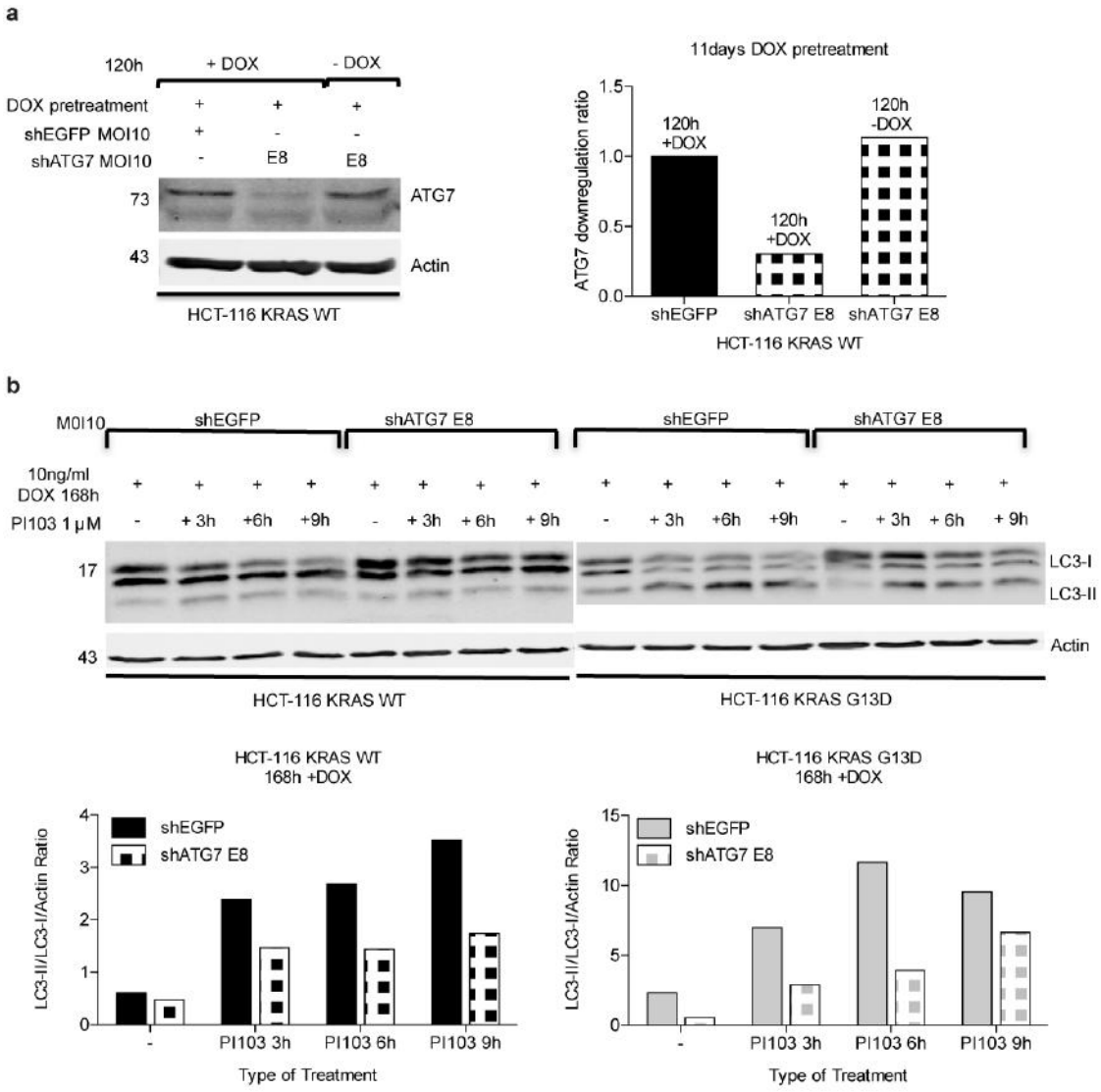

Figure 4. 5: **a pLKO-Tet-On system is reversible *in vitro*.** DOX removal can reverse ATG7 protein downregulation, Right: western blotting, Left: Bar plot represents ratio of ATG7 protein downregulation based on densitometric analysis of ATG7 protein expression levels normalised to beta-actin. **b ATG7 protein downregulation using the pLKO-Tet-On system impairs PI103-induced autophagy in three different timepoints.** 1 µM of PI103 used for autophagy induction experiment after 3, 6 and 9 hours of treatment. Bar plots represent densitometric analysis of LC3-II/LC3-I levels normalised to actin. E8= refers to the sequence used for ATG7 downregulation, DOX= Doxycycline.

In conclusion, the pLKO-Tet-On system appeared to be a better model for genetic modulation of autophagy compared to pGIPZ. Five days of DOX treatment was found to be the best condition for efficient downregulation of ATG7 protein expression in all CRC cell lines examined.

4.2.2. ATG7 downregulation affects PI3K/AKT pathway in CRC cells

Autophagy-proficient (shEGFP) and -compromised (shATG7 E8) CRC cells were analysed by western blotting for levels of phosphorylated and total AKT. Downregulation of ATG7 protein significantly reduced phosphorylation of AKT (pAKT S473) relative to levels of total AKT in all CRC cells examined (Figure 4. 6a). Specifically, HCT-116 *KRAS* WT, DLD-1 *KRAS* WT and CaCo2 autophagy-compromised cells displayed approximately 25%, 35% and 30% downregulation of pAKT S473, respectively. pAKT downregulation was more marked in the presence of *KRAS* G13D in HCT-116 and DLD-1 cells (35% and 65%, respectively; Figure 4. 6.a). The T308 phosphorylation residue on AKT protein, which is directly phosphorylated by PDK1 (Laplante and Sabatini, 2012), was examined upon autophagy downregulation in CaCo2 cells. T308 phosphorylation was found reduced only in CaCo2 autophagy-compromised cells (approximately 23%), albeit not to a statistically significant extent (Figure 4. 6.b). Finally, we examined phosphorylation of the mTORC1 downstream effector S6 ribosomal protein. No statistically significant differences in phosphorylation levels of S6 ribosomal protein residues S240/244 were observed. Specifically, HCT-116 and DLD-1 *KRAS* WT autophagy-compromised cells showed increased S6 phosphorylation (~40% and ~15% respectively) when compared with their autophagy-proficient controls. On the contrary, HCT-116 and DLD-1 *KRAS* G13D cells maintained pS6 ribosomal protein S240/244 levels stable upon autophagy downregulation. CaCo2 autophagy-compromised cells displayed approximately a 20% non-statistically significant reduction in pS6 ribosomal protein S240/244 levels (Figure 4. 6.c).

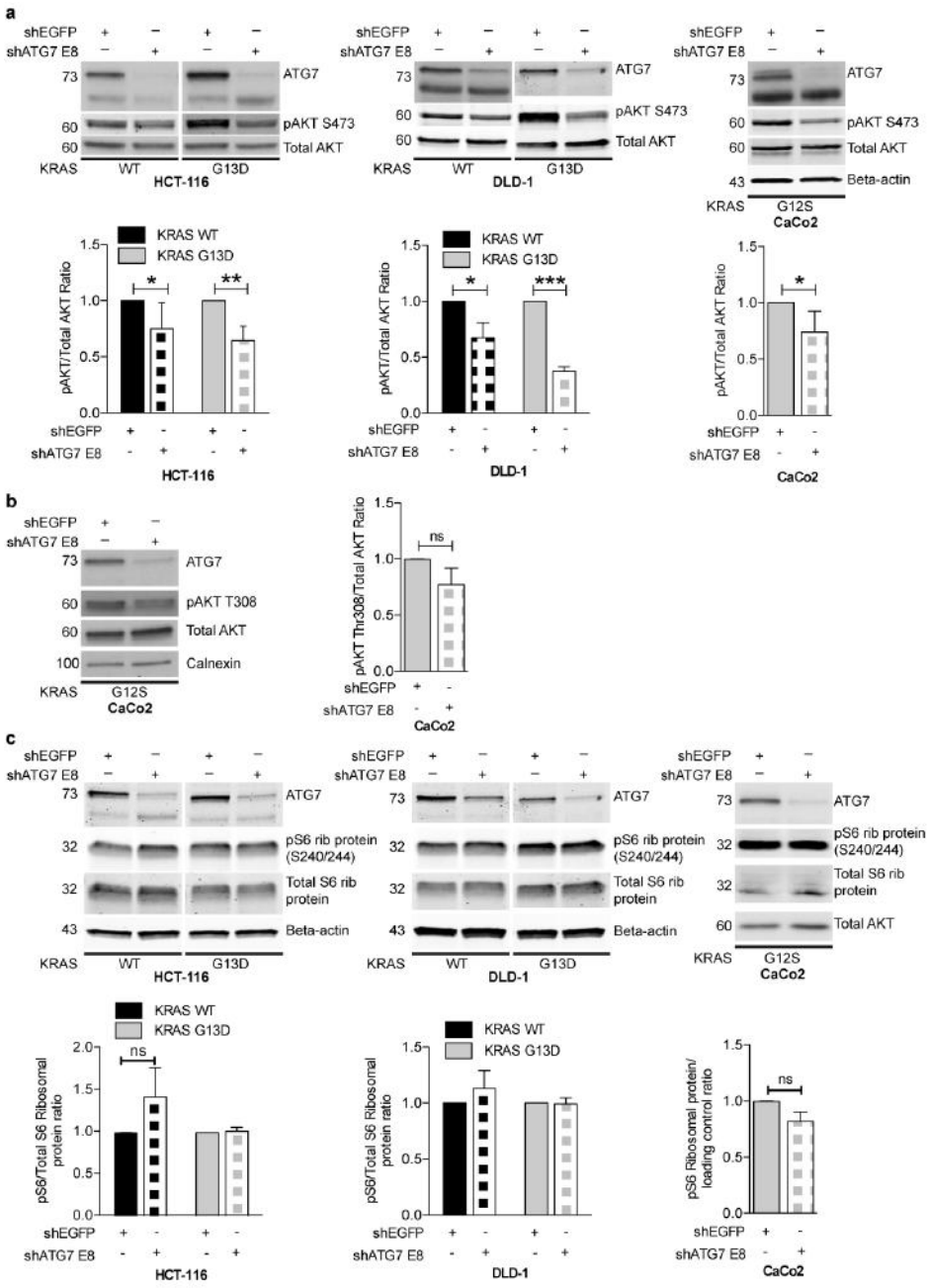

Figure 4. 6: ATG7 knockdown regulates AKT phosphorylation. Autophagy downregulation resulted in **a** reduced AKT phosphorylation at S473 residue. Two-way ANOVA with Bonferroni posttests statistical analysis was conducted for HCT-116 (n= 4) and DLD-1 (n= 3) *KRAS* WT and G13D cells and unpaired Student's t-test statistical analysis was conducted for CaCo2 (n= 4) cells. **b** reduced AKT phosphorylation at T308 residue. Unpaired Student's t-test statistical analysis was conducted for CaCo2 cells (n= 3). pAKT T308 levels were too low to be detected in HCT-116 and DLD-1 cells. **c** no difference in phosphorylation levels of S6 ribosomal protein. Unpaired Student's t-test statistical analysis was conducted for HCT-116 *KRAS* WT (n= 3) and CaCo2 (n= 3) cells. For HCT-116 *KRAS* G13D and both DLD-1 *KRAS* WT and G13D cells n= 2. HCT-116 and DLD-1 *KRAS* WT and G13D isogenic cell lines as well as CaCo2 cells were treated with DOX for 5 days and total cell lysates were subjected to western blotting analysis of the indicated proteins. Beta-actin, calnexin and total AKT proteins used as loading controls. Bar plots represent densitometric quantification of pAKT S473, pAKT T308 and pS6 ribosomal protein relative to total AKT and total S6 ribosomal protein or loading control respectively. The bars represent mean ± standard deviation; ns= non-statistically significant, * $p<0.05$, ** $p<0.01$ and *** $p<0.001$. Immunoblots presented are representative of n= 2-4 independent experiments. Autophagy-proficient and autophagy-compromised cells are denoted as shEGFP and shATG7 E8.

4.2.3. Other signalling pathways are not affected in a systematic manner upon ATG7 downregulation in CRC cells

MAPK/ERK pathway

As mentioned above, our experiments with CQ (Figure 3. 11) and a previous study reported a role for autophagy in regulation of the MAPK/ERK pathway (Martinez-Lopez *et al.*, 2013). We therefore analysed total cell lysates from shEGFP and shATG7 E8 CRC cells for total and phosphorylated ERK (pERK) 1/2 proteins. Our findings indicated that autophagy regulates phosphorylation of ERK 1/2 protein in a statistically significant manner but with a non-consistent pattern between the different cell lines tested. Particularly, ATG7 knockdown resulted in attenuated phosphorylation levels of ERK 1/2 protein in both HCT-116 *KRAS* WT and G13D cells (approximately 55% and 35%, respectively). The same statistically significant pattern of reduced pERK 1/2 was also observed in DLD-1 *KRAS* G13D cells (approximately 40%). On the contrary, autophagy downregulation resulted in a statistically significant increase in ERK 1/2 phosphorylation (approximately 65%) in DLD-1 *KRAS* WT cells. Downregulation of ATG7 protein decreased phosphorylation levels of ERK 1/2 in CaCo2 cells marginally and not significantly (Figure 4. 7.a).

We then set out to investigate whether the reduced ERK phosphorylation upon autophagy suppression is due to a direct effect on ERK or via modulation of upstream components of the MAPK/ERK cascade. To this end, we analysed phosphorylation of the MEK 1/2 proteins, which are upstream kinases regulating ERK phosphorylation. HCT-116 *KRAS* WT and G13D autophagy-compromised cells displayed a reduction in phosphorylation levels of MEK 1/2 of approximately 26% and 18%, respectively. pMEK 1/2 was increased by 50% in DLD-1 *KRAS* WT cells, whereas it decreased by 10% in DLD-1 G13D cells. In CaCo2 cells a slight up-regulation of pMEK 1/2 levels was observed upon autophagy downregulation conditions (Figure 4. 7.b).

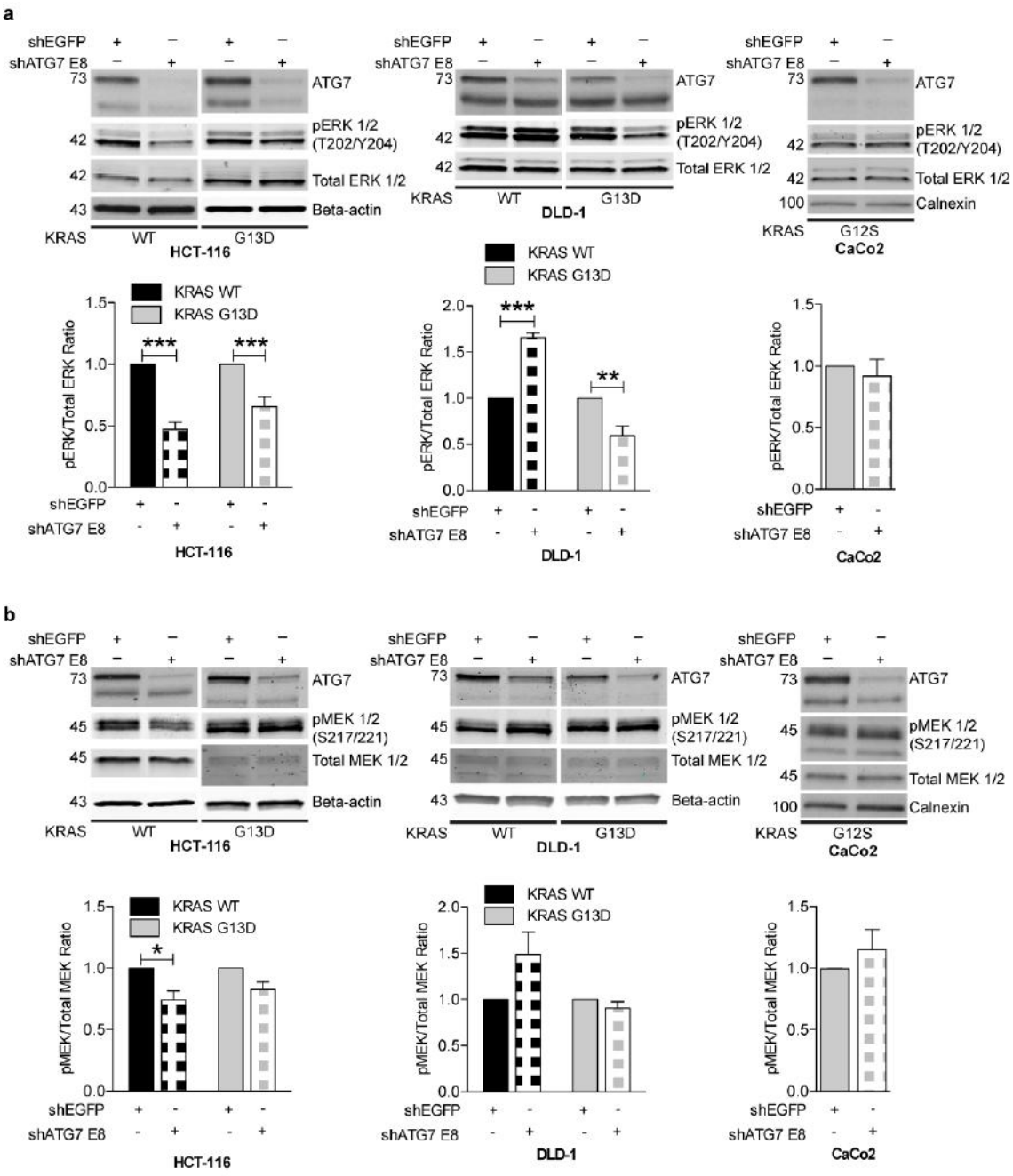

Figure 4. 7: ATG7 knockdown regulates phosphorylation of MAPK/ERK cascade components in a cell-type specific way. Autophagy downregulation resulted in **a** deregulated ERK 1/2 phosphorylation. Two-way ANOVA with Bonferroni posttests statistical analysis was conducted for HCT-116 (n= 4) and DLD-1 (n= 3) *KRAS* WT and G13D cells and unpaired Student's t-test statistical analysis was conducted for CaCo2 (n= 4) cells. **b** altered MEK 1/2 phosphorylation levels. Unpaired Student's t-test statistical analysis was conducted for HCT-116 *KRAS* WT (n= 3) and CaCo2 (n= 3) cells. Two-way ANOVA with Bonferroni posttests statistical analysis was conducted for both DLD-1 *KRAS* WT and G13D cells (n= 3). For HCT-116 *KRAS* G13D cells n= 2. HCT-116 and DLD-1 *KRAS* WT and G13D isogenic cell lines as well as CaCo2 cells were treated with DOX for 5 days and total cell lysates were subjected to western blotting analysis of the indicated proteins. Beta-actin, calnexin or total ERK 1/2 protein used as loading controls. Bar plots represent densitometric quantification of pERK 1/2 T202/Y204 and pMEK 1/2 S217/221 relative to total ERK 1/2 and total MEK 1/2 protein, respectively. The bars represent mean ± standard deviation; * $p<0.05$, ** $p<0.01$ and *** $p<0.001$. Immunoblots presented are representative of n= 2-4 independent experiments. Autophagy-proficient and autophagy-compromised cells are illustrated as shEGFP and shATG7 E8.

PI3K and MAPK/ERK pathways were additionally examined in autophagy-proficient and autophagy-compromised SW48 *KRAS* WT and G12D cells. Preliminary data performed once showing that autophagy suppression may not affect PI3K activation depicted by pAKT S473 levels in both SW48 *KRAS* WT and G12D cells (Figure 4. 8.a). pERK 1/2 activation was found upregulated in both SW48 *KRAS* WT and G12D cells following autophagy inhibition (Figure 4. 8.b). However, the abovementioned observations need further investigation.

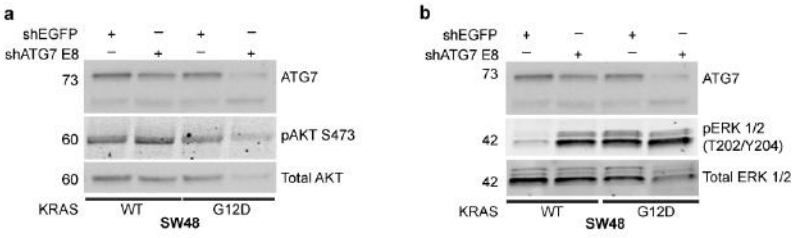

Figure 4. 8: Activation of PI3K and MAPK/ERK pathways following ATG7 downregulation in SW48 KRAS WT and G12D cells. Autophagy suppression **a** did not alter AKT phosphorylation at S473 residue and **b** increased pERK 1/2 activation levels. SW48 *KRAS* WT and G12D cells were treated with DOX for 5 days and total cell lysates were subjected to western blotting analysis of the indicated proteins. Total AKT and total ERK 1/2 proteins were used as loading controls. Immunoblots presented were only performed once. **Note**: Autophagy-compromised sample of SW48 *KRAS* G12D cells had possibly a protein-degradation problem.

In conclusion, autophagy inhibition in CRC cells leads to decreased AKT phosphorylation, whereas the effect on MAPK/ERK cascade components appears to be cell-type-dependent (Table 4. 1).

Table 4. 1: Phosphorylation modulation of PI3K and MAPK/ERK cascades upon autophagy downregulation. * denotes experiments performed once.

Cell line	HCT-116		DLD-1		CaCo2	SW48	
KRAS	WT	G13D	WT	G13D	G12S	WT	G12D
pAKT S473	↓	↓	↓	↓	↓	Stable *	Stable *
pAKT T308	Not detectable	Not detectable	Not detectable	Not detectable	↓	Not examined	Not examined
pS6 rib protein	↑	Stable	↑	Stable	↓	Not examined	Not examined
pERK 1/2	↓	↓	↑	↓	Stable	↑ *	↑ *
pMEK 1/2	↓	↓	↑	Stable	Stable	Not examined	Not examined

Given the fact that autophagy plays a role in metabolism (Guo *et al.*, 2011), it was essential to investigate whether autophagy inhibition controls phosphorylation of proteins in a systematic manner by reducing ATP production levels or metabolic substrates in the cell. To address this, five different signalling pathways were assessed for differences in protein phosphorylation in autophagy-compromised CRC cells using phospho-specific antibodies by western blotting.

Signal Transducer and Activator of Transcription 3 (STAT3)

Autophagy inhibition resulted in slightly upregulated and downregulated phosphorylation levels of STAT3 protein at Y705 residue in HCT-116 *KRAS* G13D and CaCo2 cells, respectively. STAT3 activation levels in HCT-116 *KRAS* WT cells were not detectable (Figure 4. 9.a).

p38 MAPK kinase

p38 MAPK T180/Y182 phosphorylation levels were maintained upon autophagy inhibition in all HCT-116 *KRAS* isogenic cell lines and CaCo2 cells (Figure 4. 9.b).

AMPK alpha

Besides HCT-116 *KRAS* WT cells that displayed upregulated phosphorylation levels of AMPK alpha at T172 residue, HCT-116 *KRAS* G13D and (*KRAS*-mutant) CaCo2 cells displayed reduced phosphorylation levels of AMPK alpha (Figure 4. 9. c).

Stress-Activated Protein Kinase (SAPK)/Jun N-terminal Kinase (JNK)

SAPK/JNK kinase showed reduced levels of phosphorylation in HCT-116 cells and sustained phosphorylation in CaCo2 cells upon autophagy downregulation. The presence of *KRAS* G13D mutation in HCT-116 cells attenuated the difference in phosphorylation levels of SAPK/JNK between autophagy-proficient and autophagy-compromised cells compared to *KRAS* WT cells (Figure 4. 9.d). Interestingly, SAPK/JNK presents a similar pattern in phosphorylation modulation upon autophagy inhibition with ERK 1/2 (Figure 4. 7.a).

Retinoblastoma protein (Rb)

Sustained phosphorylation levels of Rb protein at S807/811 residues were observed upon autophagy downregulation in CaCo2 cells (Figure 4. 9.e).

In summary, differences in phosphorylation levels of proteins tested upon autophagy inhibition were not consistent to support the hypothesis of a mechanism that systematically regulates phosphorylation of all proteins.

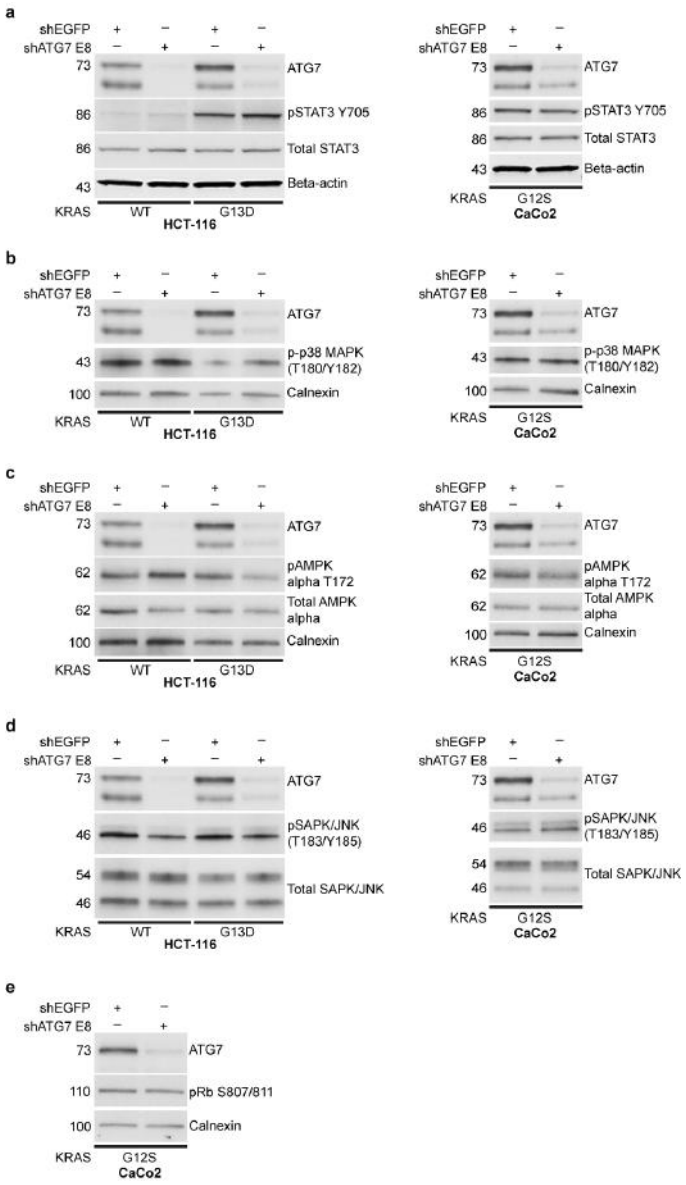

Figure 4. 9: Autophagy inhibition does not modulate phosphorylation of proteins in a systematic manner. Phosphorylation levels of **a** STAT3 Y705 residue; **b** p38 MAPK T180/Y182 residues; **c** AMPK alpha T172 residue; **d** SAPK/JNK T183/Y185 residues and **e** Rb S807/811 residues. HCT-116 *KRAS* WT and G13D isogenic cell lines as well as CaCo2 cells were treated with DOX for 5 days and total cell lysates were subjected to western blotting analysis of the indicated proteins. Beta-actin or calnexin used as loading controls. Immunoblots presented were only performed once. Autophagy-proficient and autophagy-compromised cells are shown as shEGFP and shATG7 E8. Y= tyrosine, T= threonine and S= serine residues.

Based on our abovementioned findings, we expected autophagy to regulate AKT phosphorylation via a specific mechanism. Therefore, different hypotheses were formulated and investigated that are presented below. The mechanistic studies were mainly conducted using HCT-116 cells, which showed both pAKT and pERK 1/2 downregulation following autophagy suppression.

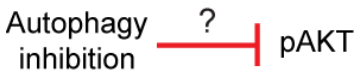

4.2.4. Hypotheses 1 and 2: PP2A and PTEN phosphatases in regulation of phosphorylation of AKT and ERK proteins upon autophagy inhibition

To understand how autophagy may regulate phosphorylation of AKT and ERK proteins, it was important to investigate whether autophagy controls degradation of phosphatases implicated in their de-phosphorylation (Figure 4. 10.a). Phosphorylation is a reversible process in which kinases and phosphatases play opposing roles. A literature search prompted us to investigate regulation of the threonine/serine Protein Phosphatase 2A (PP2A), accounting for approximately 90% of protein phosphatase activity in eukaryotes. PP2A is a heterotrimeric enzyme complex that includes three different subunits; a highly conserved catalytic subunit (PP2Ac), a structural core subunit (PP2Aa) and a highly variable regulatory subunit (PP2Ab) enabling diverse specificities to substrate proteins. Interestingly, PP2A has been previously described to negatively regulate PI3K and MAPK/ERK pathways (Sontag, 2001, Eichhorn *et al.*, 2009). In particular, PP2A has been found to directly de-phosphorylate AKT mainly at the T308 residue and to a smaller extent at S473 residue (Kuo *et al.*, 2008). Additionally, PP2A can either positively or negatively regulate ERK activation (Eichhorn *et al.*, 2009). As far as the negative regulation of ERK is concerned, PR61β or PR61γ regulatory subunits are responsible for direct de-phosphorylation of ERK by PP2A since their ablation resulted in upregulation of ERK signalling in a MEK-independent way (Letourneux *et al.*, 2006). Moreover, an indirect de-phosphorylation mechanism of ERK exists whereby PP2A de-phosphorylates and inactivates c-SRC, which in turn inactivates RAF protein, an upstream kinase in MAPK/ERK cascade, in a RAS-independent way. On the contrary, PP2A upon RAS activation directly de-phosphorylates RAF at S295 residue leading to translocation of RAF to the plasma membrane for activation of the RAS/RAF/MAPK pathway and consequent upregulation of ERK activation (Eichhorn *et al.*, 2009). Finally, Phosphatase and TENsin homolog protein (PTEN) was included in our study due to its known function in controlling PI3K activity and consequently AKT phosphorylation. PTEN is a lipid

phosphatase enabling the de-phosphorylation of phosphatidylinositol 3,4,5-trisphosphate (PIP3) to phosphatidylinositol 4,5-bisphosphate (PIP2) and therefore reverses PI3K lipid kinase activity.

To examine whether autophagy inhibition resulted in upregulation of PP2A and PTEN protein expression levels, total cell lysates from autophagy-proficient and autophagy-compromised cells were subjected to western blotting analysis for PP2Ac catalytic subunit and total PTEN expression levels. Autophagy-compromised HCT-116 cells displayed a slight increase of approximately 15% in PP2A protein levels, whereas PP2A expression was not affected in autophagy-compromised CaCo2 cells (Figure 4. 10.b and c). A marginal increase in PTEN expression levels upon autophagy inhibition was observed in CaCo2 cells (Figure 4. 10.d).

Together these data suggest that diminished phosphorylation of AKT and ERK proteins upon autophagy inhibition is not regulated by accumulation of PP2A and PTEN phosphatases.

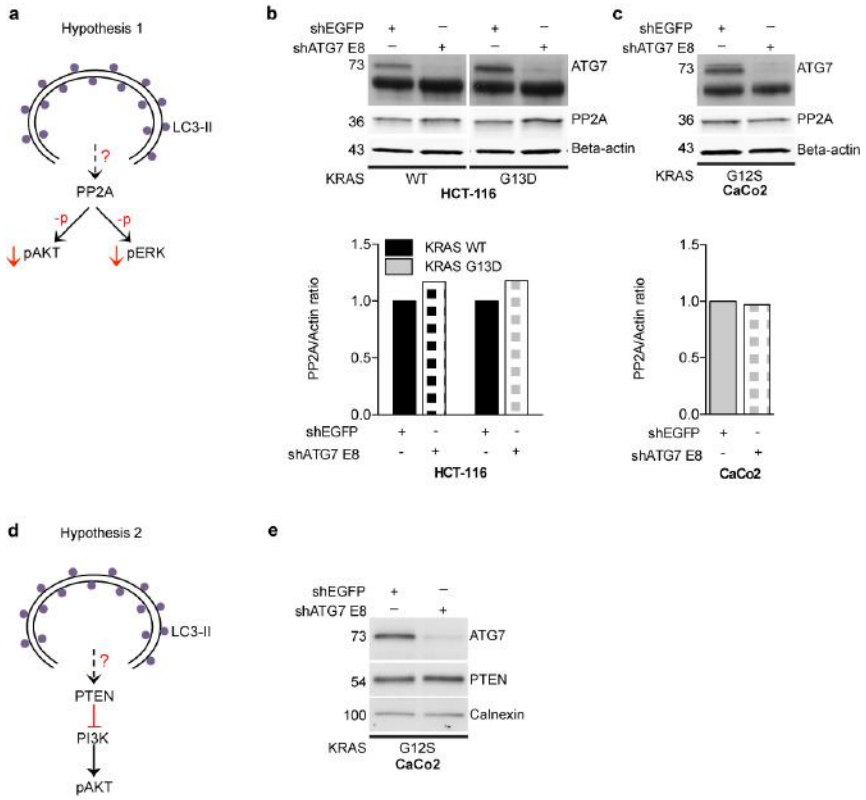

Figure 4. 10: PP2A and PTEN phosphatases are not degraded through autophagy. a Schematic representation of hypothesis that PP2A or PTEN are getting degraded through autophagy. PP2A catalytic subunit expression levels upon autophagy downregulation in **b** HCT-116 *KRAS* WT and G13D isogenic cell lines; **c** CaCo2 cells. **d** PTEN expression levels upon autophagy downregulation in CaCo2 cells. HCT-116 *KRAS* WT and G13D isogenic cell lines as well as CaCo2 cells were treated with DOX for 5 days and total cell lysates were subjected to western blotting analysis of the indicated proteins. Beta-actin or calnexin used as loading controls. Immunoblots presented were only performed once. Bar plots represent densitometric quantification of PP2A expression relative to actin levels. Autophagy-proficient and autophagy-compromised cells are denoted as shEGFP and shATG7 E8. p= phosphorylation.

4.2.5. Hypothesis 3: the Ubiquitin Proteasome System (UPS) in regulation of AKT and ERK phosphorylation upon autophagy inhibition

A crosstalk between the two major degradation pathways present in eukaryotes, autophagy and the Ubiquitin Proteasome System (UPS), has been recently revealed in the literature. The interplay between the two pathways highlights the importance of protein degradation equilibrium maintenance in the cell, since autophagic degradation is elevated as a compensatory mechanism when UPS is inhibited and *vice versa* (Pandey *et al.*, 2007, Lamark and Johansen, 2010, Wang *et al.*, 2013, Liu *et al.*, 2015). Previous reports have shown that AKT (Adachi *et al.*, 2003, Dickey *et al.*, 2008, Wakatsuki *et al.*, 2011, Wu *et al.*, 2011, Noguchi *et al.*, 2014) and ERK (Lu *et al.*, 2002) proteins are degraded by UPS. Interestingly, phosphorylation at S473 residue of AKT has been found to promote AKT ubiquitination by mTORC2 and AKT degradation (Wu *et al.*, 2011).

Firstly, we aimed to investigate whether genetic and pharmacological (CQ) modulation of autophagy resulted in upregulation of UPS activity and in that way increased degradation of pAKT and pERK 1/2 (Figure 4. 11.a). Since no difference in total AKT and ERK 1/2 levels was previously observed upon autophagy downregulation, we reasoned this may be due to a compensatory mechanism where total protein expression would be proportionally increased in order to diminish differences in phosphorylation. To test this hypothesis, autophagy-proficient and autophagy-compromised (shATG7 E8 and shEGFP+CQ conditions) cells were tested for their proteasome activity using the luminescence-based assay Proteasome-Glo. For a proteasome activity negative control in the assay, autophagy-proficient cells were treated with 2.5 μM of the proteasome inhibitor MG132. It was found that autophagy inhibition did not regulate proteasome activity since no difference was observed between autophagy-proficient and autophagy-compromised (shATG7 E8 and shEGFP+CQ) HCT-116 *KRAS* WT and G13D cells (Figure 4. 11.c).

However, this observation does not exclude the possibility that an Ubiquitin E3 ligase enzyme, responsible for ubiquitination and targeting of pAKT and pERK 1/2 protein for UPS degradation, could be specifically modulated and degraded by autophagy (Figure 4. 11.d). To this end, total cell lysates of autophagy-proficient and autophagy-compromised (shATG7 E8 and shEGFP+CQ) cells were non-treated or treated with 2.5 μM of MG132 proteasome inhibitor and the levels of AKT and ERK 1/2 protein phosphorylation relative to total protein levels were assessed by western blotting. Proteasome inhibition elevated pAKT S473 and pERK 1/2 levels of both autophagy-proficient and -compromised cells in comparison to the autophagy-proficient untreated control without remarkably affecting total levels of AKT and

ERK1/2 proteins, respectively. In particular, MG132 treatment totally and partially rescued phosphorylation levels of AKT at S473 residue in HCT-116 *KRAS* WT and G13D autophagy-compromised (shATG7 E8 and shEGFP+CQ) cells, respectively. Total rescue of phosphorylation levels of ERK 1/2 protein was observed upon autophagy inhibition conditions (shATG7 E8 and shEGFP+CQ) in both HCT-116 *KRAS* WT and G13D cells (Figure 4. 11.e). It was this observation that triggered the in-depth analysis of ERK 1/2 protein ubiquitination. In order to examine this, pERK 1/2 protein was pulled-down from total cell lysates of autophagy-proficient and -compromised HCT-116 *KRAS* WT cells in -/+ MG132-treated conditions and pERK 1/2 ubiquitination was examined using western blotting. Even though pERK 1/2 immunoprecipitation was successful, the presence of ubiquitination in pERK 1/2 protein was not verified in all conditions tested. Additionally, no rescue upon MG132 treatment could be observed in both autophagy-proficient and -compromised cells (Figure 4. 11.f).

In summary, no connection between autophagy modulation and proteasome activity and/or degradation of an E3-Ubiquitin ligase could be established.

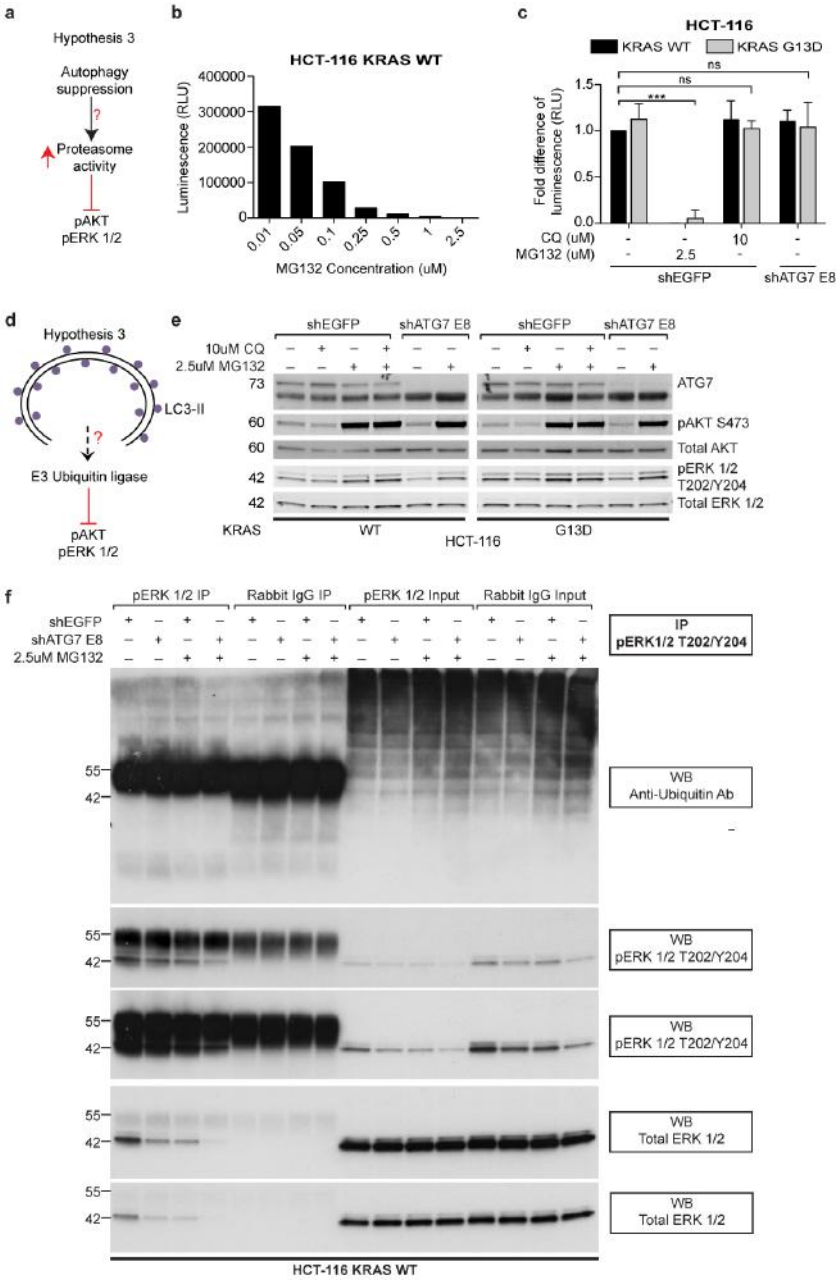

Figure 4. 11: Autophagy suppression does not affect the Ubiquitin proteasome system. a Schematic representation depicting the hypothesis that autophagy suppression could upregulate proteasome activity which in turn may lead to reduced phosphorylation of AKT and ERK 1/2 protein. b Bar plot presents proteasome activity dose-response of HCT-116 *KRAS* WT cells after treatment with the proteasome inhibitor MG132 for 6 hours. Proteasome activity was assessed using the luciferase-based assay Proteasome-Glo. c Differences in proteasome activity between autophagy-proficient and - compromised HCT-116 *KRAS* WT and G13D cells. Proteasome activity was assessed using the luciferase-based assay Proteasome-Glo. Two-way ANOVA with Bonferroni posttests statistical analysis was conducted for HCT-116 cells (n= 3). The bars represent mean ± standard deviation; ns= non-significant, *** p<0.001. d Flow chart showing the hypothesis that autophagy suppression may degrade an E3 ubiquitin ligase enzyme that targets pAKT and pERK for proteasomal degradation. e Activation levels of AKT and ERK 1/2 protein in autophagy-proficient and -compromised HCT-116 *KRAS* WT and G13D cells under basal and MG132-treated conditions. f Examination of ERK 1/2 protein ubiquitination under basal and proteasome-inhibited conditions in HCT-116 *KRAS* WT autophagy-proficient and -compromised cells. Immunoblots presented were only performed once. For proteasome inhibition cells were treated with 2.5 μM MG132 for 6 hours. Cells treated with 10 μM CQ for 6 hours in order to pharmacologically inhibit autophagy. Autophagy-proficient and autophagy-compromised t cells are shown as shEGFP and shATG7 E8. RLU= Relative light units.

4.2.6. Hypothesis 4: Receptor Tyrosine Kinase (RTK) activation in regulation of AKT/ERK phosphorylation upon autophagy suppression

Based on the findings reported above, we can conclude with some degree of confidence that the effect of autophagy suppression on signalling is not dependent on the following mechanisms: i) phosphatase degradation, ii) proteasome activity regulation or iii) proteasome activity/E3 ubiquitin ligase-dependent degradation. We therefore formulated another hypothesis whereby autophagy-mediated effects on AKT and ERK 1/2 activation are dependent on its ability to control RTKs, which, as previously described, play an important role in pathogenesis of CRC (Figure 4. 12). There is increasing evidence supporting RTK-dependent regulation of autophagy (discussed in 1.1.2.2., page 30) (Wei *et al.*, 2013, Tan *et al.*, 2015). However, to our knowledge nothing is known regarding autophagy-dependent regulation of RTK signalling. We set out to investigate this possibility. In support of this hypothesis is our finding showing CQ treatment to downregulate EGFR activation levels in DiFi cells (Figure 3. 8.e).

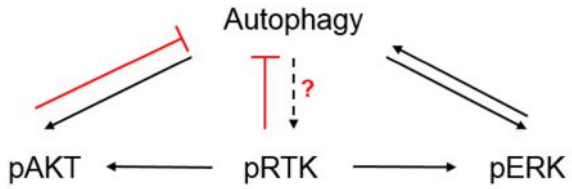

Figure 4. 12: Schematic representation depicting the hypothesis that autophagy suppression may regulate RTK phosphorylation and downstream signalling.

We utilised a phospho-RTK array to evaluate the phosphorylation of 49 different RTKs. Activated *KRAS* G13D isogenic cell lines were also included in this examination in order to assess whether the presence of oncogenic *KRAS* affects autophagy-dependent RTK regulation, as previous studies have described a reduced dependency on RTK activation in cells harbouring *KRAS* activating mutations (van Houdt *et al.*, 2010).

Interestingly, phosphorylation of eight different RTKs was decreased upon autophagy suppression in HCT-116 *KRAS* WT cells. In particular, autophagy-compromised cells displayed a decrease in phosphorylation levels of the highly activated RTKs: i) c-MET (35%), member of HGFR RTK family; ii) Dtk (35%), member of AXL RTK family; iii) c-Ret (60%), member of the RET RTK family and iv) RYK (40%). In the same cells, RTKs with lower phosphorylation activation levels than the

aforementioned also exhibited decreased phosphorylation levels upon autophagy downregulation; these were: i) TrkC (90%), belonging to NGFR family of RTKs and ii) EphA1 (46%), EphA2 (30%) and EphB2 (60%), members of the Eph family of RTKs. A similar pattern of decreased phosphorylation in RTKs upon autophagy suppression was also observed in *KRAS* G13D expressing HCT-116 cells: i) c-Met, ii) Dtk and iii) c-Ret RTKs displayed a decrease in their phosphorylation levels upon autophagy suppression (~47%, 30% and 60%, respectively). Additional RTKs with their activity found to be inhibited upon autophagy suppression in HCT-116 *KRAS* G13D cells were: i) Insulin R (26%) and IGF-I R (22%), members of Insulin R family of RTKs; ii) Axl (17%), member of AXL RTK family; iii) MSP R (42%), member of HGFR RTK family; iv) ROR2 (15%), member of ROR RTK family and v) EphA10 (38%), member of the Eph RTK family. In contrast to HCT-116 *KRAS* WT cells, autophagy suppression resulted in upregulated phosphorylation of TrkC RTK (~70%; member of NGFR RTK family) in the presence of the *KRAS* G13D mutation (Figure 4. 13).

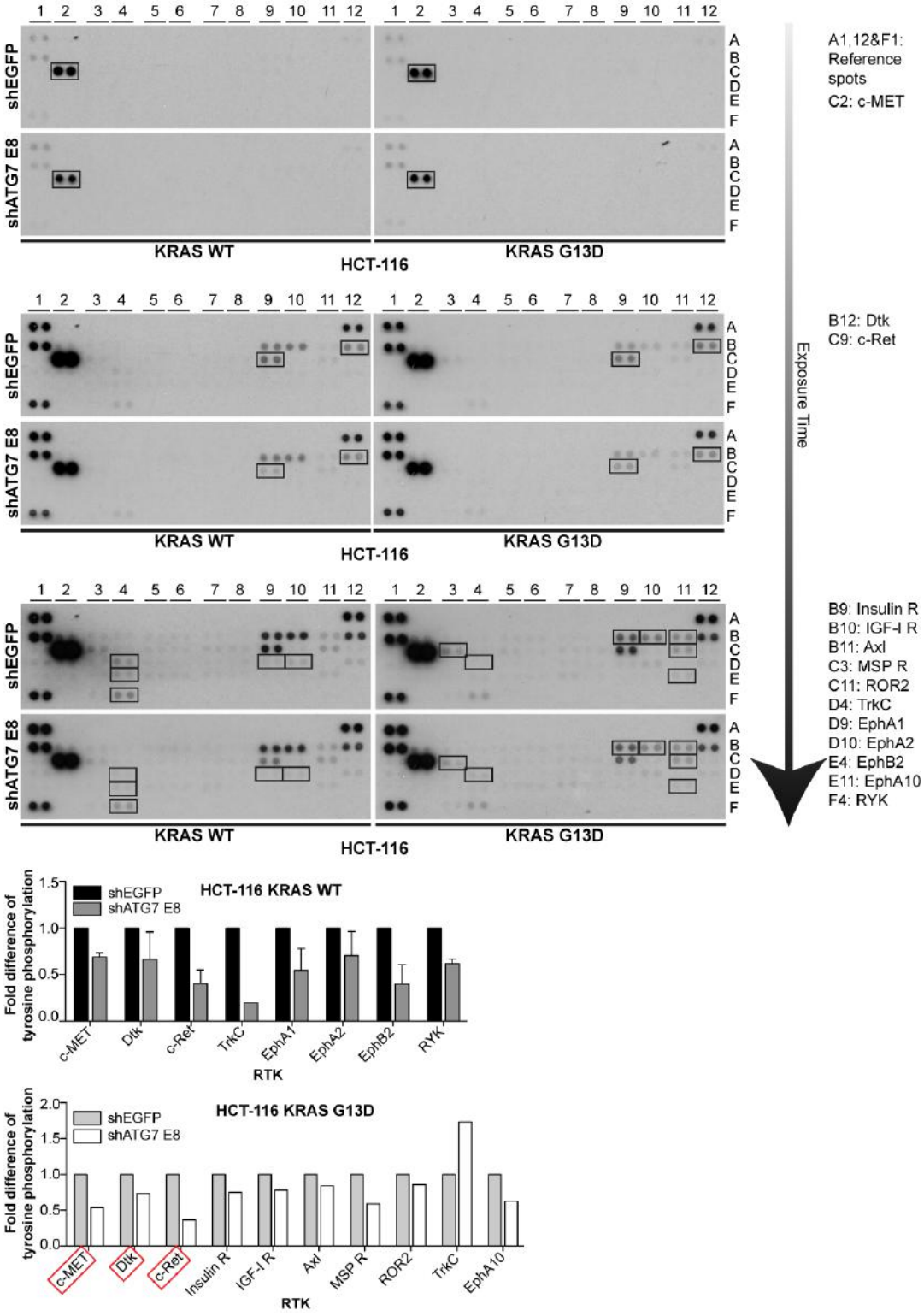

Figure 4. 13: Decreased phosphorylation levels of RTKs upon autophagy suppression in HCT-116 *KRAS* WT and G13D isogenic cells. Phospho-RTK array membranes, printed with 49 different anti-total RTK antibodies in duplicate, were incubated overnight with autophagy-proficient (shEGFP) and -compromised (shATG7 E8) cell lysates. Incubation with phospho-tyrosine HRP-conjugated antibody detected RTK activation levels. Immunoblots presented are from one complete experiment, processed simultaneously for all conditions examined and are representative of two independent experiments for *KRAS* WT and one experiment for *KRAS* G13D cells. Arrow indicates increased exposure time used to develop immunoblots. Bar plots depict densitometric quantification of phospho-RTK array spots. Bars represent mean ± standard deviation. Red boxes indicate RTKs found to be deregulated upon autophagy suppression in both HCT-116 *KRAS* WT and G13D cells.

To exclude the possibility of a cell-type specific effect of autophagy suppression in regulating RTK phosphorylation, DLD-1 *KRAS* WT and G13D cells were also examined for RTK activation levels upon autophagy suppression conditions, using the phospho-RTK array. In accordance with the reduced RTK-phosphorylation phenotype observed in HCT-116 autophagy-compromised cells, both DLD-1 *KRAS* WT and G13D autophagy-compromised cells displayed a decrease in RTK phosphorylation. In particular, we found the following reduction in RTK phosphorylation levels: i) c-MET (50%) and MSP R (50%), members of HGFR family of RTKs; ii) EGFR (15%), ErbB2 (35%) and ERBB3 (24%), members of EGFR family of RTKs; iii) IGF-I R (20%), member of Insulin RTK family; iv) Dtk (38%), member of Axl RTK family; v) SCF-R (26%), member of PDGFR family of RTKs; vi) c-Ret (31%), member of RET RTK family in DLD-1 *KRAS* WT cells. Longer developing time of the phospho-RTK array membranes revealed an additional 13 RTKs with reduced phosphorylation levels upon autophagy suppression including: i) FGFR1 (49%), FGFR2a (26%) and FGFR3 (25%), members of the FGFR family of RTKs; ii) PDGFRβ (49%) and M-CSF R (20%), members of PDGFR family of RTKs; iii) VEGF R3 (18%), member of the VEGF R family of RTKs; iv) EphA1 (11%), EphA2 (10%), EphA4 (47%), EphA7 (33%) and EphB3 (15%), members of the Eph family of RTKs and v) TrkA (50%) and TrkC (26%), members of the NGFR family of RTKs. ALK, which belongs to the insulin RTK family showed increased phosphorylation levels upon autophagy suppression (30%). Reduced RTK-phosphorylation upon autophagy suppression was also observed in DLD-1 *KRAS* G13D cells but to a lesser extent compared to WT cells: c-MET, ErbB2, Dtk and EphA4 displayed reduced phosphorylation (20%, 27%, 23% and 33%, respectively). Additional RTKs with reduced phosphorylation in DLD-1 *KRAS* G13D cells were: i) ROR2 (13%), member of the ROR RTK family; ii) Tie-2 (50%), member of TIE RTK family; iii) ALK (33%), member of Insulin R family and iv) EphA10 (25%), member of the Eph family of RTKs. In contrast to DLD-1 *KRAS* WT autophagy-compromised cells, autophagy suppression in DLD-1 *KRAS* G13D cells resulted in enhanced phosphorylation of: i) ERBB3 (52%), ii) MSP R (23%) and iii) EphA1 (16%) (Figure 4. 14).

In conclusion, autophagy suppression reduces RTK-phosphorylation in CRC cells, in most cases independently of *KRAS* mutational status. Notably, c-MET, Dtk and c-RET RTKs were hypo-phosphorylated upon autophagy suppression in both HCT-116 and DLD-1 cells.

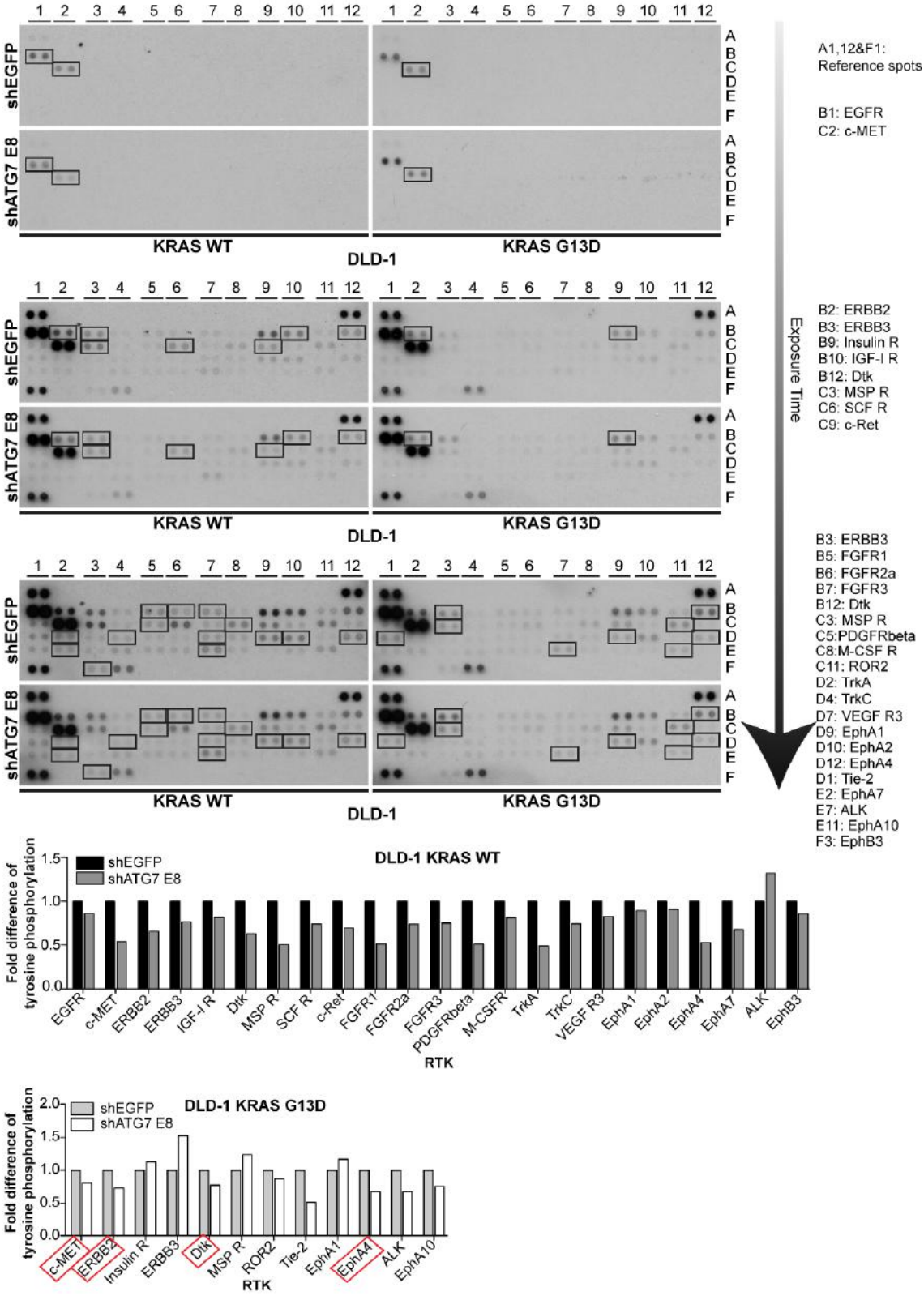

Figure 4. 14: Decreased phosphorylation levels of RTKs upon autophagy suppression in DLD-1 *KRAS* WT and G13D isogenic cells. Phospho-RTK array membranes, printed with 49 different anti-total RTK antibodies in duplicate, were incubated overnight with autophagy-proficient (shEGFP) and -compromised (shATG7 E8) cell lysates. Incubation with phospho-tyrosine HRP-conjugated antibody detected RTK activation levels. Immunoblots presented are from one complete experiment and simultaneously processed for all conditions examined. Arrow indicates increased exposure time used to develop immunoblots. Bar plots depict densitometric quantification of phospho-RTK array spots. Red boxes indicate RTKs found to be deregulated upon autophagy suppression in both DLD-1 *KRAS* WT and G13D cells.

4.2.7. Validation of RTK Array results: c-MET phosphorylation is affected upon autophagy suppression

To validate hits identified by the RTK array, we used immunoprecipitation for total-RTKs followed by western blotting with an anti-phospho-tyrosine antibody. We decided to focus our research on c-MET since its expression and signalling, apart from being highly expressed in CRC, have also been implicated in development of primary and acquired resistance of mCRC cells and patients to EGFR-targeted therapy (Bardelli *et al.*, 2013, Misale *et al.*, 2014). In addition to the high clinical importance of studying c-MET, plenty of reagents to enable our research were available.

In line with the phospho-RTK array results, immunoprecipitated total c-MET was found to be less phosphorylated in autophagy-compromised cells compared to autophagy-proficient HCT-116 *KRAS* WT cells (Figure 4. 15.a). Moreover, the ratio between phosphorylated c-MET and total c-MET was reduced in total cell lysates from autophagy-compromised cells by approximately 40%. The decrease in c-MET phosphorylation was not a secondary effect caused by reduced total c-MET levels, as total c-MET levels were unaltered in autophagy-compromised cells (Figure 4. 15.b).

In an attempt to validate additional RTKs, we studied phosphorylation levels of c-Ret but reagents were not reliable (not shown). As expected, phosphorylation levels of both IGF-I R and EGFR were not affected, in agreement with phospho-RTK array results for HCT-116 *KRAS* WT cells (Figure 4. 16). Of note, total tyrosine-phosphorylation levels were not altered upon autophagy suppression (Figures 4. 15 and 4. 16).

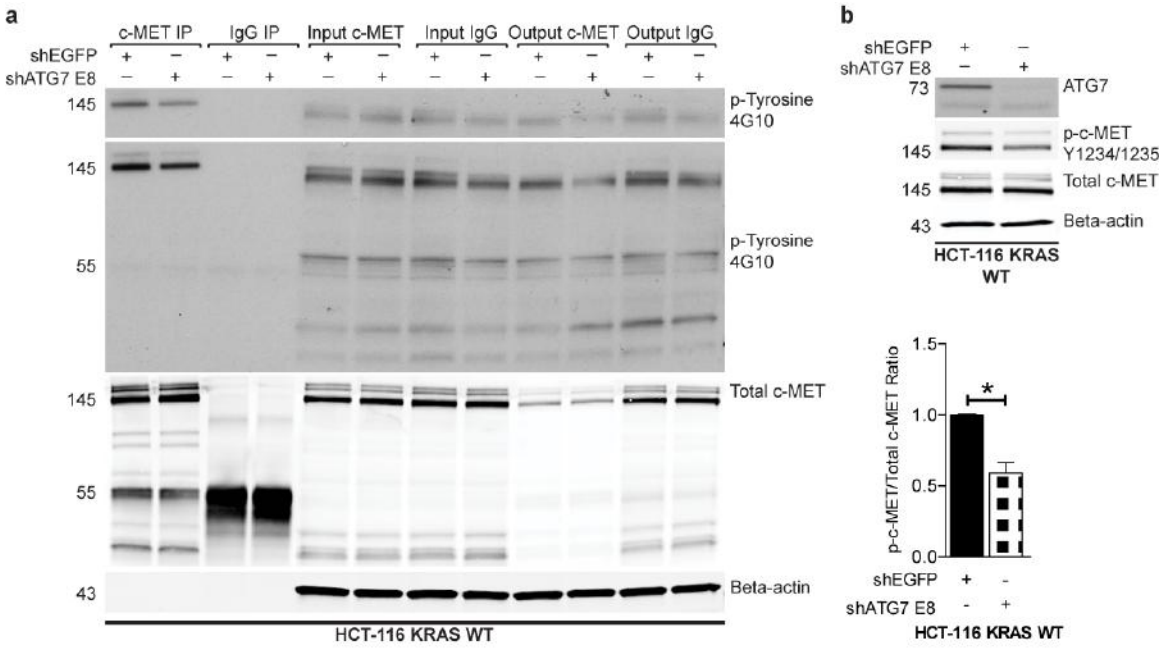

Figure 4. 15: Autophagy suppression reduces c-MET activation in HCT-116 *KRAS* WT cells. a Autophagy-proficient and -compromised cells 5 days after DOX treatment, to efficiently downregulate ATG7 protein expression, were lysed and total c-MET protein subjected to immunoprecipitation. Immunoprecipitated c-MET activity was assessed using western blotting for p-Tyrosine 4G10 antibody. Total c-MET was used to examine immunoprecipitation efficiency and loading. Beta-actin was used as loading control of total cell lysates. **b** Autophagy-proficient and -compromised total cell lysates derived from HCT-116 *KRAS* WT cells 5 days after DOX treatment, to downregulate ATG7 protein, were subjected to western blotting in order to examine p-c-MET Y1234/1235 relative to total c-MET levels. Beta-actin used as loading control. Immunoblot presented is representative of n= 3 independent experiments. Bar plot represents densitometric quantification of p-c-MET Y1234/1235 relative to total c-MET protein. The bars represent mean ± standard deviation; * $p<0.05$. Unpaired Student's t-test.

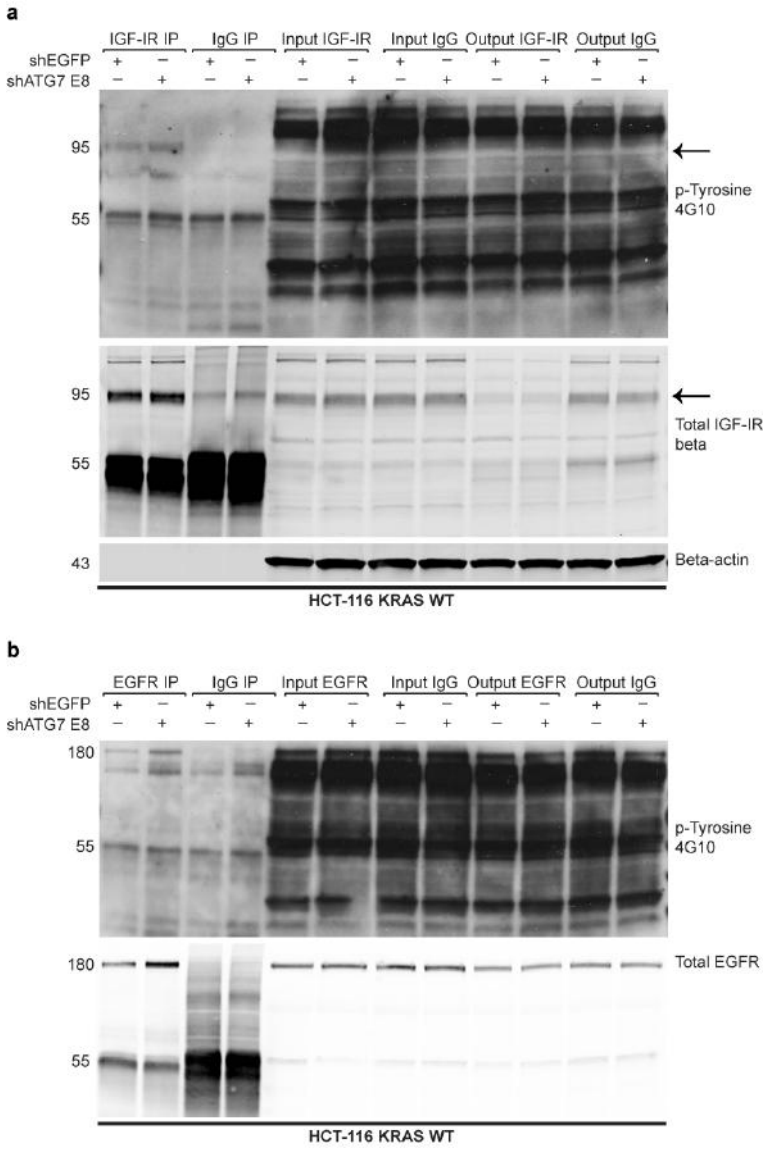

Figure 4. 16: Autophagy suppression does not alter phosphorylation levels of IGF-I R and EGFR in HCT-116 *KRAS* WT cells. Autophagy-proficient and -compromised cells 5 days after DOX treatment, to efficiently downregulate ATG7 protein expression, were lysed and total cell lysates were subjected to immunoprecipitation with **a** total IGF-I R and **b** total EGFR antibodies. Immunoprecipitated total IGF-I R and total EGFR activity was assessed using western blotting for p-Tyrosine 4G10 antibody. Total IGF-I R and total EGFR proteins used to assess immunoprecipitation efficiency and loading. Beta-actin was used as loading control of total cell lysates. Arrow indicates IGF-I R.

Overall, c-MET but not EGFR or IGF-IR beta activation was altered by autophagy suppression in immunoprecipitation studies, as the phospho-RTK array had previously indicated for HCT-116 *KRAS* WT cells. Additionally, the sustained total c-MET levels and total tyrosine-phosphorylation levels under autophagy-compromised conditions point in the direction of autophagy specifically regulating phosphorylation levels of c-MET.

4.2.8. c-MET colocalises with autophagosomes

Based on our observations and evidence from the literature showing that RTKs may colocalise with autophagic structures (Sandilands *et al.*, 2012, Jones *et al.*, 2014), we formulated the hypothesis that internalised c-MET colocalises with autophagic vesicles. To explore this possibility, HCT-116 *KRAS* WT cells were examined using confocal microscopy for endogenous c-MET and LC3B protein localisation and interaction. To increase the chances of detecting autophasosomes, the lysosomotropic agent CQ was included to enable their accumulation by preventing their fusion with lysosomes and degradation. Even though in both untreated and CQ-treated cells, c-MET was found to colocalise with LC3B protein, the distribution of colocalising domains in the cell differed between the two conditions. In particular, in -CQ conditions c-MET staining was mainly observed at the plasma membrane, where it displayed a degree of colocalisation with LC3B. After CQ treatment c-MET was observed in punctate intracellular structures around the nucleus that colocalised with LC3B (Figure 4. 17.a). To determine whether this colocalisation pattern applied to another RTK, localisation of EGFR was examined upon -/+ CQ treatment in HCT-116 *KRAS* WT cells. It was observed that EGFR was located at the plasma membrane in both -/+CQ conditions examined. In -CQ condition, EGFR seemed to colocalise with LC3B at the plasma membrane, in accordance with the c-MET/LC3B colocalisation data. In contrast to c-MET, EGFR did not accumulate in perinuclear areas upon CQ treatment and no colocalisation with LC3B was observed (Figure 4. 17.b).

As the majority of studies describe LC3B to be mainly cytoplasmic, we decided to investigate whether the staining was specific to LC3B protein. HCT-116 *KRAS* WT cells were transiently transfected with two different LC3B siRNAs and it was confirmed that intracellular LC3B staining in the +CQ condition was specific since both LC3B siRNAs abolished intracellular LC3B signal. Plasma membrane staining of endogenous LC3B could not be proved specific since staining was, to some extent, retained in cells transfected with LC3B siRNAs (Figure 4. 18).

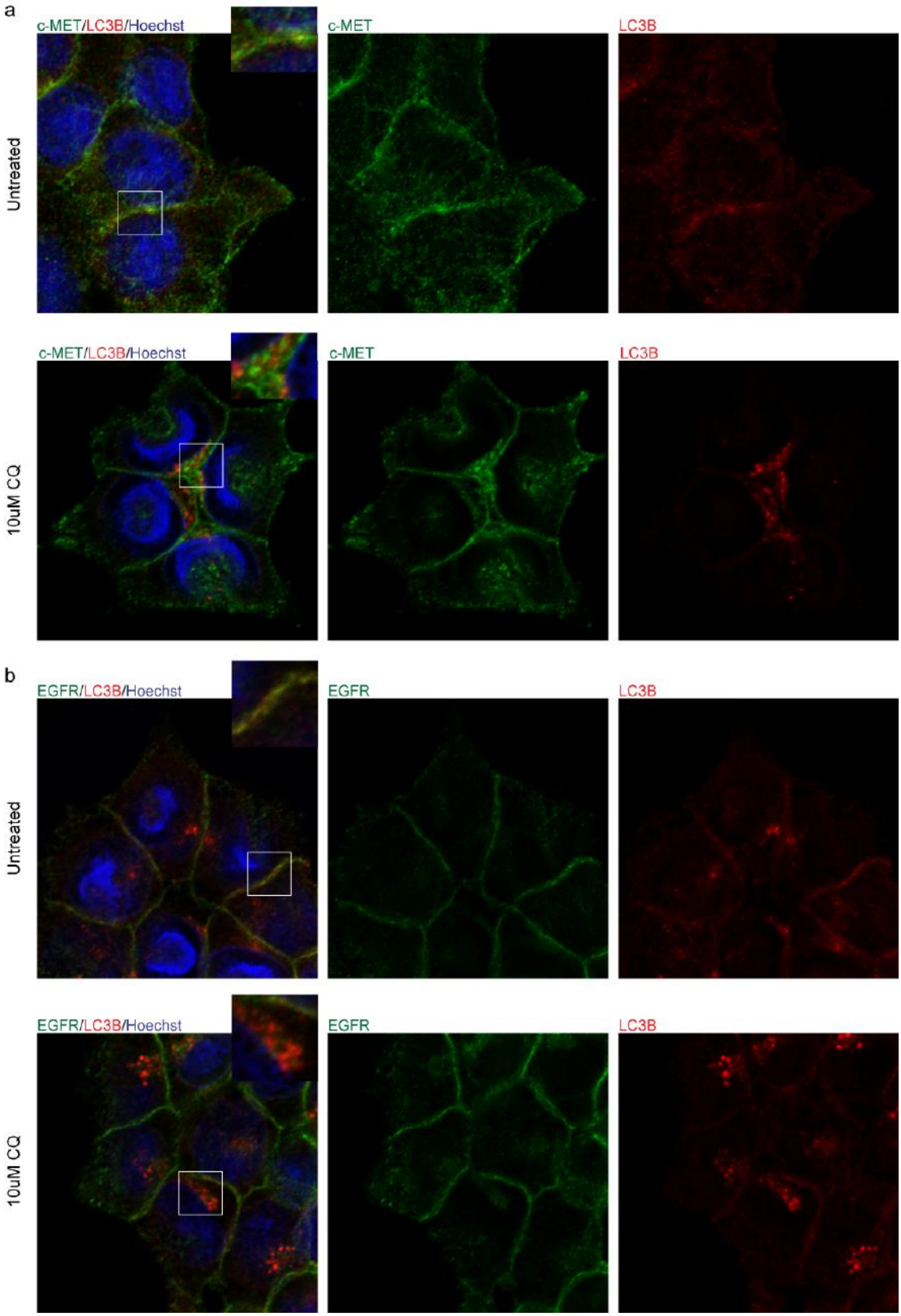

Figure 4. 17: Examination of LC3B colocalisation with a c-MET and **b** EGFR RTKs. HCT-116 *KRAS* WT cells were either treated or not with 10 μM CQ for 6 hours and then fixed. Cells were stained for total c-MET (green) or EGFR (green), LC3B (red) and nucleus (Hoechst dye-blue). Images were acquired using a Zeiss LSM 700 confocal microscope.

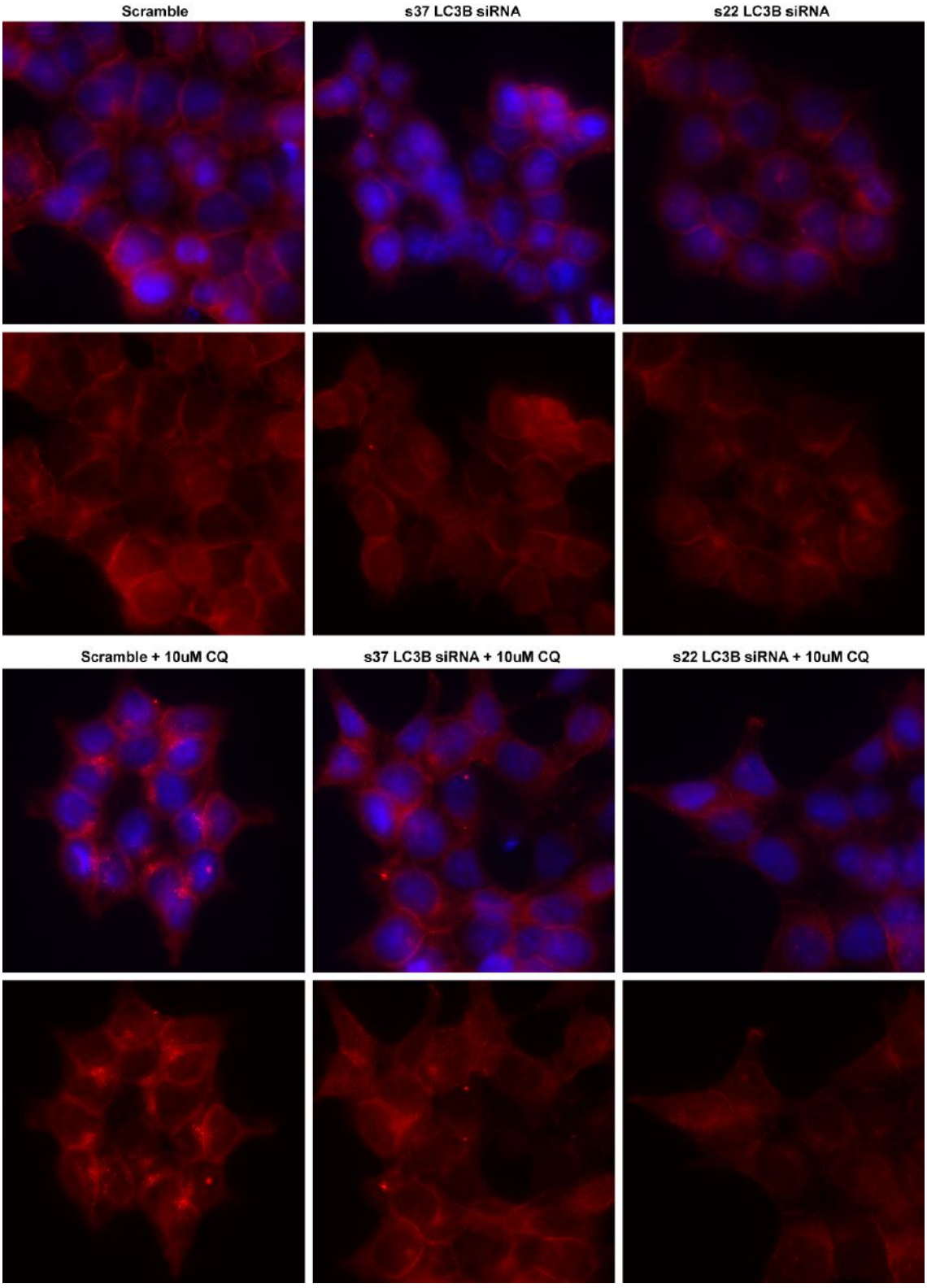

Figure 4. 18: Examination of LC3B antibody specificity. HCT-116 *KRAS* WT cells were transiently transfected with 10 nM scramble, s22- and s37- LC3B siRNAs using lipofectamineRNAiMax reagent. 48 hours post-transfection cells were treated with or without 10 μM CQ for 6 hours and then fixed. Cells were stained for LC3B (red) and nucleus (Hoechst dye-blue). Images were acquired using a Zeiss epifluorescence microscope.

4.2.9. c-MET has a putative LIR motif but interaction with LC3B could not be proved

Studies on selective autophagy, where characterised autophagy receptors such as p62 and NBR1 function as inter-mediators between cargo and autophagosome associated LC3B protein, led to the identification and characterisation of LC3-Interacting Region (LIR) motifs in proteins interacting with LC3B. LIR motifs are characterised by a consensus amino acid sequence of [W/F/Y]xx[L/I/V] where x indicates any amino acid (W stands for Tryptophan, F for Phenylalanine, Y for Tyrosine, L for Leucine, I for Isoleucine, and V for Valine). New LIR-motif-containing proteins are constantly being discovered and in many cases they can function differently to an autophagy receptor. Some examples are proteins of the core autophagy machinery, proteins associated with autophagosomes and other vesicles and signalling proteins that act as substrates for selective autophagy (Birgisdottir *et al.*, 2013).

Based on that knowledge and iLIR website (http://repeat.biol.ucy.ac.cy/iLIR/), for *in silico* identification of LIR motifs in proteins (Kalvari *et al.*, 2014), we examined whether c-MET and other RTKs contain any possible LIR motifs which would enable direct interaction with LC3B protein and consequently autophagosome. The iLIR website predicted candidate sequences that could act as LIRs in all RTKs tested (Table 4. 2). In the majority of RTKs, including c-MET; sequences located in both extracellular and cytoplasmic tyrosine kinase domains of RTKs were predicted to be good candidates for interaction with LC3B protein. Probability of good candidates was based on the position-specific scoring matrix (PSSM) value provided by iLIR.

Even though iLIR analysis indicated the presence of possible LIR motifs in c-MET and other RTKs, experimental validation of direct interaction between c-MET and LC3B was indispensable to eliminate false positive predictions. To this end, autophagy-proficient and -compromised HCT-116 *KRAS* WT total cell lysates were immunoprecipitated for total and p-c-MET proteins and the presence of LC3B protein in a complex with c-MET was examined using western blotting. CQ treatment was applied in both autophagy-proficient and -compromised cells to eliminate LC3-II degradation by autophagosomes and enhance LC3B protein detection. LC3B protein did not coimmunoprecipitate neither with total MET nor with p-c-MET protein in all conditions tested, even though pull-down of both c-MET and p-cMET was successful (Figure 4. 19). In summary, even though iLIR server predictions indicated an LC3B-dependent regulation of c-MET phosphorylation by autophagy, immunoprecipitation experiments could not prove a direct interaction between LC3B and c-MET. The latter needs further investigation since experimental limitations could have led to negative

results. In this respect, different IP conditions could reveal an interaction. Furthermore, the use of antibodies against the extracellular domain or a tagged version of c-MET could avoid problems related to antibody binding of the putative LIR region and therefore interfering with the interaction to LC3B.

Table 4. 2: iLIR server predicts possible LIR motif sequences present in RTKs. The amino acid sequence of each RTK was examined for the presence of xLIR motif sequences corresponding to the [ADEFGLPRSK][DEGMSTV][**WFY**][DEILQTV][ADEFHIKLMPSTV][**ILV**], *in silico*. PSSM stands for position-specific scoring matrix and indicates the probability of a functional LIR prediction. The higher the PSSM value, the greater the probability of a functional LIR detection is. For the identification of possible LIR motifs, a PSSM value above 10 was used as the cut-off. iLIR server uses also the ANCHOR software, which predicts disorder sequences able to stabilize upon binding to a target protein. If a sequence is characterized as an anchor and has a high PSSM value, the probability of it to be a functional LIR is increased.

RTK	Motif	Position	RTK domain	LIR Sequence	PSSM score	Anchor	Similar LIRs
c-MET	WxxL	224-229	Extracellular	DGFMFL	12 (1.1e-01)	No	
	WxxL	1247-1252	Cytoplasmic Tyrosine kinase	VKWMAL	11 (1.5e-01)	No	
c-Ret	xLIR	104-109	Extracellular	SSWEKL	19 (1.2e-02)	No	BNI3L_HUMAN 34-39
	xLIR	1013-1018	Cytoplasmic Tyrosine kinase	RDYLDL	16 (3.0e-02)	No	
	xLIR	750-755	Cytoplasmic Tyrosine kinase	AGYTTV	11 (1.5e-01)	No	
	WxxL	35-40	Extracellular	AYWEKL	14 (5.7e-02)	No	
	WxxL	83-88	Extracellular	NNWICI	13 (7.9e-02)	No	
	WxxL	915-920	Cytoplasmic Tyrosine kinase	VKWMAI	11 (1.5e-01)	No	
EGFR	xLIR	86-91	Extracellular	AGYVLI	12 (1.1e-01)	No	
	xLIR	1084-1089	Cytoplasmic	DTFLPV	12 (1.1e-01)	Yes	
	WxxL	475-480	Extracellular	INWKKL	12 (1.1e-01)	No	
	WxxL	878-883	Cytoplasmic Tyrosine kinase	IKWMAL	11 (1.5e-01)	No	
IGF-I R	xLIR	56-61	Extracellular	EGYLHI	12 (1.1e-01)	No	
	xLIR	1257-1262	Cytoplasmic Tyrosine kinase	PSFLEI	11 (1.5e-01)	No	OPTN_HUMAN 176-181
Insulin R	xLIR	392-397	Extracellular	SGYLKI	12 (1.1e-01)	No	
	xLIR	1281-1286	Cytoplasmic Tyrosine kinase	PTFLEI	11 (1.5e-01)	Yes	
PDGFR beta	xLIR	862-867	Cytoplasmic Tyrosine kinase	STFLPL	11 (1.5e-01)	No	

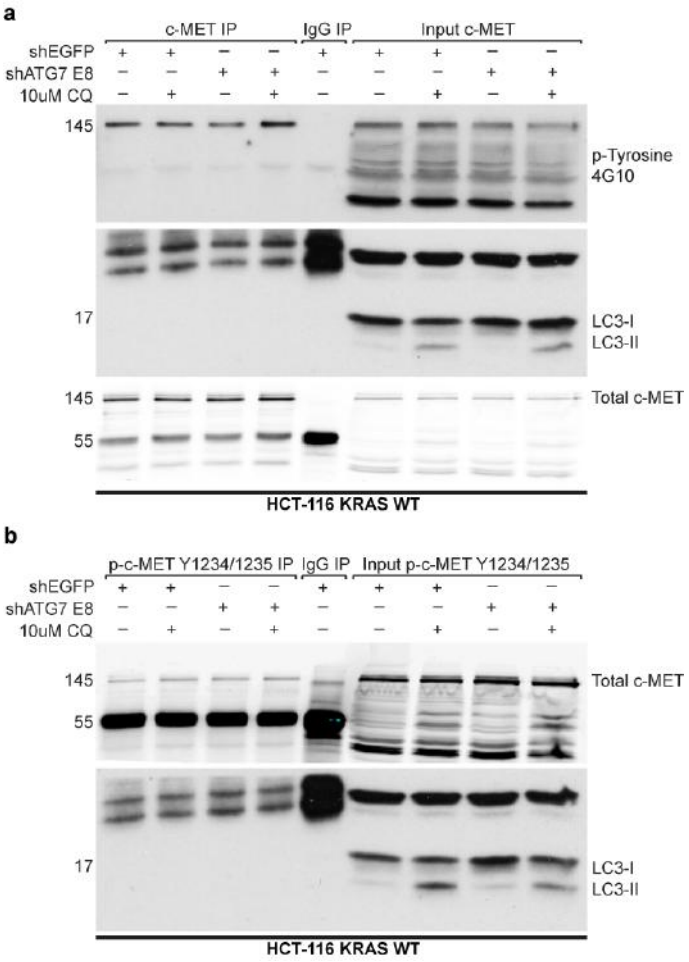

Figure 4. 19: LC3B does not immunoprecipitate either with total c-MET or with p-c-MET Y1234/1235 protein. Autophagy-proficient and -compromised cells 5 days after DOX treatment, to efficiently downregulate ATG7 protein expression, were treated with -/+ 10 μM CQ for 6 hours and then were lysed. Total cell lysates were subjected to immunoprecipitation with **a** total c-MET and **b** p-c-MET Y1234/1235 antibodies. Interaction of LC3B protein with immunoprecipitated total c-MET and p-c-MET Y1234/1235 was assessed using western blotting for LC3B. Total c-MET protein used to assess immunoprecipitation efficiency and loading. p-Tyrosine 4G10 used to assess phosphorylation levels of immunoprecipitated c-MET protein.

4.2.10. Examination of c-MET, ERK and AKT phosphorylation under LC3B protein downregulation conditions

To determine whether regulation of c-MET RTK, MAPK/ERK- and PI3K-components phosphorylation requires LC3-II positive autophagosomes, HCT-116 *KRAS* WT cells were transfected with control and LC3B siRNAs to inhibit LC3B protein expression. I hypothesised that if LC3B protein plays an active role in regulating the phosphorylation of the aforementioned proteins, LC3B depletion would recapitulate the defects in their phosphorylation observed by ATG7 downregulation. LC3B protein expression was abolished and autophagy levels measured by p62 protein expression remained stable with both LC3B siRNAs examined (Figure 4. 20.a). Preliminary data

showed that LC3B protein downregulation reduced phosphorylation levels of c-MET, ERK1/2 and possibly AKT proteins without affecting their total protein levels (Figure 4. 20). In particular, both LC3B siRNA samples exhibited modest albeit reduced phosphorylation levels of c-MET relative to total protein (approximately 16% and 21% in s22 and s37 LC3B siRNAs, respectively). ERK 1/2 phosphorylation was reduced independently of MEK 1/2 phosphorylation upon LC3B downregulation (s22~ 21% and s37~41%). Regarding PI3K pathway, even though s22 LC3B siRNA exhibited reduced AKT phosphorylation levels relative to total AKT (~25%), s37 LC3B siRNA upregulated AKT phosphorylation levels (~25%) relative to total AKT. Phosphorylation of S6 ribosomal protein remained stable with both LC3B siRNAs examined.

Collectively, in line with ATG7 knockdown experiments, LC3B downregulation reduced c-MET and ERK 1/2 phosphorylation levels whereas levels of pAKT were affected in a siRNA sequence-dependent manner. Additionally, MEK 1/2 and S6 ribosomal protein phosphorylation was sustained following LC3B siRNA in contrast to the attenuated and elevated levels, which were observed following ATG7 downregulation. Further experiments are warranted to establish whether LC3B protein has an active role in regulation of c-MET RTK, MAPK/ERK- and PI3K-components phosphorylation.

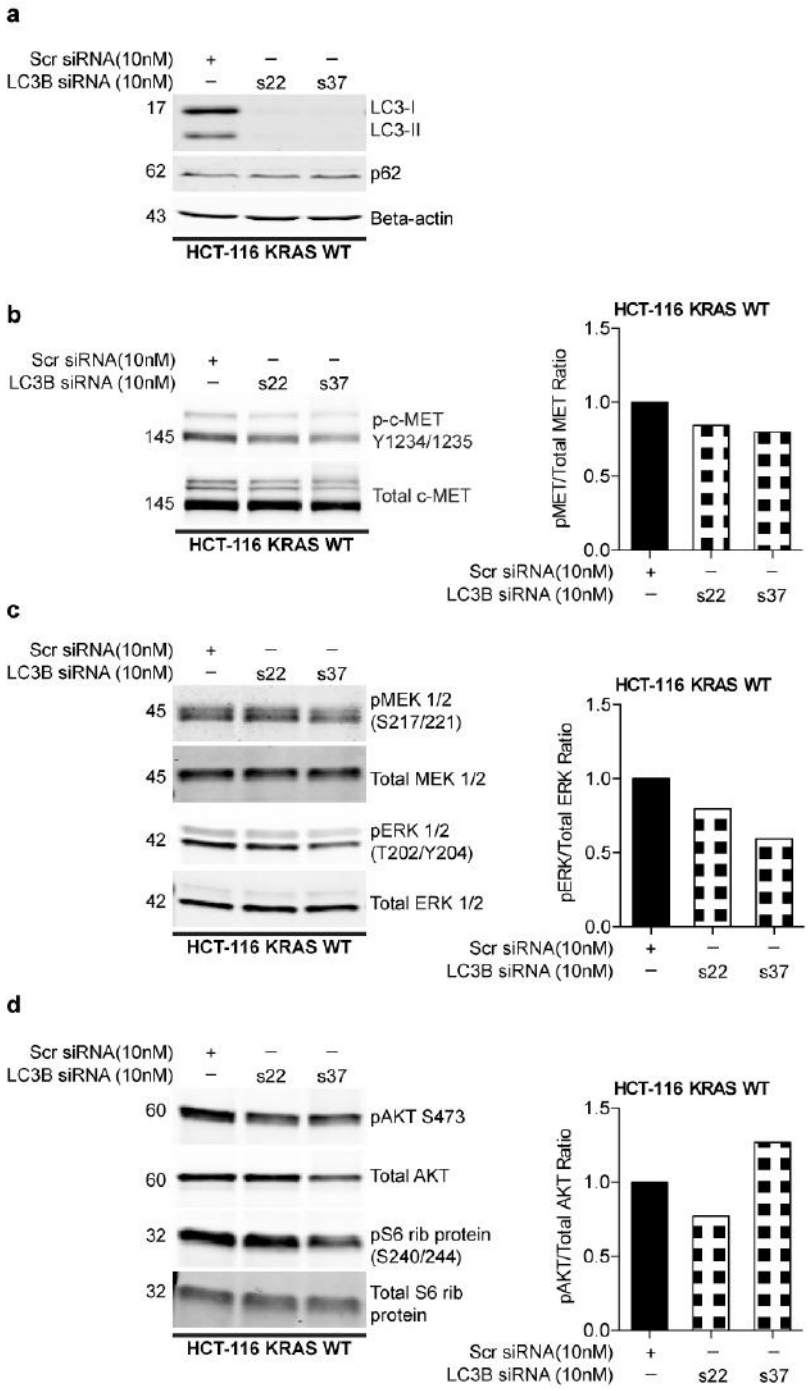

Figure 4. 20: Examination of c-MET, MAPK/ERK and PI3K pathway components phosphorylation upon LC3B downregulation. HCT-116 *KRAS* WT cells were transiently transfected with 10 nM scramble, s22- and s37- LC3B siRNAs using lipofectamineRNAiMax reagent. 48 hours post-transfection cells were lysed and total cell lysates were subjected to western blotting for corresponding proteins. Examination of: **a** LC3B and p62 protein expression levels; **b** c-MET phosphorylation levels relative to total c-MET protein expression levels; **c** MEK 1/2 and ERK 1/2 phosphorylation levels relative to total MEK 1/2 and ERK 1/2, respectively; **d** AKT S473 and S6 ribosomal protein phosphorylation levels relative to total AKT and S6 ribosomal protein, respectively upon LC3B siRNA. Beta-actin used as western blotting loading control. Bar plots represent densitometric analysis of p-c-MET/pERK 1/2/pAKT proteins relative to their corresponding total proteins. Scr= Scramble siRNA control. Immunoblot images depict results of a single experiment.

4.2.11. HGF levels are not affected by autophagy inhibition

Based on previous observations suggesting that LC3-II-positive autophagosomes may be responsible for c-MET activation regulation, we aimed to gain insight into the functional mechanism by which autophagy regulates phosphorylation of c-MET RTK.

Ligand binding in RTK extracellular domains initiates RTK dimerisation and transphosphorylation of their cytoplasmic-tyrosine kinase domain leading to RTK activation (Lemmon and Schlessinger, 2010). Hepatocyte Growth Factor (HGF) is responsible for triggering c-MET activation after its binding and leading to phosphorylation of c-MET catalytic Y1234/1235 residues. Even though c-MET activation in plasma membrane of epithelial cells is mainly catalysed in a paracrine manner by HGF that is produced in mesenchymal cells (Trusolino *et al.*, 2010), an autocrine activation mechanism of c-MET activation in cancer has been previously described (Peruzzi and Bottaro, 2006). To explore whether autophagy suppression reduces HGF expression levels and consequently autocrine c-MET activation, autophagy-proficient and -compromised HCT-116 *KRAS* WT cells were examined for HGF expression levels using western blotting. Additionally, based on the observation that LC3B siRNA-treated cells exhibit slightly reduced c-MET activation, lysates of HCT-116 *KRAS* WT cells with abolished LC3B expression were also subjected to western blotting for HGF expression. Sustained HGF expression was observed under both autophagy suppression and LC3B siRNA conditions (Figure 4. 21), discouraging the hypothesis of a reduced autocrine c-MET activation mechanism upon autophagy suppression.

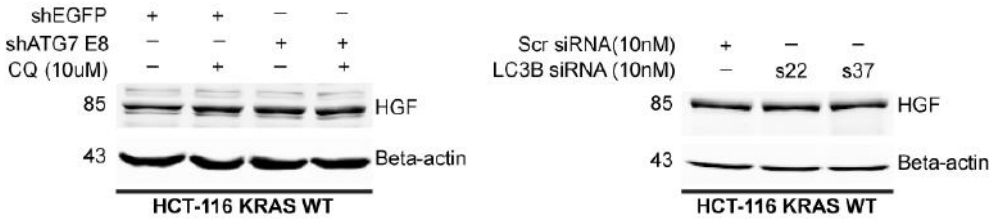

Figure 4. 21: HGF expression levels upon a autophagy suppression and **b** LC3B siRNA conditions in HCT-116 *KRAS* WT cells. For autophagy suppression experiment, autophagy-proficient and -compromised HCT-116 *KRAS* WT cells were treated with 10 ng/ml DOX for 5 days to efficiently downregulate ATG7 protein expression. At day 5, cells were treated with 10 μM CQ for 6 hours and followed cell lysis for western blotting examination of HGF protein. For LC3B siRNA experiment, HCT-116 *KRAS* WT cells were transiently transfected with 10 nM scramble or s22/s37 LC3B siRNAs using lipofectamineRNAiMax reagent. 48 hours post-transfection cells were lysed and subjected to western blotting for HGF protein. Beta-actin used as loading control. Scr= Scramble siRNA control. Immunoblot in **a** is representative image of 2 independent experiments. Immunoblot in **b** performed once.

4.2.12. Endocytosis is not negatively affected upon autophagy inhibition

Traditionally, endocytosis has been thought to be an attenuation mechanism of RTK activation and signalling through removal of the activated RTK from the signalling-active plasma membrane and leading to either RTK degradation at lysosomes or RTK recycling back to the plasma membrane (Lemmon and Schlessinger, 2010). Two distinct endocytosis mechanisms have been described for RTKs including clathrin-mediated and caveolae-mediated endocytosis. Even though the formation of either clathrin- or caveolin- positive vacuoles from the plasma membrane discriminates these endocytosis pathways, the plasma membrane-release of vesicles is catalysed in both cases by the action of dynamin protein. c-MET RTK is mainly endocytosed in a clathrin-mediated manner (Gherardi *et al.*, 2012). Interestingly, a recent publication studying the proteome differences between autophagy-proficient and -deficient (ATG5-/- and ATG7-/-) HRAS G12V expressing immortalized baby mouse kidney (iBMK) cells under nutrient-replete and -deplete conditions, reported that autophagy suppression decreased clathrin but not caveolin protein expression levels (Mathew *et al.*, 2014). We hypothesised that autophagy suppression may alter endocytosis of RTKs and impair their downstream signalling. To study the role of autophagy in RTK endocytosis a labeled-transferrin ligand approach was employed to investigate endocytosis differences in clathrin-mediated transferrin receptor internalisation between autophagy-proficient and -compromised cells. Additionally, two different endocytosis inhibitors were used as positive controls: Pitstop2 inhibiting only clathrin-mediated endocytosis and dynasore inhibiting both clathrin- and caveolin-mediated endocytosis. Preliminary data suggested that endocytosis rates of transferrin receptor were not affected upon autophagy suppression (Figure 4. 22).

In contrast to the attenuation-signalling function of RTK endocytosis, an increasing number of studies are reporting endocytosis as a mechanism for sustained intracellular signalling of RTKs (Lemmon and Schlessinger, 2010). c-MET has been proven as a competent RTK to signal from endosomes and c-MET endosomal signalling is important for full ERK1/2 and Rac1 activation upon HGF stimulation (Kermorgant *et al.*, 2004, Ménard *et al.*, 2014). Based on our observation that c-MET colocalises with LC3B protein in perinuclear regions upon CQ treatment and the work of Martinez-Lopez *et al*., (2013) suggesting autophagosomes to act as intracellular signalling-platforms for ERK 1/2, we decided to investigate whether autophagy suppression regulates intracellular c-MET accumulation and consequently signalling efficiency. To this end, autophagy-proficient and -compromised cells were compared for intracellular c-MET accumulation by confocal microscopy imaging. CQ treatment

was used to potentiate c-MET accumulation in perinuclear regions and enable comparison. Preliminary data suggested that autophagy-compromised cells exhibit modestly increased levels of intracellular c-MET (Figure 4. 23), thus potentially excluding that decreased c-MET phosphorylation is due to diminished internalisation.

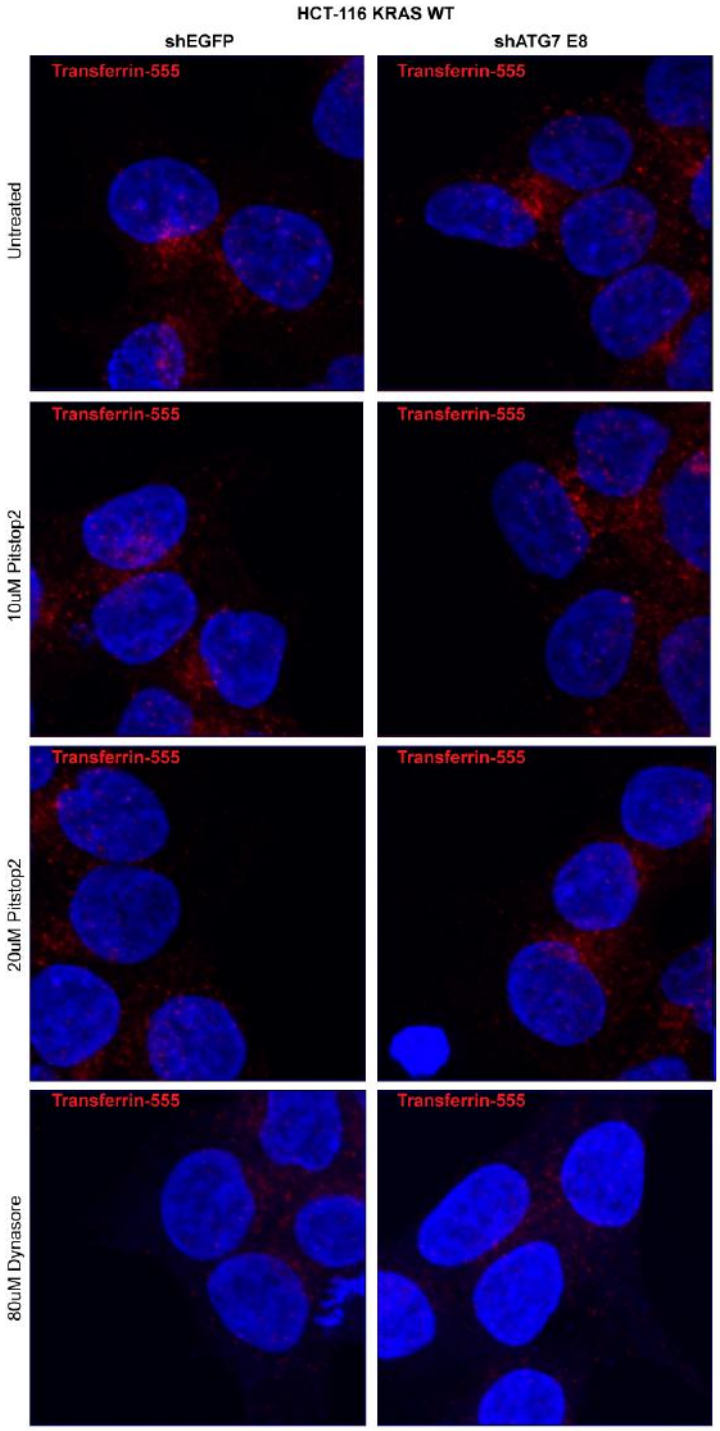

Figure 4. 22: Autophagy suppression does not alter endocytosis. HCT-116 *KRAS* WT autophagy-proficient (shEGFP) and -compromised (shATG7 E8) cells were serum starved for 4 hours to remove transferrin traces from the medium. Followed treatment with Alexa555-conjugated transferrin (red) for 15 mins before fixation in 4% formaldehyde. Pitstop2 (10 and 20 µM) and dynasore (80 µM) endocytosis inhibitors used as negative controls for transferrin endocytosis. 100 mins prior transferrin treatment cells were treated with the inhibitors in the corresponding conditions. For nucleus staining Hoechst dye (blue) was used. Images were acquired using a Zeiss LSM 700 confocal microscope. n= 1.

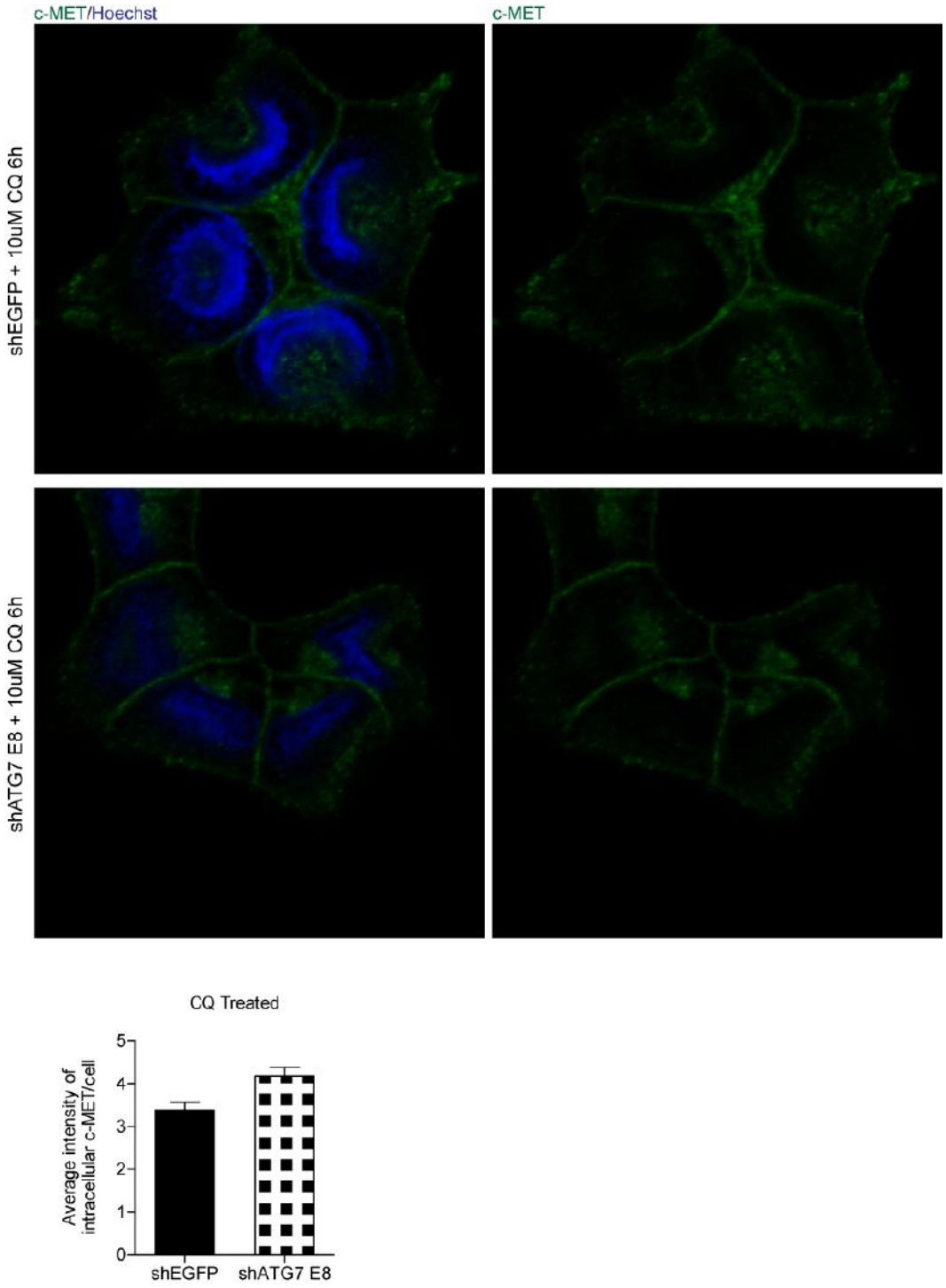

Figure 4. 23: Intracellular c-MET accumulation upon autophagy suppression. HCT-116 *KRAS* WT autophagy-proficient (shEGFP) and -compromised (shATG7 E8) cells were treated with 10 ng/ml DOX for 5 days to efficiently downregulate ATG7 protein expression. 6 hours prior fixation cells were treated with 10 μM CQ to potentiate intracellular c-MET accumulation. Cells were stained for total c-MET (green) and nucleus (Hoechst dye-blue). Images were acquired using a Zeiss LSM 700 confocal microscope. Bar plot depicts average intensity of intracellular c-MET/cell by using Fiji software (ImageJ). Quantification of intracellular c-MET was performed by manually specifying the intracellular region of interest (ROI) of every cell in a single z-stack image. Plasma membrane staining was excluded from quantification analysis. Bars represent mean ± s.e.m. of n= 40 shEGFP and n= 34 shATG7 E8 cells from three independent experiments.

4.2.13. Examination of c-MET regulation by autophagy upon exogenous hrHGF stimulation

Thus far all previous observations were centred in investigating the role of basal autophagy in endogenous c-MET regulation. However, this approach limits detailed investigation of RTK trafficking experiments due to the lack of synchronised ligand stimulation and internalised-RTK kinetics. To enable robust c-MET trafficking investigation, the use of exogenous human recombinant HGF (hrHGF) was required. An obstacle to overcome in hrHGF stimulation studies was serum-starvation prior hrHGF stimulation that is commonly used in the trafficking field to remove growth factors from the medium. Since serum-starvation induces autophagy, this approach was not compatible with basal autophagy examination. Instead, we decided to use high concentration of hrHGF and avoid serum-starvation in our experiments. By following this approach, it was important to examine whether hrHGF without starvation follows the typical trafficking route whereby hrHGF bound-c-MET is rapidly internalised and within around two hours is located at perinuclear endosomes while progressively is getting degraded (Barrow-McGee and Kermorgant, 2014). To this end, HCT-116 *KRAS* WT cells were treated with 50 ng/ml HGF for 3 hours and total c-MET localisation was examined by immunofluorescence. Concomitant treatment with or without CQ was also used in order to enable autophagosome detection in these conditions. As is depicted in Figure 4. 24, hrHGF treatment resulted in abolished plasma membrane staining and increased intracellular c-MET localisation in perinuclear areas, whereas in the untreated condition c-MET staining was more abundant in cell-cell contacts at the plasma membrane. In line with previous observations, CQ treatment resulted in intracellular c-MET accumulation along with plasma membrane staining in untreated conditions and potentiated intracellular c-MET accumulation upon hrHGF treatment. Moreover, c-MET was found to be colocalised with LC3B in perinuclear areas in both -/+hrHGF conditions upon CQ treatment. Activation of c-MET did not seem to alter autophagosome number. To gain a better insight in c-MET activation and downstream signalling upon hrHGF stimulation, lysates of untreated and hrHGF-treated -/+CQ HCT-116 *KRAS* WT cells were subjected to western blotting. As expected, hrHGF treatment increased c-MET phosphorylation. Furthermore, MAPK/ERK, PI3K and mTORC1 pathways activation was upregulated upon hrHGF stimulation. In line with immunofluorescence results, LC3B levels were retained at the same level between untreated and hrHGF treated cells (Figure 4. 25).

The aforementioned observations suggest that the intracellular accumulated c-MET colocalising with LC3B-positive autophagosomes in CQ treated cells corresponds to the kinase-activated c-MET.

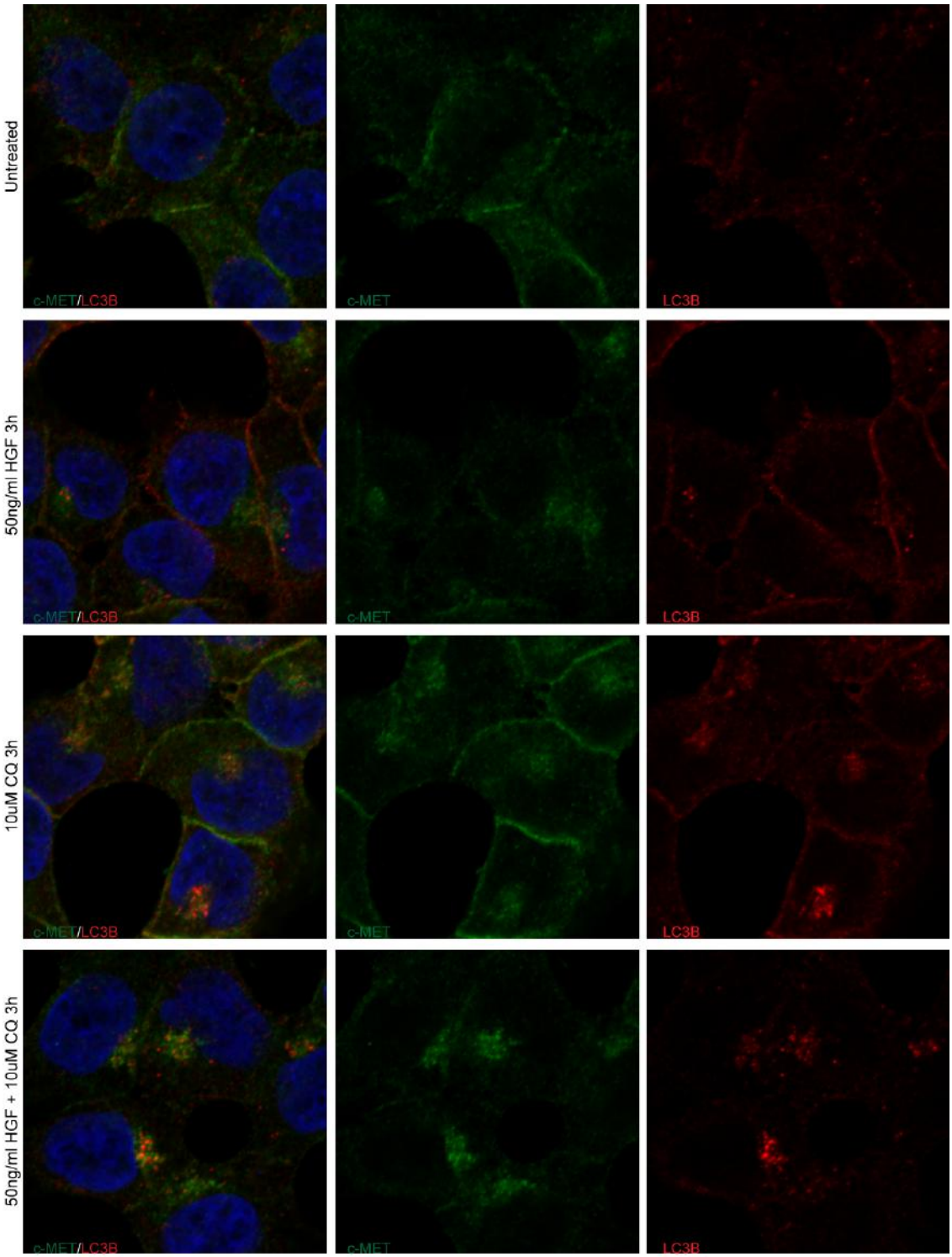

Figure 4. 24: c-MET localisation upon hrHGF stimulation. HCT-116 *KRAS* WT cells were treated concomitantly with 50 ng/ml hrHGF -/+ 10 µM CQ for 3 hours. CQ treatment was used to enable autophagosome detection and differences in autophagosome formation upon hrHGF treatment. Cells were stained for total c-MET (green), LC3B (red) and nucleus (Hoechst dye-blue). Images were acquired using a Zeiss LSM 700 confocal microscope. Single z-stack images are shown.

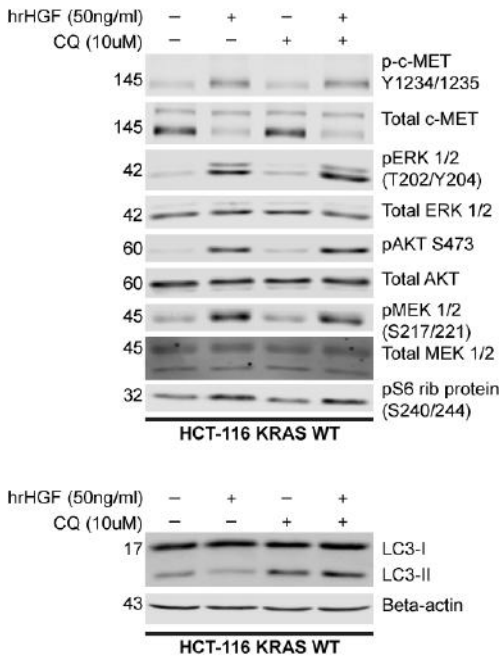

Figure 4. 25: Examination of c-MET/downstream signalling activation and autophagy induction upon hrHGF treatment. HCT-116 *KRAS* WT cells were concomitantly treated with 50 ng/ml hrHGF -/+ 10 μM CQ for 3 hours. CQ treatment was used to enable autophagic flux detection between untreated and hrHGF-treated conditions. Cells were lysed and total cell lysates were subjected to western blotting for the corresponding proteins. Beta-actin used as western blotting loading control. Immunoblot images are from a single experiment.

Ensuing characterisation of c-MET signalling and localisation upon hrHGF stimulation, we aimed to investigate c-MET internalisation along with c-MET-LC3B interaction upon autophagy suppression post-hrHGF stimulation. To this end, autophagy-proficient and -compromised cells were treated with 50 ng/ml hrHGF +CQ for 3 hours and subjected to confocal microscopy analysis for total c-MET and LC3B protein detection/colocalisation. Preliminary results showed comparable levels of intracellular c-MET between autophagy-proficient and -compromised conditions post-hrHGF stimulation (Figure 4. 26.a and b). Moreover, colocalisation of intracellular c-MET with LC3B protein was modestly reduced albeit still detectable upon autophagy suppression (Figure 4. 26.a, c and d), possibly due to remaining ATG7 protein expression enabling LC3B lipidation and autophagosome formation.

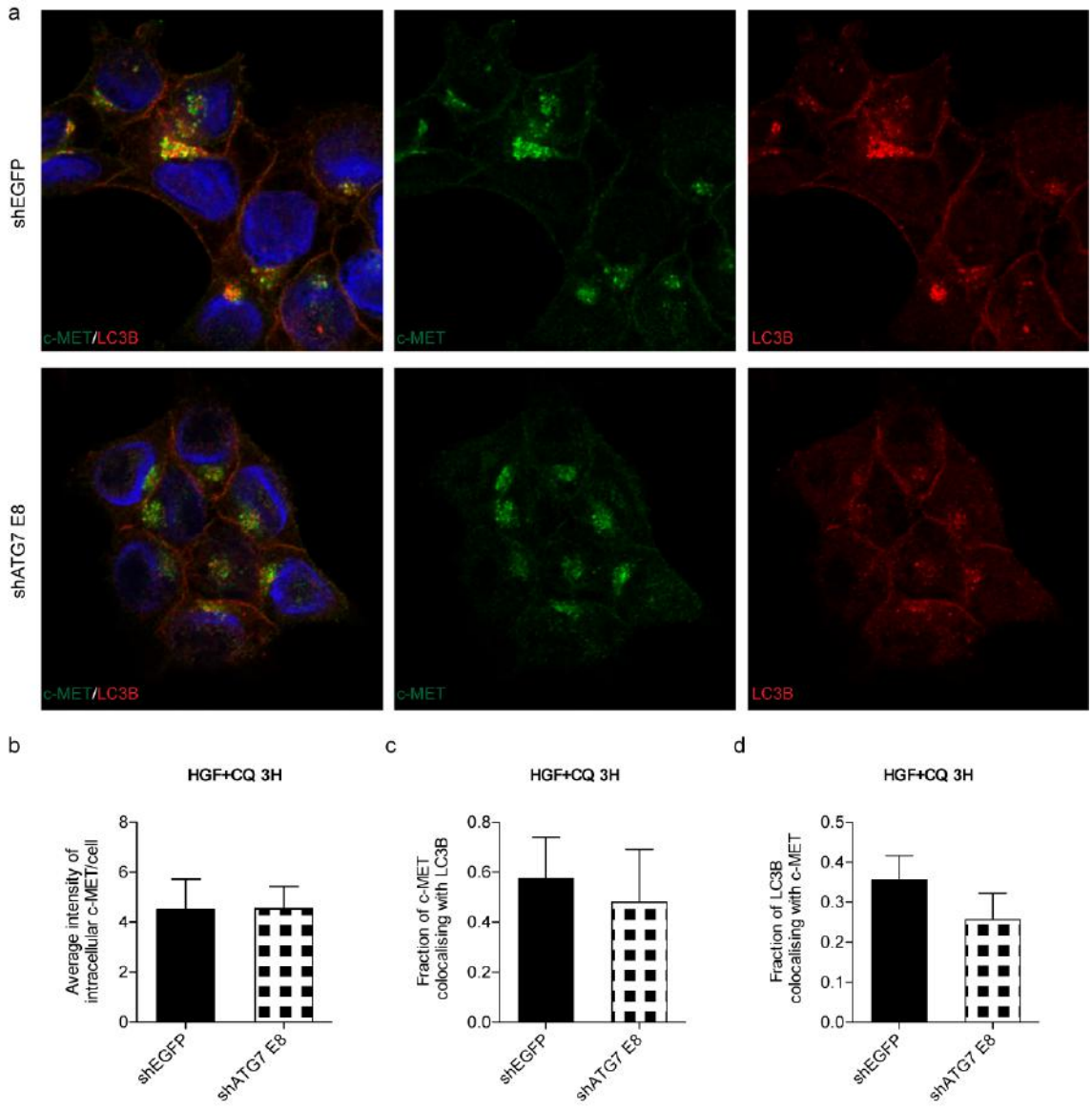

Figure 4. 26: Examination of internalised c-MET levels and colocalisation with LC3B upon autophagy suppression post-hrHGF stimulation. a HCT-116 *KRAS* WT autophagy-proficient (shEGFP) and -compromised (shATG7 E8) cells were treated with 10 ng/ml DOX for 5 days to efficiently downregulate ATG7 protein expression. 3 hours before fixation, cells were co-treated with 50 ng/ml hrHGF and 10 μM CQ. Cells were stained for total c-MET (green), LC3B (red) and nucleus (Hoechst dye-blue). Images were acquired using a Zeiss LSM 700 confocal microscope. **b** Bar plot depicts average intensity of intracellular c-MET/cell by using Fiji software (ImageJ). Quantification of intracellular c-MET was performed by manually specifying the intracellular region of interest (ROI) of every cell in a single z-stack image. Bars represent mean ± s.d. of n= 69 shEGFP and n= 79 shATG7 E8 cells from a single experiment. **c** Bar plot represents mean ± s.d. of Manders' coefficient for c-MET fraction colocalising with LC3B **d** Bar plot represents mean ± s.d. of Manders' coefficient for LC3B fraction colocalising with c-MET. **c-d** Colocalisation analysis was performed using ImageJ plugin JACoP enabling manual adjustment of threshold of single channel z-stack images to eliminate background staining. Threshold settings were identical between individual images. Images for colocalisation examination were from a single experiment.

4.2.14. c-MET-dependent regulation of autophagy

Given the observation that possibly activated c-MET colocalises with LC3B-positive autophagosomes intracellularly, we aimed to investigate the effect of c-MET inhibition in c-MET-LC3B interaction and autophagy induction. Regulation of autophagy downstream of RTKs is well studied and the vast majority of publications report autophagy induction upon RTKs inhibition, which is caused by loss of the mTORC1-dependent checkpoint. However, it is currently unclear what the effect of RTK inhibition in cells displaying constitutive activation of the PI3K/AKT/mTOR pathway is. To address this question, we employed a c-MET inhibitor that targets the tyrosine kinase domain and studied potential effects on autophagy. We found that c-MET inhibition resulted in reduced autophagic flux (~2-fold reduction, $p<0.05$); in particular LC3-II/LC3-I ratio of METi+CQ condition was lower than non-treated+CQ condition in HCT-116 *KRAS* WT cells (Figure 4. 27.a). Of note, even though autophagosome formation was reduced, p62 levels were sustained upon c-MET inhibition. The latter observation may suggest that a non-catabolic pool of autophagosomes may exist in the cell that is regulated by c-MET activation.

Additionally, differences in c-MET localisation and interaction with LC3B protein upon c-MET inhibitor treatment were examined using confocal microscopy. Interestingly, reduced c-MET activation resulted in attenuated intracellular c-MET accumulation upon CQ treatment, supporting the observation that intracellular c-MET that interacts with autophagosomes is phosphorylated (Figure 4. 27.b and c). In line with western blotting results, c-MET inhibition resulted in reduced autophagosome formation and consequently interaction with LC3B (Figure 4. 27.a and d).

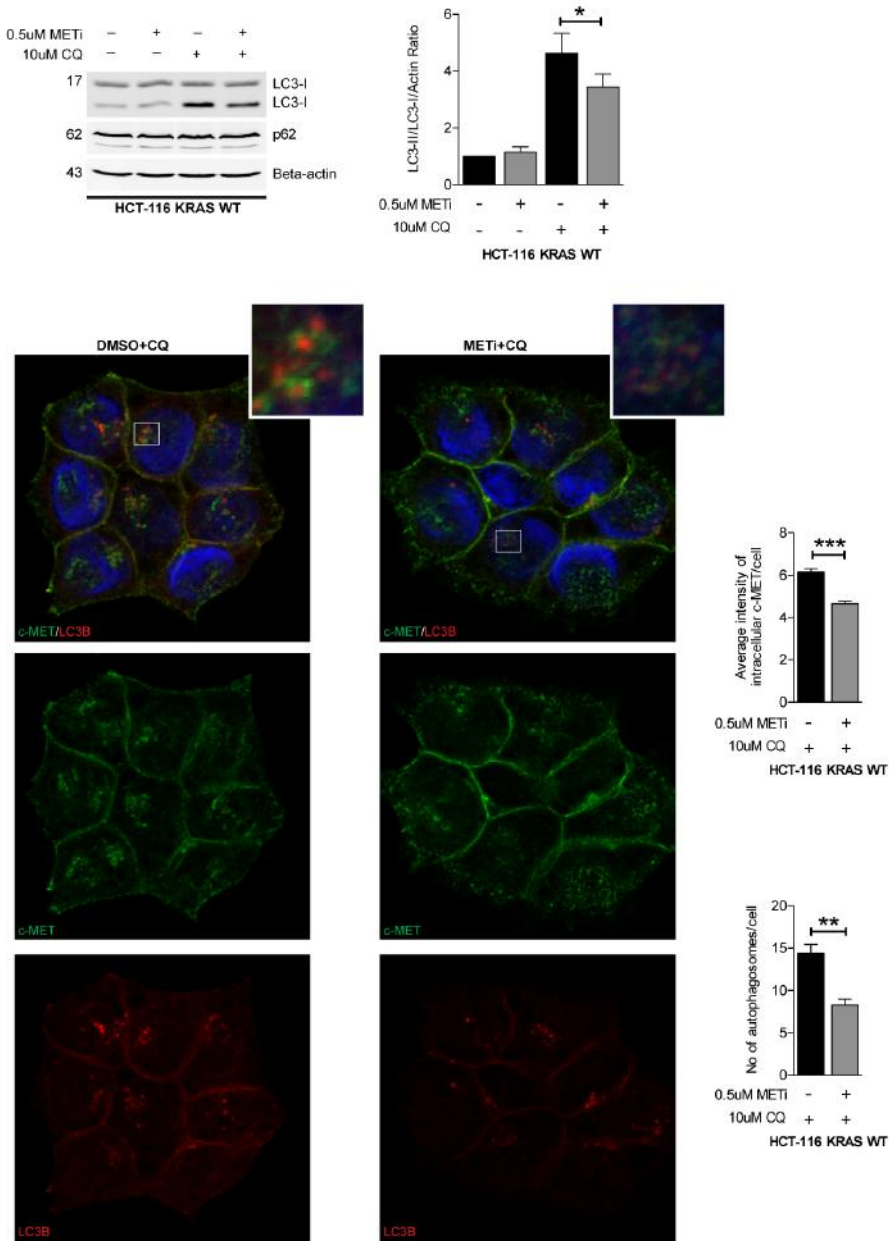

Figure 4. 27: c-MET-dependent regulation of autophagy. HCT-116 *KRAS* WT cells were concomitantly treated with 0.5 µM METi (SGX 523) -/+ 10 µM CQ for 6 hours. CQ treatment was used to enable autophagic flux detection between untreated and METi-treated conditions. **a** Western blotting of untreated and METi-treated -/+10 µM CQ total cell lysates. LC3B and p62 antibodies were used for measuring autophagy induction. Beta-actin used as western blotting loading control. Immunoblot images are representative of 3 independent experiments. Bar plot represents densitometric quantification of LC3-II/LC3-I ratio normalised to beta-actin loading control. The bars represent mean ± s.d.; * $p<0.05$. Unpaired Student's t-test statistical analysis was conducted. **b** Confocal images of untreated and 0.5 µM METi treated cells. Cells were stained for total c-MET (green), LC3B (red) and nucleus (Hoechst dye-blue). Images were acquired using a Zeiss LSM 700 confocal microscope. **c** Bar plot depicts average intensity of intracellular c-MET/cell quantification conducted using Fiji software (ImageJ). Quantification of intracellular c-MET was performed by manually specifying the intracellular region of interest (ROI) of every cell in a single z-stack image. Bars represent mean ± s.e.m. of n= 223 untreated and n= 221 METi-treated cells from 3 independent experiments. **d** Bar plot represents mean of autophagosomes/cell calculated automatically using Imaris software. A manual adjustment of threshold of single channel z-stack images to eliminate background staining was performed. Threshold settings were identical between individual images from the same experiment. Bars represent mean ± s.e.m. of n= 223 untreated and n= 221 METi-treated cells from 3 independent experiments.

4.2.15. Effect of autophagy inhibition on CRC growth and invasion/migration

Autophagy has been found to play a tumour-promoting role in established tumours with various mechanisms regulating such a function. Autophagy may regulate tumour growth by fulfilling the elevated nutritional and metabolic demands of cancer cells enabling in that way their accelerated proliferation. Additionally, autophagy may potentiate tumour cell metastasis by enhancing the capability of cancer cells to migrate and invade in distant organs (previously discussed in 1.2.2). These observations prompted us to investigate the role of autophagy in CRC growth and invasion/migration. We hypothesised that autophagy would promote cancer cell survival/proliferation and migration/invasion in CRC and that genetic inhibition of autophagy would eliminate cell proliferation and migration/invasion of CRC cells.

Previous work from our group and others suggested that autophagy promote tumour invasion and metastasis (Macintosh *et al.*, 2012, Galavotti *et al.*, 2013, Li *et al.*, 2013a). To study the role of autophagy in CRC migration/invasion an *in vitro* model to assess the invasive/migratory capacity of CRC cell lines was established using BD Biocoat chambers (Figure 4. 28).

Since *KRAS* activating mutations are known to promote migration/invasion (Campbell and Der, 2004), we investigated whether the presence of the activating *KRAS* mutation affects the migration and/or invasion capacity of CRC cells. To this end, HCT-116 *KRAS* WT and G13D cells were cultured for 60hours in matrigel-coated invasion and non-coated migration chambers. As expected, the *KRAS* G13D activating mutation was found to accelerate the invasive and migratory capacity of HCT-116 cells (Figure 4. 29.a).

Having established that the presence of *KRAS* G13D mutation enhances the invasive and migratory capacity of CRC cells (Figure 4. 29.a) and taking into account that cells with activating *KRAS* mutations show enhanced autophagy levels (Guo *et al.*, 2011), the HCT-116 *KRAS* G13D cell line model was selected to examine the role of autophagy in regulating invasion and/or migration capacity in CRC cells.

Autophagy-proficient and -compromised HCT-116 *KRAS* G13D cells were cultured in matrigel-coated invasion and non-coated migration chambers for 60 hours. Pharmacological modulation of autophagy by CQ treatment was used in parallel. It was found that autophagy downregulation did not affect the invasive and migratory capacity of HCT-116 *KRAS* G13D cells under basal-autophagy conditions. CQ treatment was found to inhibit invasive but not migratory capacity of HCT-116 *KRAS* G13D cells (Figure 4. 29.b).

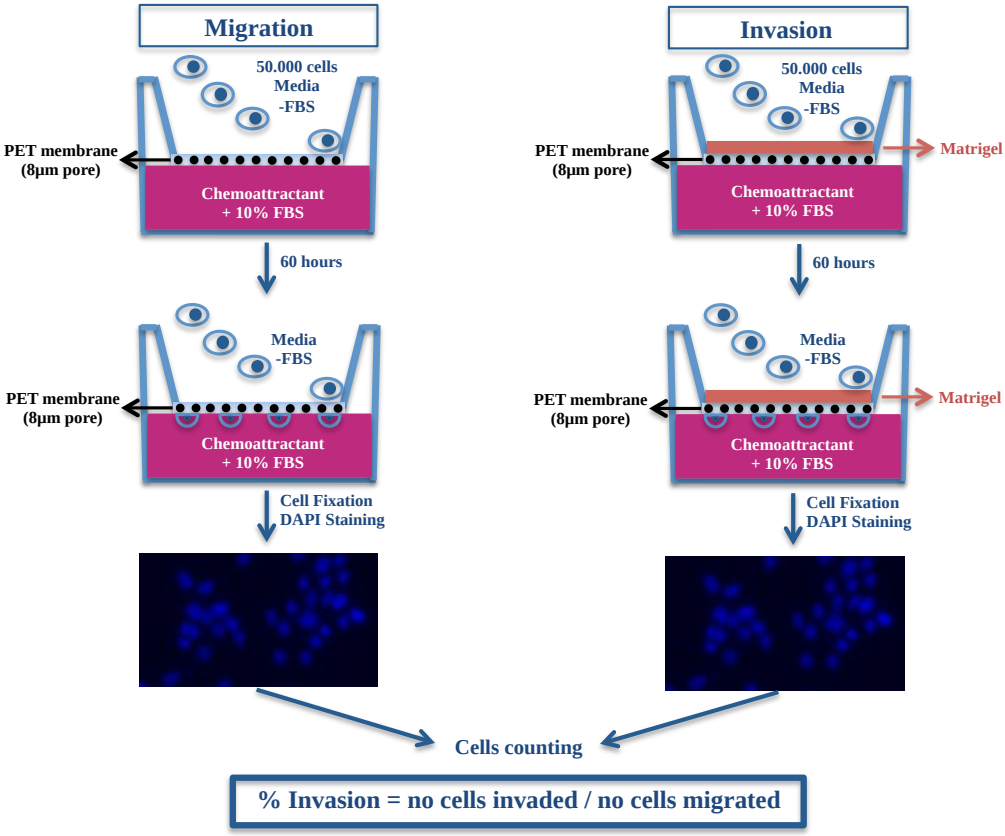

Figure 4. 28: ***In vitro* model for studying invasion/migration in CRC cells.** Both migration and invasion studies performed using BD Biocoat chambers, which are characterised by the presence of a PET membrane with 8 µm pores. Only migratory and invasive cells could pass through the pores of the membrane. Invasion chambers have a layer of matrigel resembling extracellular matrix on top of the PET membrane enabling the examination of invasion *in vitro*. Cells were plated in corresponding chambers in the absence of FBS and let to incubate for 60 hours. As a chemoattractant, media containing 10% FBS was used in the bottom of the well. Non-migrated and non-invaded cells were removed from the top of the PET membrane. Cells that passed through the membrane fixed and stained with Hoechst nucleus staining. Counting of cells was performed using the automatic programme Cell Profiler.

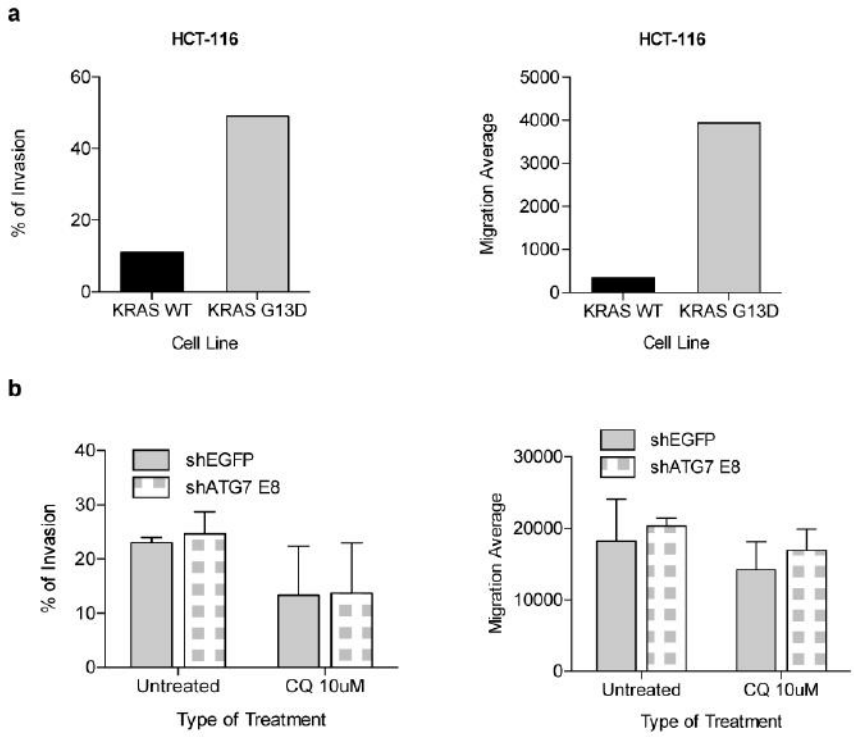

Figure 4. 29: Role of a *KRAS* oncogene activation in invasion/migration capacity of HCT-116 CRC cell line and **b** autophagy suppression in invasion/migration capacity of HCT-116 *KRAS* G13D cells. For both **a** and **b** 50000 cells were plated in either migration or invasion chambers in the absence of FBS and were incubated for 60 hours. As a chemoattractant, media containing 10% FBS was used in the bottom of the well. Non-migrated and non-invaded cells were removed from the top of the PET membrane. Migrated and invaded cells that passed through the membrane fixed in methanol and stained with Hoechst nucleus staining. Counting of cells was performed using the automatic programme Cell Profiler.

To study the role of basal autophagy in CRC cell growth, two different approaches were followed. Firstly, the proliferation rates of autophagy-proficient and -compromised HCT-116 cells were examined under adhered conditions using SRB assay. It was found that autophagy suppression does not alter cell proliferation rate of HCT-116 *KRAS* WT and G13D isogenic cells, under adhered conditions (Figure 4. 30.a). Another method that established to examine the role of autophagy in CRC cell growth was the anchorage-independent cell growth approach using soft agar. Unexpectedly, it was found that autophagy suppression potentiates HCT-116 *KRAS* WT cell growth in anchorage-independent conditions (approximately 3-fold; Figure 4. 30.b).

Overall, it was found that inhibition of basal autophagy does not affect growth of HCT-116 *KRAS* isogenic cells cultured in adhesion whereas it resulted in increased anchorage-independent growth of HCT-116 *KRAS* WT cells. Finally, while basal autophagy suppression does not affect migration/invasion capacity of HCT-116 *KRAS* G13D cells, CQ treatment shows a trend in attenuating invasive capacity of CRC cells possibly through an autophagy-independent manner.

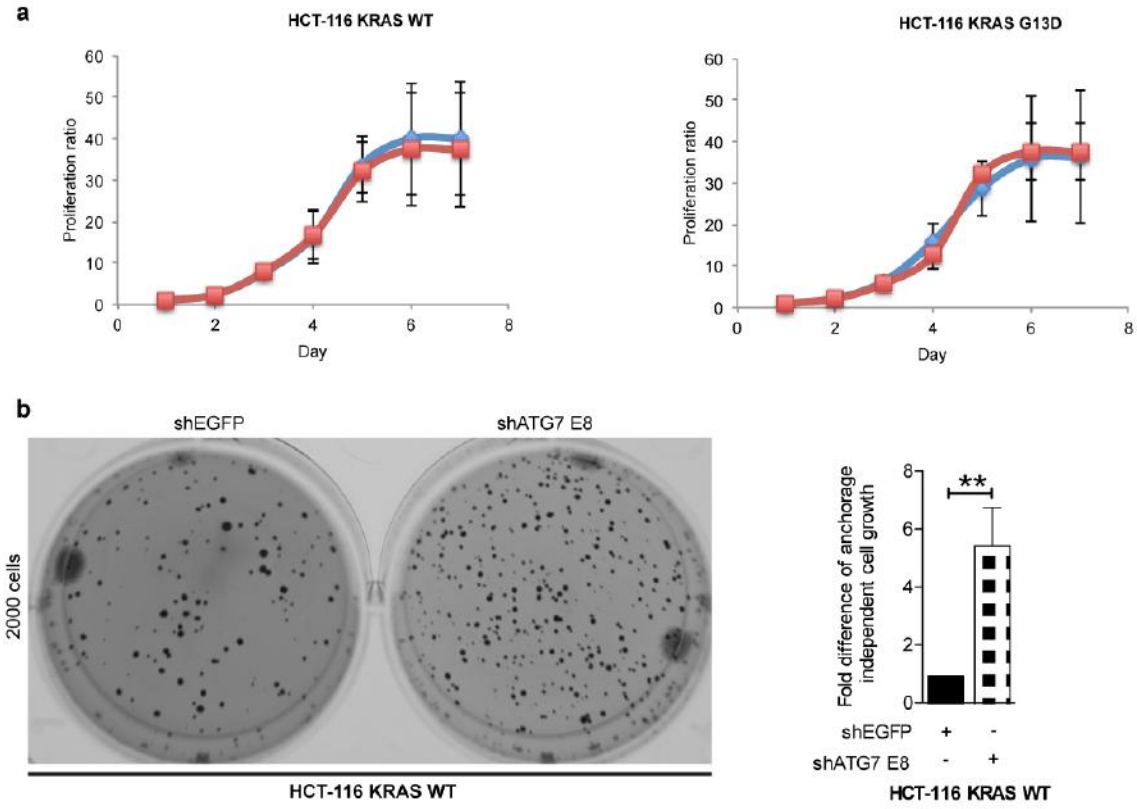

Figure 4. 30: Role of autophagy in CRC cell proliferation in: a adhered-cultured conditions and **b** in anchorage-independent conditions. Cell proliferation was assessed in autophagy-proficient and -compromised HCT-116 cells using **a** the SRB proliferation assay. Graphs represent mean ± SD of three independent experiments; and **b** anchorage-independent cell growth assay. Graph represent mean ± SD of two independent experiments each of them including two internal experimental repeats. Unpaired Student's t-test statistical analysis was conducted.

4.3. Discussion

4.3.1. Basal autophagy suppression attenuates AKT phosphorylation of CRC cells in a systematic manner while it affects ERK and other protein phosphorylation in a cell-type specific manner

The function of the autophagosome as a cell signalling regulator has only recently been reported in the literature and its role remains elusive. The study by Martinez-Lopez *et al*., (2013) was the first to show that autophagy regulates ERK activation in brown adipose tissue and liver extracts since inhibition of autophagy resulted in decreased pERK levels (Martinez-Lopez *et al.*, 2013). Additionally, Bernard *et al*., (2014) reported that autophagy could regulate AKT activation at S473 residue in myofibroblasts upon serum-starved conditions (Bernard *et al.*, 2014). Hitherto, our knowledge regarding the role of autophagy in regulation of cell signalling in CRC cells is limited and further investigation is needed. Our work reveals for the first time that basal autophagy suppression impairs AKT phosphorylation in CRC cell lines under endogenous growth factor and nutrient replete conditions. In particular, genetic suppression of basal autophagy results in reduced phosphorylation of AKT at S473 residue in all CRC cell lines utilised and AKT T308 residue in CaCo2 cells, without affecting total levels of AKT (Figure 4. 6.a and b).

AKT protein is phosphorylated at T308 and S473 residues by two distinct upstream kinases, named PDK1 and mTORC2 respectively. Both PDK1 and mTORC2 are under the control of growth factor-dependent signalling and they both transmit signals downstream of PI3K. However, regulation of mTORC2 under PI3K is still not well defined (Laplante and Sabatini, 2012, Efeyan *et al.*, 2015). These observations indicate that an upstream regulator of both PDK1 and mTORC2 is regulated by autophagy suppression. Interestingly, autophagy suppression reduced pAKT S473 even in *PI3K* mutant CRC cells and this downregulation was accelerated when *KRAS* and *PI3K* activating mutations were both present. The abovementioned results are in consistence with the reduced levels of pAKT S473 observed following pharmacological inhibition of autophagy by CQ in all CRC cells (Figure 3. 5; discussed in 3.3.5). CQ is a neutralising compound, which raises the acidic lysosomal pH and in that way blocks degradation of lysosomal content. It has been suggested that CQ could interfere with autophagosome fusion to the lysosome (Klionsky *et al.*, 2012). Taken together, this observed consistency between genetic- and CQ-mediated inhibition of autophagy might point in the direction that late steps of the autophagic process such as autophagosome to lysosome fusion are important for autophagy-induced AKT activation.

Basal autophagy suppression did not alter mTORC1 signalling residing downstream of AKT in a consistent manner between cell lines. In fact, autophagy-compromised *KRAS* WT CRC cell lines upregulated mTORC1 activation levels depicted by pS6 activation, while *KRAS* mutant cells sustained mTORC1 levels with the exception of CaCo2 cells that marginally decreased mTORC1 signalling (Figure 4. 6.c). Altered phosphorylation levels of AKT in autophagy-compromised conditions could not be correlated to mTORC1 signalling activation. This observation suggests that the pool of pAKT being regulated by autophagy might have other downstream signalling targets than mTORC1, such as Glycogen Synthase Kinase-3 (GSK-3) and/or Forkhead box O (FOXO) proteins (Brunet *et al.*, 1999, Manning and Cantley, 2007, Carracedo and Pandolfi, 2008, Hemmings and Restuccia, 2012). Growth factors and amino acids are the main regulators of mTORC1 and both are required for its full activation. Amino acids are required for lysosomal localisation of mTORC1 and growth factors are responsible for AKT-mediated activation of mTORC1 (Laplante and Sabatini, 2012, Efeyan *et al.*, 2015). No additional serum or amino acids were added to the cell culture medium during our experimental conditions. Hence, increased activation of mTORC1 upon autophagy suppression in *KRAS* WT cells could suggest that levels of intracellular amino acids or growth factors were elevated. The decreased phosphorylation of AKT upon autophagy suppression may rule out the possibility that increased levels of growth factors control mTORC1 activity. A possible explanation for mTORC1 upregulation upon autophagy suppression would be that the remaining AKT activation is sufficient to cooperate with high levels of amino acids to increase mTORC1 activity. Future experiments could shed more light on the functional consequences of AKT hypo-phosphorylation mediated by basal autophagy suppression.

When signalling pathways other than PI3K/AKT were examined it was found that autophagy modulates activation of proteins in a cell type-specific manner. Regarding MAPK/ERK pathway it was found that, in contrast to the systematic decrease of AKT phosphorylation observed upon autophagy suppression, phosphorylation of ERK and MEK was regulated in a cell-type specific manner (Figure 4. 7). In particular, basal autophagy suppression resulted in reduced ERK activation in HCT-116 cells independently of their *KRAS* status. However, in DLD-1 cells *KRAS* activation differentially controlled phosphorylation of ERK upon autophagy suppression. In fact, it resulted in ERK hypo-phosphorylation in *KRAS* mutant DLD-1 cells, whereas DLD-1 *KRAS* WT cells presented increased ERK activation. CaCo2 cells showed only marginally decreased levels in ERK activation. CQ treatment recapitulated genetic inhibition of autophagy only in short time treatments (6 hours) in HCT-116 cells (Figure 3. 11.e). In DLD-1 cells CQ treatment resembled ATG7 downregulation after 24 hours

(Figure 3. 10.a) and 6 hours (Figure 3. 18.b) treatment for *KRAS* WT and *KRAS* G13D cells, respectively. Inconsistency of CQ results between different treatment time points prevents us from reaching a conclusion regarding similarity in regulation of ERK activation between inhibition of autophagy in early and late steps of the autophagic process. When MEK 1/2 residing upstream of ERK 1/2 was tested, it was found that autophagy inhibition regulates activation of MEK 1/2 in a similar pattern to ERK1/2 in *KRAS* WT cells; however, this was not observed in *KRAS* mutant cells (Figure 4. 7.b). This suggests that defects in ERK activation following autophagy suppression in *KRAS* WT cells might be indirect and an upstream regulator of both MEK and ERK is regulated by autophagy. However, in the study by Martinez-Lopez *et al*., (2013) autophagy-mediated regulation of ERK protein was a direct effect and MEK activation levels were not altered (Martinez-Lopez *et al.*, 2013). This supports our results showing that ERK activation is directly regulated by autophagy in *KRAS* mutant cells.

For other signalling pathways, it was found that activation of STAT3, p38 MAPK and Rb proteins was not altered following autophagy suppression. On the contrary, autophagy inhibition altered AMPK alpha and SAPK/JNK activity in a cell-type specific manner (Figure 4. 9). In particular, autophagy suppression reduced AMPK alpha in *KRAS* mutant CaCo2 and HCT-116 cells, whereas AMPK alpha was increased in HCT-116 *KRAS* WT cells. Given the known role of AMPK alpha as an energy sensor in the cell (Efeyan *et al.*, 2015), these observations suggest that autophagy suppression might alter metabolism of CRC cells in a *KRAS*-dependent manner. A recent study by Levy *et al*., (2015) has shown that AMPK alpha is upregulated following ATG7-deletion in intestinal epithelial cancer cells with *APC* deletion (Levy *et al.*, 2015). SAPK/JNK kinase phosphorylation was downregulated in HCT-116 cells following autophagy inhibition and the presence of *KRAS* activation further enhanced pSAPK/JNK inhibition. CaCo2 cells sustained pSAPK/JNK levels following autophagy suppression. The abovementioned were following the same pattern as ERK 1/2 following autophagy suppression.

PI3K/AKT, MAPK/ERK, AMPK alpha and JNK1 signalling cascades are known regulators of autophagy induction (discussed in 1.1.2.). However, little is known regarding the role of autophagy itself in the regulation of these signalling pathways. Our findings reveal a novel bi-directional relationship between basal autophagy and these signalling kinases. Collectively, we have clearly shown that autophagy plays an active role in regulation of AKT phosphorylation of CRC cells in a systematic manner. On the other hand, MAPK/ERK, AMPK alpha and SAPK/JNK pathways are regulated in a cell-type specific manner upon autophagy-compromised conditions, whereas phosphorylation levels of STAT3, p38 and Rb proteins are not affected. The inconsistency in the cell signalling defects following autophagy suppression observed

in this work exclude the possibility of a general mechanism systematically reducing phosphorylation levels of proteins to be controlled via autophagy and point in the direction of a specific mechanism by which autophagy controls cell signalling including AKT activation in CRC cells.

4.3.2. Basal autophagy suppression inhibits endogenous RTK activation in CRC

In an attempt to unravel the specific mechanism by which autophagy regulates cell signalling in CRC cells, different hypotheses were tested using HCT-116 *KRAS* WT cells as a model system that presented efficient downregulation of both ERK and AKT activation following autophagy suppression. This study reveals for the first time that genetic inhibition of basal autophagy diminishes endogenous RTK phosphorylation in CRC cells regardless of their *KRAS* mutational status (Figures 4. 13 and 4. 14). Using a phospho-RTK array it was observed that phosphorylation of various RTKs was reduced upon autophagy suppression in two different CRC cell lines. Amongst the various RTKs being de-regulated via autophagy suppression c-MET, c-RET and Dtk were common in the two different CRC cell lines tested. Similarity in observations between the two different cell lines highlights the reliability of phospho-RTK results. In support of this, validation experiments confirmed that endogenous c-MET phosphorylation but not EGFR or IGF-I R was reduced upon basal autophagy suppression (Figures 4. 15 and 4. 16). The reduction in c-MET phosphorylation was not caused by degradation or reduced protein expression since levels of total c-MET were sustained upon autophagy suppression (Figure 4. 15.b). These observations suggest the presence of a non-catabolic mechanism by which autophagy controls c-MET phosphorylation.

But how is c-MET activation regulated by autophagy? To shed light on the mechanism by which autophagy regulates c-MET phosphorylation a number of hypotheses were tested. Firstly, the autocrine production of HGF upon autophagy suppression was examined and it was revealed that HGF production deregulation is not responsible for c-MET phosphorylation reduction (Figure 4. 21). However, this observation does not exclude the likelihood that ATG7 downregulation attenuates secretion of the autocrine-produced HGF and thereby reducing c-MET stimulation and phosphorylation. Another possibility tested was whether c-MET endocytosis is de-regulated upon autophagy suppression. Preliminary data showed that endocytosis was not altered upon autophagy suppression (Figure 4. 22). This observation suggests that endocytosis might not be responsible for diminished c-MET activation; however, additional experiments employing quantification of endocytosed-transferrin-555 are

needed to confirm this observation. On the other hand, preliminary data also shows that intracellular c-MET might be increased following autophagy suppression (Figure 4. 23). This observation suggests that recycling or exocytosis of c-MET back to the plasma membrane might be attenuated upon autophagy suppression and in that way diminished levels of c-MET in the plasma membrane eliminate c-MET activation. When localisation of c-MET was examined it was found that intracellular c-MET colocalises with LC3B positive autophagosomes (Figure 4. 17.a). Treatment with hrHGF was found to increase intracellular c-MET (Figure 4. 24) and conversely tyrosine kinase inhibition of c-MET was found to attenuate its intracellular localisation (Figure 4. 27). Taken together, all the above suggest that activated internalised c-MET colocalises with autophagosomes. Based on the study by Martinez-Lopez *et al*., (2013) showing that autophagosomes act as intracellular scaffolds for maintaining ERK signalling (Martinez-Lopez *et al.*, 2013), we could hypothesise that c-MET activation is regulated in a similar manner. A possible explanation would be that even though c-MET following activation at the plasma membrane is properly endocytosed, autophagosomes are needed to sustain c-MET activation intracellularly. In autophagy-compromised conditions where autophagosomes are not present, the intracellular pool of c-MET cannot remain active. Furthermore, the observation that CQ treatment does not attenuate c-MET activation in basal and hrHGF-stimulated conditions (Figure 4. 25) could be in support of this hypothesis. In particular, the presence of the autophagosome *per se* might be important regardless of the functionality of the autophagic process. In that respect, we hypothesised that LC3B protein, which resides at the outer-membrane of autophagosomes may be a mediator between autophagosomes and c-MET. When c-MET and other RTKs identified to be regulated by autophagy using the phospho-RTK array were examined *in silico* (via the iLIR server) for the existence of LIR motifs, it was found that all of them were good candidates for direct interaction with LC3B protein (Table 4. 2). However, co-immunoprecipiation studies failed to prove a direct interaction between c-MET/p-c-MET and LC3B (Figure 4. 19). This observation suggests either limitations in the immunoprecipitation protocol used or an indirect interaction between c-MET/p-c-MET and LC3B.

Earlier studies reported RTKs' interaction with autophagosome precursors /autophagosomes (Sandilands *et al.*, 2012, Jones *et al.*, 2014). In particular, the study by Jones *et al*., (2014) proposed that the non-receptor tyrosine kinase Ack1 modulates a non-canonical degradative trafficking of a small portion of EGFR to pre-autophagosomal structures upon EGF stimulation. In particular, they showed that Ack1 upon serum-stravation conditions is colocalised within ubiquitin rich compartments containing p62. EGF stimulation facilitates relocalisation of Ack1 to early endosomal

and pre-autophagosomal structures positive for ATG16L1. Even though colocalisation of Ack1 with p62 is reduced upon EGF stimulation there is still some small portion of Ack1 protein colocalising with p62 and EGFR. The small portion of EGFR colocalising with p62 was proposed to be through Ack1 interaction with both proteins (even though Ack1 inhibition did not alter this colocalisation). Ack1 inhibition results in increased localisation of EGFR to lysosomes upon EGF stimulation that however did not affect degradation of EGFR (Jones *et al.*, 2014). Nevertheless, it was not investigated whether these p62 structures partially colocalising with EGFR are LC3B positive autophagosomal structures. Of note, in our study EGFR was not found to colocalise with intracellular LC3B positive autophagosomes (Figure 4. 17.b). The study by Sandilands *et al*., (2012) reported that c-RET RTK colocalises with autophagosomes and that autophagy facilitates c-RET degradation in cancer cells with defects or reduced FAK signalling. In the latter conditions, c-RET loses its peripheral adhesion localisation and presents a cytosolic localisation in autophagosomes with the specific mechanism enabling c-RET interaction to autophagosomes remaining unknown (Sandilands *et al.*, 2012). c-RET was identified as a promising hit for autophagy-mediated activation in both cell lines tested in our work; albeit experimental limitations that did not allow for validation and localisation experiments. However, based on c-MET observations and the decreased activation of c-RET following autophagy suppression, a catabolic role of autophagy in regulation of c-RET activation could not be supported in our study.

Collectively, this work suggests that autophagy regulates RTK activation including c-MET in CRC cells. A novel bi-directional relationship between basal autophagy and RTK activation has been established. At this point no conclusion can be made regarding the specific mechanism by which basal autophagy could regulate RTK/c-MET phosphorylation and future investigations are warranted.

4.3.3. Does autophagy regulate cell signalling via attenuation of c-MET RTK activation?

RTKs including c-MET are the starting points for stimulation of various signalling cascades (discussed in 1.5.1). c-MET activation and signalling is primed by the binding of c-MET ligand, HGF, to the extracellular domain of c-MET at the plasma membrane. Dimerisation of two c-MET molecules and transphosphorylation of two catalytic tyrosine residues (Y1234 and Y1235) in the tyrosine kinase domain of the receptor follows. This leads to the subsequent phosphorylation of the two tyrosine residues Y1349 and Y1356 in c-MET carboxy-terminal tail. This forms a

"multisubstrate docking site", which is essential for Met signalling. c-MET regulates the activation of MAPK/ERK, PI3K/AKT, JNK, p38 MAPK, STAT and LKB1/AMPK downstream signalling pathways either through direct interaction with signalling molecules or through adaptor proteins (Vázquez *et al.*, 2009, Trusolino *et al.*, 2010, Barrow-McGee and Kermorgant, 2014).

c-MET activates PI3K/AKT pathway either through direct interaction with its docking site or indirectly through RAS (Ponzetto *et al.*, 1994, Trusolino *et al.*, 2010). In our work, basal autophagy suppression reduced activation of both c-MET and AKT in HCT-116 *KRAS* WT cells. Moreover, c-MET phosphorylation was also attenuated in HCT-116 *KRAS* G13D cells and both DLD-1 *KRAS* isogenic cells lines (phospho-RTK array observations; Figures 4. 13 and 4. 14) in which pAKT downregulation was also observed. These observations suggest that AKT downregulation could be a secondary effect caused by the attenuated c-MET activation residing upstream of PI3K pathway. However, a recent study has shown that accelerated autophagy upon prolonged serum starvation upregulates AKT activation through mTORC2 which drives myofibroblast differentiation (Bernard *et al.*, 2014). This may imply that autophagy regulates AKT via mTORC2 independently of c-MET in our system. Even though both studies observed downregulation of AKT upon autophagy suppression the different experimental procedures and *in vitro* models used may differentiate the mechanism by which autophagy controls mTORC2 in serum-replete and deplete conditions. Additionally, a recent study has shown that lysosomal associated AKT can modulate CMA activation. Lysosomal- mTORC2 and PHLLP1 are responsible for the phosphorylation and de-phosphorylation of AKT at lysosomes, respectively (Arias *et al.*, 2015). The intracellular AKT might be located at the cytosolic phase of autophagosomes. In that case, the latter could function as scaffolds and upon fusion of autophagosomes with lysosomes, where mTORC2 resides; activation and consequently phosphorylation of AKT could be facilitated. In support of this hypothesis is the consistent AKT downregulation between genetic and pharmacological inhibition of autophagy that we observed.

c-MET triggers MAPK/ERK pathway and activates ERK 1/2 through activation of the upstream kinase MEK 1/2 *via* the following pathways: Grb2-SOS-RAS (Ponzetto *et al.*, 1994) or SHC-Grb2-SOS-RAS (Pelicci *et al.*, 1995) or Gab1-Shp2-RAS (Maroun *et al.*, 2000). In our study, pMEK 1/2 and pERK 1/2 alterations followed the same pattern upon autophagy suppression in *KRAS* WT cells. This observation implies that signalling mediated by growth factors is impaired in autophagy-compromised cells. In support of this, downregulated MEK 1/2 and ERK 1/2 activation following autophagy suppression is following a similar pattern with c-MET in HCT-116 *KRAS* WT cells. However, these findings cannot be generalised in DLD-1 *KRAS* WT cells since even

though c-MET activation was downregulated following autophagy suppression, ERK 1/2 was hyper-phosphorylated. Additionally, as expected, *KRAS* mutant cells did not present alterations in MEK signalling and the theory of an upstream regulator such as c-MET controlling autophagy-regulated cell signalling activation cannot be supported. These observations may imply variability in regulation of ERK phosphorylation in a *KRAS* dependent manner but at the same time underline the importance of a conserved mechanism for ERK regulation by autophagy. CRC cells harbouring *KRAS* activating mutation may have developed a different mechanism for regulating ERK activation independently of growth factor signalling. As suggested in the study by Martinez-Lopez *et al*., (2013) autophagosomes may serve as signalling platforms for intracellular ERK independently of MEK regulation and growth factor signalling (Martinez-Lopez *et al.*, 2013).

JNK can be activated by c-MET through RAS-PI3K-RAC pathway (Trusolino *et al.*, 2010) and JNK downregulation following autophagy suppression could be correlated with the reduced levels of c-MET activation in HCT-116 *KRAS* WT cells. However, in *KRAS* mutant cells the constant activation of *KRAS* downstream of c-MET may restrict a growth factor signalling dependent mechanism by which autophagy regulates JNK activation. c-MET has been shown to induce AMPK activation through phosphorylation of its upstream kinase LKB1 (Vázquez *et al.*, 2009). Our results have shown that autophagy suppression decreases phosphorylation of AMPK alpha in *KRAS* mutant cells. Based on our findings showing reduced activation of c-MET upon autophagy suppression, a c-MET-mediated AMPK alpha regulation can be suggested.

Additional mechanisms by which autophagy could regulate AKT and/or ERK activation in CRC cells independently of c-MET were tested mainly in HCT-116 cells showing downregulated phosphorylation of both proteins. Initially, we investigated mechanisms implicating the catabolic function of autophagy and therefore autophagy-mediated degradation of phosphatases controlling AKT and/or ERK were tested (Figure 4. 10). It was found that autophagy suppression resulted in a slight accumulation of PP2A in HCT-116 cells, whereas this increase was not evident in autophagy-compromised CaCo2 cells. Both HCT-116 and CaCo2 cells presented downregulation of pAKT following autophagy suppression so inconsistency in PP2A regulation could exclude the likelihood PP2A accumulation to control AKT activation following autophagy suppression. ERK activation following autophagy suppression was found reduced in HCT-116 cells, whereas it was maintained in CaCo2 cells. These observations could be positively correlated with the slight PP2A accumulation in HCT-116 cells and the stable levels of PP2A in CaCo2 cells and may suggest that PP2A accumulation may be responsible for pERK inhibition in autophagy-compromised conditions. However, Martinez-Lopez *et al*., (2013) have shown that

ERK de-activation following autophagy inhibition is PP2A-independent since PP2A knockdown by siRNA did not rescue pERK upon ATG7 deletion (Martinez-Lopez *et al.*, 2013). Our results suggest that autophagy may regulate AKT activation in a PP2A-independent manner while PP2A accumulation could be implicated in autophagy-mediated pERK regulation and future investigation with a specific PP2A inhibitor is needed.

Based on previous studies showing that autophagy suppression upregulates proteasomal activity (Wang *et al.*, 2013, Liu *et al.*, 2015), the implication of the proteasome system in control of pAKT and pERK degradation was tested. However, no difference in proteasomal activity between autophagy-proficient and -compromised cells was observed (Figure 4. 11.c). In agreement with our findings, autophagy suppression via CQ was not found to affect proteasome activity in HCT-116 cells under nutrient-replete conditions (Wang *et al.*, 2013).

The hypothesis that an Ubiquitin E3 ligase responsible for ubiquitination and targeting of pAKT and pERK proteins for proteasome degradation to be specifically regulated by autophagy was also examined (Figure 4. 11.e and f). We firstly employed a proteasome inhibitor approach to examine whether AKT and/or ERK activation is rescued upon autophagy-compromised conditions. Preliminary data showed total rescue of ERK activation in autophagy-compromised conditions in the presence of a proteasome inhibitor. However, when ubiquitination of pERK protein was tested by immunoprecipitation the results were inconclusive. Even though pERK immunoprecipitation was successful, the presence of ubiquitination in pERK protein could not be verified. Additionally, ERK activation levels were not rescued this time in the presence of the proteasome inhibitor. The inconsistency of the abovementioned observations restricts us from reaching a conclusion regarding the implication of an Ubiquitin E3 ligase in control of AKT and/or ERK activation following autophagy suppression and future experiments are still needed.

Collectively, this work suggests that reduction in AKT and/or other signalling cascades via autophagy suppression might be regulated through autophagy-mediated regulation of c-MET activation.

4.3.4. c-MET kinase activation may control basal autophagy levels in CRC

RTKs have been extensively described as indirect negative modulators of autophagy induction through mTOR, AKT and ERK downstream pathways activation. Interestingly, EGFR has been recently described by two different groups to regulate autophagy induction through direct regulation of autophagic machinery components

via either kinase-dependent or -independent mechanisms (Wei *et al.*, 2013, Tan *et al.*, 2015) (previously discussed in 1.1.2.2.). As previously described for EGFR RTK, it is generally accepted that RTK inhibition induces autophagy. In our study, while EGFR inhibition did not alter levels of autophagy in HCT-116 *KRAS* WT cells (Figure 3. 6 and Figure 3. 12), inhibition of c-MET reduced a portion of basal autophagy (Figure 4. 27). In line with our observations another group showed negative regulation of autophagy upon IGF-I tyrosine kinase inhibition (by picropodophyllin) and IGF-I genetic knockdown (by IGF-I siRNA in HeLa cells and heterozygous deletion in MEFs) (Renna *et al.*, 2013). However, a contradictory study by Humbert *et al*., (2013) reports that c-MET inhibition upregulates cytoprotective autophagy in human gastric adenocarcinoma cells (Humbert *et al.*, 2013). Discrepancies between studies could be attributed to cell type-specific effects in regulation of autophagy downstream of c-MET. Additionally, variability in results could also be due to c-MET inhibitor-specific effects since different pharmacological compounds were used. Future experiments using different c-MET inhibitors and c-MET downregulation approaches are needed to shed light on the regulation and the role of autophagy downstream of c-MET in CRC.

Our study implies heterogeneity in regulation of autophagy downstream of RTKs and contradicts the traditional belief describing autophagy to be induced following RTK inhibition. Additionally, even though autophagosome formation was reduced, p62 levels were sustained upon c-MET inhibition (Figure 4. 27). The latter observation could suggest that a non-catabolic pool of autophagosomes regulated by c-MET activation may exist. Based on the observation that c-MET inhibition suppresses basal autophagy, we hypothesised that growth factor stimulation would instead induce autophagy. However, no further increase in levels of basal autophagy was observed upon hrHGF stimulation in our study (Figure 4. 25). This could further suggest that activated c-MET is responsible solely for the regulation of basal autophagy. Interestingly, difference in tyrosine kinase activation status of c-MET resulted in disparate localisation; hrHGF stimulation increased perinuclear, while tyrosine kinase inhibition increased plasma membrane localisation (Figures 4. 24 and 4. 27). The loss of c-MET intracellular localisation may be responsible for the reduction of basal autophagy levels observed following c-MET inhibition. How could c-MET tyrosine kinase inhibition or localisation reduce levels of basal autophagy in CRC?

A potential scenario could be that tyrosine kinase activation of c-MET represents the initial step that facilitates intracellular translocation of c-MET whereby it interacts with autophagosome initiation precursors thus enabling autophagosome biogenesis. Upon hrHGF stimulation, active c-MET is rapidly internalised and soon (approximately after two hours) it is located at perinuclear endosomes (Barrow-McGee and Kermorgant, 2014). Regulation of autophagy initiation by RTKs at endosomes has

been previously described for EGFR (Wei *et al.*, 2013, Tan *et al.*, 2015). In particular, the study by Tan *et al*., (2015) reported decreased basal autophagy levels upon EGFR downregulation, however not evident for c-MET. Notably, regulation of autophagy upon c-MET tyrosine kinase inhibition was not investigated. Additionally, c-MET similarly to EGFR was found to colocalise with LAMPT4B-positive endosomes while LAMPT4B downregulation altered c-MET localisation (Tan *et al.*, 2015). Future experiments are warranted to investigate the specific localisation of c-MET and its interaction with potential target proteins in intracellular compartments important for regulation of autophagy.

Another explanation would be that c-MET tyrosine kinase inhibition results in mTORC2 activity downregulation, which in turn inhibits PKC alpha activity. PKC alpha could derange actin cytoskeleton and suppress rates of endocytosis resulting in this way to formation inhibition of autophagosome precursors from the plasma membrane, such as ATG16L1. This mechanism was previously described by Renna *et al*., (2013) in IGF-I-mediated autophagy inhibition (Renna *et al.*, 2013). Since c-MET downstream pathways were not tested following tyrosine kinase inhibition we cannot exclude the possibility that an mTORC2-PKC alpha mechanism controls autophagy downregulation in our system too. However, results may differ due to the experimental approaches (i.e. prolonged serum deprivation) followed.

Finally, c-MET-driven transcriptional regulation of autophagy related genes would be another possible mechanism by which c-MET activation/localisation could alter autophagosome biogenesis. A recent publication by Perera *et al*., (2015) described that increased levels of autophagy, which characterise pancreatic ductal adenocarcinoma (PDA), is controlled by accelerated nuclear translocation and consequent activation of the MiT/TFE proteins that concomitantly regulate lysosome biogenesis. Interestingly, RNA-sequencing data across 10 solid cancers, revealed high relative expression of TFE3 factor in CRC (Perera *et al.*, 2015). Earlier studies have shown that MiT and TFE proteins transcriptionally upregulate MET signalling (McGill *et al.*, 2006, Tsuda *et al.*, 2007) and we cannot exclude the possibility that a feedback loop exists where c-MET regulates MiT/TFE activation and or localisation.

In conclusion, this work shows that c-MET tyrosine kinase inhibition results in reduced levels of basal autophagy and the specific mechanism regulating c-MET-induced basal autophagy remains to be identified.

4.3.5. Basal autophagy plays a tumour suppressive role in HCT-116 cells under anchorage-independent cell growth conditions

The role of autophagy in cancer remains debatable. The general model suggested describes a tumour suppressive role for autophagy in cancer initiation whereas autophagy is considered to be a tumour-promoting mechanism in cancer progression. Even though important progress in deconvoluting the role of autophagy in cancer has been made the last years, the role of autophagy in CRC initiation and progression remains elusive. Our work shows that inhibition of basal autophagy does not affect growth of HCT-116 cells in adhesion (Figures 4. 30.a and 3. 7.a). The main disadvantage of *in vitro* culture systems in adhesion is their inadequacy to resemble the tumour microenvironment. For that reason, 3D culture systems and anchorage independent cell growth assays are used alongside with experimental models in adhesion. The aforementioned assays are better correlated with tumourigenicity in animal models (2012). In this study we employed an anchorage independent cell growth assay, which examined the ability of cancer cells to grow and survive in the absence of attachment to extracellular matrix and neighboring cells. In contrast to the sustained proliferation of HCT-116 cells in adhesion, autophagy inhibition resulted in increased anchorage-independent growth of HCT-116 *KRAS* WT cells (Figure 4. 30.b); an observation supporting a tumour suppressive role of autophagy in CRC progression. This observation is inconsistent with a recent study by Levy *et al*., (2015) showing that autophagy plays a tumour-promoting role in both early and later stages of CRC development (Levy *et al.*, 2015). Nevertheless, these differences could be explained by the different experimental approaches and the genetic differences of the samples utilised. Levy *et al*., (2015) used an *in vivo* model for CRC cancer initiation and progression where autophagy was suppressed (ATG7 deletion) along with heterozygous deletion of *APC* gene in intestinal epithelial cells. This model differs from our *in vitro* assessment of cell growth in established CRC cell lines. In our model, autophagy is downregulated in already transformed cells whereas in their study the inhibition of autophagy precedes malignant transformation. Moreover, Levy *et al*., (2015) studied autophagy under *APC* deletion whereas HCT-116 cells were found not to harbour any frameshift mutation in *APC* gene (Cosmic website). It is possible that autophagy in CRC progression plays a tumour-promoting role mainly under an APC-dependent context. Of note, in our model autophagy suppression using CQ was found to attenuate cell growth of DiFi cells (Figure 3. 7.e), which are expressing a truncated version of APC gene (Olive *et al.*, 1993). Autophagy has been previously shown to decrease DNA damage and maintain genomic integrity of a cell (Karantza-Wadsworth *et al.*, 2007). In that way autophagy may function as a barrier for cancer cells to lose

their genomic stability and accumulate further mutations leading to more aggressive cancer progression. CRC it is anyway characterised by increased genomic instability (Al-Sohaily *et al.*, 2012) and particularly HCT-116 cells are characterised as high MSI (He *et al.*, 2015). The tumour suppressive role of autophagy observed in HCT-116 cells in anchorage-independent conditions could be attributed to the high genomic instability caused by autophagy suppression. Differences in cell growth phenotypes upon autophagy suppression between adherent and anchorage-independent conditions have been previously reported (Guo *et al.*, 2011). Our findings on RTK and cell signalling in autophagy-compromised conditions cannot explain the increased cell growth phenotype of HCT-116 *KRAS* WT cells in anchorage-independent conditions. Based on earlier studies showing that AKT, ERK and JNK signalling downstream of c-MET confers cell proliferation and survival (Lamorte *et al.*, 2000, Xiao *et al.*, 2001), it would have been expected the reduced RTK and AKT/ERK/JNK signalling to attenuate cell growth of cells. However our observations are inversely correlated. A possible explanation for these contradictory results could be that the signalling defects we observed in attached cultured conditions upon autophagy suppression were not present in anchorage-independent conditions of *in vitro* model systems. Future studies would be valuable to investigate whether the signalling defects on p-c-MET, pAKT and pERK following autophagy suppression in adherent-cultured conditions are also sustained upon anchorage-independent growth.

Collectively, autophagy seems to play a tumour suppressive role in CRC progression in anchorage-independent conditions. *In vivo* studies investigating the role of autophagy in cancer progression of *KRAS*-driven tumours consistently show that autophagy enables cancer cell survival. However, the tumour-promoting role of autophagy in cancer progression switches to tumour suppressive when p53 gene is deleted concurrently with *KRAS* activating mutations. These observations highlight a context-dependent role of autophagy in cancer progression (discussed in 1.2.2.). Further investigations are warranted to investigate how the inhibition of autophagy affects the progression of different cancer types with variable mutational signatures. In CRC future *in vivo* work to characterise the role of autophagy under the presence of *KRAS* and *PI3K* activating mutations, important in CRC development and responsible for cancer therapy resistance, would be valuable.

4.3.6. Basal autophagy is not implicated in invasion/migration of CRC cells

Autophagy has been found to regulate migration/invasion in cancer (Macintosh *et al.*, 2012, Galavotti *et al.*, 2013, Li *et al.*, 2013a) with the precise mechanism being

less defined. It has been shown that autophagy inhibition could suppress invasion/migration in glioma cells (Macintosh *et al.*, 2012, Galavotti *et al.*, 2013) and Epithelial to Mesenchymal Transition (EMT) in hepatocellular carcinoma (Li *et al.*, 2013a). Currently, the role of autophagy in migration/invasion of CRC is elusive. Our work in accordance with the literature has shown that the presence of *KRAS* activating mutation accelerates migration/invasion of cancer cells (Campbell and Der, 2004). In particular, higher invasion and migration capacity was observed in HCT-116 *KRAS* G13D cells compared to their isogenic WT version (Figure 4. 29.a). Cancer cell invasion and metastasis is a process with high metabolic requirements. Based on the abovementioned findings and the known role of *KRAS* activation in increasing levels of basal autophagy and enabling cancer cell survival (Guo *et al.*, 2011), we hypothesised that aggressive tumours characterised by *KRAS* activation could use autophagy not only to survive but also to invade extracellular matrix and then metastasise and colonise to distant organs. HCT-116 *KRAS* G13D autophagy-proficient and -compromised cells were used as a model system to assess the role of autophagy in migration/invasion capacity of CRC cells *in vitro*. In contrast to the previously reported invasion-promoting role of autophagy, this study reveals that basal autophagy is not controlling CRC migration/invasion (Figure 4. 29.b). Discrepancies between studies could be attributed to cell-type and cancer-type specific effects. Earlier studies have shown that activation of c-MET, AKT and/or ERK pathways is positively correlated with increased invasion/migration of cancer cells, including CRC cells (Takeuchi *et al.*, 2003, Samuels *et al.*, 2005, Cancer Genome Atlas, 2012, Zhu *et al.*, 2012, Caramel *et al.*, 2013, Pérez-Vargas *et al.*, 2013, Urosevic *et al.*, 2014, Ye *et al.*, 2014). Based on the reduced RTKs, AKT and ERK activation that was observed in our study following autophagy suppression, it would have been expected autophagy suppression to diminish migration/invasion of CRC cells. However, our results were not indicative of such a correlation.

4.3.7. Summary

The work presented in this chapter aimed to unravel the role of basal autophagy in regulating cell signalling in CRC cells. Our findings establish a novel bi-directional relationship between basal autophagy and RTK activation and cell signalling. In particular basal autophagy is implicated in c-MET activation and *vice versa* c-MET tyrosine-kinase inhibition attenuates basal autophagy levels; however, the exact mechanism of this interplay remains to be determined. Basal autophagy was found to play an active role in regulation of AKT phosphorylation of CRC cells in a systematic

manner. On the other hand, MAPK/ERK, AMPK alpha and SAPK/JNK pathways are regulated in a cell-type specific manner upon autophagy-compromised conditions. Our work suggests that basal autophagy regulates AKT, ERK, JNK and AMPK alpha phosphorylation through regulating RTK activation. While basal autophagy was found to play a tumour suppressive role in HCT-116 cells under anchorage-independent cell growth conditions, this was not evident in adhered-cultured conditions. Finally, basal autophagy was not implicated in invasion/migration of CRC cells.

The main conclusions and future directions of this work are presented in Chapter 5.

Chapter 5

Conclusions and Future Perspectives

5. Conclusions and Future Perspectives

This study aimed to define the role of autophagy in CRC in two different but interconnected contexts: a) upon EGFR targeted therapy and b) upon basal non-induced autophagy conditions. It was identified that *PI3K* activating mutations and high AKT activation levels render CRC cells refractory to autophagy induction following pharmacological inhibition or downregulation of EGFR. Additionally, concomitant EGFR and autophagy inhibition did not potentiate EGFR-targeted therapy response. Only *PI3K* WT cells with deactivated AKT signalling following EGFR inhibition were found to induce cyto-protective autophagy. Even though *PI3K* mutated CRC cells are refractory to EGFR-mediated autophagy induction, they display basal levels of autophagy despite the presence of constitutive PI3K/mTOR signalling. Genetic inhibition of basal autophagy results in downregulation of AKT and/or ERK phosphorylation possibly through hypo-phosphorylation of several RTKs, including c-MET. Interestingly, vice versa c-MET activation was found to regulate basal autophagy induction since c-Met inhibition results in reduction of basal autophagy. While inhibition of basal autophagy did not affect growth of CRC cells cultured in adhesion, it resulted in increased anchorage-independent growth. Finally, autophagy suppression did not affect migration/invasion capacity of CRC cells.

In this work, EGFR inhibition targeted therapy with the use of the monoclonal antibody Cetuximab has been shown to yield a largely varied and differential response when tested in CRC cells. Resistant, intermediate-response, sensitive and highly-sensitive cell lines were identified and associated with activation levels of EGFR downstream pathways. MAPK/ERK and PI3K/AKT activation was found to inversely correlate with Cetuximab treatment response. Cetuximab resistant cell lines were characterized by high AKT and ERK activation while highly sensitive to Cetuximab cells demonstrated decreased AKT and ERK activation following EGFR inhibition. Intermediate resistant and sensitive cells were shown to exhibit solely ERK downregulation. We suggest that following EGFR inhibition, ERK activation regulates cell proliferation and AKT activation determines cell death. To further investigate and prove this hypothesis a number of purpose-designed experiments can be conducted. Cell viability testing on the aforementioned cell lines under EGFR inhibition will allow for discrimination and correlation of the cytostatic and the cytotoxic effects of ERK and AKT, respectively. A fluorescence-based cell Live/Dead double staining assay could be utilised to this purpose. Additional experimental conditions where MEK, ERK and/or AKT inhibitors are assessed in combination with Cetuximab should be conducted in resistant cells (HCT-116 and CaCo2) to further explore response to EGFR inhibition. In turn, we could constitutively activate MEK and/or AKT (myr_AKT) proteins in

Cetuximab sensitive cell lines to assess reversibility of cytostatic and/or cytotoxic effects, respectively. Should our hypotheses proven to be valid, the cell cycle positioning (via BrdU assay) and the type of cell death (via Annexin V staining) upon Cetuximab treatment will be further defined and quantified using flow cytometry.

The majority of CRC cell lines were found to be refractory to autophagy induction following EGFR targeted therapy and did not benefit from EGFR-autophagy combinational treatment. PI3K/AKT pathway was found to regulate autophagy induction following EGFR inhibition. All CRC cells harbouring *PI3K* mutations were refractory to autophagy induction, with the exception of *PI3K* WT DiFi cells. Specifically, *PI3K* mutations were positively correlated with AKT activation levels, which in turn were inversely correlated with autophagy induction. On the other hand, AKT inhibition approaches reversed the impotency of *PI3K* mutant cells to autophagy induction. To exploit the direct link between *PI3K* mutational status, AKT activation and autophagy induction in CRC cells it would be fundamental to use *PI3K* isogenic cell lines. *In vivo* experiments are warranted to establish the role of *PI3K* mutational status in Cetuximab treatment response in combination with autophagy inhibition, which will pave the way to future clinical trials.

Which factor controls autophagy induction downstream of PI3K/AKT upon EGFR targeted therapy? In order to address this, DiFi cells could be used as a model system since they were found capable of inducing autophagy. Two kinases residing downstream of AKT, namely mTORC1 and Beclin1, will be assessed for their ability to induce autophagy upon EGFR inhibition as follows: i) To exploit whether an mTORC1-dependent mechanism regulates Cetuximab-induced autophagy in CRC cells we should first evaluate mTORC1 activation levels as depicted by phosphorylation of S6 using western blotting. To further prove a direct link of mTORC1 in the regulation of Cetuximab-induced autophagy we could either constitutively activate mTORC1 or downregulate Raptor in both control and myr_AKT-expressing DiFi cells treated with Cetuximab. We expect the constitutively activated mTORC1 cells not to induce autophagy and *vice versa* the Raptor downregulated DiFi cells to induce autophagy even in the presence of constitutively active myr_AKT. ii) To define whether an mTORC1-independent mechanism controls autophagy induction upon EGFR inhibition, Beclin1 protein will be examined. Firstly, immunoprecipitation of Beclin1 protein in control and myr_AKT cells -/+ Cetuximab and phosphorylation of Beclin1 will be assessed using western blotting with an anti-phosphoserine antibody. The rationale behind the phosphoserine antibody selection resides to the fact that AKT phosphorylates Beclin 1 at S295 residue and thus inactivates autophagy induction. myr_AKT cells are expected to have increased phosphorylation (inactivation) of Beclin1 in comparison to control cells following Cetuximab treatment in accordance to

reduced autophagy levels. In addition, a Beclin1 downregulation approach via siRNA could be utilised in order to examine whether autophagy induction is reversed, following Cetuximab treatment in DiFi cells.

Basal autophagy is controlled in an mTORC1-independent manner in CRC cells, despite the presence of *PI3K* activating mutations and mTORC1 activation. Interestingly, c-MET tyrosine kinase inhibition resulted in reduced levels of basal autophagy in our system. These findings suggest a novel function of c-MET RTK in controlling basal autophagy in CRC independently of mTORC1 activation. Based on our observations and other studies, the following two hypotheses can be suggested: i) c-MET-driven transcriptional regulation of autophagy might be a possible mechanism by which c-MET activation regulates autophagosome biogenesis. Basal autophagy in PDA is controlled by accelerated nuclear translocation and consequent activation of the MiT/TFE proteins and interestingly high relative expression of TFE3 factor is present in CRC (Perera *et al.*, 2015). Since MiT and TFE proteins are transcriptionally upregulating MET signalling (McGill *et al.*, 2006, Tsuda *et al.*, 2007) we could hypothesise that a feedback loop exists where c-MET regulates MiT/TFE activation and or localisation. To exploit whether c-MET transcriptionally regulates autophagy induction we could initially examine the expression of MiT/TFE in CRC cells. Following that, siRNA downregulation will be used to investigate whether basal levels of autophagy are abolished through MiT/TFE deletion. ii) c-MET intracellular activation and/or localisation might be another factor regulating basal autophagy in CRC since reduction of intracellular localised c-MET upon tyrosine kinase inhibition attenuated autophagosome biogenesis. Earlier studies have shown that autophagy induction is directly regulated by EGFR at intracellular endosomal compartments where autophagosome precursors and regulators reside. To exploit this hypothesis we could specifically restrict c-MET internalisation and subsequent localisation at intracellular compartments independently of its activation levels. To this end, endocytosis inhibitors (Dynasore and Pitstop2) could be used under c-MET tyrosine kinase-stimulated and -inhibited conditions to examine levels of basal autophagy. In addition and in order to further investigate whether c-MET regulates basal autophagy in a tyrosine kinase-independent manner, siRNA could be utilised to downregulate c-MET expression and assess levels of basal autophagy.

We showed for the first time that genetic inhibition of basal autophagy diminishes endogenous RTK activation in CRC cells, an effect evident even in the presence of *KRAS* activating mutations. This mechanism was proven by focusing on c-MET, a highly expressed and activated RTK and also known contributor of acquired Cetuximab resistance in CRC cells. The activated c-MET was found to intracellularly colocalise with autophagosomes. Despite the fact that these organelles are commonly

implicated in protein degradation, total c-MET levels remained stable, thus signifying that a non-catabolic mechanism by which autophagy controls c-MET and possibly other RTK activation exists. In order to further investigate the potential mechanism by which basal autophagy regulates c-MET RTK activation we could examine the following hypotheses: i) Basal autophagy-mediated regulation of protein-tyrosine phosphatases controls c-MET phosphorylation and activation. Protein-tyrosine phosphatases are reversing c-MET phosphorylation and activation (Trusolino *et al.*, 2010). Specifically, PTP1B and PTPN2 phosphatases are responsible for the de-phosphorylation of the catalytic tyrosines of c-MET (Y1234/1235) (Sangwan *et al.*, 2008). A general pharmacological inhibitor of protein-tyrosine phosphatases could be used in autophagy-proficient and -compromised cells. Additionally, PTP1B and PTPN2 phosphatases can be specifically downregulated using a siRNA approach. ii) Since c-MET colocalises with autophagosome the latter could potentially function as a signalling scaffold for c-MET activation. To prove such a mechanism we firstly need to examine whether there is a direct interaction between autophagosomes and c-MET. To this end, we can overexpress GFP-tagged c-MET in autophagy-proficient and -compromised CRC cells and follow a co-immunoprecipitation approach for pulling down GFP and detecting LC3B using western blotting. It is expected that only proficient cells will interact with LC3B. If such an interaction is proven we could overexpress a lipidated-deficient LC3B mutant ($LC3B^{\Delta G}$) in CRC autophagy-proficient cells. Since non-lipidated LC3B protein cannot bind to autophagosomes we expect autophagy- proficient $LC3B^{\Delta G}$ expressing cells to recapitulate the attenuation of c-MET activation that was observed in autophagy-compromised cells. In turn, to rescue p-c-MET inhibition in autophagy-compromised cells we could downregulate ATG4B protein responsible for LC3B de-lipidation. In that way we expect increased levels and localisation of LC3B-II on autophagosomes and an increase in c-MET phosphorylation. iii) Basal-autophagy-mediated regulation of HGF secretion controls c-MET activation. ELISA could examine differences in secretion of HGF regulated by basal autophagy using a quantitative assessment of HGF. It is expected that autophagy-compromised cells with reduced c-MET activation to present lower levels of HGF. iv) Basal autophagy decreases RTK exocytosis and RTK plasma membrane activation. If our preliminary data, which indicate increased levels of intracellular c-MET following basal autophagy suppression, are confirmed we could further exploit regulation of exocytosis in autophagy-proficient and -compromised conditions. To this end, Vamp2-pluorin and/or Vamp7-pluorin constructs would be overexpressed in autophagy-proficient and -compromised cells to monitor differences in exocytosis (Mohankumar *et al.*, 2015). v) proteasome-mediated degradation of p-c-MET is potentially controlled by basal autophagy. This can be further examined by using the proteasome inhibitor MG132 in

autophagy-proficient and -compromised cells and examine whether c-MET downregulation is rescued in autophagy-compromised cells using western blotting.

Our work suggests that basal autophagy regulates cell signalling through RTKs and more specifically c-MET in CRC cells. In particular, inhibition of c-MET activation was positively correlated with inhibition of c-MET downstream kinases, namely PI3K/AKT, MAPK/ERK, JNK, and AMPK alpha in autophagy-compromised conditions. Amongst the above kinases, activation of AKT was the one consistently regulated by basal autophagy in all CRC cell lines tested. To investigate whether autophagy modulates cell signalling via c-MET we could examine AKT activation in autophagy-proficient and -compromised cells in the absence of growth factors. To this end, prolonged serum starved conditions and additionally HGF siRNA in serum-replete conditions could be applied to abolish HGF-induced c-MET activation. If c-MET acts as the intermediate effector, discrepancies in cell signalling between autophagy-proficient and -compromised cells will not be observed. In parallel a potential c-MET independent mechanism controlling AKT activation via autophagy could be examined. An ideal candidate for this would be mTORC2 as it is a known regulator of AKT activation at S473 residue. If mTORC2 activity is regulated by basal autophagy, downstream signalling effectors other than AKT could also be affected. To this purpose, serum- and glucocorticoid-induced protein kinase 1 (SGK1) and PKC alpha will be examined in autophagy-proficient and -compromised cells using western blotting. Additionally an mTORC2 downregulation approach through siRNA of Rictor (a component of mTORC2 complex) will allow us to examine differences in AKT.

This study also highlights the importance of a later step in the autophagic process controlling AKT activation since both genetic and pharmacological inhibition of autophagy consistently downregulated AKT phosphorylation. This later step was suggested to be the autophagosome to lysosome fusion whereby the former acts as scaffold for AKT. Based on this and on the fact that mTROC2 signalling can be present on lysosomes it would be valuable to examine colocalisation of pAKT with autophagosome (LC3B), lysosomes (LAMP1) and mTORC2 (Rictor) in autophagy-proficient and -compromised cells using immunofluorescence.

We have also described that growth of CRC cells in adhesion is not affected upon basal autophagy inhibition and that a tumour suppressive role is evident under anchorage-independent cell growth conditions. Signalling defects present in adhered culture conditions upon autophagy suppression but not in anchorage-independent conditions could be a possible hypothesis. To further investigate how c-MET and cell signalling activation is regulated by autophagy in an anchorage independent milieu, CRC cells in detached conditions can be cultured aiming to evaluate phosphorylation of RTKs and cell signalling effectors using western blotting.

Conclusion

RTKs are commonly overactivated or overexpressed in a variety of cancer types including CRC. RTKs activation and downstream signalling has been correlated with tumourigenesis, metastatic potential, poor survival and resistance to therapy. Basal autophagy is activated in a variety of cancer types including CRC and confers to tumour progression. A fine interplay between RTKs and basal autophagy was illustrated in this work. Basal autophagy suppression results in inhibition of RTKs activation and downstream signalling. The presence of a dynamic equilibrium between basal autophagy and cancer is suggesting that aberrant activation of autophagy leads to cancer cells “addiction” to RTK activation and AKT signalling. However, CRC cell growth on anchorage-independent conditions is potentiated following basal autophagy suppression, suggesting a tumour suppressive role of basal autophagy in CRC progression. It would be crucial to determine in the future whether basal autophagy-mediated regulation of RTK and cell signalling in CRC is responsible for the tumour suppressive role of basal autophagy. Regarding the role of autophagy in RTK targeted therapy; it is generally believed that inhibition of autophagy can potentially sensitize cancer cells to treatment. However, autophagy regulation downstream of RTKs and specifically EGFR and c-MET is complex and characterized by variability. Similarly, variability is also present in autophagy induction between CRC cells. Autophagy inhibition via targeted therapy is considered a promising therapeutic approach and increasing number of clinical trials are using autophagy inhibitors in combination with conventional cancer therapy. *PI3K* activating mutations are present in 18% of non-hypermutated CRC and are associated with tumour aggressiveness. Our work highlights the importance of *PI3K* screening when using autophagy inhibitors in combination with EGFR targeted therapy in CRC. Only *PI3K* WT CRC cells may benefit from autophagy inhibition and Cetuximab combinational treatment, whereas *PI3K* mutant cells might remain unresponsive.

Care should be taken before using autophagy-modulating compounds into the therapeutic approaches used for the treatment of CRC patients. Most certainly, purpose-designed *in vivo* studies must be conducted before implementing bench-top model findings into the clinical practice. Autophagy inhibition approaches could be detrimental for *PI3K* mutant CRC patients, which do not induce autophagy following EGFR targeted therapy, due to a tumour suppressive role of basal autophagy in *PI3K* mutant CRC.

Bibliography

Bibliography

(2012) Anchorage-Independent Cell Growth. In: Encyclopedia of Cancer (Schwab, M., ed), pp 173-173: Springer Berlin Heidelberg.

Adachi M, Katsumura KR, Fujii K, Kobayashi S, Aoki H, Matsuzaki M (2003) Proteasome-dependent decrease in Akt by growth factors in vascular smooth muscle cells. FEBS Letters 554:77-80.

Adrain C, Freeman M (2014) Regulation of receptor tyrosine kinase ligand processing. Cold Spring Harbor perspectives in biology 6.

Al-Sohaily S, Biankin A, Leong R, Kohonen-Corish M, Warusavitarne J (2012) Molecular pathways in colorectal cancer. Journal of gastroenterology and hepatology 27:1423-1431.

Amaravadi RK, Lippincott-Schwartz J, Yin XM, Weiss WA, Takebe N, Timmer W, DiPaola RS, Lotze MT, White E (2011) Principles and current strategies for targeting autophagy for cancer treatment. Clinical cancer research : an official journal of the American Association for Cancer Research 17:654-666.

Arias E, Koga H, Diaz A, Mocholi E, Patel B, Cuervo Ana M (2015) Lysosomal mTORC2/PHLPP1/Akt Regulate Chaperone-Mediated Autophagy. Molecular cell 59:270-284.

Arvelo F, Sojo F, Cotte C (2015) Biology of colorectal cancer. ecancermedicalscience 9:520.

Ashraf SQ, Nicholls AM, Wilding JL, Ntouroupi TG, Mortensen NJ, Bodmer WF (2012) Direct and immune mediated antibody targeting of ERBB receptors in a colorectal cancer cell-line panel. Proceedings of the National Academy of Sciences of the United States of America 109:21046-21051.

Bardelli A, Corso S, Bertotti A, Hobor S, Valtorta E, Siravegna G, Sartore-Bianchi A, Scala E, Cassingena A, Zecchin D, Apicella M, Migliardi G, Galimi F, Lauricella C, Zanon C, Perera T, Veronese S, Corti G, Amatu A, Gambacorta M, Diaz LA, Jr., Sausen M, Velculescu VE, Comoglio P, Trusolino L, Di Nicolantonio F, Giordano S, Siena S (2013) Amplification of the MET receptor drives resistance to anti-EGFR therapies in colorectal cancer. Cancer discovery 3:658-673.

Bardelli A, Siena S (2010) Molecular mechanisms of resistance to cetuximab and panitumumab in colorectal cancer. Journal of clinical oncology : official journal of the American Society of Clinical Oncology 28:1254-1261.

Barrow-McGee R, Kermorgant S (2014) Met endosomal signalling: In the right place, at the right time. The International Journal of Biochemistry & Cell Biology 49:69-74.

Bellodi C, Lidonnici MR, Hamilton A, Helgason GV, Soliera AR, Ronchetti M, Galavotti S, Young KW, Selmi T, Yacobi R, Van Etten RA, Donato N, Hunter A, Dinsdale D, Tirro E, Vigneri P, Nicotera P, Dyer MJ, Holyoake T, Salomoni P, Calabretta B (2009) Targeting autophagy potentiates tyrosine kinase inhibitor-induced cell death in Philadelphia chromosome-positive cells, including primary CML stem cells. The Journal of clinical investigation 119:1109-1123.

Benvenuti S, Sartore-Bianchi A, Di Nicolantonio F, Zanon C, Moroni M, Veronese S, Siena S, Bardelli A (2007) Oncogenic activation of the RAS/RAF signaling pathway impairs the response of metastatic colorectal cancers to anti-epidermal growth factor receptor antibody therapies. Cancer research 67:2643-2648.

Bernard M, Dieudé M, Yang B, Hamelin K, Underwood K, Hébert M-J (2014) Autophagy fosters myofibroblast differentiation through MTORC2 activation and downstream upregulation of CTGF. Autophagy 10:2193-2207.

Berry DL, Baehrecke EH (2007) Growth arrest and autophagy are required for salivary gland cell degradation in Drosophila. Cell 131:1137-1148.

Bertotti A, Migliardi G, Galimi F, Sassi F, Torti D, Isella C, Cora D, Di Nicolantonio F, Buscarino M, Petti C, Ribero D, Russolillo N, Muratore A, Massucco P, Pisacane A, Molinaro L, Valtorta E, Sartore-Bianchi A, Risio M, Capussotti L, Gambacorta M, Siena S, Medico E, Sapino A, Marsoni S, Comoglio PM, Bardelli A, Trusolino L (2011) A molecularly annotated platform of patient-derived xenografts ("xenopatients") identifies HER2 as an effective therapeutic target in cetuximab-resistant colorectal cancer. Cancer discovery 1:508-523.

Bertotti A, Sassi F (2015) Molecular Pathways: Sensitivity and Resistance to Anti-EGFR Antibodies. Clinical cancer research : an official journal of the American Association for Cancer Research 21:3377-3383.

Birgisdottir ÅB, Lamark T, Johansen T (2013) The LIR motif – crucial for selective autophagy. Journal of cell science 126:3237-3247.

Brand TM, Iida M, Wheeler DL (2011) Molecular mechanisms of resistance to the EGFR monoclonal antibody cetuximab. Cancer biology & therapy 11:777-792.

Brunet A, Bonni A, Zigmond MJ, Lin MZ, Juo P, Hu LS, Anderson MJ, Arden KC, Blenis J, Greenberg ME (1999) Akt Promotes Cell Survival by Phosphorylating and Inhibiting a Forkhead Transcription Factor. Cell 96:857-868.

Cadwell K, Patel KK, Komatsu M, Virgin HWt, Stappenbeck TS (2009) A common role for Atg16L1, Atg5 and Atg7 in small intestinal Paneth cells and Crohn disease. Autophagy 5:250-252.

Calabretta B, Salomoni P (2011) Inhibition of autophagy: a new strategy to enhance sensitivity of chronic myeloid leukemia stem cells to tyrosine kinase inhibitors. Leukemia & lymphoma 52 Suppl 1:54-59.

Campbell PM, Der CJ (2004) Oncogenic Ras and its role in tumor cell invasion and metastasis. Seminars in cancer biology 14:105-114.

Cancer Genome Atlas N (2012) Comprehensive molecular characterization of human colon and rectal cancer. Nature 487:330-337.

Cantor JR, Sabatini DM (2012) Cancer Cell Metabolism: One Hallmark, Many Faces. Cancer discovery 2:881-898.

Caramel J, Papadogeorgakis E, Hill L, Browne Gareth J, Richard G, Wierinckx A, Saldanha G, Osborne J, Hutchinson P, Tse G, Lachuer J, Puisieux A, Pringle JH, Ansieau S, Tulchinsky E (2013) A Switch in the Expression of Embryonic EMT-Inducers Drives the Development of Malignant Melanoma. Cancer cell 24:466-480.

Carpenter G, King L, Jr., Cohen S (1978) Epidermal growth factor stimulates phosphorylation in membrane preparations in vitro. Nature 276:409-410.

Carracedo A, Pandolfi PP (2008) The PTEN-PI3K pathway: of feedbacks and cross-talks. Oncogene 27:5527-5541.

Chukkapalli S, Amessou M, Dilly AK, Dekhil H, Zhao J, Liu Q, Bejna A, Thomas RD, Bandyopadhyay S, Bismar TA, Neill D, Azoulay L, Batist G, Kandouz M (2014) Role of the EphB2 receptor in autophagy, apoptosis and invasion in human breast cancer cells. Experimental Cell Research 320:233-246.

Chung KY, Shia J, Kemeny NE, Shah M, Schwartz GK, Tse A, Hamilton A, Pan D, Schrag D, Schwartz L, Klimstra DS, Fridman D, Kelsen DP, Saltz LB (2005) Cetuximab shows activity in colorectal cancer patients with tumors that do not express the epidermal growth factor receptor by immunohistochemistry. Journal of clinical oncology : official journal of the American Society of Clinical Oncology 23:1803-1810.

Cianfanelli V, Fuoco C, Lorente M, Salazar M, Quondamatteo F, Gherardini PF, De Zio D, Nazio F, Antonioli M, D'Orazio M, Skobo T, Bordi M, Rohde M, Dalla Valle L, Helmer-Citterich M, Gretzmeier C, Dengjel J, Fimia GM, Piacentini M, Di Bartolomeo S, Velasco G, Cecconi F (2015) AMBRA1 links autophagy to cell proliferation and tumorigenesis by promoting c-Myc dephosphorylation and degradation. Nature cell biology 17:20-30.

Cohen S (1962) Isolation of a mouse submaxillary gland protein accelerating incisor eruption and eyelid opening in the new-born animal. The Journal of biological chemistry 237:1555-1562.

Cohen S (1965) The stimulation of epidermal proliferation by a specific protein (EGF). Developmental biology 12:394-407.

Colotta F, Allavena P, Sica A, Garlanda C, Mantovani A (2009) Cancer-related inflammation, the seventh hallmark of cancer: links to genetic instability. Carcinogenesis 30:1073-1081.

Cuervo AM, Wong E (2014) Chaperone-mediated autophagy: roles in disease and aging. Cell research 24:92-104.

De Roock W, Claes B, Bernasconi D, De Schutter J, Biesmans B, Fountzilas G, Kalogeras KT, Kotoula V, Papamichael D, Laurent-Puig P, Penault-Llorca F, Rougier P, Vincenzi B, Santini D, Tonini G, Cappuzzo F, Frattini M, Molinari F, Saletti P, De Dosso S, Martini M, Bardelli A, Siena S, Sartore-Bianchi A, Tabernero J, Macarulla T, Di Fiore F, Gangloff AO, Ciardiello F, Pfeiffer P, Qvortrup C, Hansen TP, Van Cutsem E, Piessevaux H, Lambrechts D, Delorenzi M, Tejpar S (2010) Effects of KRAS, BRAF, NRAS, and PIK3CA mutations on the efficacy of cetuximab plus chemotherapy in chemotherapy-refractory metastatic colorectal cancer: a retrospective consortium analysis. The lancet oncology 11:753-762.

De Roock W, De Vriendt V, Normanno N, Ciardiello F, Tejpar S (2011) KRAS, BRAF, PIK3CA, and PTEN mutations: implications for targeted therapies in metastatic colorectal cancer. The lancet oncology 12:594-603.

Denton D, Shravage B, Simin R, Mills K, Berry DL, Baehrecke EH, Kumar S (2009) Autophagy, not apoptosis, is essential for midgut cell death in Drosophila. Current biology : CB 19:1741-1746.

DeSantis CE, Lin CC, Mariotto AB, Siegel RL, Stein KD, Kramer JL, Alteri R, Robbins AS, Jemal A (2014) Cancer treatment and survivorship statistics, 2014. CA: a cancer journal for clinicians 64:252-271.

Di Nicolantonio F, Martini M, Molinari F, Sartore-Bianchi A, Arena S, Saletti P, De Dosso S, Mazzucchelli L, Frattini M, Siena S, Bardelli A (2008) Wild-type BRAF is required for response to panitumumab or cetuximab in metastatic colorectal cancer. Journal of clinical oncology : official journal of the American Society of Clinical Oncology 26:5705-5712.

Diaz LA, Jr., Williams RT, Wu J, Kinde I, Hecht JR, Berlin J, Allen B, Bozic I, Reiter JG, Nowak MA, Kinzler KW, Oliner KS, Vogelstein B (2012) The molecular evolution of acquired resistance to targeted EGFR blockade in colorectal cancers. Nature 486:537-540.

Dickey CA, Koren J, Zhang Y-J, Xu Y-f, Jinwal UK, Birnbaum MJ, Monks B, Sun M, Cheng JQ, Patterson C, Bailey RM, Dunmore J, Soresh S, Leon C, Morgan D, Petrucelli L (2008) Akt and CHIP coregulate tau degradation through coordinated interactions. Proceedings of the National Academy of Sciences 105:3622-3627.

Dou Z, Pan JA, Dbouk HA, Ballou LM, DeLeon JL, Fan Y, Chen JS, Liang Z, Li G, Backer JM, Lin RZ, Zong WX (2013) Class IA PI3K p110beta subunit promotes autophagy through Rab5 small GTPase in response to growth factor limitation. Molecular cell 50:29-42.

Dowdle WE, Nyfeler B, Nagel J, Elling RA, Liu S, Triantafellow E, Menon S, Wang Z, Honda A, Pardee G, Cantwell J, Luu C, Cornella-Taracido I, Harrington E, Fekkes P, Lei H, Fang Q, Digan ME, Burdick D, Powers AF, Helliwell SB, D'Aquin S, Bastien J, Wang H, Wiederschain D, Kuerth J, Bergman P, Schwalb D, Thomas J, Ugwonali S, Harbinski F, Tallarico J, Wilson CJ, Myer VE, Porter JA, Bussiere DE, Finan PM, Labow MA, Mao X, Hamann LG, Manning BD, Valdez Reginald A, Nicholson T, Schirle M, Knapp MS, Keaney EP, Murphy LO (2014) Selective VPS34 inhibitor blocks autophagy and uncovers a role for NCOA4 in ferritin degradation and iron homeostasis in vivo. Nature cell biology 16:1069-1079.

Dragowska WH, Weppler SA, Wang JC, Wong LY, Kapanen AI, Rawji JS, Warburton C, Qadir MA, Donohue E, Roberge M, Gorski SM, Gelmon KA, Bally MB (2013) Induction of autophagy is an early response to gefitinib and a potential therapeutic target in breast cancer. PloS one 8:e76503.

Du J, Teng RJ, Guan T, Eis A, Kaul S, Konduri GG, Shi Y (2012) Role of autophagy in angiogenesis in aortic endothelial cells. American journal of physiology Cell physiology 302:C383-391.

Efeyan A, Comb WC, Sabatini DM (2015) Nutrient-sensing mechanisms and pathways. Nature 517:302-310.

Egan Daniel F, Chun Matthew GH, Vamos M, Zou H, Rong J, Miller Chad J, Lou Hua J, Raveendra-Panickar D, Yang C-C, Sheffler Douglas J, Teriete P, Asara John M, Turk Benjamin E, Cosford Nicholas DP, Shaw Reuben J (2015) Small Molecule Inhibition of the Autophagy Kinase ULK1 and Identification of ULK1 Substrates. Molecular cell 59:285-297.

Eichhorn PJA, Creyghton MP, Bernards R (2009) Protein phosphatase 2A regulatory subunits and cancer. Biochimica et Biophysica Acta (BBA) - Reviews on Cancer 1795:1-15.

Eimer S, Belaud-Rotureau MA, Airiau K, Jeanneteau M, Laharanne E, Veron N, Vital A, Loiseau H, Merlio JP, Belloc F (2011) Autophagy inhibition cooperates with

erlotinib to induce glioblastoma cell death. Cancer biology & therapy 11:1017-1027.

Elgendy M, Sheridan C, Brumatti G, Martin SJ (2011) Oncogenic Ras-induced expression of Noxa and Beclin-1 promotes autophagic cell death and limits clonogenic survival. Molecular cell 42:23-35.

Engelman JA, Luo J, Cantley LC (2006) The evolution of phosphatidylinositol 3-kinases as regulators of growth and metabolism. Nature reviews Genetics 7:606-619.

Fearon ER (2011) Molecular genetics of colorectal cancer. Annual review of pathology 6:479-507.

Feng Y, He D, Yao Z, Klionsky DJ (2014) The machinery of macroautophagy. Cell research 24:24-41.

Fuchs Y, Steller H (2015) Live to die another way: modes of programmed cell death and the signals emanating from dying cells. Nature reviews Molecular cell biology 16:329-344.

Furuta S, Hidaka E, Ogata A, Yokota S, Kamata T (2004) Ras is involved in the negative control of autophagy through the class I PI3-kinase. Oncogene 23:3898-3904.

Galavotti S, Bartesaghi S, Faccenda D, Shaked-Rabi M, Sanzone S, McEvoy A, Dinsdale D, Condorelli F, Brandner S, Campanella M, Grose R, Jones C, Salomoni P (2013) The autophagy-associated factors DRAM1 and p62 regulate cell migration and invasion in glioblastoma stem cells. Oncogene 32:699-712.

Galluzzi L, Pietrocola F, Bravo-San Pedro JM, Amaravadi RK, Baehrecke EH, Cecconi F, Codogno P, Debnath J, Gewirtz DA, Karantza V, Kimmelman A, Kumar S, Levine B, Maiuri MC, Martin SJ, Penninger J, Piacentini M, Rubinsztein DC, Simon HU, Simonsen A, Thorburn AM, Velasco G, Ryan KM, Kroemer G (2015) Autophagy in malignant transformation and cancer progression. The EMBO journal 34:856-880.

Gherardi E, Birchmeier W, Birchmeier C, Woude GV (2012) Targeting MET in cancer: rationale and progress. Nature reviews Cancer 12:89-103.

Goldberg SB, Supko JG, Neal JW, Muzikansky A, Digumarthy S, Fidias P, Temel JS, Heist RS, Shaw AT, McCarthy PO, Lynch TJ, Sharma S, Settleman JE, Sequist LV (2012) A Phase I Study of Erlotinib and Hydroxychloroquine in Advanced Non-Small Cell Lung Cancer. Journal of thoracic oncology : official publication of the International Association for the Study of Lung Cancer 7:1602-1608.

Gorzalczany Y, Gilad Y, Amihai D, Hammel I, Sagi-Eisenberg R, Merimsky O (2011) Combining an EGFR directed tyrosine kinase inhibitor with autophagy-inducing drugs: a beneficial strategy to combat non-small cell lung cancer. Cancer letters 310:207-215.

Goussetis DJ, Altman JK, Glaser H, McNeer JL, Tallman MS, Platanias LC (2010) Autophagy is a critical mechanism for the induction of the antileukemic effects of arsenic trioxide. The Journal of biological chemistry 285:29989-29997.

Gschwind A, Fischer OM, Ullrich A (2004) The discovery of receptor tyrosine kinases: targets for cancer therapy. Nature reviews Cancer 4:361-370.

Guo JY, Chen HY, Mathew R, Fan J, Strohecker AM, Karsli-Uzunbas G, Kamphorst JJ, Chen G, Lemons JM, Karantza V, Coller HA, Dipaola RS, Gelinas C, Rabinowitz JD, White E (2011) Activated Ras requires autophagy to maintain oxidative metabolism and tumorigenesis. Genes & development 25:460-470.

Guo JY, Karsli-Uzunbas G, Mathew R, Aisner SC, Kamphorst JJ, Strohecker AM, Chen G, Price S, Lu W, Teng X, Snyder E, Santanam U, DiPaola RS, Jacks T, Rabinowitz JD, White E (2013) Autophagy suppresses progression of K-ras-induced lung tumors to oncocytomas and maintains lipid homeostasis. Genes & development 27:1447-1461.

Gwinn DM, Shackelford DB, Egan DF, Mihaylova MM, Mery A, Vasquez DS, Turk BE, Shaw RJ (2008) AMPK phosphorylation of raptor mediates a metabolic checkpoint. Molecular cell 30:214-226.

Han W, Pan H, Chen Y, Sun J, Wang Y, Li J, Ge W, Feng L, Lin X, Wang X, Wang X, Jin H (2011) EGFR tyrosine kinase inhibitors activate autophagy as a cytoprotective response in human lung cancer cells. PloS one 6:e18691.

Hanahan D, Weinberg RA (2011) Hallmarks of cancer: the next generation. Cell 144:646-674.

Hara T, Nakamura K, Matsui M, Yamamoto A, Nakahara Y, Suzuki-Migishima R, Yokoyama M, Mishima K, Saito I, Okano H, Mizushima N (2006) Suppression of basal autophagy in neural cells causes neurodegenerative disease in mice. Nature 441:885-889.

He C, Klionsky DJ (2009) Regulation mechanisms and signaling pathways of autophagy. Annual review of genetics 43:67-93.

He S, Zhao Z, Yang Y, O'Connell D, Zhang X, Oh S, Ma B, Lee J-H, Zhang T, Varghese B, Yip J, Dolatshahi Pirooz S, Li M, Zhang Y, Li G-M, Ellen Martin S, Machida K, Liang C (2015) Truncating mutation in the autophagy gene UVRAG confers oncogenic properties and chemosensitivity in colorectal cancers. Nat Commun 6.

Hecht JR, Mitchell E, Neubauer MA, Burris HA, 3rd, Swanson P, Lopez T, Buchanan G, Reiner M, Gansert J, Berlin J (2010) Lack of correlation between epidermal growth factor receptor status and response to Panitumumab monotherapy in metastatic colorectal cancer. Clinical cancer research : an official journal of the American Association for Cancer Research 16:2205-2213.

Helgason GV, Holyoake TL, Ryan KM (2013) Role of autophagy in cancer prevention, development and therapy. Essays In Biochemistry 55:133-151.

Hemmings BA, Restuccia DF (2012) PI3K-PKB/Akt Pathway. Cold Spring Harbor perspectives in biology 4.

Hosokawa N, Hara T, Kaizuka T, Kishi C, Takamura A, Miura Y, Iemura S-i, Natsume T, Takehana K, Yamada N, Guan J-L, Oshiro N, Mizushima N (2009) Nutrient-dependent mTORC1 Association with the ULK1–Atg13–FIP200 Complex Required for Autophagy. Molecular biology of the cell 20:1981-1991.

Humbert M, Medová M, Aebersold DM, Blaukat A, Bladt F, Fey MF, Zimmer Y, Tschan MP (2013) Protective autophagy is involved in resistance towards MET inhibitors in human gastric adenocarcinoma cells. Biochemical and Biophysical Research Communications 431:264-269.

Hynes NE, Lane HA (2005) ERBB receptors and cancer: the complexity of targeted inhibitors. Nature reviews Cancer 5:341-354.

Inami Y, Waguri S, Sakamoto A, Kouno T, Nakada K, Hino O, Watanabe S, Ando J, Iwadate M, Yamamoto M, Lee MS, Tanaka K, Komatsu M (2011) Persistent activation of Nrf2 through p62 in hepatocellular carcinoma cells. The Journal of cell biology 193:275-284.

Inno A, Di Salvatore M, Cenci T, Martini M, Orlandi A, Strippoli A, Ferrara AM, Bagala C, Cassano A, Larocca LM, Barone C (2011) Is there a role for IGF1R and c-MET pathways in resistance to cetuximab in metastatic colorectal cancer? Clinical colorectal cancer 10:325-332.

Issa JP (2004) CpG island methylator phenotype in cancer. Nature reviews Cancer 4:988-993.

Jhawer M, Goel S, Wilson AJ, Montagna C, Ling YH, Byun DS, Nasser S, Arango D, Shin J, Klampfer L, Augenlicht LH, Perez-Soler R, Mariadason JM (2008) PIK3CA mutation/PTEN expression status predicts response of colon cancer cells to the epidermal growth factor receptor inhibitor cetuximab. Cancer research 68:1953-1961.

Jones S, Cunningham DL, Rappoport JZ, Heath JK (2014) The non-receptor tyrosine kinase Ack1 regulates the fate of activated EGFR by inducing trafficking to the p62/NBR1 pre-autophagosome. Journal of cell science 127:994-1006.

Jung CH, Jun CB, Ro S-H, Kim Y-M, Otto NM, Cao J, Kundu M, Kim D-H (2009) ULK-Atg13-FIP200 Complexes Mediate mTOR Signaling to the Autophagy Machinery. Molecular biology of the cell 20:1992-2003.

Jutten B, Keulers TG, Schaaf MBE, Savelkouls K, Theys J, Span PN, Vooijs MA, Bussink J, Rouschop KMA (2013) EGFR overexpressing cells and tumors are dependent on autophagy for growth and survival. Radiotherapy and Oncology 108:479-483.

Kalvari I, Tsompanis S, Mulakkal NC, Osgood R, Johansen T, Nezis IP, Promponas VJ (2014) iLIR. Autophagy 10:913-925.

Kandouz M, Haidara K, Zhao J, Brisson M-L, Batist G (2010) The EphB2 tumor suppressor induces autophagic cell death via concomitant activation of the ERK1/2 and PI3K pathways. Cell cycle 9:398-407.

Kanzawa T, Kondo Y, Ito H, Kondo S, Germano I (2003) Induction of autophagic cell death in malignant glioma cells by arsenic trioxide. Cancer research 63:2103-2108.

Karantza-Wadsworth V, Patel S, Kravchuk O, Chen G, Mathew R, Jin S, White E (2007) Autophagy mitigates metabolic stress and genome damage in mammary tumorigenesis. Genes & development 21:1621-1635.

Karapetis CS, Jonker D, Daneshmand M, Hanson JE, O'Callaghan CJ, Marginean C, Zalcberg JR, Simes J, Moore MJ, Tebbutt NC, Price TJ, Shapiro JD, Pavlakis N, Gibbs P, Van Hazel GA, Lee U, Haq R, Virk S, Tu D, Lorimer IA, Group NCT, the Australasian Gastro-Intestinal Trials G (2014) PIK3CA, BRAF, and PTEN status and benefit from cetuximab in the treatment of advanced colorectal cancer--results from NCIC CTG/AGITG CO.17. Clinical cancer research : an official journal of the American Association for Cancer Research 20:744-753.

Karapetis CS, Khambata-Ford S, Jonker DJ, O'Callaghan CJ, Tu D, Tebbutt NC, Simes RJ, Chalchal H, Shapiro JD, Robitaille S, Price TJ, Shepherd L, Au HJ, Langer C, Moore MJ, Zalcberg JR (2008) K-ras mutations and benefit from cetuximab in advanced colorectal cancer. The New England journal of medicine 359:1757-1765.

Karnes WE, Jr., Weller SG, Adjei PN, Kottke TJ, Glenn KS, Gores GJ, Kaufmann SH (1998) Inhibition of epidermal growth factor receptor kinase induces protease-dependent apoptosis in human colon cancer cells. Gastroenterology 114:930-939.

Kermorgant S, Zicha D, Parker PJ (2004) PKC controls HGF-dependent c-Met traffic, signalling and cell migration. The EMBO journal 23:3721-3734.

Khambata-Ford S, Garrett CR, Meropol NJ, Basik M, Harbison CT, Wu S, Wong TW, Huang X, Takimoto CH, Godwin AK, Tan BR, Krishnamurthi SS, Burris HA, 3rd, Poplin EA, Hidalgo M, Baselga J, Clark EA, Mauro DJ (2007) Expression of epiregulin and amphiregulin and K-ras mutation status predict disease control in metastatic colorectal cancer patients treated with cetuximab. Journal of clinical oncology : official journal of the American Society of Clinical Oncology 25:3230-3237.

Kim J, Kundu M, Viollet B, Guan K-L (2011a) AMPK and mTOR regulate autophagy through direct phosphorylation of Ulk1. Nature cell biology 13:132-141.

Kim MJ, Woo SJ, Yoon CH, Lee JS, An S, Choi YH, Hwang SG, Yoon G, Lee SJ (2011b) Involvement of autophagy in oncogenic K-Ras-induced malignant cell transformation. The Journal of biological chemistry 286:12924-12932.

Kim Y-M, Jung Chang H, Seo M, Kim Eun K, Park J-M, Bae Sun S, Kim D-H (2015) mTORC1 Phosphorylates UVRAG to Negatively Regulate Autophagosome and Endosome Maturation. Molecular cell 57:207-218.

Kimmelman AC (2011) The dynamic nature of autophagy in cancer. Genes & development 25:1999-2010.

Kimura T, Takabatake Y, Takahashi A, Isaka Y (2013) Chloroquine in cancer therapy: a double-edged sword of autophagy. Cancer research 73:3-7.

Kingston RE, Chen CA, Okayama H (2001) Calcium Phosphate Transfection. In: Current Protocols in Neuroscience: John Wiley & Sons, Inc.

Klionsky DJ, Abdalla FC, Abeliovich H, Abraham RT, Acevedo-Arozena A, Adeli K, Agholme L, Agnello M, Agostinis P, Aguirre-Ghiso JA, Ahn HJ, Ait-Mohamed O, Ait-Si-Ali S, Akematsu T, Akira S, Al-Younes HM, Al-Zeer MA, Albert ML, Albin RL, Alegre-Abarrategui J, Aleo MF, Alirezaei M, Almasan A, Almonte-Becerril M, Amano A, Amaravadi R, Amarnath S, Amer AO, Andrieu-Abadie N, Anantharam V, Ann DK, Anoopkumar-Dukie S, Aoki H, Apostolova N, Arancia G, Aris JP, Asanuma K, Asare NY, Ashida H, Askanas V, Askew DS, Auberger P, Baba M, Backues SK, Baehrecke EH, Bahr BA, Bai XY, Bailly Y, Baiocchi R, Baldini G, Balduini W, Ballabio A, Bamber BA, Bampton ET, Banhegyi G, Bartholomew CR, Bassham DC, Bast RC, Jr., Batoko H, Bay BH, Beau I, Bechet DM, Begley TJ, Behl C, Behrends C, Bekri S, Bellaire B, Bendall LJ, Benetti L, Berliocchi L, Bernardi H, Bernassola F, Besteiro S, Bhatia-Kissova I, Bi X, Biard-Piechaczyk M, Blum JS, Boise LH, Bonaldo P, Boone DL, Bornhauser BC, Bortoluci KR, Bossis I, Bost F, Bourquin JP, Boya P, Boyer-Guittaut M, Bozhkov PV, Brady NR, Brancolini C, Brech A, Brenman JE, Brennand A, Bresnick EH, Brest P, Bridges D, Bristol ML, Brookes PS, Brown EJ, Brumell JH, Brunetti-Pierri N, Brunk UT, Bulman DE, Bultman SJ, Bultynck

G, Burbulla LF, Bursch W, Butchar JP, Buzgariu W, Bydlowski SP, Cadwell K, Cahova M, Cai D, Cai J, Cai Q, Calabretta B, Calvo-Garrido J, Camougrand N, Campanella M, Campos-Salinas J, Candi E, Cao L, Caplan AB, Carding SR, Cardoso SM, Carew JS, Carlin CR, Carmignac V, Carneiro LA, Carra S, Caruso RA, Casari G, Casas C, Castino R, Cebollero E, Cecconi F, Celli J, Chaachouay H, Chae HJ, Chai CY, Chan DC, Chan EY, Chang RC, Che CM, Chen CC, Chen GC, Chen GQ, Chen M, Chen Q, Chen SS, Chen W, Chen X, Chen X, Chen X, Chen YG, Chen Y, Chen Y, Chen YJ, Chen Z, Cheng A, Cheng CH, Cheng Y, Cheong H, Cheong JH, Cherry S, Chess-Williams R, Cheung ZH, Chevet E, Chiang HL, Chiarelli R, Chiba T, Chin LS, Chiou SH, Chisari FV, Cho CH, Cho DH, Choi AM, Choi D, Choi KS, Choi ME, Chouaib S, Choubey D, Choubey V, Chu CT, Chuang TH, Chueh SH, Chun T, Chwae YJ, Chye ML, Ciarcia R, Ciriolo MR, Clague MJ, Clark RS, Clarke PG, Clarke R, Codogno P, Coller HA, Colombo MI, Comincini S, Condello M, Condorelli F, Cookson MR, Coombs GH, Coppens I, Corbalan R, Cossart P, Costelli P, Costes S, Coto-Montes A, Couve E, Coxon FP, Cregg JM, Crespo JL, Cronje MJ, Cuervo AM, Cullen JJ, Czaja MJ, D'Amelio M, Darfeuille-Michaud A, Davids LM, Davies FE, De Felici M, de Groot JF, de Haan CA, De Martino L, De Milito A, De Tata V, Debnath J, Degterev A, Dehay B, Delbridge LM, Demarchi F, Deng YZ, Dengjel J, Dent P, Denton D, Deretic V, Desai SD, Devenish RJ, Di Gioacchino M, Di Paolo G, Di Pietro C, Diaz-Araya G, Diaz-Laviada I, Diaz-Meco MT, Diaz-Nido J, Dikic I, Dinesh-Kumar SP, Ding WX, Distelhorst CW, Diwan A, Djavaheri-Mergny M, Dokudovskaya S, Dong Z, Dorsey FC, Dosenko V, Dowling JJ, Doxsey S, Dreux M, Drew ME, Duan Q, Duchosal MA, Duff K, Dugail I, Durbeej M, Duszenko M, Edelstein CL, Edinger AL, Egea G, Eichinger L, Eissa NT, Ekmekcioglu S, El-Deiry WS, Elazar Z, Elgendy M, Ellerby LM, Eng KE, Engelbrecht AM, Engelender S, Erenpreisa J, Escalante R, Esclatine A, Eskelinen EL, Espert L, Espina V, Fan H, Fan J, Fan QW, Fan Z, Fang S, Fang Y, Fanto M, Fanzani A, Farkas T, Farre JC, Faure M, Fechheimer M, Feng CG, Feng J, Feng Q, Feng Y, Fesus L, Feuer R, Figueiredo-Pereira ME, Fimia GM, Fingar DC, Finkbeiner S, Finkel T, Finley KD, Fiorito F, Fisher EA, Fisher PB, Flajolet M, Florez-McClure ML, Florio S, Fon EA, Fornai F, Fortunato F, Fotedar R, Fowler DH, Fox HS, Franco R, Frankel LB, Fransen M, Fuentes JM, Fueyo J, Fujii J, Fujisaki K, Fujita E, Fukuda M, Furukawa RH, Gaestel M, Gailly P, Gajewska M, Galliot B, Galy V, Ganesh S, Ganetzky B, Ganley IG, Gao FB, Gao GF, Gao J, Garcia L, Garcia-Manero G, Garcia-Marcos M, Garmyn M, Gartel AL, Gatti E, Gautel M, Gawriluk TR, Gegg ME, Geng J, Germain M, Gestwicki JE, Gewirtz DA,

Ghavami S, Ghosh P, Giammarioli AM, Giatromanolaki AN, Gibson SB, Gilkerson RW, Ginger ML, Ginsberg HN, Golab J, Goligorsky MS, Golstein P, Gomez-Manzano C, Goncu E, Gongora C, Gonzalez CD, Gonzalez R, Gonzalez-Estevez C, Gonzalez-Polo RA, Gonzalez-Rey E, Gorbunov NV, Gorski S, Goruppi S, Gottlieb RA, Gozuacik D, Granato GE, Grant GD, Green KN, Gregorc A, Gros F, Grose C, Grunt TW, Gual P, Guan JL, Guan KL, Guichard SM, Gukovskaya AS, Gukovsky I, Gunst J, Gustafsson AB, Halayko AJ, Hale AN, Halonen SK, Hamasaki M, Han F, Han T, Hancock MK, Hansen M, Harada H, Harada M, Hardt SE, Harper JW, Harris AL, Harris J, Harris SD, Hashimoto M, Haspel JA, Hayashi S, Hazelhurst LA, He C, He YW, Hebert MJ, Heidenreich KA, Helfrich MH, Helgason GV, Henske EP, Herman B, Herman PK, Hetz C, Hilfiker S, Hill JA, Hocking LJ, Hofman P, Hofmann TG, Hohfeld J, Holyoake TL, Hong MH, Hood DA, Hotamisligil GS, Houwerzijl EJ, Hoyer-Hansen M, Hu B, Hu CA, Hu HM, Hua Y, Huang C, Huang J, Huang S, Huang WP, Huber TB, Huh WK, Hung TH, Hupp TR, Hur GM, Hurley JB, Hussain SN, Hussey PJ, Hwang JJ, Hwang S, Ichihara A, Ilkhanizadeh S, Inoki K, Into T, Iovane V, Iovanna JL, Ip NY, Isaka Y, Ishida H, Isidoro C, Isobe K, Iwasaki A, Izquierdo M, Izumi Y, Jaakkola PM, Jaattela M, Jackson GR, Jackson WT, Janji B, Jendrach M, Jeon JH, Jeung EB, Jiang H, Jiang H, Jiang JX, Jiang M, Jiang Q, Jiang X, Jiang X, Jimenez A, Jin M, Jin S, Joe CO, Johansen T, Johnson DE, Johnson GV, Jones NL, Joseph B, Joseph SK, Joubert AM, Juhasz G, Juillerat-Jeanneret L, Jung CH, Jung YK, Kaarniranta K, Kaasik A, Kabuta T, Kadowaki M, Kagedal K, Kamada Y, Kaminskyy VO, Kampinga HH, Kanamori H, Kang C, Kang KB, Kang KI, Kang R, Kang YA, Kanki T, Kanneganti TD, Kanno H, Kanthasamy AG, Kanthasamy A, Karantza V, Kaushal GP, Kaushik S, Kawazoe Y, Ke PY, Kehrl JH, Kelekar A, Kerkhoff C, Kessel DH, Khalil H, Kiel JA, Kiger AA, Kihara A, Kim DR, Kim DH, Kim DH, Kim EK, Kim HR, Kim JS, Kim JH, Kim JC, Kim JK, Kim PK, Kim SW, Kim YS, Kim Y, Kimchi A, Kimmelman AC, King JS, Kinsella TJ, Kirkin V, Kirshenbaum LA, Kitamoto K, Kitazato K, Klein L, Klimecki WT, Klucken J, Knecht E, Ko BC, Koch JC, Koga H, Koh JY, Koh YH, Koike M, Komatsu M, Kominami E, Kong HJ, Kong WJ, Korolchuk VI, Kotake Y, Koukourakis MI, Kouri Flores JB, Kovacs AL, Kraft C, Krainc D, Kramer H, Kretz-Remy C, Krichevsky AM, Kroemer G, Kruger R, Krut O, Ktistakis NT, Kuan CY, Kucharczyk R, Kumar A, Kumar R, Kumar S, Kundu M, Kung HJ, Kurz T, Kwon HJ, La Spada AR, Lafont F, Lamark T, Landry J, Lane JD, Lapaquette P, Laporte JF, Laszlo L, Lavandero S, Lavoie JN, Layfield R, Lazo PA, Le W, Le Cam L, Ledbetter DJ, Lee AJ, Lee BW, Lee GM, Lee J, Lee JH, Lee M, Lee MS, Lee SH,

Leeuwenburgh C, Legembre P, Legouis R, Lehmann M, Lei HY, Lei QY, Leib DA, Leiro J, Lemasters JJ, Lemoine A, Lesniak MS, Lev D, Levenson VV, Levine B, Levy E, Li F, Li JL, Li L, Li S, Li W, Li XJ, Li YB, Li YP, Liang C, Liang Q, Liao YF, Liberski PP, Lieberman A, Lim HJ, Lim KL, Lim K, Lin CF, Lin FC, Lin J, Lin JD, Lin K, Lin WW, Lin WC, Lin YL, Linden R, Lingor P, Lippincott-Schwartz J, Lisanti MP, Liton PB, Liu B, Liu CF, Liu K, Liu L, Liu QA, Liu W, Liu YC, Liu Y, Lockshin RA, Lok CN, Lonial S, Loos B, Lopez-Berestein G, Lopez-Otin C, Lossi L, Lotze MT, Low P, Lu B, Lu B, Lu B, Lu Z, Luciano F, Lukacs NW, Lund AH, Lynch-Day MA, Ma Y, Macian F, MacKeigan JP, Macleod KF, Madeo F, Maiuri L, Maiuri MC, Malagoli D, Malicdan MC, Malorni W, Man N, Mandelkow EM, Manon S, Manov I, Mao K, Mao X, Mao Z, Marambaud P, Marazziti D, Marcel YL, Marchbank K, Marchetti P, Marciniak SJ, Marcondes M, Mardi M, Marfe G, Marino G, Markaki M, Marten MR, Martin SJ, Martinand-Mari C, Martinet W, Martinez-Vicente M, Masini M, Matarrese P, Matsuo S, Matteoni R, Mayer A, Mazure NM, McConkey DJ, McConnell MJ, McDermott C, McDonald C, McInerney GM, McKenna SL, McLaughlin B, McLean PJ, McMaster CR, McQuibban GA, Meijer AJ, Meisler MH, Melendez A, Melia TJ, Melino G, Mena MA, Menendez JA, Menna-Barreto RF, Menon MB, Menzies FM, Mercer CA, Merighi A, Merry DE, Meschini S, Meyer CG, Meyer TF, Miao CY, Miao JY, Michels PA, Michiels C, Mijaljica D, Milojkovic A, Minucci S, Miracco C, Miranti CK, Mitroulis I, Miyazawa K, Mizushima N, Mograbi B, Mohseni S, Molero X, Mollereau B, Mollinedo F, Momoi T, Monastyrska I, Monick MM, Monteiro MJ, Moore MN, Mora R, Moreau K, Moreira PI, Moriyasu Y, Moscat J, Mostowy S, Mottram JC, Motyl T, Moussa CE, Muller S, Muller S, Munger K, Munz C, Murphy LO, Murphy ME, Musaro A, Mysorekar I, Nagata E, Nagata K, Nahimana A, Nair U, Nakagawa T, Nakahira K, Nakano H, Nakatogawa H, Nanjundan M, Naqvi NI, Narendra DP, Narita M, Navarro M, Nawrocki ST, Nazarko TY, Nemchenko A, Netea MG, Neufeld TP, Ney PA, Nezis IP, Nguyen HP, Nie D, Nishino I, Nislow C, Nixon RA, Noda T, Noegel AA, Nogalska A, Noguchi S, Notterpek L, Novak I, Nozaki T, Nukina N, Nurnberger T, Nyfeler B, Obara K, Oberley TD, Oddo S, Ogawa M, Ohashi T, Okamoto K, Oleinick NL, Oliver FJ, Olsen LJ, Olsson S, Opota O, Osborne TF, Ostrander GK, Otsu K, Ou JH, Ouimet M, Overholtzer M, Ozpolat B, Paganetti P, Pagnini U, Pallet N, Palmer GE, Palumbo C, Pan T, Panaretakis T, Pandey UB, Papackova Z, Papassideri I, Paris I, Park J, Park OK, Parys JB, Parzych KR, Patschan S, Patterson C, Pattingre S, Pawelek JM, Peng J, Perlmutter DH, Perrotta I, Perry G, Pervaiz S, Peter M, Peters GJ, Petersen M, Petrovski G, Phang JM, Piacentini M, Pierre P, Pierrefite-Carle V, Pierron G, Pinkas-

Kramarski R, Piras A, Piri N, Platanias LC, Poggeler S, Poirot M, Poletti A, Pous C, Pozuelo-Rubio M, Praetorius-Ibba M, Prasad A, Prescott M, Priault M, Produit-Zengaffinen N, Progulske-Fox A, Proikas-Cezanne T, Przedborski S, Przyklenk K, Puertollano R, Puyal J, Qian SB, Qin L, Qin ZH, Quaggin SE, Raben N, Rabinowich H, Rabkin SW, Rahman I, Rami A, Ramm G, Randall G, Randow F, Rao VA, Rathmell JC, Ravikumar B, Ray SK, Reed BH, Reed JC, Reggiori F, Regnier-Vigouroux A, Reichert AS, Reiners JJ, Jr., Reiter RJ, Ren J, Revuelta JL, Rhodes CJ, Ritis K, Rizzo E, Robbins J, Roberge M, Roca H, Roccheri MC, Rocchi S, Rodemann HP, Rodriguez de Cordoba S, Rohrer B, Roninson IB, Rosen K, Rost-Roszkowska MM, Rouis M, Rouschop KM, Rovetta F, Rubin BP, Rubinsztein DC, Ruckdeschel K, Rucker EB, 3rd, Rudich A, Rudolf E, Ruiz-Opazo N, Russo R, Rusten TE, Ryan KM, Ryter SW, Sabatini DM, Sadoshima J, Saha T, Saitoh T, Sakagami H, Sakai Y, Salekdeh GH, Salomoni P, Salvaterra PM, Salvesen G, Salvioli R, Sanchez AM, Sanchez-Alcazar JA, Sanchez-Prieto R, Sandri M, Sankar U, Sansanwal P, Santambrogio L, Saran S, Sarkar S, Sarwal M, Sasakawa C, Sasnauskiene A, Sass M, Sato K, Sato M, Schapira AH, Scharl M, Schatzl HM, Scheper W, Schiaffino S, Schneider C, Schneider ME, Schneider-Stock R, Schoenlein PV, Schorderet DF, Schuller C, Schwartz GK, Scorrano L, Sealy L, Seglen PO, Segura-Aguilar J, Seiliez I, Seleverstov O, Sell C, Seo JB, Separovic D, Setaluri V, Setoguchi T, Settembre C, Shacka JJ, Shanmugam M, Shapiro IM, Shaulian E, Shaw RJ, Shelhamer JH, Shen HM, Shen WC, Sheng ZH, Shi Y, Shibuya K, Shidoji Y, Shieh JJ, Shih CM, Shimada Y, Shimizu S, Shintani T, Shirihai OS, Shore GC, Sibirny AA, Sidhu SB, Sikorska B, Silva-Zacarin EC, Simmons A, Simon AK, Simon HU, Simone C, Simonsen A, Sinclair DA, Singh R, Sinha D, Sinicrope FA, Sirko A, Siu PM, Sivridis E, Skop V, Skulachev VP, Slack RS, Smaili SS, Smith DR, Soengas MS, Soldati T, Song X, Sood AK, Soong TW, Sotgia F, Spector SA, Spies CD, Springer W, Srinivasula SM, Stefanis L, Steffan JS, Stendel R, Stenmark H, Stephanou A, Stern ST, Sternberg C, Stork B, Stralfors P, Subauste CS, Sui X, Sulzer D, Sun J, Sun SY, Sun ZJ, Sung JJ, Suzuki K, Suzuki T, Swanson MS, Swanton C, Sweeney ST, Sy LK, Szabadkai G, Tabas I, Taegtmeyer H, Tafani M, Takacs-Vellai K, Takano Y, Takegawa K, Takemura G, Takeshita F, Talbot NJ, Tan KS, Tanaka K, Tanaka K, Tang D, Tang D, Tanida I, Tannous BA, Tavernarakis N, Taylor GS, Taylor GA, Taylor JP, Terada LS, Terman A, Tettamanti G, Thevissen K, Thompson CB, Thorburn A, Thumm M, Tian F, Tian Y, Tocchini-Valentini G, Tolkovsky AM, Tomino Y, Tonges L, Tooze SA, Tournier C, Tower J, Towns R, Trajkovic V, Travassos LH, Tsai TF, Tschan MP, Tsubata T, Tsung A, Turk B,

Turner LS, Tyagi SC, Uchiyama Y, Ueno T, Umekawa M, Umemiya-Shirafuji R, Unni VK, Vaccaro MI, Valente EM, Van den Berghe G, van der Klei IJ, van Doorn W, van Dyk LF, van Egmond M, van Grunsven LA, Vandenabeele P, Vandenberghe WP, Vanhorebeek I, Vaquero EC, Velasco G, Vellai T, Vicencio JM, Vierstra RD, Vila M, Vindis C, Viola G, Viscomi MT, Voitsekhovskaja OV, von Haefen C, Votruba M, Wada K, Wade-Martins R, Walker CL, Walsh CM, Walter J, Wan XB, Wang A, Wang C, Wang D, Wang F, Wang F, Wang G, Wang H, Wang HG, Wang HD, Wang J, Wang K, Wang M, Wang RC, Wang X, Wang X, Wang YJ, Wang Y, Wang Z, Wang ZC, Wang Z, Wansink DG, Ward DM, Watada H, Waters SL, Webster P, Wei L, Weihl CC, Weiss WA, Welford SM, Wen LP, Whitehouse CA, Whitton JL, Whitworth AJ, Wileman T, Wiley JW, Wilkinson S, Willbold D, Williams RL, Williamson PR, Wouters BG, Wu C, Wu DC, Wu WK, Wyttenbach A, Xavier RJ, Xi Z, Xia P, Xiao G, Xie Z, Xie Z, Xu DZ, Xu J, Xu L, Xu X, Yamamoto A, Yamamoto A, Yamashina S, Yamashita M, Yan X, Yanagida M, Yang DS, Yang E, Yang JM, Yang SY, Yang W, Yang WY, Yang Z, Yao MC, Yao TP, Yeganeh B, Yen WL, Yin JJ, Yin XM, Yoo OJ, Yoon G, Yoon SY, Yorimitsu T, Yoshikawa Y, Yoshimori T, Yoshimoto K, You HJ, Youle RJ, Younes A, Yu L, Yu L, Yu SW, Yu WH, Yuan ZM, Yue Z, Yun CH, Yuzaki M, Zabirnyk O, Silva-Zacarin E, Zacks D, Zacksenhaus E, Zaffaroni N, Zakeri Z, Zeh HJ, 3rd, Zeitlin SO, Zhang H, Zhang HL, Zhang J, Zhang JP, Zhang L, Zhang L, Zhang MY, Zhang XD, Zhao M, Zhao YF, Zhao Y, Zhao ZJ, Zheng X, Zhivotovsky B, Zhong Q, Zhou CZ, Zhu C, Zhu WG, Zhu XF, Zhu X, Zhu Y, Zoladek T, Zong WX, Zorzano A, Zschocke J, Zuckerbraun B (2012) Guidelines for the use and interpretation of assays for monitoring autophagy. Autophagy 8:445-544.

Klippel A, Reinhard C, Kavanaugh WM, Apell G, Escobedo MA, Williams LT (1996) Membrane localization of phosphatidylinositol 3-kinase is sufficient to activate multiple signal-transducing kinase pathways. Molecular and Cellular Biology 16:4117-4127.

Kroemer G, Marino G, Levine B (2010) Autophagy and the integrated stress response. Molecular cell 40:280-293.

Kuo Y-C, Huang K-Y, Yang C-H, Yang Y-S, Lee W-Y, Chiang C-W (2008) Regulation of Phosphorylation of Thr-308 of Akt, Cell Proliferation, and Survival by the B55α Regulatory Subunit Targeting of the Protein Phosphatase 2A Holoenzyme to Akt. Journal of Biological Chemistry 283:1882-1892.

Lamark T, Johansen T (2010) Autophagy: links with the proteasome. Current opinion in cell biology 22:192-198.

Lamorte L, Kamikura DM, Park M (2000) A switch from p130Cas/Crk to Gab1/Crk signaling correlates with anchorage independent growth and JNK activation in cells transformed by the Met receptor oncoprotein. Oncogene 19:5973-5981.

Laplante M, Sabatini David M (2012) mTOR Signaling in Growth Control and Disease. Cell 149:274-293.

Laurent-Puig P, Cayre A, Manceau G, Buc E, Bachet JB, Lecomte T, Rougier P, Lievre A, Landi B, Boige V, Ducreux M, Ychou M, Bibeau F, Bouche O, Reid J, Stone S, Penault-Llorca F (2009) Analysis of PTEN, BRAF, and EGFR status in determining benefit from cetuximab therapy in wild-type KRAS metastatic colon cancer. Journal of clinical oncology : official journal of the American Society of Clinical Oncology 27:5924-5930.

Lemmon MA, Schlessinger J (2010) Cell signaling by receptor tyrosine kinases. Cell 141:1117-1134.

Lemmon MA, Schlessinger J, Ferguson KM (2014) The EGFR family: not so prototypical receptor tyrosine kinases. Cold Spring Harbor perspectives in biology 6:a020768.

Lengauer C, Kinzler KW, Vogelstein B (1998) Genetic instabilities in human cancers. Nature 396:643-649.

Letourneux C, Rocher G, Porteu F (2006) B56-containing PP2A dephosphorylate ERK and their activity is controlled by the early gene IEX-1 and ERK. The EMBO journal 25:727-738.

Levi-Montalcini R (1952) Effects of mouse tumor transplantation on the nervous system. Annals of the New York Academy of Sciences 55:330-344.

Levy J, Cacheux W, Bara MA, L'Hermitte A, Lepage P, Fraudeau M, Trentesaux C, Lemarchand J, Durand A, Crain AM, Marchiol C, Renault G, Dumont F, Letourneur F, Delacre M, Schmitt A, Terris B, Perret C, Chamaillard M, Couty JP, Romagnolo B (2015) Intestinal inhibition of Atg7 prevents tumour initiation through a microbiome-influenced immune response and suppresses tumour growth. Nature cell biology 17:1062-1073.

Li C, Iida M, Dunn EF, Ghia AJ, Wheeler DL (2009) Nuclear EGFR contributes to acquired resistance to cetuximab. Oncogene 28:3801-3813.

Li J, Yang B, Zhou Q, Wu Y, Shang D, Guo Y, Song Z, Zheng Q, Xiong J (2013a) Autophagy promotes hepatocellular carcinoma cell invasion through activation of epithelial-mesenchymal transition. Carcinogenesis 34:1343-1351.

Li S, Schmitz KR, Jeffrey PD, Wiltzius JJ, Kussie P, Ferguson KM (2005) Structural basis for inhibition of the epidermal growth factor receptor by cetuximab. Cancer cell 7:301-311.

Li X, Fan Z (2010) The epidermal growth factor receptor antibody cetuximab induces autophagy in cancer cells by downregulating HIF-1alpha and Bcl-2 and activating the beclin 1/hVps34 complex. Cancer research 70:5942-5952.

Li X, Lu Y, Pan T, Fan Z (2010) Roles of autophagy in cetuximab-mediated cancer therapy against EGFR. Autophagy 6:1066-1077.

Li Y-y, Lam S-k, Mak JC-w, Zheng C-y, Ho JC-m (2013b) Erlotinib-induced autophagy in epidermal growth factor receptor mutated non-small cell lung cancer. Lung Cancer 81:354-361.

Liang XH, Jackson S, Seaman M, Brown K, Kempkes B, Hibshoosh H, Levine B (1999) Induction of autophagy and inhibition of tumorigenesis by beclin 1. Nature 402:672-676.

Lièvre A, Bachet J-B, Le Corre D, Boige V, Landi B, Emile J-F, Côté J-F, Tomasic G, Penna C, Ducreux M, Rougier P, Penault-Llorca F, Laurent-Puig P (2006) KRAS Mutation Status Is Predictive of Response to Cetuximab Therapy in Colorectal Cancer. Cancer research 66:3992-3995.

Lipinski MM, Hoffman G, Ng A, Zhou W, Py BF, Hsu E, Liu X, Eisenberg J, Liu J, Blenis J, Xavier RJ, Yuan J (2010) A genome-wide siRNA screen reveals multiple mTORC1 independent signaling pathways regulating autophagy under normal nutritional conditions. Developmental cell 18:1041-1052.

Liu B, Fang M, Schmidt M, Lu Y, Mendelsohn J, Fan Z (2000) Induction of apoptosis and activation of the caspase cascade by anti-EGF receptor monoclonal antibodies in DiFi human colon cancer cells do not involve the c-jun N-terminal kinase activity. British journal of cancer 82:1991-1999.

Liu EY, Xu N, O'Prey J, Lao LY, Joshi S, Long JS, O'Prey M, Croft DR, Beaumatin F, Baudot AD, Mrschtik M, Rosenfeldt M, Zhang Y, Gillespie DA, Ryan KM (2015) Loss of autophagy causes a synthetic lethal deficiency in DNA repair. Proceedings of the National Academy of Sciences 112:773-778.

Lock R, Roy S, Kenific CM, Su JS, Salas E, Ronen SM, Debnath J (2011) Autophagy facilitates glycolysis during Ras-mediated oncogenic transformation. Molecular biology of the cell 22:165-178.

Lu Z, Xu S, Joazeiro C, Cobb MH, Hunter T (2002) The PHD Domain of MEKK1 Acts as an E3 Ubiquitin Ligase and Mediates Ubiquitination and Degradation of ERK1/2. Molecular cell 9:945-956.

Luca T, Barresi V, Privitera G, Musso N, Caruso M, Condorelli DF, Castorina S (2014) In vitro combined treatment with cetuximab and trastuzumab inhibits growth of colon cancer cells. Cell proliferation 47:435-447.

Ma X-H, Piao S-F, Dey S, McAfee Q, Karakousis G, Villanueva J, Hart LS, Levi S, Hu J, Zhang G, Lazova R, Klump V, Pawelek JM, Xu X, Xu W, Schuchter LM,

Davies MA, Herlyn M, Winkler J, Koumenis C, Amaravadi RK (2014) Targeting ER stress–induced autophagy overcomes BRAF inhibitor resistance in melanoma. The Journal of clinical investigation 124:1406-1417.

Macintosh RL, Timpson P, Thorburn J, Anderson KI, Thorburn A, Ryan KM (2012) Inhibition of autophagy impairs tumor cell invasion in an organotypic model. Cell cycle 11:2022-2029.

Mahalingam D, Mita M, Sarantopoulos J, Wood L, Amaravadi RK, Davis LE, Mita AC, Curiel TJ, Espitia CM, Nawrocki ST, Giles FJ, Carew JS (2014) Combined autophagy and HDAC inhibition. Autophagy 10:1403-1414.

Mammucari C, Milan G, Romanello V, Masiero E, Rudolf R, Del Piccolo P, Burden SJ, Di Lisi R, Sandri C, Zhao J, Goldberg AL, Schiaffino S, Sandri M (2007) FoxO3 Controls Autophagy in Skeletal Muscle In Vivo. Cell metabolism 6:458-471.

Manne U, Shanmugam C, Katkoori VR, Bumpers HL, Grizzle WE (2010) Development and progression of colorectal neoplasia. Cancer biomarkers : section A of Disease markers 9:235-265.

Manning BD, Cantley LC (2007) AKT/PKB Signaling: Navigating Downstream. Cell 129:1261-1274.

Marino G, Niso-Santano M, Baehrecke EH, Kroemer G (2014) Self-consumption: the interplay of autophagy and apoptosis. Nature reviews Molecular cell biology 15:81-94.

Markowitz SD, Bertagnolli MM (2009) Molecular Basis of Colorectal Cancer. New England Journal of Medicine 361:2449-2460.

Maroun CR, Naujokas MA, Holgado-Madruga M, Wong AJ, Park M (2000) The Tyrosine Phosphatase SHP-2 Is Required for Sustained Activation of Extracellular Signal-Regulated Kinase and Epithelial Morphogenesis Downstream from the Met Receptor Tyrosine Kinase. Molecular and Cellular Biology 20:8513-8525.

Martin DDO, Beauchamp E, Berthiaume LG (2011) Post-translational myristoylation: Fat matters in cellular life and death. Biochimie 93:18-31.

Martinez-Lopez N, Athonvarangkul D, Mishall P, Sahu S, Singh R (2013) Autophagy proteins regulate ERK phosphorylation. Nat Commun 4.

Mathew R, Khor S, Hackett Sean R, Rabinowitz Joshua D, Perlman David H, White E (2014) Functional Role of Autophagy-Mediated Proteome Remodeling in Cell Survival Signaling and Innate Immunity. Molecular cell 55:916-930.

McGill GG, Haq R, Nishimura EK, Fisher DE (2006) c-Met Expression Is Regulated by Mitf in the Melanocyte Lineage. Journal of Biological Chemistry 281:10365-10373.

McKay MM, Morrison DK (2007) Integrating signals from RTKs to ERK/MAPK. Oncogene 26:3113-3121.

Mehrpour M, Esclatine A, Beau I, Codogno P (2010) Overview of macroautophagy regulation in mammalian cells. Cell research 20:748-762.

Ménard L, Parker PJ, Kermorgant S (2014) Receptor tyrosine kinase c-Met controls the cytoskeleton from different endosomes via different pathways. Nat Commun 5.

Mendoza MC, Er EE, Blenis J (2011) The Ras-ERK and PI3K-mTOR pathways: cross-talk and compensation. Trends in biochemical sciences 36:320-328.

Michaud M, Martins I, Sukkurwala AQ, Adjemian S, Ma Y, Pellegatti P, Shen S, Kepp O, Scoazec M, Mignot G, Rello-Varona S, Tailler M, Menger L, Vacchelli E, Galluzzi L, Ghiringhelli F, di Virgilio F, Zitvogel L, Kroemer G (2011) Autophagy-Dependent Anticancer Immune Responses Induced by Chemotherapeutic Agents in Mice. Science 334:1573-1577.

Mijaljica D, Prescott M, Devenish RJ (2011) Microautophagy in mammalian cells: Revisiting a 40-year-old conundrum. Autophagy 7:673-682.

Misale S, Di Nicolantonio F, Sartore-Bianchi A, Siena S, Bardelli A (2014) Resistance to Anti-EGFR Therapy in Colorectal Cancer: From Heterogeneity to Convergent Evolution. Cancer discovery 4:1269-1280.

Misale S, Yaeger R, Hobor S, Scala E, Janakiraman M, Liska D, Valtorta E, Schiavo R, Buscarino M, Siravegna G, Bencardino K, Cercek A, Chen CT, Veronese S, Zanon C, Sartore-Bianchi A, Gambacorta M, Gallicchio M, Vakiani E, Boscaro V, Medico E, Weiser M, Siena S, Di Nicolantonio F, Solit D, Bardelli A (2012) Emergence of KRAS mutations and acquired resistance to anti-EGFR therapy in colorectal cancer. Nature 486:532-536.

Mizushima N (2007) Autophagy: process and function. Genes & development 21:2861-2873.

Mizushima N, Komatsu M (2011) Autophagy: renovation of cells and tissues. Cell 147:728-741.

Mizushima N, Levine B, Cuervo AM, Klionsky DJ (2008) Autophagy fights disease through cellular self-digestion. Nature 451:1069-1075.

Mohankumar KM, Currle DS, White E, Boulos N, Dapper J, Eden C, Nimmervoll B, Thiruvenkatam R, Connelly M, Kranenburg TA, Neale G, Olsen S, Wang YD, Finkelstein D, Wright K, Gupta K, Ellison DW, Thomas AO, Gilbertson RJ (2015) An in vivo screen identifies ependymoma oncogenes and tumor-suppressor genes. Nature genetics 47:878-887.

Montagut C, Dalmases A, Bellosillo B, Crespo M, Pairet S, Iglesias M, Salido M, Gallen M, Marsters S, Tsai SP, Minoche A, Seshagiri S, Serrano S,

Himmelbauer H, Bellmunt J, Rovira A, Settleman J, Bosch F, Albanell J (2012) Identification of a mutation in the extracellular domain of the Epidermal Growth Factor Receptor conferring cetuximab resistance in colorectal cancer. Nature medicine 18:221-223.

Moroni M, Veronese S, Benvenuti S, Marrapese G, Sartore-Bianchi A, Di Nicolantonio F, Gambacorta M, Siena S, Bardelli A (2005) Gene copy number for epidermal growth factor receptor (EGFR) and clinical response to antiEGFR treatment in colorectal cancer: a cohort study. The lancet oncology 6:279-286.

Nakai A, Yamaguchi O, Takeda T, Higuchi Y, Hikoso S, Taniike M, Omiya S, Mizote I, Matsumura Y, Asahi M, Nishida K, Hori M, Mizushima N, Otsu K (2007) The role of autophagy in cardiomyocytes in the basal state and in response to hemodynamic stress. Nature medicine 13:619-624.

Noguchi M, Hirata N, Suizu F (2014) The links between AKT and two intracellular proteolytic cascades: Ubiquitination and autophagy. Biochimica et Biophysica Acta (BBA) - Reviews on Cancer 1846:342-352.

Ogier-Denis E, Pattingre S, El Benna J, Codogno P (2000) Erk1/2-dependent Phosphorylation of Gα-interacting Protein Stimulates Its GTPase Accelerating Activity and Autophagy in Human Colon Cancer Cells. Journal of Biological Chemistry 275:39090-39095.

Ohsumi Y (2014) Historical landmarks of autophagy research. Cell research 24:9-23.

Olive M, Untawale S, Coffey RJ, Siciliano MJ, Wildrick DM, Fritsche H, Pathak S, Cherry LM, Blick M, Lointier P, Roubein LD, Levin B, Boman BM (1993) Characterization of the DiFi Rectal Carcinoma Cell Line Derived from a Familial Adenomatous Polyposis Patient. In Vitro Cellular & Developmental Biology 29A:239-248.

Pandey UB, Nie Z, Batlevi Y, McCray BA, Ritson GP, Nedelsky NB, Schwartz SL, DiProspero NA, Knight MA, Schuldiner O, Padmanabhan R, Hild M, Berry DL, Garza D, Hubbert CC, Yao T-P, Baehrecke EH, Taylor JP (2007) HDAC6 rescues neurodegeneration and provides an essential link between autophagy and the UPS. Nature 447:860-864.

Park S, Chapuis N, Bardet V, Tamburini J, Gallay N, Willems L, Knight ZA, Shokat KM, Azar N, Viguie F, Ifrah N, Dreyfus F, Mayeux P, Lacombe C, Bouscary D (2008) PI-103, a dual inhibitor of Class IA phosphatidylinositide 3-kinase and mTOR, has antileukemic activity in AML. Leukemia 22:1698-1706.

Pattingre S, Bauvy C, Codogno P (2003) Amino Acids Interfere with the ERK1/2-dependent Control of Macroautophagy by Controlling the Activation of Raf-1 in Human Colon Cancer HT-29 Cells. Journal of Biological Chemistry 278:16667-16674.

Pelicci G, Giordano S, Zhen Z, Salcini AE, Lanfrancone L, Bardelli A, Panayotou G, Waterfield MD, Ponzetto C, Pelicci PG, *et al*. (1995) The motogenic and mitogenic responses to HGF are amplified by the Shc adaptor protein. Oncogene 10:1631-1638.

Pentheroudakis G, Kotoula V, De Roock W, Kouvatseas G, Papakostas P, Makatsoris T, Papamichael D, Xanthakis I, Sgouros J, Televantou D, Kafiri G, Tsamandas AC, Razis E, Galani E, Bafaloukos D, Efstratiou I, Bompolaki I, Pectasides D, Pavlidis N, Tejpar S, Fountzilas G (2013) Biomarkers of benefit from cetuximab-based therapy in metastatic colorectal cancer: interaction of EGFR ligand expression with RAS/RAF, PIK3CA genotypes. BMC cancer 13:49.

Perera RM, Stoykova S, Nicolay BN, Ross KN, Fitamant J, Boukhali M, Lengrand J, Deshpande V, Selig MK, Ferrone CR, Settleman J, Stephanopoulos G, Dyson NJ, Zoncu R, Ramaswamy S, Haas W, Bardeesy N (2015) Transcriptional control of autophagy-lysosome function drives pancreatic cancer metabolism. Nature 524:361-365.

Pérez-Vargas JCS, Biondani P, Maggi C, Gariboldi M, Gloghini A, Inno A, Volpi CC, Gualeni AV, di Bartolomeo M, de Braud F, Castano A, Bossi I, Pietrantonio F (2013) Role of cMET in the Development and Progression of Colorectal Cancer. International Journal of Molecular Sciences 14:18056-18077.

Peruzzi B, Bottaro DP (2006) Targeting the c-Met Signaling Pathway in Cancer. Clinical Cancer Research 12:3657-3660.

Ponzetto C, Bardelli A, Zhen Z, Maina F, dalla Zonca P, Giordano S, Graziani A, Panayotou G, Comoglio PM (1994) A multifunctional docking site mediates signaling and transformation by the hepatocyte growth factor/scatter factor receptor family. Cell 77:261-271.

Qu X, Yu J, Bhagat G, Furuya N, Hibshoosh H, Troxel A, Rosen J, Eskelinen EL, Mizushima N, Ohsumi Y, Cattoretti G, Levine B (2003) Promotion of tumorigenesis by heterozygous disruption of the beclin 1 autophagy gene. The Journal of clinical investigation 112:1809-1820.

Rabinowitz JD, White E (2010) Autophagy and Metabolism. Science (New York, NY) 330:1344-1348.

Rangwala R, Chang YC, Hu J, Algazy KM, Evans TL, Fecher LA, Schuchter LM, Torigian DA, Panosian JT, Troxel AB, Tan K-S, Heitjan DF, DeMichele AM, Vaughn DJ, Redlinger M, Alavi A, Kaiser J, Pontiggia L, Davis LE, O'Dwyer PJ, Amaravadi RK (2014a) Combined MTOR and autophagy inhibition. Autophagy 10:1391-1402.

Rangwala R, Leone R, Chang YC, Fecher LA, Schuchter LM, Kramer A, Tan K-S, Heitjan DF, Rodgers G, Gallagher M, Piao S, Troxel AB, Evans TL, DeMichele

AM, Nathanson KL, O'Dwyer PJ, Kaiser J, Pontiggia L, Davis LE, Amaravadi RK (2014b) Phase I trial of hydroxychloroquine with dose-intense temozolomide in patients with advanced solid tumors and melanoma. Autophagy 10:1369-1379.

Rao S, Tortola L, Perlot T, Wirnsberger G, Novatchkova M, Nitsch R, Sykacek P, Frank L, Schramek D, Komnenovic V, Sigl V, Aumayr K, Schmauss G, Fellner N, Handschuh S, Glösmann M, Pasierbek P, Schlederer M, Resch GP, Ma Y, Yang H, Popper H, Kenner L, Kroemer G, Penninger JM (2014) A dual role for autophagy in a murine model of lung cancer. Nat Commun 5.

Ravikumar B, Sarkar S, Davies JE, Futter M, Garcia-Arencibia M, Green-Thompson ZW, Jimenez-Sanchez M, Korolchuk VI, Lichtenberg M, Luo S, Massey DC, Menzies FM, Moreau K, Narayanan U, Renna M, Siddiqi FH, Underwood BR, Winslow AR, Rubinsztein DC (2010) Regulation of mammalian autophagy in physiology and pathophysiology. Physiological reviews 90:1383-1435.

Rebecca VW, Amaravadi RK (2015) Emerging strategies to effectively target autophagy in cancer. Oncogene.

Renna M, Bento CF, Fleming A, Menzies FM, Siddiqi FH, Ravikumar B, Puri C, Garcia-Arencibia M, Sadiq O, Corrochano S, Carter S, Brown SD, Acevedo-Arozena A, Rubinsztein DC (2013) IGF-1 receptor antagonism inhibits autophagy. Human molecular genetics 22:4528-4544.

Roberts PJ, Der CJ (2007) Targeting the Raf-MEK-ERK mitogen-activated protein kinase cascade for the treatment of cancer. Oncogene 26:3291-3310.

Rojas M, Yao S, Lin YZ (1996) Controlling epidermal growth factor (EGF)-stimulated Ras activation in intact cells by a cell-permeable peptide mimicking phosphorylated EGF receptor. The Journal of biological chemistry 271:27456-27461.

Ronan B, Flamand O, Vescovi L, Dureuil C, Durand L, Fassy F, Bachelot M-F, Lamberton A, Mathieu M, Bertrand T, Marquette J-P, El-Ahmad Y, Filoche-Romme B, Schio L, Garcia-Echeverria C, Goulaouic H, Pasquier B (2014) A highly potent and selective Vps34 inhibitor alters vesicle trafficking and autophagy. Nat Chem Biol 10:1013-1019.

Rosenfeld MR, Ye X, Supko JG, Desideri S, Grossman SA, Brem S, Mikkelson T, Wang D, Chang YC, Hu J, McAfee Q, Fisher J, Troxel AB, Piao S, Heitjan DF, Tan K-S, Pontiggia L, O'Dwyer PJ, Davis LE, Amaravadi RK (2014) A phase I/II trial of hydroxychloroquine in conjunction with radiation therapy and concurrent and adjuvant temozolomide in patients with newly diagnosed glioblastoma multiforme. Autophagy 10:1359-1368.

Rosenfeldt MT, O'Prey J, Morton JP, Nixon C, MacKay G, Mrowinska A, Au A, Rai TS, Zheng L, Ridgway R, Adams PD, Anderson KI, Gottlieb E, Sansom OJ, Ryan KM (2013) p53 status determines the role of autophagy in pancreatic tumour development. Nature 504:296-300.

Rosenfeldt MT, Ryan KM (2011) The multiple roles of autophagy in cancer. Carcinogenesis 32:955-963.

Rubinsztein DC, Shpilka T, Elazar Z (2012) Mechanisms of autophagosome biogenesis. Current biology : CB 22:R29-34.

Russell RC, Yuan HX, Guan KL (2014) Autophagy regulation by nutrient signaling. Cell research 24:42-57.

Samuels Y, Diaz Jr LA, Schmidt-Kittler O, Cummins JM, DeLong L, Cheong I, Rago C, Huso DL, Lengauer C, Kinzler KW, Vogelstein B, Velculescu VE (2005) Mutant PIK3CA promotes cell growth and invasion of human cancer cells. Cancer cell 7:561-573.

Samuels Y, Wang Z, Bardelli A, Silliman N, Ptak J, Szabo S, Yan H, Gazdar A, Powell SM, Riggins GJ, Willson JK, Markowitz S, Kinzler KW, Vogelstein B, Velculescu VE (2004) High frequency of mutations of the PIK3CA gene in human cancers. Science 304:554.

Sancak Y, Bar-Peled L, Zoncu R, Markhard AL, Nada S, Sabatini DM (2010) Ragulator-Rag Complex Targets mTORC1 to the Lysosomal Surface and Is Necessary for Its Activation by Amino Acids. Cell 141:290-303.

Sancak Y, Peterson TR, Shaul YD, Lindquist RA, Thoreen CC, Bar-Peled L, Sabatini DM (2008) The Rag GTPases Bind Raptor and Mediate Amino Acid Signaling to mTORC1. Science 320:1496-1501.

Sandilands E, Serrels B, Wilkinson S, Frame MC (2012) Src-dependent autophagic degradation of Ret in FAK-signalling-defective cancer cells. EMBO reports 13:733-740.

Sangwan V, Paliouras GN, Abella JV, Dubé N, Monast A, Tremblay ML, Park M (2008) Regulation of the Met Receptor-tyrosine Kinase by the Protein-tyrosine Phosphatase 1B and T-cell Phosphatase. Journal of Biological Chemistry 283:34374-34383.

Sarkar S (2013) Regulation of autophagy by mTOR-dependent and mTOR-independent pathways: autophagy dysfunction in neurodegenerative diseases and therapeutic application of autophagy enhancers. Biochemical Society transactions 41:1103-1130.

Sarkar S, Floto RA, Berger Z, Imarisio S, Cordenier A, Pasco M, Cook LJ, Rubinsztein DC (2005) Lithium induces autophagy by inhibiting inositol monophosphatase. The Journal of cell biology 170:1101-1111.

Sartore-Bianchi A, Bencardino K, Cassingena A, Venturini F, Funaioli C, Cipani T, Amatu A, Pietrogiovanna L, Schiavo R, Di Nicolantonio F, Artale S, Bardelli A, Siena S (2010) Therapeutic implications of resistance to molecular therapies in metastatic colorectal cancer. Cancer treatment reviews 36 Suppl 3:S1-5.

Schlessinger J (2000) Cell Signaling by Receptor Tyrosine Kinases. Cell 103:211-225.

Schlessinger J (2014) Receptor tyrosine kinases: legacy of the first two decades. Cold Spring Harbor perspectives in biology 6.

Selvakumaran M, Amaravadi RK, Vasilevskaya IA, O'Dwyer PJ (2013) Autophagy inhibition sensitizes colon cancer cells to antiangiogenic and cytotoxic therapy. Clinical cancer research : an official journal of the American Association for Cancer Research 19:2995-3007.

Shchors K, Massaras A, Hanahan D (2015) Dual Targeting of the Autophagic Regulatory Circuitry in Gliomas with Repurposed Drugs Elicits Cell-Lethal Autophagy and Therapeutic Benefit. Cancer cell 28:456-471.

Shia J, Klimstra DS, Li AR, Qin J, Saltz L, Teruya-Feldstein J, Akram M, Chung KY, Yao D, Paty PB, Gerald W, Chen B (2005) Epidermal growth factor receptor expression and gene amplification in colorectal carcinoma: an immunohistochemical and chromogenic in situ hybridization study. Modern pathology : an official journal of the United States and Canadian Academy of Pathology, Inc 18:1350-1356.

Shibutani ST, Yoshimori T (2014) A current perspective of autophagosome biogenesis. Cell research 24:58-68.

Shimizu S, Kanaseki T, Mizushima N, Mizuta T, Arakawa-Kobayashi S, Thompson CB, Tsujimoto Y (2004) Role of Bcl-2 family proteins in a non-apoptotic programmed cell death dependent on autophagy genes. Nature cell biology 6:1221-1228.

Singh R, Cuervo AM (2011) Autophagy in the cellular energetic balance. Cell metabolism 13:495-504.

Solomon VR, Lee H (2009) Chloroquine and its analogs: a new promise of an old drug for effective and safe cancer therapies. European journal of pharmacology 625:220-233.

Sontag E (2001) Protein phosphatase 2A: the Trojan Horse of cellular signaling. Cellular signalling 13:7-16.

Strohecker AM, Guo JY, Karsli-Uzunbas G, Price SM, Chen GJ, Mathew R, McMahon M, White E (2013) Autophagy Sustains Mitochondrial Glutamine Metabolism and Growth of BrafV600E–Driven Lung Tumors. Cancer discovery 3:1272-1285.

Takamura A, Komatsu M, Hara T, Sakamoto A, Kishi C, Waguri S, Eishi Y, Hino O, Tanaka K, Mizushima N (2011) Autophagy-deficient mice develop multiple liver tumors. Genes & development 25:795-800.

Takeuchi H, Bilchik A, Saha S, Turner R, Wiese D, Tanaka M, Kuo C, Wang H-J, Hoon DSB (2003) c-MET Expression Level in Primary Colon Cancer: A Predictor of Tumor Invasion and Lymph Node Metastases. Clinical Cancer Research 9:1480-1488.

Tan X, Thapa N, Sun Y, Anderson Richard A (2015) A Kinase-Independent Role for EGF Receptor in Autophagy Initiation. Cell 160:145-160.

Tang MC, Wu MY, Hwang MH, Chang YT, Huang HJ, Lin AM, Yang JC (2015) Chloroquine enhances gefitinib cytotoxicity in gefitinib-resistant nonsmall cell lung cancer cells. PloS one 10:e0119135.

Tennant DA, Duran RV, Gottlieb E (2010) Targeting metabolic transformation for cancer therapy. Nature reviews Cancer 10:267-277.

Tooze SA, Yoshimori T (2010) The origin of the autophagosomal membrane. Nature cell biology 12:831-835.

Torre LA, Bray F, Siegel RL, Ferlay J, Lortet-Tieulent J, Jemal A (2015) Global cancer statistics, 2012. CA: a cancer journal for clinicians 65:87-108.

Trusolino L, Bertotti A, Comoglio PM (2010) MET signalling: principles and functions in development, organ regeneration and cancer. Nature reviews Molecular cell biology 11:834-848.

Tsuda M, Davis IJ, Argani P, Shukla N, McGill GG, Nagai M, Saito T, Laé M, Fisher DE, Ladanyi M (2007) TFE3 Fusions Activate MET Signaling by Transcriptional Up-regulation, Defining Another Class of Tumors as Candidates for Therapeutic MET Inhibition. Cancer research 67:919-929.

Untawale S, Zorbas MA, Hodgson CP, Coffey RJ, Gallick GE, North SM, Wildrick DM, Olive M, Blick M, Yeoman LC, *et al*. (1993) Transforming growth factor-alpha production and autoinduction in a colorectal carcinoma cell line (DiFi) with an amplified epidermal growth factor receptor gene. Cancer research 53:1630-1636.

Urosevic J, Garcia-Albéniz X, Planet E, Real S, Céspedes MV, Guiu M, Fernandez E, Bellmunt A, Gawrzak S, Pavlovic M, Mangues R, Dolado I, Barriga FM, Nadal C, Kemeny N, Batlle E, Nebreda AR, Gomis RR (2014) Colon cancer cells colonize the lung from established liver metastases through p38 MAPK signalling and PTHLH. Nature cell biology 16:685-694.

Valtorta E, Misale S, Sartore-Bianchi A, Nagtegaal ID, Paraf F, Lauricella C, Dimartino V, Hobor S, Jacobs B, Ercolani C, Lamba S, Scala E, Veronese S, Laurent-Puig P, Siena S, Tejpar S, Mottolese M, Punt CJ, Gambacorta M, Bardelli A, Di

Nicolantonio F (2013) KRAS gene amplification in colorectal cancer and impact on response to EGFR-targeted therapy. International journal of cancer Journal international du cancer 133:1259-1265.

van Houdt WJ, Hoogwater FJH, de Bruijn MT, Emmink BL, Nijkamp MW, Raats DAE, van der Groep P, van Diest P, Borel Rinkes IHM, Kranenburg O (2010) Oncogenic KRAS Desensitizes Colorectal Tumor Cells to Epidermal Growth Factor Receptor Inhibition and Activation. Neoplasia (New York, NY) 12:443-452.

Vanhaesebroeck B, Guillermet-Guibert J, Graupera M, Bilanges B (2010) The emerging mechanisms of isoform-specific PI3K signalling. Nature reviews Molecular cell biology 11:329-341.

Vaughn CP, Zobell SD, Furtado LV, Baker CL, Samowitz WS (2011) Frequency of KRAS, BRAF, and NRAS mutations in colorectal cancer. Genes, chromosomes & cancer 50:307-312.

Vázquez M, Ariz U, Varela-Rey M, Embade N, Martínez N, Fernández D, Gómez L, Lamas S, Lu SC, Martínez-Chantar ML, Mato JM (2009) Evidence for an LKB1/AMPK/eNOS Cascade Regulated by HGF, S-Adenosylmethionine and NO in Hepatocyte Proliferation. Hepatology (Baltimore, Md) 49:608-617.

Vichai V, Kirtikara K (2006) Sulforhodamine B colorimetric assay for cytotoxicity screening. Nature protocols 1:1112-1116.

Vincenzi B, Schiavon G, Silletta M, Santini D, Tonini G (2008) The biological properties of cetuximab. Critical reviews in oncology/hematology 68:93-106.

Vlacich G, Coffey RJ (2011) Resistance to EGFR-targeted therapy: a family affair. Cancer cell 20:423-425.

Vogelstein B, Papadopoulos N, Velculescu VE, Zhou S, Diaz LA, Kinzler KW (2013) Cancer Genome Landscapes. Science 339:1546-1558.

Voss V, Senft C, Lang V, Ronellenfitsch MW, Steinbach JP, Seifert V, Kogel D (2010) The pan-Bcl-2 inhibitor (-)-gossypol triggers autophagic cell death in malignant glioma. Molecular cancer research : MCR 8:1002-1016.

Wakatsuki S, Saitoh F, Araki T (2011) ZNRF1 promotes Wallerian degeneration by degrading AKT to induce GSK3B-dependent CRMP2 phosphorylation. Nature cell biology 13:1415-1423.

Wang J, Whiteman MW, Lian H, Wang G, Singh A, Huang D, Denmark T (2009) A Non-canonical MEK/ERK Signaling Pathway Regulates Autophagy via Regulating Beclin 1. The Journal of biological chemistry 284:21412-21424.

Wang RC, Wei Y, An Z, Zou Z, Xiao G, Bhagat G, White M, Reichelt J, Levine B (2012) Akt-Mediated Regulation of Autophagy and Tumorigenesis Through Beclin 1 Phosphorylation. Science 338:956-959.

Wang XJ, Yu J, Wong SH, Cheng ASL, Chan FKL, Ng SSM, Cho CH, Sung JJY, Wu WKK (2013) A novel crosstalk between two major protein degradation systems. Autophagy 9:1500-1508.

Wee S, Wiederschain D, Maira SM, Loo A, Miller C, deBeaumont R, Stegmeier F, Yao YM, Lengauer C (2008) PTEN-deficient cancers depend on PIK3CB. Proceedings of the National Academy of Sciences of the United States of America 105:13057-13062.

Wei Y, Pattingre S, Sinha S, Bassik M, Levine B (2008) JNK1-Mediated Phosphorylation of Bcl-2 Regulates Starvation-Induced Autophagy. Molecular cell 30:678-688.

Wei Y, Zou Z, Becker N, Anderson M, Sumpter R, Xiao G, Kinch L, Koduru P, Christudass Christhunesa S, Veltri Robert W, Grishin Nick V, Peyton M, Minna J, Bhagat G, Levine B (2013) EGFR-Mediated Beclin 1 Phosphorylation in Autophagy Suppression, Tumor Progression, and Tumor Chemoresistance. Cell 154:1269-1284.

White E (2012) Deconvoluting the context-dependent role for autophagy in cancer. Nature reviews Cancer 12:401-410.

Wiederschain D, Wee S, Chen L, Loo A, Yang G, Huang A, Chen Y, Caponigro G, Yao YM, Lengauer C, Sellers WR, Benson JD (2009) Single-vector inducible lentiviral RNAi system for oncology target validation. Cell cycle 8:498-504.

Williams A, Sarkar S, Cuddon P, Ttofi EK, Saiki S, Siddiqi FH, Jahreiss L, Fleming A, Pask D, Goldsmith P, O'Kane CJ, Floto RA, Rubinsztein DC (2008) Novel targets for Huntington's disease in an mTOR-independent autophagy pathway. Nat Chem Biol 4:295-305.

Wolpin BM, Rubinson DA, Wang X, Chan JA, Cleary JM, Enzinger PC, Fuchs CS, McCleary NJ, Meyerhardt JA, Ng K, Schrag D, Sikora AL, Spicer BA, Killion L, Mamon H, Kimmelman AC (2014) Phase II and Pharmacodynamic Study of Autophagy Inhibition Using Hydroxychloroquine in Patients With Metastatic Pancreatic Adenocarcinoma. The Oncologist 19:637-638.

Wu Y-T, Ouyang W, Lazorchak AS, Liu D, Shen H-M, Su B (2011) mTOR Complex 2 Targets Akt for Proteasomal Degradation via Phosphorylation at the Hydrophobic Motif. Journal of Biological Chemistry 286:14190-14198.

Xiao G-H, Jeffers M, Bellacosa A, Mitsuuchi Y, Vande Woude GF, Testa JR (2001) Anti-apoptotic signaling by hepatocyte growth factor/Met via the phosphatidylinositol 3-kinase/Akt and mitogen-activated protein kinase pathways. Proceedings of the National Academy of Sciences of the United States of America 98:247-252.

Yang A, Rajeshkumar NV, Wang X, Yabuuchi S, Alexander BM, Chu GC, Von Hoff DD, Maitra A, Kimmelman AC (2014) Autophagy is critical for pancreatic tumor growth and progression in tumors with p53 alterations. Cancer discovery 4:905-913.

Yang S, Wang X, Contino G, Liesa M, Sahin E, Ying H, Bause A, Li Y, Stommel JM, Dell'antonio G, Mautner J, Tonon G, Haigis M, Shirihai OS, Doglioni C, Bardeesy N, Kimmelman AC (2011a) Pancreatic cancers require autophagy for tumor growth. Genes & development 25:717-729.

Yang YP, Hu LF, Zheng HF, Mao CJ, Hu WD, Xiong KP, Wang F, Liu CF (2013) Application and interpretation of current autophagy inhibitors and activators. Acta pharmacologica Sinica 34:625-635.

Yang Z, Klionsky DJ (2010) Mammalian autophagy: core molecular machinery and signaling regulation. Current opinion in cell biology 22:124-131.

Yang ZJ, Chee CE, Huang S, Sinicrope FA (2011b) The role of autophagy in cancer: therapeutic implications. Molecular cancer therapeutics 10:1533-1541.

Ye Q, Cai W, Zheng Y, Evers BM, She Q-B (2014) ERK and AKT signaling cooperate to translationally regulate survivin expression for metastatic progression of colorectal cancer. Oncogene 33:1828-1839.

Yonesaka K, Zejnullahu K, Okamoto I, Satoh T, Cappuzzo F, Souglakos J, Ercan D, Rogers A, Roncalli M, Takeda M, Fujisaka Y, Philips J, Shimizu T, Maenishi O, Cho Y, Sun J, Destro A, Taira K, Takeda K, Okabe T, Swanson J, Itoh H, Takada M, Lifshits E, Okuno K, Engelman JA, Shivdasani RA, Nishio K, Fukuoka M, Varella-Garcia M, Nakagawa K, Janne PA (2011) Activation of ERBB2 signaling causes resistance to the EGFR-directed therapeutic antibody cetuximab. Science translational medicine 3:99ra86.

Young AR, Narita M, Ferreira M, Kirschner K, Sadaie M, Darot JF, Tavare S, Arakawa S, Shimizu S, Watt FM, Narita M (2009) Autophagy mediates the mitotic senescence transition. Genes & development 23:798-803.

Zandi R, Larsen AB, Andersen P, Stockhausen MT, Poulsen HS (2007) Mechanisms for oncogenic activation of the epidermal growth factor receptor. Cellular signalling 19:2013-2023.

Zhao J, Brault JJ, Schild A, Cao P, Sandri M, Schiaffino S, Lecker SH, Goldberg AL (2007) FoxO3 Coordinately Activates Protein Degradation by the Autophagic/Lysosomal and Proteasomal Pathways in Atrophying Muscle Cells. Cell metabolism 6:472-483.

Zhu Y-F, Yu B-H, Li D-L, Ke H-L, Guo X-Z, Xiao X-Y (2012) PI3K expression and PIK3CA mutations are related to colorectal cancer metastases. World Journal of Gastroenterology : WJG 18:3745-3751.

Zou Y, Ling Y-H, Sironi J, Schwartz EL, Perez-Soler R, Piperdi B (2013) The autophagy inhibitor chloroquine overcomes the innate resistance to erlotinib of non-small cell lung cancer cells with wild-type EGFR. Journal of thoracic oncology : official publication of the International Association for the Study of Lung Cancer 8:10.1097/JTO.1090b1013e31828c37210.

Appendix I

Table 1: Clinical trials using autophagy inhibitors in combination with Targeted Therapy agents

A/A	Cancer Type	Autophagy Inhibitor	Cancer Therapy	Status	Title
1	Advance Solid Tumors	HCQ	**Vorinostat**	Recruiting	Hydroxychloroquine + Vorinostat in Advanced Solid Tumors
2	Advanced Malignancies	HCQ	**Sirolimus** or **Vorinostat**	Recruiting	Sirolimus or Vorinostat and Hydroxychloroquine in Advanced Cancer
3	Breast Cancer	CQ	**-**	Recruiting	A Phase 2 Randomized, Double-blind Trial Evaluating the Effects of Chloroquine in Breast Cancer (CUBiC)
4	Chronic Myeloid Leukemia	HCQ	**Imatinib Mesylate**	Recruiting	Imatinib Mesylate With or Without Hydroxychloroquine in Treating Patients With Chronic Myeloid Leukemia
5	Colorectal cancer	HCQ	FOLFOX **Bevacizumab**	Recruiting	FOLFOX/Bevacizumab/Hydroxychloroquine (HCQ) in Colorectal Cancer
6	Colorectal Cancer	HCQ	**Regorafenib Vorinostat**	Recruiting	Vorinostat Plus Hydroxychloroquine Versus Regorafenib in Colorectal Cancer
7	Ductal Carcinoma in Situ	CQ	**-**	Recruiting	Study of the Efficacy of Chloroquine in the Treatment of Ductal Carcinoma in Situ (The PINC Trial)
8	Glioma, Intrahepatic Cholangiocarcinoma or Chondrosarcoma	CQ	**Metformin**	Not yet recruiting	Metformin And Chloroquine in IDH1/2-mutated Solid Tumors (MACIST)
9	Lung Cancer	HCQ	Paclitaxel Carboplatin **Bevacizumab**	Recruiting	Modulation of Autophagy in Patients With Advanced/Recurrent Non-small Cell Lung Cancer - Phase II
10	Lung Cancer	HCQ	Paclitaxel Carboplatin **Bevacizumab**	Active, Not yet recruiting	Hydroxychloroquine + Carboplatin, Paclitaxel and Bevacizumb in Non-Small Cell Lung Cancer (NSCLC)
11	Lung Cancer	HCQ	Paclitaxel Carboplatin **Bevacizumab**	Terminated	Hydroxychloroquine, Carboplatin, Paclitaxel, and Bevacizumab in Treating Patients With Recurrent Advanced Non-Small Cell Lung Cancer
12	Lung Cancer	HCQ	**Gefitinib**	Recruiting	Hydroxychloroquine and Gefitinib to Treat Lung Cancer
13	Lung Cancer	HCQ	**Erlotinib**	Terminated	Hydroxychloroquine With or Without Erlotinib in Advanced Non-small Cell Lung Cancer (NSCLC)

A/A	Cancer Type	Autophagy Inhibitor	Cancer Therapy	Status	Title
14	Lung Cancer	HCQ	**Erlotinib**	Active, Not yet recruiting	Erlotinib With or Without Hydroxychloroquine in Chemo-Naive Advanced NSCLC and (EGFR) Mutations
15	Melanoma	HCQ	**Vemurafenib**	Recruiting	A Phase I Trial of Vemurafenib and Hydroxychloroquine in Patients With Advanced BRAF Mutant Melanoma
16	Melanoma	HCQ	**Dabrafenib Trametinib**	Recruiting	The BAMM Trial: BRAF, Autophagy and MEK Inhibition in Metastatic Melanoma: A Phase I/2 Trial of Dabrafenib, Trametinib and Hydroxychloroquine in Patients With Advanced BRAF Mutant Melanoma
17	Metastatic colorectal cancer	HCQ	Capecitabine Oxaliplatin **Bevacizumab**	Recruiting	Hydroxychloroquine, Capecitabine, Oxaliplatin, and Bevacizumab in Treating Patients With Metastatic Colorectal Cancer
18	Metastatic Solid Tumours	HCQ	**Temsirolimus**	Unknown	Hydroxychloroquine and Temsirolimus in Treating Patients With Metastatic Solid Tumors That Have Not Responded to Treatment
19	Myeloma	HCQ	Cyclophosphamid Pulse Dexamethasone **Rapamycin**	Terminated	Cyclophosphamide and Pulse Dexamethasone With Rapamycin or Hydroxychloroquine
20	Myeloma	HCQ	Cyclophosphamide Dexamethasone **Rapamycin**	Recruiting	Cyclophosphamide(Cy)/ Dexamethasone(Dex)/Rapamycin (Rapa)/Hydroxychloroquine (HCQ) for Relapsed or Refractory Myeloma(Rel/Ref MM)
21	Myeloma	HCQ	**Bortezomib**	Unknown	Hydroxychloroquine and Bortezomib in Treating Patients With Relapsed or Refractory Multiple Myeloma
22	Prostate cancer	HCQ	**ABT-263 Abiraterone**	Not yet recruiting	Phase II Study of ABT-263/Abiraterone or ABT-263/Abiraterone/Hydroxychloroquine in Prostrate Cancer
23	Prostate or Kidney Cancer	HCQ	**MK2206**	Recruiting	Akt Inhibitor MK2206 and Hydroxychloroquine in Treating Patients With Advanced Solid Tumors or Prostate or Kidney Cancer
24	Renal Cancer	HCQ	**Aldesleukin**	Recruiting	Study of Hydroxychloroquine and Aldesleukin in Renal Cell Carcinoma Patients (RCC)

A/A	Cancer Type	Autophagy Inhibitor	Cancer Therapy	Status	Title
25	Renal Cell Carcinoma	HCQ	**RAD001**	Recruiting	Autophagy Inhibition to Augment mTOR Inhibition: A Phase I/II Trial of RAD001 and Hydroxychloroquine in Patients With Previously Treated Renal Cell Carcinoma
26	Sarcoma	HCQ	**Sirolimus**	Recruiting	A Phase II Trial of Combined Hydroxychloroquine and Sirolimus in Drug Refractory Advanced Sarcoma
27	Solid Tumors, Melanoma, Renal and Prostate Cancer	HCQ	**MK-2206**	Recruiting	Akt Inhibitor MK2206 and Hydroxychloroquine in Treating Patients With Advanced Solid Tumors, Melanoma, Prostate or Kidney Cancer
28	Solid Tumours	HCQ	**Sorafenib**	Recruiting	Oral Hydroxychloroquine Plus Oral Sorafenib to Treat Patients With Refractory or Relapsed Solid Tumors
29	Solid Tumours	HCQ	**Sunitinib Malate**	Active, Not yet recruiting	Sunitinib Malate and Hydroxychloroquine in Treating Patients With Advanced Solid Tumors That Have Not Responded to Chemotherapy
Information for Clinical trials obtained by **Clinicaltrials.gov** website					
Bevacizumab = VEGF-A inhibitor, **Gefitinib & Erlotinib =** EGFR inhibitors, **Temsirolimus/Sirolimus/Rapamycin & RAD001** = mTOR inhibitor, **Vorinostat** = histone deacetylase HDAC inhibitor, **Sorafenib** = KIT, VEGFR, PDGFR and MAPK/ERK serine/threonine kinases inhibitor, **Sunitinib Malate** = VEGFR2, PDGFRb, c-kit and FLT3 tyrosine kinases inhibitor, **ABT-263** =Bcl-2 inhibitor, **MK2206** = AKT inhibitor, **Vemurafenib** = BRAF inhibitor, **Imatinib Mesylate** = BCR/ABL, c-KIT and PDGFR inhibitor, **Aldesleukin =** IL-2 Receptor activator, **Dabrafenib** = B-raf inhibitor, **Trametinib** = MEC inhibitor, **Regorafenib** = VEGFR2-TIE2 tyrosine kinase inhibitor					